

1995

# Profiling the Organic Emissions from a Light-Duty Direct Injection Diesel Engine over a range of Speeds and Loads

Collier, Anthony Richard

<http://hdl.handle.net/10026.1/2214>

---

<http://dx.doi.org/10.24382/4696>

University of Plymouth

---

*All content in PEARL is protected by copyright law. Author manuscripts are made available in accordance with publisher policies. Please cite only the published version using the details provided on the item record or document. In the absence of an open licence (e.g. Creative Commons), permissions for further reuse of content should be sought from the publisher or author.*

**Profiling the Organic Emissions from a Light-Duty Direct  
Injection Diesel Engine over a range of Speeds  
and Loads**

by

**Anthony Richard Collier**

A thesis submitted to the University of Plymouth in partial fulfilment for the degree of

**Doctor of Philosophy**

Department of Environmental Sciences  
Faculty of Science

In collaboration with Perkins Technology, Peterborough

March 1995

S

UNIVERSITY OF PLYMOUTH	
Item No.	900 242248 2
Date	21 AUG 1995
Class No.	T 629.2506 COL
Contl. No.	X703114300
LIBRARY SERVICES	

90 0242248 2



REFERENCE ONLY

# **Profiling the Organic Emissions from a Light-Duty Direct Injection Diesel Engine over a range of Speeds and Loads**

Anthony Richard Collier

## **Abstract**

Diesel engines account for a large percentage of the particulates in urban city environments. Polycyclic aromatic compounds (PAC), some proven carcinogens, have been found on diesel particulates. The trace level nitro-PAC emissions, such as 1-nitropyrene and dinitropyrenes, contribute a large proportion of the mutagenicity in the particulates; in the case of 1-nitropyrene between 10 to 40% of the total mutagenicity of the particulate has been claimed. The potential health hazards of PAC require the levels and sources of such emissions to be evaluated over a range of speeds and loads.

PAC emissions are dependant on the engine specification, such as normally aspirated compared with turbocharged, and the operating conditions (speed and load). The effect of such variables can be determined using emission profiling, in which profiles of the exhaust are compared at varying engine powers. In this way the effect of speed and load on the combustion efficiency can be established.

Identification of PAC sources may be further complicated when engine sampling systems, such as the conventional dilution tunnel/filter system, are prone to artefact formation. This is especially relevant to secondary nitro-PAC emissions, which are prone to forming as artefacts of the filter installed in the dilution tunnel. In this study, organic emission maps were constructed using the unique total exhaust solvent-stripping apparatus (TESSA) developed at the University of Plymouth. TESSA allowed rapid sampling with a minimum potential for artefact formation. The close proximity of TESSA to the engine allowed the role of the combustion chamber in the formation of emissions to be evaluated.

Primary organic emissions, such as pyrene, are derived from survival of compounds in the fuel/oil and by combustion generation. Establishment of emission maps for the primary emissions are vital to resolving the formation of secondary emissions, such as 1-nitropyrene. Profiling of primary emissions sampled 26 different speeds and loads using TESSA (sampling times as low as 15 seconds). Following simple work-up, quantification of the  $n$ -alkanes was by gas chromatography with flame ionisation detection and PAH by gas chromatography/mass spectrometry operated in electron impact mode. Emissions were expressed as a recovery of the compound emitted as a percentage of the same compound entering the chamber in the fuel. The  $n$ -alkane and PAH emission maps correlated with the gaseous unburnt hydrocarbon emissions, indicating that fuel survival was an important source of emissions, whereas lubricating oil contributions were minimal. Fuel survival contributions decreased with load; at 1000 rpm the average PAH survival of 0.95% at idling decreased to 0.2% at full load. High survivals under idling was a consequence of the low chamber temperatures and air:fuel ratios mixed beyond the lean flammability limits, whereas at full load, the high temperatures resulted in the greatest combustion efficiency. The  $n$ -alkane emission trends replicated those of PAH; at 1000 rpm the average  $n$ -alkane survival was 0.48% at idle compared with 0.084% at full load. Correlations between the distribution of the emissions and fuel at high load, suggested fuel survival unchanged was responsible. At low loads the exhaust/fuel PAH ratios were more varied, with the range of percentage recoveries at low loads increasing with speed (difference between percentage recovery of fluorene and phenanthrene at idling for 1000 rpm and 3000 rpm was 0.05 and 0.18 respectively).

At high load, the combustion environment can be envisaged as producing areas under which complete combustion and survival unchanged occur. In between the complete combustion and unburnt fuel zones, a narrow range of temperatures and time for combustion reduce the opportunity for combustion generation reactions and/or preferential survival. Low load at 3000 rpm may increase the intermediate zone, allowing preferential survival and/or combustion generation reactions to evolve. Possible pyrolytic cracking of  $n$ -alkanes and demethylation of PAH at low loads and 3000 rpm was evident. The optimum time, swirl, and temperature for efficient combustion at low loads was generated at 2000 rpm to 2500 rpm, whereas at the higher temperatures corresponding to high loads, the effect of speed was much smaller. The primary emissions map show engineering improvements, particularly at low loads, could be implemented to lower the PAH emissions. The correlation between the emissions and fuel input suggest modifications to the PAH content of fuels may lower emissions.



The formation of secondary nitro- and oxy-PAC emissions is by transformation of primary emissions. In the case of nitro-PAC, nitration has been proposed to occur by free radical processes between PAH and oxides of nitrogen,  $\text{NO}_x$ , within the chamber and by electrophilic substitution of PAH surviving combustion by nitrogen dioxide and nitric acid, *via* the nitronium ion. The combustion contribution to nitro-PAC emissions was investigated using an upgraded TESSA system, and 3 speeds at low, mid, and high  $\text{NO}_x$  for each speed were sampled. Following initial extraction, concentration and clean-up of the samples, the nitro-PAC fractions of interest were isolated by normal phase high performance liquid chromatography. The nitro-PAC were identified and quantified by gas chromatography with electron capture detection, and gas chromatography/mass spectrometry operated in the negative ion chemical ionisation mode (the detection limits for both analytical systems was of the order of 40-50 pg of nitro-PAC standards injected). The profiling indicated that a proportion of the fuel underwent nitration within the combustion chamber across a range of speeds and loads. The extract concentrations (average of 5.3 ppm) found in this study were much lower than those previously found (ranging from 55 to 2280 ppm). The majority of the previous studies relied on sampling using dilution tunnel/filter systems, for which post combustion contributions are simulated; suggesting that a major source of nitro-PAC is derived from post-combustion nitration of PAH surviving combustion, some of which may be artefacts of the filter. Different speeds produced different trends for nitro-PAC emissions with respect to engine load. It was not until the high temperature speed of 3500 rpm was reached that both  $\text{NO}_x$  and nitro-PAC increased with load ( $R\text{-sq} = 0.989$  &  $p = 0.067$  for 1-nitronaphthalene &  $\text{NO}_x$ ).

Nitro-PAC emissions at 3500 rpm were primarily the result of combustion chamber nitration of PAH at high  $\text{NO}_x$ . In the case of 1-nitropyrene, there was strong evidence to support pyrosynthetic contributions to the pyrene mass, which in turn became nitrated. The nitro-PAC emissions at low loads were the result of post-combustion nitration of PAH surviving combustion with the nitronium ion. The correlation of the PAH precursors to nitro-PAC in the fuel and nitro-PAC emissions suggest fuel modifications may to some extent lower the nitro-PAC emissions. The combustion generation of nitro-PAC at high engine powers may require post-combustion after treatment.

### Acknowledgements

I would like to thank my supervisors, Dr Colin Trier, Dr Mike Rhead, and Dr Murray Bell for their guidance and support throughout the research. I also thank the other members of the diesel research group at the University, in particular Professor David Fussey, Dr Paul Tancell and Robin Pemberton.

I wish to thank the staff at Perkins Technology for their advice in interpreting the results from an engineering viewpoint. Special thanks goes to Fred Brear for his assistance whilst at Perkins.

I must thank all the support from the staff at the University of Plymouth. I would mention in particular Roger Shrodzinski for his help with the GC/MS work and Dr Anthony Gachanja for his help with the chemiluminescence experimentation. I also thank Roy Cox and Don Ryder in the Thermodynamics laboratory for helping with maintaining and upgrading the engine sampling facilities.

I also wish to thank the staff, particularly Jim Carter, at the GC/MS facility at the University of Bristol for help and guidance with the use of their GC/MS facilities.

Finally I express many thanks to my family for their support throughout the research. A special thanks goes to Rachel Rossitter for helping me through the research.

### Author's Declaration

At no time during registration for the degree of Doctor of Philosophy has the author been registered for any other University award.

Throughout the research I regularly attended and presented research seminars at the University of Plymouth. I also attended a number of key external conferences:

Emissions. Organised by UnICEG. Shell Thornton Research Centre, 22/9/93.

Petroleum Analysis. Organised by The Chromatographic Society. Shell Thornton Research Centre, 10/11/93.

Alternative Fuels. Organised by UnICEG. Coventry University, 20/12/93.

Fundamentals of Combustion. Organised by UnICEG. University of Warwick, 13/4/94

Urban Air Pollution and Public health. Organised by the Environmental Change Research Centre, University College London. 23/9/94.


Lecture given at the Fundamentals of Combustion Conference: Relationship between Fuel and Emissions in Diesel Engine Combustion.

Poster presented at the Urban Air Pollution and Public Health conference: Nitro-Polycyclic Aromatic Compound Profiles for a Light-Duty Diesel Engine.

I have also frequently consulted with external institutions and the following papers were prepared for publication:

Collier, A.R. (1994) Organic emissions from light-duty diesel engines. *Proceedings of a Seminar: Urban Air Pollution and Public Health*. Environmental Change Research Centre. University College London,

Collier, A.R., Rhead, M.M., Trier, C.J., & Bell, M.A. (1995) Polycyclic Aromatic Compound Profiles from a Light-Duty Direct Injection Diesel Engine. *Fuel*. 74 (3), 362-367.

Signed   
Date 24.1.95

## Contents

<b>Chapter 1 - Introduction</b>	<b>1</b>
1.1 The Emergence of High-Speed Passenger Car Diesels	1
1.2 Environmental Impact of Diesel Emissions	6
1.3 Legislation and Control of Diesel Emissions	10
1.4 Diesel Combustion and the Formation of Organic Emissions	13
1.5 Profiling of the Organic Emissions from Diesels	17
 <b>Chapter 2 - Review of Diesel Emission Profiling</b>	 <b>19</b>
2.1 Review of Profiling Techniques	19
2.1.1 Sampling of Engines for Organic Emissions	19
2.1.2 Laboratory Work-up & Analytical Techniques for Organic Compounds	23
2.1.2.1 Extraction and Concentration of Organics	23
2.1.2.2 Fractionation of Organic	24
2.1.2.3 Detection of Organics	24
2.2 Review of Previous Profiling Studies	28
2.2.1 PAH Profiling	28
2.2.2 Alkane Profiling	37
2.2.3 Nitro-PAC Profiling	39
2.2.4 Oxy-PAC Profiling	48
2.3 Summary of Emission Profiling & Aims of Investigation	50
 <b>Chapter 3 - Experimental Procedures &amp; Facilities</b>	 <b>53</b>
3.1 Facilities and Fuel/Oil Description	53
3.1.1 Engine Details	53
3.1.2 Engine Management	53
3.1.3 Total Exhaust Solvent-Stripping Apparatus (TESSA)	53
3.1.4 Fuels and Oils	56
 3.2 Profiling of the Primary Emissions using the initial TESSA configuration	 57
3.2.1 Engine Sampling for Primary Emissions	57
3.2.2 Sample work-up	60
3.2.2.1 Internal Standards for Aromatics	60
3.2.2.2 Extraction and Concentration of TES	62
3.2.2.3 Open column Silica Gel Fractionation	62
3.2.2.4 Fuel work-up	63
3.2.2.5 Lubricating Oil work-up	63
3.2.2.6 Recovery of Aromatic Internal Standards	64
3.2.2.7 Laboratory losses for Selected $n$ -Alkanes	65
3.2.3 Quantification of $n$ -Alkanes by Gas Chromatography with Flame Ionisation Detection	66

3.2.4 Quantification of Major PAC by Gas Chromatography/Mass Spectrometry operated in Electron Impact Mode .....	69
3.3 Relocation and Modification of TESSA	75
3.3.1 Improvements to the Engine Sampling Rig	75
3.3.2 Initial testing of the upgraded TESSA	79
3.4 Profiling of the Secondary Emissions using the upgraded TESSA	80
3.4.1 Engine Sampling for Nitro-PAC Profiling	80
3.4.1.1 Engine Sampling for Nitro-PAC at 2500 rpm	80
3.4.1.2 Engine Sampling for Nitro-PAC at 1500 rpm & 3500 rpm	83
3.4.2 Sample Work-up for Nitro-PAC Profiling	85
3.4.2.1 Extraction and Concentration of TES for Nitro-PAC Profiling	85
3.4.2.2 Clean-up of TES	86
3.4.2.2.1 Octadecylsilane Cartridge Clean-up	86
3.4.2.2.2 Silica gel Clean-up	89
3.4.2.3 High-Performance Liquid Chromatography Fractionation	90
3.4.2.3.1 Initial HPLC Fractionations and Method Development	91
3.4.2.3.2 HPLC Fractionations of TES collected at 1500 rpm & 3500 rpm	93
3.4.2.4 Fuel and Oil work-up	93
3.4.2.5 Recovery of Nitro-PAC for Laboratory Work-up	95
3.4.3 Analysis Nitro- and Oxy-PAC	95
3.4.3.1 Evaluation of Detection Systems for Nitro-PAC Analysis	96
3.4.3.1.1 Gas Chromatography with Nitrogen-Phosphorous Detection	96
3.4.3.1.2 Reverse Phase HPLC with Fluorescence/Chemiluminescence Detection	97
3.4.3.1.3 Gas Chromatography/Mass Spectrometry operated in the Electron Impact Mode	101
3.4.3.1.4 Gas Chromatography with Electron Capture Detection	101
3.4.3.1.4.1 Analysis of Mononitro-PAC HPLC Fractions by GC-ECD	103
3.4.3.1.4.2 Analysis of Dinitro-PAC HPLC Fractions by GC-ECD	108
3.4.3.1.4.3 Analysis of Nitro-oxy-PAC HPLC Fractions by GC-ECD	108
3.4.3.1.5 Gas Chromatography/Mass Spectrometry operated in the Negative Ion Chemical Ionisation mode .....	111
3.4.3.2 Gas Chromatography/Mass Spectrometry operated in Electron Impact mode for Oxy-PAC	115
3.4.3.3 Analysis of n-Alkanes by Gas Chromatography with Flame Ionisation Detection	115
3.4.3.4 Analysis of major PAC by Gas Chromatography/Mass Spectrometry in the Electron Impact Mode .....	117

<b>Chapter 4 - Primary Organic Emissions</b>	<b>118</b>
4.1 The Contributions of Fuel and Oil Survival to the Emissions	118
4.2 Profiling of the Primary Emissions using the initial TESSA configuration	128
4.2.1 The Concept of Percentage Recoveries	129
4.2.2 The Effect of Engine Load on the Percentage Recovery of Primary Organics	134
4.2.3 The Effect of Engine Speed on the Percentage Recovery of Primary Organics	142
4.2.4 Combined Effect of Engine Speed and Load on Primary Emissions	145
4.2.5 Comparison of the $n$ -Alkanes with the Major PAC emissions	149
4.2.6 The contribution of combustion generation to the organic emissions	152
4.3 Comparison of Primary Emissions collected using Initial & Upgraded TESSA	160
4.3.1 Combustion of Fluorene at low loads and low speed	160
4.3.2 Effect of Engine Load on the Percentage Recovery of Primary Emissions	162
4.3.3 Effect of Engine Speed for the Combined Sampling Sets	165
4.4 Summary of Major Organic Emissions	167
 <b>Chapter 5 - Secondary Nitro- &amp; Oxy-PAC Emissions</b>	 <b>169</b>
5.1 The Contribution of Different PAC classes to the Emissions	169
5.2 Nitro-PAC Emissions	171
5.2.1 Analysis of the Mononitro-PAC HPLC fractions by Gas Chromatography with Electron Capture Detection .....	172
5.2.1.2 Analysis of the Mononitro-PAC HPLC fraction derived at High Speed and High Load by Gas Chromatography/Mass Spectrometry operated in Negative Ion Chemical Ionisation Mode	178
5.2.1.3 Comparison of the Levels and distribution of Nitro-PAC found using TESSA with Previous Studies .....	183
5.2.1.4 The Effect of Engine Speed and Load on the Mononitro-PAC Emissions	189
5.2.1.5 Factors controlling the Nitration in the Combustion Chamber	195
5.2.1.6 Nitration mechanisms involved	198
5.2.2 Dinitro-PAC & Nitro-oxy-PAC Profiles for the Prima Diesel Engine	207
5.3 Oxy-PAC Emissions	207
5.4 Summary of Findings for Secondary Nitro- and Oxy-PAC Emissions	213
 <b>Chapter 6 -Final Discussions, Conclusions, &amp; Future Work</b>	 <b>215</b>
6.1 Final Discussions	215
6.1.1 Primary Organic Emissions	216
6.1.2 Secondary Organic Emissions	223
6.2 Conclusions from research	232
6.3 Future Research Proposals	234
Literature Cited	236
Appendix - Nitro-PAC Calculations	A1

## List of Figures

### Chapter 1 - Introduction

1.1 The superior fuel economy of diesel engines compared with petrol engines, especially for urban driving. ....	2
1.2 The configuration of direct injection (DI) and indirect injection (IDI) combustion chambers. ....	3
1.3 The Perkins Prima high speed direct injection (HSDI) engine. ....	5
1.4 Structures of polycyclic aromatic compounds (PAC) common to diesel emissions ....	8
1.5 The trade-off between emissions of particulate and oxides of nitrogen (NO <sub>x</sub> ) ....	12
1.6 The four cycles of the diesel engine, consisting of the induction (a), compression (b), power (c), and exhaust (d) stages ....	14
1.7 Axisymmetric idealization of a diesel fuel spray. The lower section of the figure shows the lines of constant equivalence ratio (stoichiometric air:fuel ratio / actual air:fuel ratio, denoted by $\phi$ ). The areas of the fuel spray corresponding to the rich and lean flammability limits are indicated..	15

### Chapter 2 - Review of Diesel Emission Profiling

2.1 A typical dilution tunnel and filter collection engine sampling system ....	20
2.2 The total exhaust solvent-stripping apparatus (TESSA). ....	22
2.3 An idealised example of the chromatography for three model compounds (a) and the resulting chromatogram (b).....	25
2.4 The effect of speed and load on the PAH emissions from IDI (a) and DI (b) diesels. ....	30
2.5 Effect of engine load on the PAH and Alkyl-PAH emissions from a light-duty DI diesel. ....	32
2.6 Effect of engine speed on the survival of PAH from a medium-duty DI diesel. ....	34
2.7 The ratio between PAC in TES relative to the PAC in the fuel for a) low engine power and b) high power.....	36
2.8 The effect of engine load on the survival of <i>n</i> -Alkanes from a light-duty IDI diesel. ....	38
2.9 The effect of engine conditions on 1-nitropyrene emissions from a heavy-duty diesel. ....	41
2.10 Effect of different segments of a FTP cycle on emissions of 1-nitropyrene (a), emissions of NO <sub>x</sub> (b), and temperature (c).....	42
2.11 Effect of engine load on the nitro-PAC emissions from a heavy-duty turbocharged diesel ....	45
2.12 The effect of engine load and Speed on the 1-nitropyrene emissions from a medium-duty DI diesel.....	47
2.13 Effect of engine load on the Oxy-PAC emissions from a heavy-duty diesel. ....	49

### Chapter 3 - Experimental Procedures & Facilities

3.1 The operation of the solvent delivery system (a) and exhaust transfer mechanism (b) used for engine sampling with TESSA.....	55
3.2 The overall experimental procedure for the profiling of the primary organics. ....	58
3.3 Gas chromatogram of the <i>n</i> -alkane standard mix. GC conditions: DB-5 column, 50°C for 1 min., 10°C/min. up to 270°C.....	67
3.4 Calibration curve for heptadecane using gas chromatography with flame ionisation detection. ....	68
3.5 The identification of PAC on a retention and molecular ion basis. GC conditions: PTE-5 column, 40°C for 1 min., 6°C/min. up to 300°C, held for 15 mins.....	70
3.6 The confirmation of pyrene by matching the spectra in the sample (a) to that of the standard spectra stored in the computer library (b).....	71
3.7 Identification of phenanthrene and methylphenanthrenes by the respective molecular ions, 178 = phenanthrene, 192 = monomethylphenanthrenes, 206 = dimethylphenanthrenes, and 220 = trimethylphenanthrenes. GC conditions: PTE-5 column, 40°C for 1 min., 6°C/min. up to 300°C, held for 15 mins.....	72
3.8 Total ion chromatogram of the standard PAC used for the primary PAC profiling. GC conditions: PTE-5 column, 40°C for 1 min., 6°C/min. up to 300°C, held for 15 mins.....	74
3.9 The overall experimental procedure aimed at profiling the secondary nitro- and oxy-PAC. ....	81
3.10 The effect of engine speed and load on the gaseous oxides of nitrogen, NO <sub>x</sub> . ....	82
3.11 The evaluation of the acidic aqueous methanol phase for the formation of nitronaphthalenes. The comparison of the nitration check (a) to both the solvent blank (b) and the mononitro-PAC standard mix (c) proved there was no such nitration occurring. (Chromatographic conditions given in Section 3.4.3.1.4.1.).....	87

3.12 The evaluation of the acidic aqueous methanol phase for the formation of 3-nitrofluoranthene and 1-nitropyrene. The comparison of the nitration check (a) to both the solvent blank (b) and the mononitro- PAC standard mix (c) proved there was no such nitration occurring. (Chromatographic conditions given in Section 3.4.3.1.4.1.).....	88
3.13 The chromatogram of the HPLC fractionation standard mix and the establishment of the initial HPLC fraction elution windows. HPLC conditions: Spherisorb silica column, 100% hexane (5 min.), increased to 100% DCM (20 min.), held for 10 min., increased to 100% acetonitrile (10 min.), and held for 10 min. Flow rate of 4 ml/min.....	92
3.14 The HPLC fractionation of the aromatic fraction from the ODS clean-up of TES collected at 2500 rpm and low load. HPLC conditions: Spherisorb silica column, 100% hexane (5 min.), increased to 100% DCM (20 min.), held for 10 min., increased to 100% acetonitrile (10 min.), and held for 10 min. Flow rate of 4 ml/min.....	94
3.15 The sensitivity of fluorescence detection with on-line pre-column reduction for the determination of 1-nitropyrene (2.5 pg injected) in the reduced form of 1-aminopyrene. HPLC conditions: Spherisorb ODS-2 column, isocratic elution with acetonitrile:water (80:20), and ammonium acetate (30 mM). $Ex_1 = 260$ nm and $Em_1 = 430$ nm. Flow rate of 1 ml/min.....	98
3.16 The sensitivity of the bis (2,4-dinitrophenyl)oxalate (DNPO) chemiluminescence reaction to the detection of 1-aminopyrene (20 ng injected each time) using flow-injection analysis. Flow rate of 1 ml/min for mobile phase (100% acetonitrile) and 0.5 ml/min for each reagent stream (DNPO and $H_2O_2$ ).....	100
3.17 The low sensitivity of gas chromatography/mass spectrometry operated in the electron impact mode to mononitro-PAC standard mix. GC conditions: $Rt_1$ -5 column, 60°C for 1 min., 5°C/min. to 300°C, held for 10 min.....	102
3.18 The high sensitivity of gas chromatography with electron capture detection to a) the nitronaphthalenes, and b) 3-nitrofluoranthene and 1-nitropyrene. GC conditions: Supelchem PTE-5 column, 60°C for 1 min., 5°C/min to 300°C, held for 10 min.....	104
3.19 The establishment of the integration temperature windows for nitro-PAC using the mononitro-PAC standard mix. GC conditions: Supelchem PTE-5 column, 60°C for 1 min., 5°C/min. to 300°C, held for 10 min.....	105
3.20 The confirmation of the nitronaphthalenes in the mononitro-PAC HPLC fraction collected at high load and 1500 rpm (a) by comparing the nitronaphthalene temperature window (b) with that of the same sample co-injected with the mononitro-PAC standard mix (c) (Chromatographic conditions given in Section 3.4.3.1.4.1.).....	107
3.21 Calibration curves for 1-nitronaphthalene and 1-nitropyrene using gas chromatography with electron capture detection.....	109
3.22 The gas chromatogram of the dinitro-PAC standard mix. GC conditions: Supelchem PTE-5, 60°C for 1 min., 10°C/min to 180°C, 5°C/min to 300°C, held for 10 min.....	110
3.23 The gas chromatogram of the nitro-oxy-PAC standard mix. GC conditions: Supelchem PTE-5, 60°C for 1 min., 10°C/min to 200°C, 5°C/min to 300°C, held for 10 min.....	112
3.24 The sensitivity of gas chromatography/mass spectrometry operated in the negative ion chemical ionisation and selective ion modes to a) 1- & 2-nitronaphthalene, b) 2-methyl-1-nitronaphthalene, and c) 3-nitrofluoranthene and 1-nitropyrene. GC conditions: Supelchem PTE-5 column, 60°C for 1 min., 5°C/min. to 300°C, held for 10 min.....	113
3.25 The analysis of the mononitro-PAC HPLC fraction obtained at 3500 rpm and high load by gas chromatography/mass spectrometry operated in negative ion chemical ionisation mode, using selective ion monitoring (a) and the confirmation of 1-nitropyrene by scanning for the 247 molecular ion (b). GC conditions: Supelchem PTE-5 column, 60°C for 1 min., 5°C/min. to 300°C, held for 10 min.....	114
3.26 Total ion chromatogram of the oxy-PAC standard mix. GC conditions: $Rt_1$ -5 column, 60°C for 1 min., 5°C/min to 300°C, held for 10 min.....	116

## Chapter 4 - Primary Organic Emissions

4.1 Comparison of the aliphatic fractions of diesel fuel (a), and lubricating oil (b), with the TESSA sample (TES) at 1% of full load and 1000 rpm (c) (Chromatographic conditions given in Section 3.2.3).....	119
4.2 Close examination of the oil hump temperature window (a) to the same temperature range of the TESSA extracted sample (TES) at 1% of full load and 1000 rpm (b) (Chromatographic conditions given in Section 3.2.3).....	121
4.3 Examination of the aliphatic fractions of TESSA extracted samples (TES) for evidence of oil contributions at three power settings; 50% of full load & 1000 rpm (a), full load and 1000 rpm (b), and 1% of full load and 3000 rpm (c) (Chromatographic conditions given in Section.3.2.3)...	122



4.4 Comparison of the aromatic fractions of fuel (a), and lubricating oil (b), with the TESSA extracted sample (TES) at 1% of full load and 1500 rpm (c) (Chromatographic conditions given in Section 3.2.4).....	124
4.5 Examination of the aliphatic fractions of sump oils for accumulation of unburnt fuel. Fresh oil (a), sump after 50 hours use (b), and sump after 105 hours use (c) (Chromatographic conditions given in Section 3.2.3).....	125
4.6 Examination of the aromatic fractions of sump oils for accumulation of unburnt fuel. Fresh oil (a), sump after 50 hours use (b), and sump after 105 hours use (c) (Chromatographic conditions given in Section 3.2.4).....	126
4.7 Accumulation of phenanthrene and methyl derivatives in sump oil over time.....	127
4.8 Interpretation of percentage recoveries for identification of the source of emissions.....	131
4.9 Effect of engine load on the percentage recovery of selected PAC (a) and $n$ -alkanes (b) at 1000 rpm.....	135
4.10 Effect of engine load on the emissions of unburnt hydrocarbons (UHC) (a), TESSA extracted sample (TES) (b), and bosch smoke (c) at 1000 rpm.....	136
4.11 Effect of engine load on the percentage recovery of selected PAC (a) and $n$ -alkanes (b) at 3000 rpm.....	143
4.12 Effect of engine load on the emissions of unburnt hydrocarbons (UHC) (a), TESSA extracted sample (TES) (b), and bosch smoke (c) at 3000 rpm.....	144
4.13 Effect of engine speed and load on the percentage recovery of fluorene (a), dibenzothiophene (b), phenanthrene (c), and pyrene (d).....	146
4.14 Effect of engine speed and load on the percentage recovery of tetradecane (a), hexadecane (b), octadecane (c), and eicosane (d).....	148
4.15 Comparison of the percentage recovery of fluorene compared with hexadecane at 1000 rpm (a), 2000 rpm (b), and 3000 rpm (c).....	150
4.16 Comparison of the percentage recovery of phenanthrene compared with nonadecane at 1000 rpm (a), 2000 rpm (b), and 3000 rpm (c).....	151
4.17 Effect of molecular weight on the percentage recovery of PAH (a) and $n$ -alkanes (b).....	153
4.18 Comparison of dibenzothiophene with methyl-dibenzothiophenes at 1000 rpm (a) and 3000 rpm (b). Comparison of fluorene with methyl-derivatives at 3000 rpm (c).....	154
4.19 Comparison of the $n$ -alkane distribution in diesel fuel (a) with the TESSA extracted (TES) at 1% of full load & 3000 rpm (b).....	157
4.20 Effect of low loads on the percentage recovery of fluorene.....	161
4.21 Effect of engine load on the percentage recovery of selected PAC at 1500 rpm (a), 2500 rpm (b), and 3500 rpm (c).....	163
4.22 Effect of engine load on the percentage recovery of selected $n$ -alkanes at 1500 rpm (a) and 3500 rpm (b).....	164
4.23 Effect of speed on the percentage recovery of fluorene and hexadecane at low load.....	166

## **Chapter 5 - Secondary Nitro- & Oxy-PAC Emissions**

5.1 Overall chemical composition of the aromatic fractions of TES at 1500 rpm and a) low load, b) mid load, and c) high load, determined using normal-phase high-performance liquid chromatography (Chromatographic conditions given in Section 3.4.2.3.2).....	170
5.2 The analysis of the mononitro-PAC HPLC fractions derived from sampling at 1500 rpm and across the load range, by gas chromatography with electron capture detection (Chromatographic conditions given in Section 3.4.3.1.4.1).....	173
5.3 The profile of the nitronaphthalenes at 1500 rpm and across the load range, determined using gas chromatography with electron capture detection (Chromatographic conditions given in Section 3.4.3.1.4.1).....	174
5.4 The analysis of the mononitro-PAC HPLC fraction of diesel fuel by gas chromatography with electron capture detection (a), and the verification of the lack of nitro-PAC in the fuel (b&c). Retention times for nitro-PAC standards: 1-nitronaphthalene (22.237 mins.), 2-methyl-1-nitronaphthalene (22.919 mins.), 2-nitronaphthalene (23.487 mins.), and 1-nitropyrene (42.054 mins.) (Chromatographic conditions given in Section 3.4.3.1.4.1)...	176
5.5 The analysis of the mononitro-PAC HPLC fraction of sump oil (after 50 hours use) by gas chromatography with electron capture detection (a), and the verification of the lack of nitro-PAC in the fuel (b&c). Retention times for nitro-PAC standards: 1-nitronaphthalene (22.237 mins.), 2-methyl-1-nitronaphthalene (22.919 mins.), 2-nitronaphthalene (23.487 mins.), and 1-nitropyrene (42.054 mins.) (Chromatographic conditions given in Section 3.4.3.1.4.1).....	177

5.6	Distribution of the nitronaphthalenes in TES collected at 3500 rpm and high load, determined by gas chromatography/mass spectrometry (GC/MS) operated in the negative ion chemical ionisation mode (a) compared with the distribution of naphthalenes in the fuel, as determined by GC/MS in the electron impact mode (b) (Chromatographic conditions given in Sections 3.4.3.1.5 and 3.2.4 respectively).....	180
5.7	Distribution of molecular ions 211 and 225 in the mononitro-PAC HPLC fraction collected at 3500 rpm and high load. Determined using gas chromatography/mass spectrometry operated in the negative ion chemical ionisation mode (Chromatographic conditions given in Section 3.4.3.1.5).....	181
5.8	Distribution of molecular ions 223 and 237 in the mononitro-PAC HPLC fraction collected at 3500 rpm and high load. Determined by gas chromatography/mass spectrometry operated in the negative ion chemical ionisation mode (Chromatographic conditions given in Section 3.4.3.1.5)..	182
5.9	The effect of engine load on nitro-PAC at 1500 rpm	190
5.10	The effect of engine load on nitro-PAC at 2500 rpm	191
5.11	The effect of engine load on nitro-PAC at 3500 rpm	192
5.12	The combined effect of speed and load on the emissions of a) 1-nitronaphthalene and b) 1-nitropyrene.....	193
5.13	The investigation of correlations between the nitro-PAC and NO <sub>x</sub> emissions at a) 1500 rpm and b) 3500 rpm.....	197
5.14	Emissions of 1-nitronaphthalene (a), naphthalene (b), NO <sub>x</sub> (c) relative to the fuel burned at 1500 rpm.....	200
5.15	Emissions of 1-nitropyrene (a), pyrene (b), NO <sub>x</sub> (c), relative to the fuel burned at 1500 rpm	201
5.16	Emissions of 1-nitronaphthalene (a), naphthalene (b), NO <sub>x</sub> (c) relative to the fuel burned at 3500 rpm.....	203
5.17	Emissions of 1-nitropyrene (a), pyrene (b), NO <sub>x</sub> (c) relative to the fuel burned at 3500 rpm	204
5.18	Emissions of 1-nitropyrene (a), pyrene (b), NO <sub>x</sub> (c) relative to the fuel burned at low load	205
5.19	Emissions of 1-nitropyrene (a), pyrene (b), NO <sub>x</sub> (c) relative to the fuel burned at high load	206
5.20	The gas chromatographic analysis of the dinitro-PAC HPLC fractions collected at 3500 rpm and a) low load, b) mid load, and c) high load, by gas chromatography with electron capture detection (Chromatographic conditions given in Section 3.4.3.1.4.2).....	208
5.21	The gas chromatographic analysis of the nitro-oxy-PAC HPLC fractions collected at 3500 rpm and a) low load, b) mid load, and c) high load, by gas chromatography with electron capture detection (Chromatographic conditions given in Section 3.4.3.1.4.3).....	209
5.22	The analysis of the oxy-PAC HPLC fractions of TES collected at low engine power (a) and high engine power (b), by gas chromatography/mass spectrometry operated in the electron impact mode (Chromatographic conditions given in Section 3.4.3.2).....	211
5.23	The analysis of the polar fractions from the silica gel clean-up of TES collected at low engine power (a) and high engine power (b), by gas chromatography/mass spectrometry operated in the electron impact mode (Chromatographic conditions given in Section 3.4.3.2).....	212

## Chapter 6 - Final Discussions, Conclusions, & Future Work

6.1	Concept of different temperature and time zones necessary for complete combustion. High loads result in the highest temperatures, resulting in a large complete combustion zone (Z <sub>c</sub> ), and a much smaller zone in which fuel survives intact (Z <sub>w</sub> ). The gradient in terms of the temperature and time existing in the intermediate combustion zone (Z <sub>i</sub> ) is narrow. At low load and high speed the unburnt fuel zone is greater and the range of temperatures and time available for combustion is large, enabling preferential survival and/or combustion chamber generation of PAC.....	224
6.2	Two zone nitration concept, such that the free radical combustion generation of nitro-PAC is favoured at high loads and high speeds (a), whereas electrophilic substitution of surviving PAC is favoured at low loads and low speeds (b).....	230

## List of Tables

### Chapter 1 - Introduction

1.1 Chemical compounds and species found in diesel emissions	7
1.2 Carcinogenicity associated with different PAC Classes	9
1.3 Diesel Engine Passenger Car European Legislation	10

### Chapter 2 - Review of Profiling of Organic Emissions from Light-Duty Diesels

2.1 Detection systems for $\mu$ -Alkanes and major PAH	26
2.2 Detection systems for nitro-PAC	27
2.3 PAH Emission Rates (mg/kg) in DI exhausts at two different air:fuel ratios and for four fuels blends.....	33
2.4 Effect of two different engine conditions on the Nitro-PAC Emissions from a heavy-duty diesel	43
2.5 Effect of Driving Conditions on 1-Nitropyrene Emissions from Light- and Heavy-Duty diesels	46

### Chapter 3 - Experimental Procedures & Facilities

3.1 Perkins Prima Engine Details	54
3.2 Standard No. 2 Diesel Fuel Properties	56
3.3 Engine sampling series at 1000 rpm	59
3.4 Engine sampling series at 2000 rpm	59
3.5 Engine sampling series at 3000 rpm	59
3.6 Results from Internal Standard & PAH Laboratory Recovery Experiment	61
3.7 Internal standards added to TES & Fuel for Primary Emission Profiling	62
3.8 Laboratory Recovery for Internal Standards added to TES and Fuels	65
3.9 Laboratory Recovery of $\mu$ -Alkanes from Spiking Experiment	65
3.10 $\mu$ -Alkane standard mix used for analysis and recovery experiments	66
3.11 Response factors of PAC to Undecane	73
3.12 Engine sampling for Nitro-PAC at 2500 rpm	83
3.13 Engine sampling for Nitro-PAC at 1500 rpm	84
3.14 Engine sampling for Nitro-PAC at 3500 rpm	84
3.15 HPLC fractionation standard mix	91
3.16 Reproducibility of Retention Times ( $R_t$ ) for NP HPLC Fractionation	91
3.17 Laboratory recovery of nitro-PAC	95
3.18 Mononitro-PAC standard mix	96
3.19 Retention Index (RI) based on 1-nitropyrene	106
3.20 Response factors ( $R_f$ ) for PAC based on $d_{10}$ -Fluorene	117

### Chapter 4 - Primary Organic Emissions

4.1 Concentration of Selected $\mu$ -alkanes in the A2 Fuel	120
4.2 Concentration of Selected PAC in the A2 Fuel	123
4.3 The Exhaust PAC emissions relative to the corresponding fuel PAC consumed during sampling	132
4.4 The Exhaust $\mu$ -alkane emissions relative to the corresponding fuel $\mu$ -alkane consumed during sampling.....	133
4.5 Previous studies on Fuel Survival for Diesel Engines	138
4.6 The effect of engine load on the combustion and exhaust temperatures	139
4.7 Effect of Speed on the Percentage Recovery (PR) of PAC between 1% and 25% of Full Load	147
4.8 Effect of Speed on the Percentage Recovery (PR) of $\mu$ -alkanes between 1% and 25% of Full Load	147
4.9 $\mu$ -Alkane areas normalised to Hexadecane for a range of Speeds and Loads	159

### Chapter 5 - Secondary Nitro- & Oxy-PAC Emissions

5.1 Nitro-PAC emitted from the Prima Engine at different engine conditions	178
5.2 Previous Nitro-PAC levels from Light-Duty Diesel Engines	183
5.3 Previous Nitro-PAC levels from Medium- & Heavy-Duty Diesel Engines	184

### Chapter 6 - Final Discussions, Conclusions, & Future Work

6.1 Overview of the Emissions Profiling Research Programme	215
--	-----

## List of Plates

Plate 1 The spray head attachment used to evenly disperse the solvents with the oncoming exhaust	77
Plate 2 The transfer line from the engine to TESSA	77
Plate 3 The overall engine test bay, showing the upgraded TESSA	78

# **Chapter 1 - Introduction**

## **1.1 The Emergence of High Speed Passenger Car Diesels**

The development of the diesel engine relies to a large extent on the greater thermal efficiency associated with compression-ignition compared with spark-ignition (SI) used for petrol engines (Amann *et al.* 1980, Haddad 1984, Kamimoto & Kobayashi 1991, Schindler 1992, and Poulton 1994). The improved fuel economy of a diesel relative to a similarly powered SI engine, in the region of 25% to 40% greater (Hillier 1991, Schindler 1992, and QUARG 1993), results from the higher compression ratios and varying only the fuel supply to produce the power (Hillier 1991 and Stone 1992). The mixing of fuel and air in the carburettor generates large pumping losses at low loads for SI engines (Stone 1992). The difference in fuel economy is greatest under urban driving conditions, where high air:fuel ratios are encountered (Andrews 1986 and Poulton 1994) (Figure 1.1).

Commercial vehicle operators have long recognised the efficiency and reliability of the diesel engine, resulting in diesel engines being used to power heavy goods vehicles (HGV), buses, coaches, tractors, taxis, and light vans (Fukuda *et al.* 1992 and QUARG 1993). The diesel engine used for commercial use was the open chamber or direct injection (DI) configuration (Figure 1.2a). The fuel is injected directly into the chamber shortly before top dead centre (TDC) whereupon the temperature of the compressed gases is sufficient to initiate combustion. The necessary air motion, termed swirl, for efficient combustion is generated from the chamber bowl and air inlet design.

Up until the mid-1980s only indirect injection (IDI) diesels were used in passenger cars (Figure 1.2b). Fuel injected into the hot pre-chamber region is rapidly atomized and combusted. The combustion generates high swirl and carries the remaining fuel charge into the main chamber whereupon combustion is completed. Compared to the traditional heavy-duty DI system, the IDIs produced a smoother power delivery and were able to operate over a wider speed range.

Early diesels were noisy, smelly, and much less responsive than SI engines, and also suffered from cold start problems (Langley 1991 and Hillier 1991).

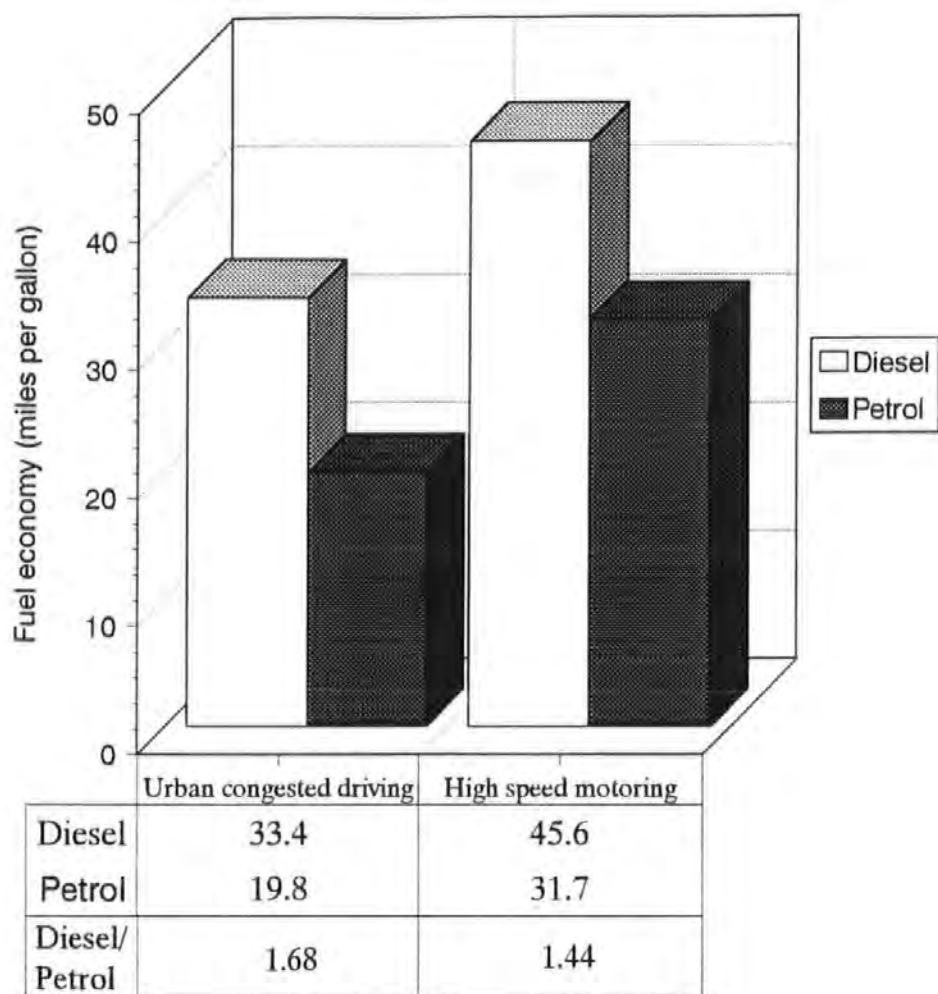


Figure 1.1 The superior fuel economy of diesel engines compared with petrol engines, especially for urban driving. (Andrews 1986)

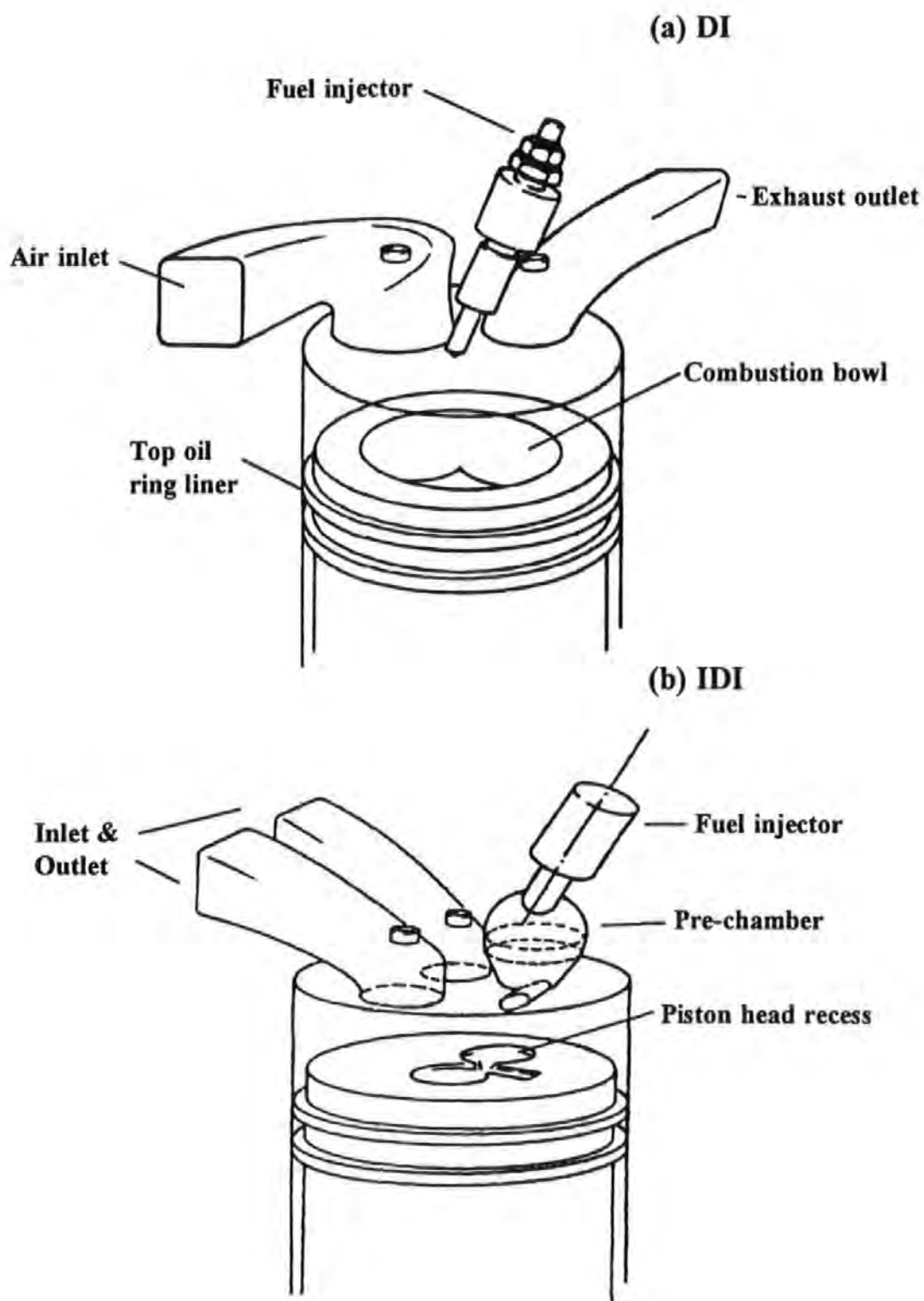
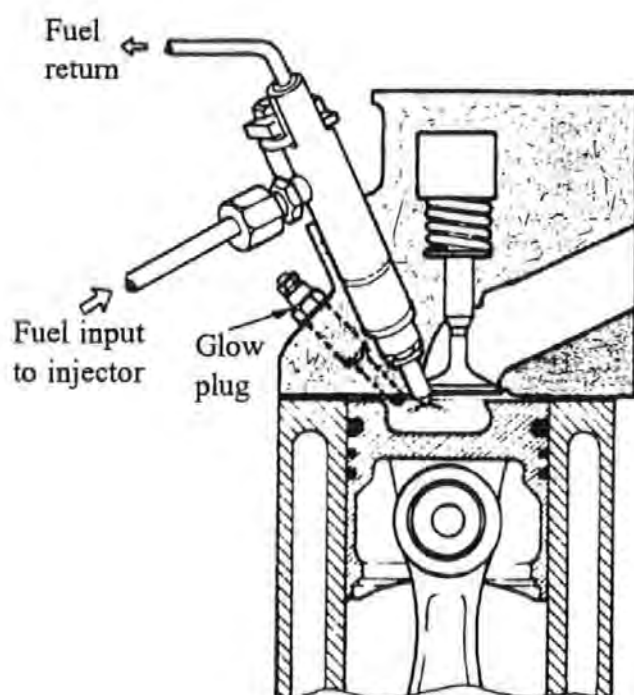


Figure 1.2 The configuration of direct injection (DI) and indirect injection (IDI) combustion chambers. (Monaghan 1981)

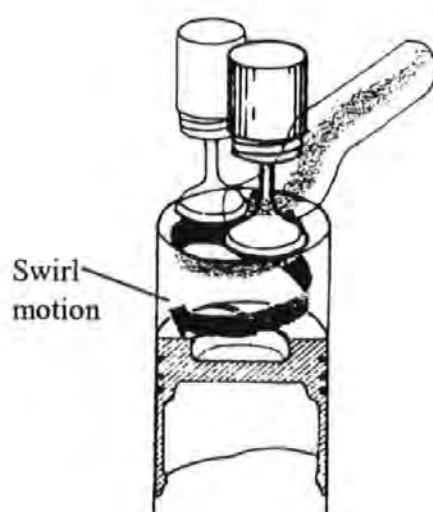
The power output is increased by upgrading the naturally air aspirated system to a turbocharged inlet system, in which a greater density of air molecules are forced into the chamber, thus enabling more fuel to be burned (Lilly 1984).

The IDI design suffers from large heat losses through the pre-chamber at high speeds, reducing the fuel economy closer to that of SI counterparts (Monaghan 1981, Nahum 1989, and Hillier 1991). The problems associated with the IDIs led to the development of high speed direct injection (HSDI) diesel engines for passenger cars (Monaghan 1981, Nahum 1989, Hillier 1991, Belardini *et al.* 1993, and Horrocks 1993). One example of an advanced HSDI diesel suitable for light-duty applications is the Prima engine developed by the Perkins Group, United Kingdom (UK) (Figure 1.3a). The bowl-in-piston combustion cavity combined with the helically shaped air inlet port enables high speed rotary swirl to be generated (Figure 1.3b), resulting in high power and good fuel economy up to a rated speed of around 4500 rpm (Hillier 1991).

The improved performance of the HSDI diesel engines combined with the fiscal benefits of diesel motoring has led to increased market penetrations in most European countries. For example, the market penetration of diesel cars increased from around 5% in 1988 to nearly 20% in the Autumn of 1993 within the UK market (QUARG 1993), and in France diesels have reached 40% of the market share (Kerswill 1992). The increasing popularity of the diesel engine in European countries is contrasted by almost no diesel sales in the United States (US) (Henk *et al.* 1992). This is largely due to the very stringent particulate legislation implemented in the US by the Environmental Protection Agency (EPA). The increasing proportion of passenger cars utilizing diesel engines in the European markets makes an environmental assessment of diesel emissions increasingly necessary.



(a) Perkins Prima DI combustion chamber



(b) High-speed rotary swirl produced by inclined air inlet port

Figure 1.3 The Perkins Prima high speed direct injection (HSDI) engine. (Hillier 1991)



## 1.2 Environmental Impact of Diesel Emissions

The higher thermal efficiency of the diesel engine results in much less gaseous carbon monoxide (CO) and hydrocarbons (HC) than equivalent powered SI engines (Williams *et al.* 1989, Stone 1992, and QUARG 1993). The higher fuel economy and corresponding lower greenhouse gases per mile travelled may help to reduce global warming (Hammerle *et al.* 1991, Springer 1991, Schindler 1992, and QUARG 1993). However, the higher density of diesel fuel and the possible warming effects of the particulates emitted from diesels may narrow the difference between the contributions of diesel and SI engines to global warming (QUARG 1993). The diesel engine can also run on a much wider selection of fuels compared to SI engines (Shore 1986, Ziejewski *et al.* 1991, Zeijewski & Goettler 1992, Amann 1993, and Shay 1993).

On the negative side, diesels emit more particulates than similar SI engines (Fukuda *et al.* 1992). The QUARG report (1993) on diesel emissions in the urban environment, estimated that diesel particulates contribute as much as 87% of the total particulates in an urban environment such as London. The particulates soil buildings, reduce visibility, whilst also affecting atmospheric conditions (El-Shobokshy 1984, Trijonis 1984, Richards *et al.* 1986, Ball 1987, Hamilton & Mansfield 1993, and QUARG 1993). The sub-micron size of the particles allows deep penetration of the human respiratory systems (Cuddihy *et al.* 1984, Scheepers & Bos 1992a, and Seaton *et al.* 1995). The health aspects of the particulates is of great concern, since recent research suggests that the small size of the particles may in themselves cause heart and lung problems, and exacerbate breathing disorders, such as asthma (Wade & Newman 1993 and Seaton *et al.* 1995).

The high surface area of carbon particles facilitates adsorption and condensation of organic compounds present in the gas phase, providing a medium for HCs to be transported deep into the human body. An indication of the complexity of the organic fraction of diesel exhaust is given in Table 1.1. The polycyclic aromatic compounds (PAC) have received a great deal of attention since some PAC are established carcinogens in laboratory tests (IARC 1989).

Table 1.1 Chemical compounds and species found in diesel emissions

Gas phase	Particulate Phase
Acrolein, ammonia	Heterocyclics and derivatives <sup>1</sup>
Benzene, 1,3-butadiene	Hydrocarbons (C <sub>14</sub> -C <sub>34</sub> ) and derivatives <sup>1</sup>
Formaldehyde, formic acid	Polycyclic aromatic compounds
Heterocyclics and derivatives <sup>1</sup>	
<sup>1</sup> Hydrocarbons (C <sub>1</sub> -C <sub>18</sub> ) and derivatives	
Hydrogen cyanide, hydrogen sulphide	
Methane, methanol	
Nitric acid, nitrous acid, oxides of nitrogen	
Polycyclic aromatic compounds	
Sulphur dioxide	
Toluene	

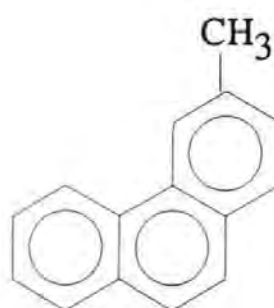
<sup>1</sup> Derivatives include acids, alcohols, aldehydes, anhydrides, esters, ketones, nitriles, quinones, sulphonates and halogenated and nitrated compounds, and multi-functional derivatives.

(Adapted from IARC 1989)

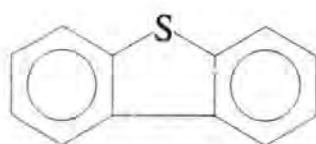
The PAC are sub-divided into different chemical classes, such as polycyclic aromatic hydrocarbons (PAH), alkyl-PAC, sulphur containing PAH (PASH), nitrogen containing PAH (PANH), and nitro- and oxy-PAC (Figure 1.4). There has been a great deal of research into whether the levels of PAC emitted from diesel engines are harmful, and these studies are reviewed by Schenker 1980, Grasso *et al.* 1988, IARC 1989, Scheepers & Bos 1992a, Stöber 1992, and Kingston 1994. Table 1.2 indicates the relative contributions of different sub-classes of PAC and the relative carcinogenic potencies. The table illustrates the extent to which the chemical structure influences the carcinogenicity, such that 6-methylchrysene is much less potent than 5-methylchrysene (Melikian *et al.* 1983). Some members of the nitro-PAC group are extremely hazardous in both mutagenic and carcinogenic testing (Beland *et al.* 1981, Mermelstein *et al.* 1981, Pederson & Siak 1981, Salmeen *et al.* 1982, Andrews *et al.* 1983, Rosenkranz & Mermelstein 1983, Wei & Shu 1983, Ohgaki *et al.* 1984, Tokiwa & Ohnishi 1986, and IARC 1989).



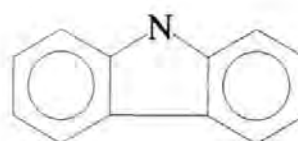
Naphthalene (PAH)



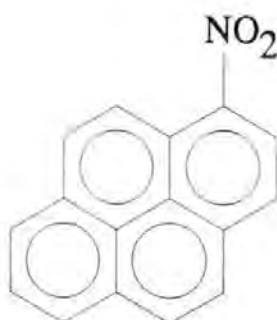
1-Methylphenanthrene (Alkyl-PAH)



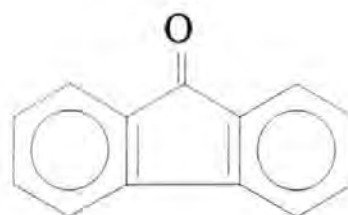
Dibenzothiophene (PASH)



Carbazole (PANH)



1-Nitropyrene (Nitro-PAC)



Fluoren-9-one (Oxy-PAC)

Figure 1.4 Structures of polycyclic aromatic compounds (PAC) common to diesel emissions.

Table 1.2 Carcinogenicity associated with different PAC Classes

Compound	Class	Carcinogenicity in animals	Carcinogenicity group
Fluorene	PAH	I	3
Phenanthrene	PAH	I	3
Anthracene	PAH	I	3
Pyrene	PAH	I	3
Chrysene	PAH	L	3
Benz( $\alpha$ )pyrene	PAH	S	2A
5-Methylchrysene	Alkyl-PAH	S	2B
6-Methylchrysene	Alkyl-PAH	L	3
1-Nitronaphthalene	nitro-PAC	I	3
2-Nitrofluorene	nitro-PAC	S	2B
1-Nitropyrene	nitro-PAC	S	2B
6-Nitrochrysene	nitro-PAC	S	2B
1,3-Dinitropyrene	nitro-PAC	L	3
1,6-Dinitropyrene	nitro-PAC	S	2B

I, inadequate evidence; L, limited evidence; S, sufficient evidence; 2A, Group 2A - the agent is probably carcinogenic to humans; 2B, Group 2B - the agent is possibly carcinogenic to humans; 3, Group 3 - the agent is not classifiable to its carcinogenicity to humans  
(Adapted from IARC 1989)

Oxy-PAC and polar PAC are also possible candidates for the mutagenicity and carcinogenicity associated with diesel extracts, although less information is available on which specific compounds are responsible (Scheepers & Bos 1992a). Some oxy-PAC, such as fluoren-9-one, are non-mutagenic, whereas others, such as benzo( $\alpha$ )pyrene-3,6-quinone and 9,10-phenanthrenequinone are mutagenic in Ames testing (Scheepers & Bos 1992a).

The International Agency into Research on Cancer (IARC) classified diesel exhaust as a probable carcinogen in 1989 (Group 2A), and in 1994 Pfeffer established a correlation between diesel engine emissions and the carcinogenic risk in traffic-related sites in Germany. The PAC content of diesel particulates may have been an important factor in the IARC carcinogenic classification of diesel exhaust and the findings of Pfeffer.

The other emission problem associated with diesel engines is the production of higher quantities of oxides of nitrogen, termed NO<sub>x</sub>, compared to SI engines. This is particularly relevant at the high load and speed working conditions for HGV transport travelling along motorways. The QUARG report (1993) estimated that 43% of the NO<sub>x</sub> in London was attributable to diesel engines. The NO<sub>x</sub> is emitted primarily as nitric oxide (NO), which is then later oxidised to nitrogen dioxide (NO<sub>2</sub>) in the environment (Kuhler *et al.* 1994 and Rudolf 1994). At high ambient levels NO<sub>2</sub> can cause health problems and NO<sub>x</sub> contributes to the formation of photochemical oxidants, acid deposition and the global warming (QUARG 1993). The NO<sub>x</sub> content of the combustion chamber and the exhaust may be of significance to the formation of the hazardous nitro-PAC emissions (Section 1.4).

### 1.3 Legislation and Control of Diesel Emissions

European legislation has come a long way from 1963 when smoke emissions from diesel vehicles were visually appraised by a panel of experts (Ball 1982). Vehicle legislation now requires certification of new engine designs over a set of specified driving conditions or cycle followed by derogation testing later in the vehicle's usage. The present European legislation covers the emissions of HCs, CO, NO<sub>x</sub>, and particulates (Table 1.3). The inclusion of a division in Stage II between DI and IDI engines arises from the HSDI engines producing as much as three times more NO<sub>x</sub> and HCs, and two times more particulates than IDIs (Belardini *et al.* 1993).

Table 1.3 Diesel Engine Passenger Car European Legislation

Legislation	Year for approval	CO g/km	HC + NO <sub>x</sub> g/km	Particulates g/km
91/444/EEC	1991	2.72	0.97	0.14
Stage 2 - IDI - DI	1996/7	1.0	0.7	0.08
		1.0	0.9	0.10
Stage 3	2000	0.5	0.5	0.04

(Adapted from Horrocks 1993)

The proposed tighter limits to control particulates and NO<sub>x</sub> are regarded as particularly difficult to meet (Poulton 1994). This is due to measures, such as fuel injection retardation, aimed at reducing the high temperature pre-mixed combustion phase associated with NO<sub>x</sub> production, resulting in an increased diffusion burning phase within which particulates tend to form, and *vice versa* (Signer & Steinke 1987 and Horrocks 1993) (Figure 1.5).

Exhaust gas recirculation in which a degree of the exhaust is mixed with the fresh air entering the chamber, results in less oxygen available for combustion, and culminates in lower NO<sub>x</sub> emissions (Amstutz & Del Re 1992). Improved combustion chambers can reduce both NO<sub>x</sub> and particulates (Konno *et al.* 1992b & 1993), as can pilot two-stage and electronic fuel injection (Signer & Steinke 1987 and Shakal & Martin 1990). Post-combustion after-treatment using reductive catalysts can be used to lower NO<sub>x</sub> (Konno *et al.* 1992a and Davies *et al.* 1993), whilst flow-through oxidation and particle traps can be used to reduce particulates (Signer & Steinke 1987, Henk *et al.* 1992, and Davies *et al.* 1993). Such post-combustion techniques are in the early stages of development with regards to light-duty passenger diesels (Andrews & Gibbs 1993, Davies *et al.* 1993, and Zelenka & Herzog 1993). Increasingly computer technology is being used to control the different emission control systems, allowing the optimum conditions for the lowest emissions to be achieved at varying engine conditions (French 1987, Carroll 1991, Bazari & French 1993, and Ladommatos *et al.* 1993).

Recently, legislators in the US and Sweden have imposed tight limits on the aromatic contents of diesel fuels in an attempt to lower particulate emissions (Cooper *et al.* 1993 and Nikanjam 1993). The introduction of new fuel blends enables the benefits to be realised for all the vehicles on the road, whilst engineering improvements take time to filter down into the car market.

Presently, no legislation covers the emissions of PAC. However, increasingly studies of the urban environment are identifying the presence of PAC derived from diesel engines (Viras *et al.* 1990, Aceeves & Grimalt 1993, Escrivá *et al.* 1994, and Pfeffer 1994), providing pressure on governments and legislators to evaluate the hazard associated with PAC.

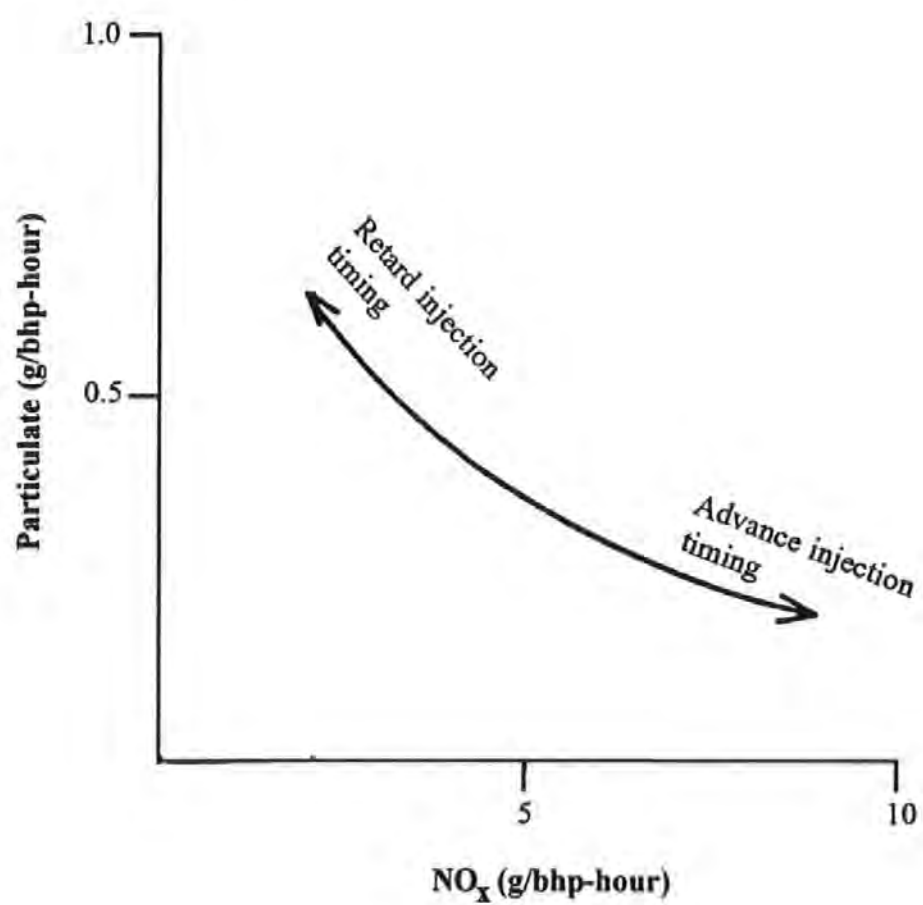


Figure 1.5 The trade-off between emissions of particulate and oxides of nitrogen ( $\text{NO}_x$ ).  
(Kamimoto & Kobayashi 1991)

It follows that an understanding of the combustion and formation of organic emissions, especially the hazardous nitro- and oxy-PAC, from diesel engines would enable control strategies to be employed were PAH legislation to be introduced. As it is, the increasingly tighter particulate emissions require the organic contribution to be assessed and if possible reduced to lower the particulate mass collected as a whole.

#### 1.4 Diesel Combustion and the Formation of Organic Emissions

The diesel engine works by using four cycles to draw air into the cylinder, compress the air to generate high cylinder temperatures, inject and combust the fuel, and finally discharge the chamber contents (Figure 1.6). The combustion phase itself can be separated into three stages; the ignition delay, pre-mixed uncontrolled combustion, and controlled or diffusive periods (Amann & Siegl 1982 and Kamimoto & Kobayashi 1991). During the ignition delay the fuel is heated, vaporised and mixed with the swirling air. Chemical reactions occur, such as pyrolysis and/or partial oxidation of the fuel. Combustion is initiated in the areas where the air:fuel ratio relative to the ideal mix or stoichiometric ratio, termed the equivalence ratio ( $\phi$ ), is close to unity<sup>1</sup> (Stone 1992). The ignition occurs in many places and there follows a rapid pressure rise due to the uncontrolled combustion of the fuel (Schindler 1992). Following the rapid uncontrolled combustion period, the remainder of the fuel must be injected, and in the case of full load the remaining fuel constitutes a considerable amount of the total fuel injected. During this diffusive phase of combustion a range of equivalence ratios, ranging from fuel rich at the flame core to fuel lean at the spray edges, are generated (Figure 1.7). Compounds will only be completely combusted if they exist within certain equivalence limits, termed the flammability limits. The upper flammability limit ( $\phi_R$ ) refers fuel rich zones, whereas the lower limit ( $\phi_L$ ) equates to fuel lean areas (Stone 1992).

---

<sup>1</sup>Equivalence ratio ( $\phi$ ) = stoichiometric air:fuel ratio / actual air:fuel



## Key

In. = Air inlet

Ex. = Exhaust outlet

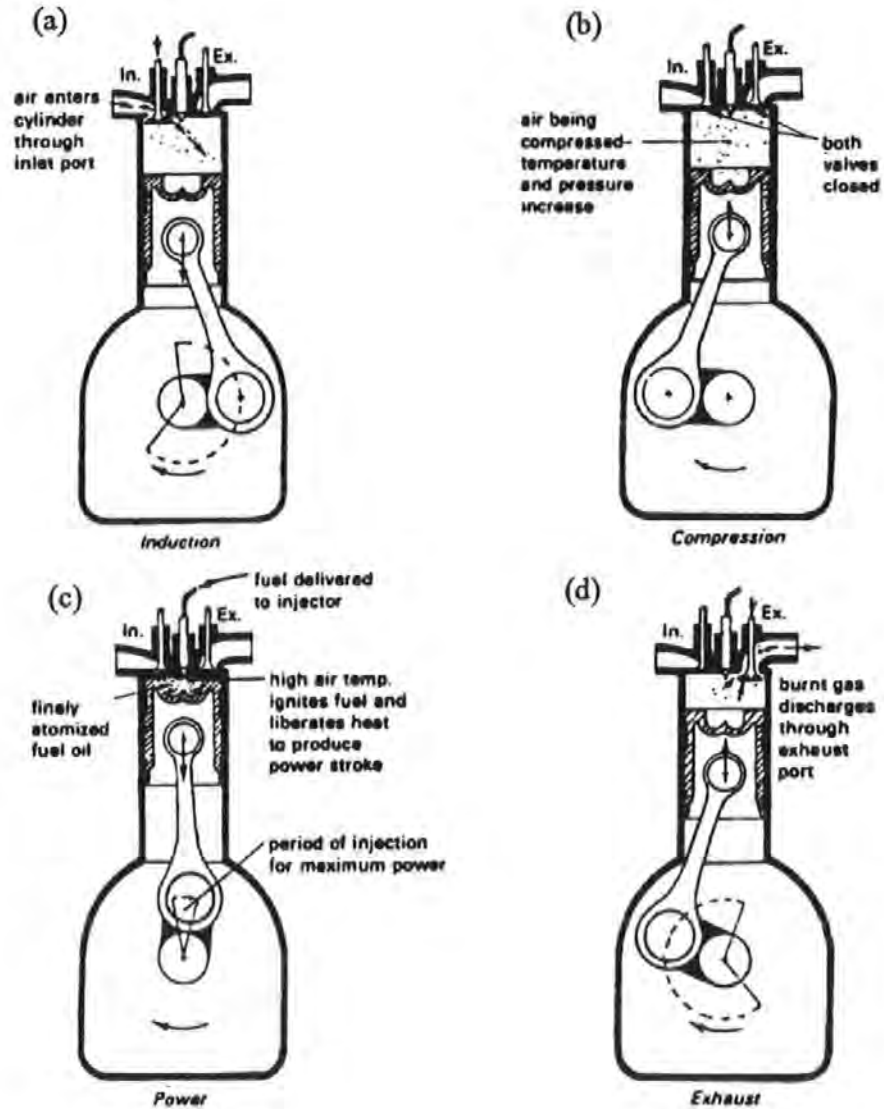


Figure 1.6 The four cycles of the diesel engine, consisting of the induction (a), compression (b), power (c), and exhaust (d) stages. (Hillier 1991)

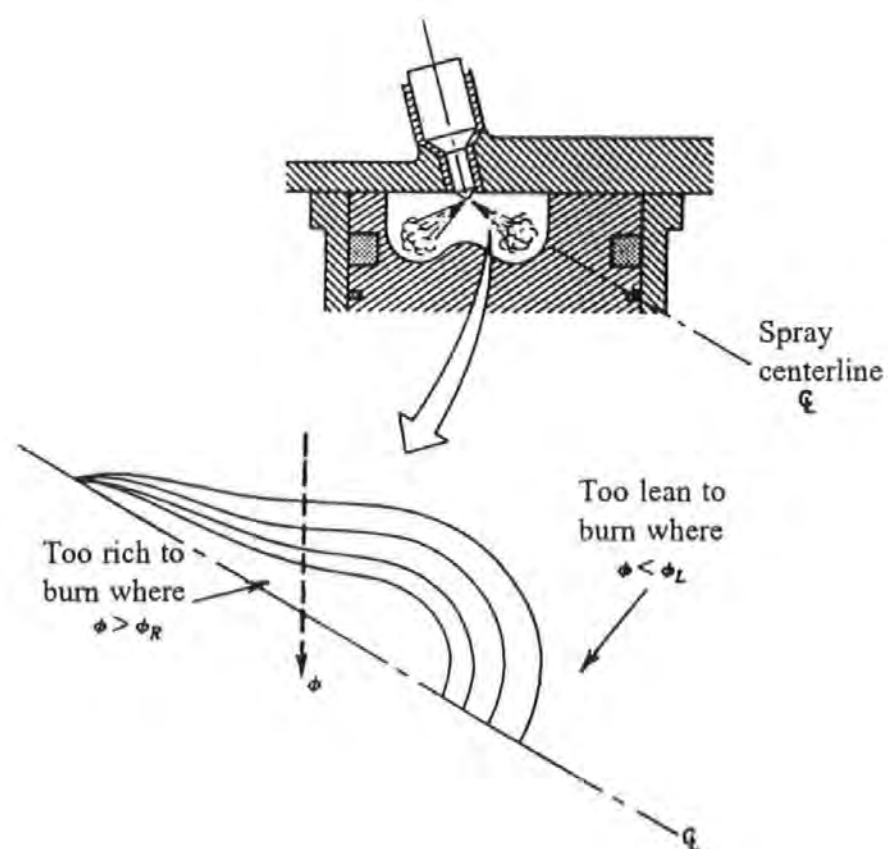


Figure 1.7 Axisymmetric idealization of a diesel fuel spray. The lower section of the figure shows the lines of constant equivalence ratio (stoichiometric air:fuel ratio / actual air:fuel ratio, denoted by  $\phi$ ). The areas of the fuel spray corresponding to the rich and lean flammability limits are indicated. (Ferguson 1986)

The organic fraction of the particulates are derived from organics in the gas-phase adsorbing and condensing onto the particulates during the expansion and exhaust strokes. The origin of the primary organics leaving the combustion chamber are derived from:

- 1) Survival of organics.
- 2) Combustion generation of organics.

The first source is derived from fuel and lubricating oil surviving combustion and entering the exhaust. Standard diesel fuel is removed from the distillation process between 160°C - 390°C and contains predominately aliphatic hydrocarbon chains of 9-28 carbon atoms (IARC 1989 and Scheepers & Bos 1992b). The fuel also contains a range of PAC, mostly 2-4 ring PAH and their alkyl-derivatives (Williams *et al.* 1986 & 1989, Nelson 1989, Bundt *et al.* 1991, and Trier *et al.* 1991). Fuel 'packets' mixed outside of the flammability limits may survive combustion and enter the exhaust (Andrews *et al.* 1983 and Williams *et al.* 1989). Similarly lubricating oil leakages, containing scavenged organics, add to the particulates by surviving combustion intact (Williams *et al.* 1987).

The second source is from combustion generation; either by pyrosynthetic reactions or by pyrolysis of the fuel/oil components (Badger *et al.* 1964, Howard & Longwell 1983, Cole *et al.* 1984, Williams *et al.* 1989, and Trier *et al.* 1990 & 1991). Pyrosynthetic reactions have been linked with the formation of particulate, and PAC may be a by-product of the process (Calcote 1981, Smith 1981, Serageldin 1981, Howard & Longwell 1983, Williams *et al.* 1989, and Burtscher 1992). The pyrosynthetic reactions take place inside the flammability limits whereas pyrolysis occurs in fuel rich or low temperature areas (Williams *et al.* 1989). Evidence for combustion generation can be masked by fuel/oil survival effects. Nelson (1989) concluded that since the major aromatic species in diesel exhaust, phenylacetylene, styrene, naphthalene, methylnaphthalenes, and acenaphthene, were not in the fuel they were a result of combustion generation. More recently, carbon 14 (<sup>14</sup>C) experiments by both Pemberton (1995) and Tancell (1995) have established the exact combustion generation contribution to specific PAC. For example, Tancell *et al.* (1995a) determined that of the benz(α)pyrene emitted from a light-duty DI diesel engine *ca.* 20%. was derived from combustion generation.

The emission of the primary organics can further react with surrounding oxygen and  $\text{NO}_x$  to form secondary emissions, such as nitro- and oxy-PAC. In the case of nitro-PAC, formation is by nitration of PAH and PANH. Formation mechanisms for nitro-PAC have been proposed by reactions with NO and  $\text{NO}_2$  within the combustion chamber and by reactions with  $\text{NO}_2$  in the presence of nitric acid in the exhaust (Scheepers & Bos 1992b). Sump oil has been shown to accumulate nitro-PAC, although evidence for the oil contributing to nitro-PAC emissions has not been proved (Jensen *et al.* 1986). The excess air and high temperatures involved with diesel combustion favour the oxidation of hydrocarbons, forming oxy-PAC such as fluoren-9-one (Schuetzle *et al.* 1981 and Choudhury 1982).

Organic emissions can also originate from engine and/or exhaust deposits (Abbass *et al.* 1988), and also from the engine sampling system itself. This is particularly relevant to secondary emissions, such as nitro- and oxy-PAC, for which transformations of PAH can occur on the filter used to collect the particulates (Section 2.1).

To reduce the contribution of both survival and combustion/exhaust generation to diesel emissions may require different technical approaches. In order to lower emissions, an understanding of the combustion of diesel fuel and subsequent organic emissions over a range of speeds and loads is needed.

### 1.5 Profiling of Organic Emissions from Diesels

Diesel combustion at a particular speed and load results in a wide range of fuel:air ratios and temperatures within the combustion chamber (Ferguson 1986). The fuel:air ratio ranges from infinite at the injector nozzle to less than unity in the swirling air zone beyond the edge of the flame front (Amann & Sieglä 1982). Similarly, the areas of the combustion chamber associated with the combustion ignition correspond to high peak gas temperatures, while areas further from the flame front, such as the crevice volume space between the top oil ring liner and the top of the chamber have much lower temperatures (Li 1982 and Signer & Steinke 1987). These two parameters of fuel:air interaction and temperature will be central to the organic emissions (Rubey *et al.* 1983 and Scheepers & Bos 1992b).

The time available for complete combustion will also be a factor in the combustion process (Rubey *et al.* 1983), with less reaction time existing at high speed compared with lower speeds (Zeijewski *et al.* 1991). The length and temperature of the exhaust section which the emissions travel may also effect the final composition of the exhaust entering the environment (Williams *et al.* 1985).

The combustion process will also be influenced by the type and configuration of diesel engine. The type of fuel injector, injection timing, aspiration (normal, turbocharged, or supercharged), and air inlet ports may all influence the combustion process (Scheepers & Bos 1992b and Poulton 1994).

Emission profiling, in which emissions from an engine are characterised over varying speeds and loads, enables the elucidation of relationships between the emissions and the outlined combustion factors to be achieved for a specific engine set-up. The results can be compared with other engines sampled in a similar way, and areas of significant emissions focused on. Similarly, as compounds are classified as potentially harmful to human health, the role of combustion and exhaust stages on such emissions can be followed with respect to speed and load. Those PAC, especially those possessing nitro- and oxy- groups, which constitute a health risk, require the levels of such compounds under different driving environments to be established. This is particularly important for the low load and low speed driving conditions associated with congested city centres.

It is of great importance that a detailed understanding of the formation pathways, including precursor compounds (some of which may be not be carcinogenic but crucial to the subsequent formation of compounds that are) which lead to high risk PAC are discovered. Information concerning the degree to which the combustion chamber or the exhaust section determines the PAC emissions under changing speeds and loads is vital for meaningful control strategies to be formulated, in anticipation of possible future PAH legislation.

The different engine sampling and analytical techniques involved with emission profiling and the previous profiling studies on diesel engines are reviewed in Chapter 2.

## **Chapter 2 - Review of Diesel Emission Profiling**

This chapter reviews the research to date on the chemical characterisation and profiling of organic emissions from diesel engines. The chapter is divided into three main sections. Firstly, the sampling, work-up, and analysis techniques required for the profiling to proceed are reviewed in Section 2.1. Previous studies on specific classes of organics are reviewed in Section 2.2. The shortcomings highlighted in the review lead to outlining the aims and objectives of this study in Section 2.3.

### **2.1 Review of Profiling Techniques**

There have been a number of reviews on the sampling and analytical techniques available for chemical characterisation of diesel emissions (Lee *et al.* 1981, Björseth 1983, Stenborg *et al.* 1983, White 1985, and Williams 1990). This review is aimed at highlighting those sampling and detection techniques most appropriate to comprehensive emission profiling. The section is divided into sampling (Section 2.1.1) and analytical techniques (Section 2.1.2).

#### **2.1.1 Sampling of Engines for Organic Emissions**

The standard method for sampling diesels, proposed by the US EPA, recommends sampling the exhaust following dilution. The method was devised to simulate the dilution processes following the exit of the exhaust into the environment (Schuetzle 1983). A typical dilution tunnel configuration is shown in Figure 2.1. The exhaust is diluted by a known ratio of air drawn through by the fan situated at the end of the tunnel. Dilution cools the exhaust and the sample is collected on filters. The recommended collection of 52°C on the filters determines the degree of dilution required for particular engines. The collection of gaseous phase compounds in the exhaust which are not trapped by the filter, can be collected on a chemical adsorbent trap behind the filter.

There are many forms of the dilution tunnel arrangements and each design can affect the mixing in the tunnel and reactions in the transfer of the exhaust to the tunnel (Williams *et al.* 1985 and Trier 1988).

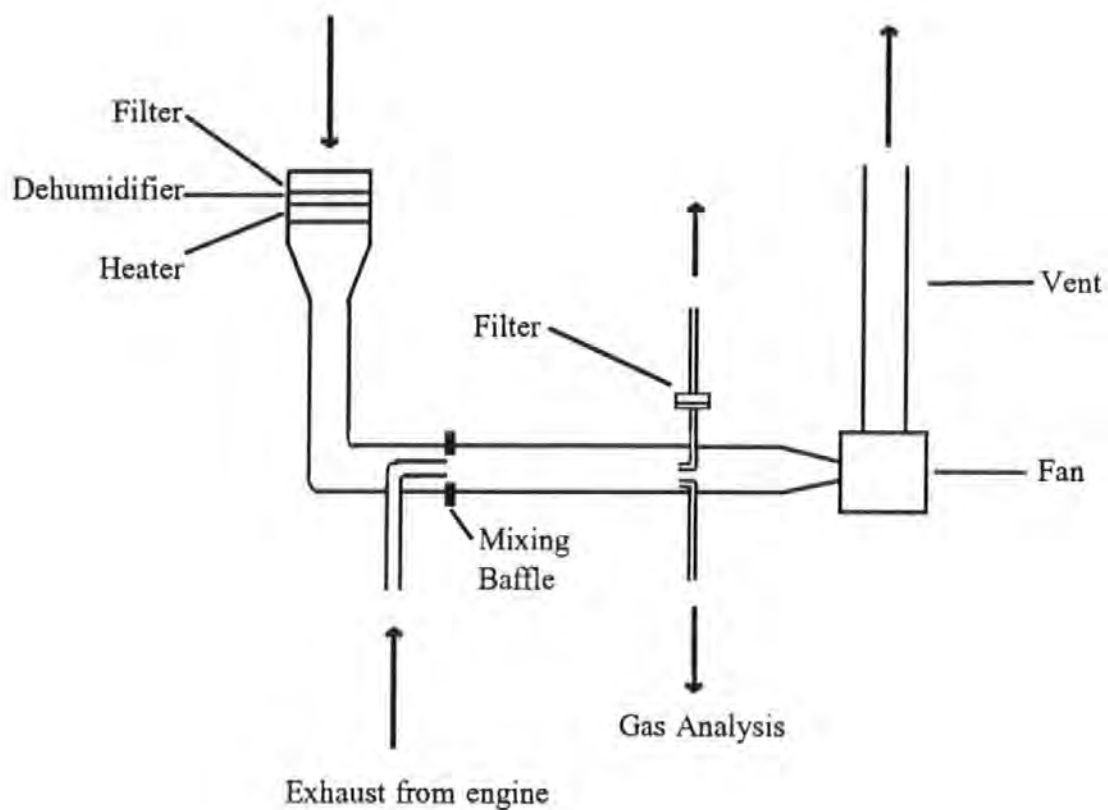


Figure 2.1 A typical dilution tunnel and filter collection engine sampling system.  
(Williams 1990)

An inherent problem associated with the system, is the possible reaction of organics held on the filter with the incoming gaseous stream (Duleep 1980, Lindskog 1983, Hartung *et al.* 1984, Chan & Gibson 1985, and Trier 1988). Laboratory exposure of filters and reactor vessels containing PAH to oxidising and nitrating agents have proved that transformations can occur (Jäger & Hanuš 1978, Pitts *et al.* 1978, and Hisamatsu 1986). Furthermore, the studies by Herr *et al.* (1982) and Lach & Winckler (1988) showed that the exposure of pyrene on filters to increasing higher exhaust NO<sub>2</sub> led to increasing 1-nitropyrene emissions.

The artefact potential for dilution tunnel/filter systems is exacerbated by the prolonged sampling times needed for adequate sample collection. For example, a common transient test cycle such as the US federal transient procedure (FTP) lasts for 23 minutes and may result in a organic extract weight of *ca.* 50 mg (Bechtold *et al.* 1984). The lengthy sampling times not only present logistical problems in terms of collecting a range of replicated samples on the same day, but more importantly encourage artefact conversions of the sample on the filter. This is especially relevant for the analysis of trace nitro-PAC, where repeated runs may need combining in order to gain sufficient organic mass (Bechtold *et al.* 1984).

The other approach to diesel engine sampling is to directly sample the exhaust stream leaving the combustion chamber. Early systems suffered greatly from filter degradation at the high exhaust temperatures (Trier 1988). This led to cooling the exhaust by condensation methods before collection on filters (Stenburg *et al.* 1983), but the filter collection remained prone to artefact problems.

To overcome the problems associated with dilution and filter systems Petch with co-workers (1987) devised a sampling system which dispensed filter collection, termed the total exhaust solvent-stripping apparatus (TESSA). The system comprises a stainless steel tower into which the exhaust is transferred at the base (Figure 2.2). The organic component of the exhaust is rapidly extracted by the downward flow of solvent mix ((dichloromethane(DCM):methanol, 1:1)) entering at the top of the middle section. The interaction between the solvents and exhaust is encouraged on the glass tubing, which are packed into the middle tower section. The extracted organics are removed, in the solvents, from the base of the tower.



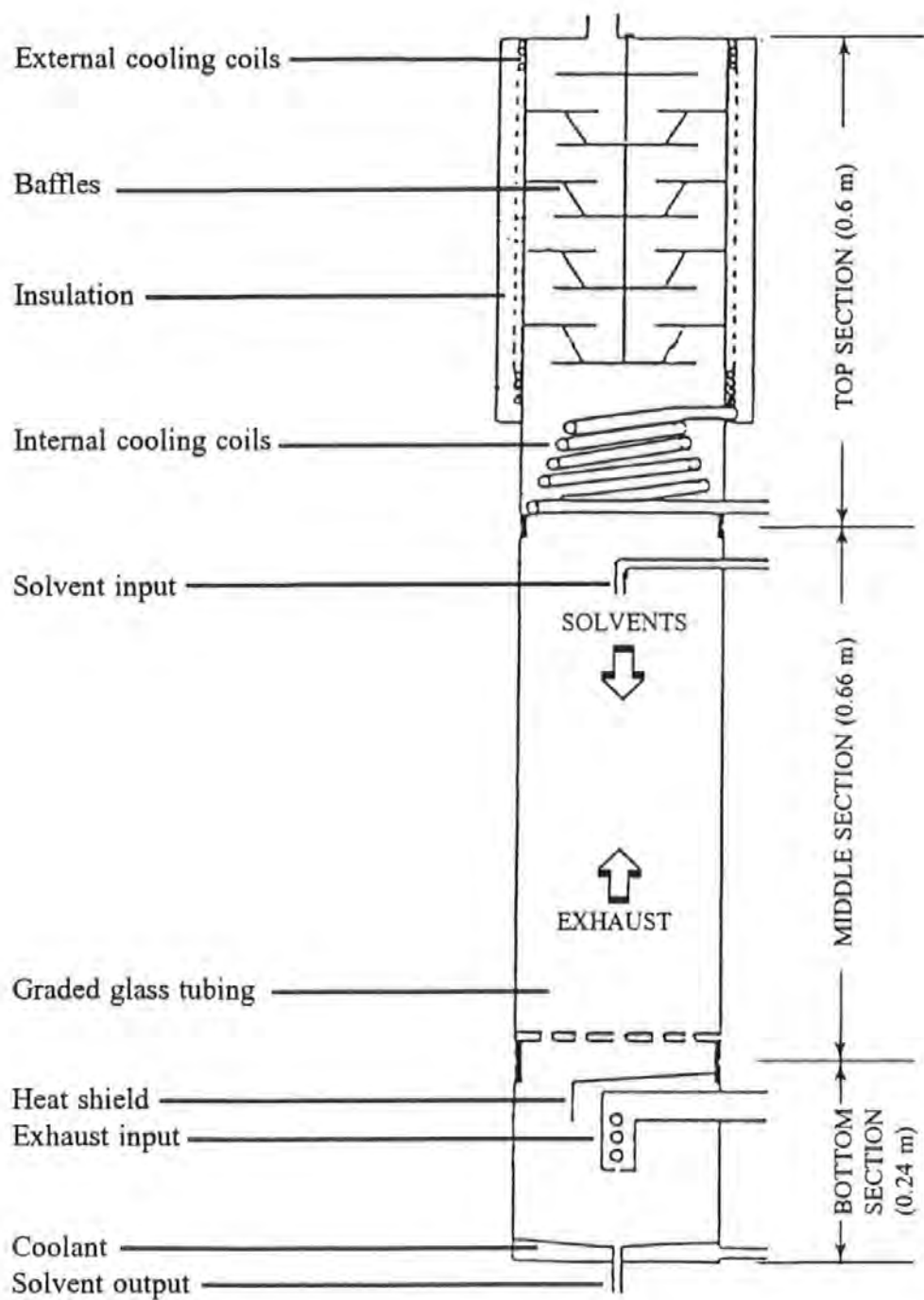


Figure 2.2 The total exhaust solvent-stripping apparatus (TESSA). (Trier 1988)

The tower is cooled at the top and bottom to reduce post-combustion reactions and enhance the condensation of the solvents. The system has a higher collection efficiency of gaseous organics than is possible with filters alone, and combines rapid sampling with low artefacts (Trier *et al.* 1988 and Rhead & Trier 1992).

The system devised by Kruzel *et al.* (1991) was similar in concept to TESSA, in that it extracted raw exhaust by passing the exhaust through three progressively cooled flasks containing DCM. The system designed for biological testing has the advantage of extracting a large organic mass rapidly combined with low artefact potentials, due to the very low collection temperatures (down to as low as -70°C in the last flask). The disadvantages of the system for rapid profiling work is the complexity of the work-up for the large volumes of DCM involved.

#### 2.1.2 Laboratory Work-up & Analytical Techniques for Organic Compounds

Following collection, samples require processing before the required chemical information of interest can be obtained. The degree of laboratory work-up and sophistication of the detection systems depend on the level of the analytes in the extracts; trace components require complicated work-up and sensitive/selective detectors. The majority of chemical characterization procedures follow an extraction (Section 2.1.2.1), fractionation (Section 2.1.2.2), and detection (Section 2.1.2.3) pathway.

##### 2.1.2.1 Extraction and Concentration of Organics

Following sampling, the organics collected on filters and adsorbent traps require extraction. The most common extraction techniques are those of soxhlet and ultrasonic extraction, with the former being more effective and the latter considerably quicker (6-8 hours compared with 30 minutes)(Williams 1990). Dichloromethane is an ideal candidate for such extractions, since it extracts 97% of the mutagenicity of diesel particles (Montreuil *et al* 1992). The extracted samples are termed the solvent-soluble organic fractions (SOF).

Engine sampling utilizing solvents as the collection medium dispense with soxhlet and ultrasonication extractions, and in the case of TESSA the samples are termed the TESSA extracted samples (TES).

#### 2.1.2.2 Fractionation of Organics

Following extraction and concentration, the more prominent compounds, such as the *n*-alkanes and two to four ring PAH, can be analyzed directly after extraction and concentration (Farrar-Khan *et al.* 1992). For detailed characterisation, the extract is fractionated into different chemical classes. There are many ways to achieve fractionations, with the degree of isolation required determining the complexity of the method. For compounds prominent in the extracts, fractionation commonly proceeds by employing silica gel packed into open glass columns (Yu & Hites 1981 and Williams *et al.* 1986) or solid-phase extraction cartridges (May & Wise 1984, Obuchi *et al.* 1984, Robbat *et al.* 1986, Theobald 1988, and Bundt *et al.* 1991). Other fractionation methods include liquid-liquid partitioning, for example with dimethylsulphoxide (Lee *et al.* 1981 and Henderson *et al.* 1984).

The analysis of minor exhaust constituents, such as nitro-PAC, commonly uses multi-step fractionation, involving a simple preliminary clean-up step, followed by semi-preparative normal-phase (NP) high-performance liquid chromatography (HPLC) (Levine & Skewes 1982, Liberti *et al.* 1984, Tong *et al.* 1984, Cicciooli *et al.* 1986, and Bayona *et al.* 1988). The complexity of HPLC fractionations are offset by isolating the specific elution window associated with the analytes, allowing a much greater concentration step.

#### 2.1.2.3 Detection of Organics

End analysis for organics is generally based on chromatographical techniques, and can be divided between HPLC and gas chromatographic (GC) systems. Chromatography is used to separate components of a sample, in which the components are distributed between two phases, one phase is stationary, whilst the other moves (Braithwaite & Smith 1985). As the compounds are carried over the mobile phase, there will be competition between the affinity to remain with the stationary phase and carry on with the mobile phase (Figure 2.3). Since, different compounds have varying distribution coefficients<sup>1</sup> between the two phases, separation of the mixture occurs.

---

<sup>1</sup> Distribution coefficient (D) = [stationary phase]/[mobile phase]

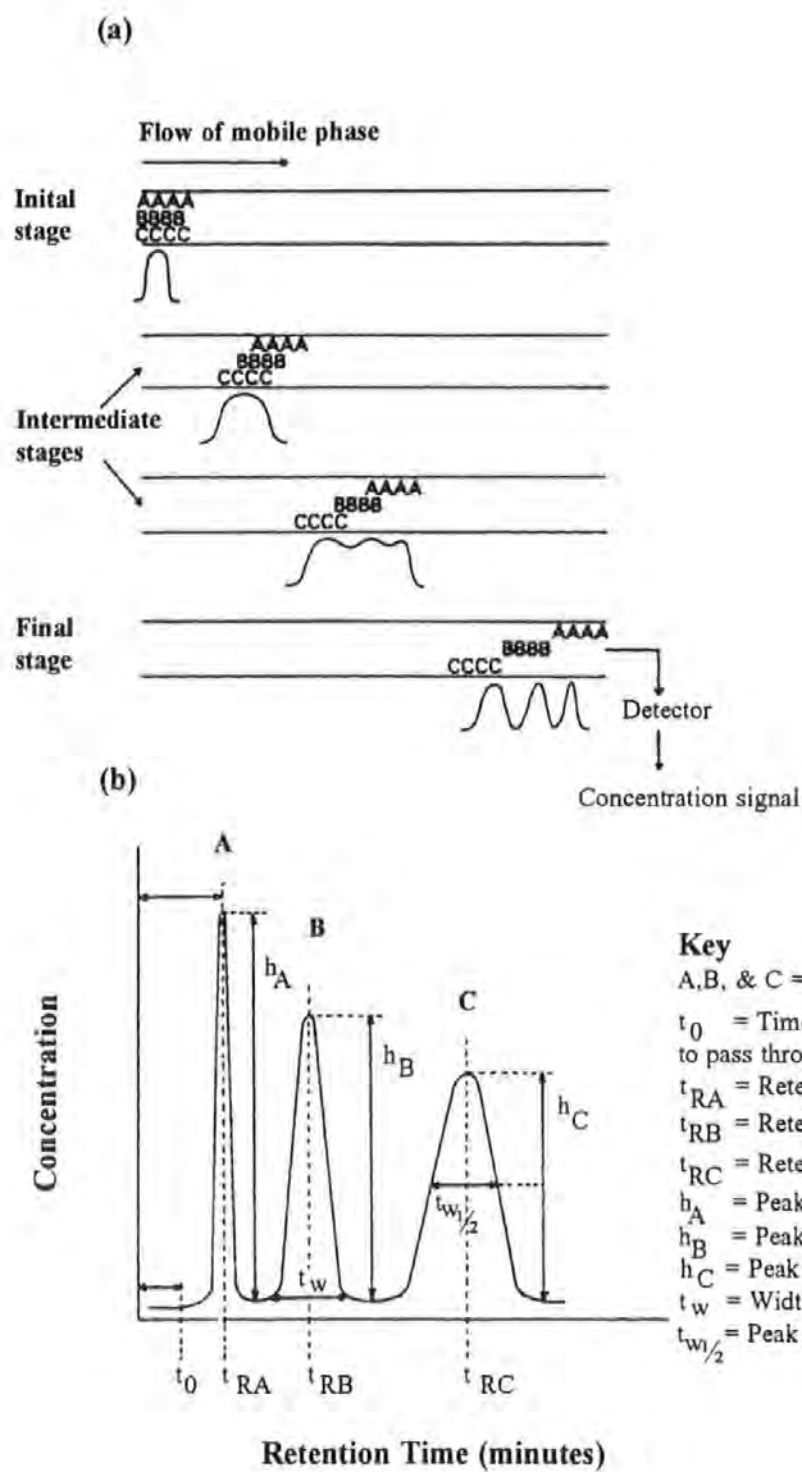


Figure 2.3 An idealised example of the chromatography for three model compounds (a) and the resulting chromatogram (b) (Braithwaite & Smith 1985)

The larger the distribution coefficient, the greater period of time will elapse before the compound is eluted, termed retention time, compared with a compound which has a smaller distribution coefficient. Once, the separation has occurred the individual components can be detected. The detection of the major constituents of diesel organic extracts, such as PAH and *n*-alkanes, are well established (Table 2.1).

Table 2.1 Detection systems for *n*-alkanes and major PAH

Detection system	Advantages	Disadvantages	References
Reverse phase (RP)-HPLC with UV detection	Fast analysis times, simple set-up	Resolution and alkanes undetected	Maher <i>et al.</i> (1989)
RP-HPLC with fluorescence	Greater selectivity than with UV	Same as UV	Hansen <i>et al.</i> (1991), Ganchanja (1993), and Williams <i>et al.</i> (1994)
GC with flame ionisation detection (FID)	High resolution, stable, large linear range	Low sensitivity and non-selective	Yu & Hites (1981), Niles & Tan (1989), Bundt <i>et al.</i> (1991), and Castello & Gerbino (1993)
Gas chromatography/mass spectrometry (GC/MS) in electron impact (EI) mode	Improved identification	Greater complexity	Hites (1989) and Farrar-Khan <i>et al.</i> (1992)

Minor constituents, such as nitro-PAC, require more selective and sensitive chromatographic systems (Table 2.2). Higher sensitivities can be achieved for the fluorescence and chemiluminescence detection if the nitro- group is reduced to the amino moiety. This can be achieved on-line with the HPLC system (Tejada *et al.* 1982, MacCrehan *et al.* 1988, and Liu & Robbat 1991), or off-line (Campbell & Lee 1984, Sellström *et al.* 1987, and Hayawaka *et al.* 1992). Derivatization techniques can be used to increase the selectivity and sensitivity of ECD, and GC/MS in both EI and NICI modes (Campbell & Lee 1984, Sellström 1987, and Scheepers *et al.* 1994). Selective ion monitoring also greatly increases sensitivity for GC/MS in EI and NICI modes (Ramdahl & Urdal 1982, D'Agostino *et al.* 1983, and Schneider *et al.* 1990). Gas chromatographic analysis, offers the greatest resolution.

Table 2.2 Detection systems for nitro-PAC

Detection system	Advantages	Disadvantages	References
RP-HPLC with fluorescence detection	Speed and selective	Resolution	MacCrehan <i>et al.</i> (1988), Tejada <i>et al.</i> (1986), Liu & Robbat 1991, and Veigl <i>et al.</i> (1994)
RP-HPLC with chemiluminescence detection	Sensitive and very selective	Resolution	Sigvardson & Birks (1984), Liu & Robbat 1991, and Li & Westerholm (1994)
RP-HPLC with electrochemical detector	Sensitive and large linear range	Interferences from carbonyl compounds	Rappaport <i>et al.</i> (1982), Jin & Rappaport (1982), and Galceran & Moyano (1993)
GC with electron capture detection (ECD)	Sensitive & good resolution	Limited linear range & prone to contamination	Oehme <i>et al.</i> (1982), Campbell & Lee (1984), and Draper (1986)
GC with nitrogen/phosphorus detection (NPD)	Highly selective	Baseline unstable	D'Agostino <i>et al.</i> (1983), Paputa-Peck <i>et al.</i> (1983), White <i>et al.</i> (1984), and Fetzer (1989)
GC with thermal energy analyzer (TEA)	Highly selective, similar responses	Prone to peak tailing & thermal degradations	Tomkins <i>et al.</i> (1984) and Yu <i>et al.</i> (1984)
GC/MS in EI mode	Distinctive spectra	Poor sensitivity	Schuetzle <i>et al.</i> (1982), Tong <i>et al.</i> (1984), and Ramdahl <i>et al.</i> (1985)
GC/MS in negative ion chemical ionisation (NICI) mode	Selective and highly sensitive. Provides molecular ion data	Limited spectra	Oehme <i>et al.</i> (1982), Newton <i>et al.</i> (1982), Ramdahl & Urdal (1982), and Bayona <i>et al.</i> (1988)
Mass spectrometry/mass spectrometry (MS/MS)	Highly selective	Complex instrumentation	Henderson <i>et al.</i> (1982) and Schuetzle <i>et al.</i> (1982)

However, the GC injection systems must be kept well maintained to prevent thermal decomposition, and hydrogen gas is not suitable as a carrier due to possible reductions of nitro-PAC to amino-PAC in its presence (Tong *et al.* 1983 and White 1985). Liquid chromatographic analysis have a faster sample throughput and do not suffer from the thermal

problems associated with some GC detection systems. Increasingly HPLC systems are being used to detect nitro-PAC, especially those employing fluorescence/chemiluminescence detection with on-line reduction (Li & Westerholm 1994 and Veigl *et al.* 1994). The technique of LC/MS is increasingly being used to identify the polar PAC present in diesel extracts (Galceran & Moyano 1994).

## 2.2 Review of Previous Profiling Studies

The review is primarily focused on naturally aspirated light-duty DI engines (capacity no greater than 2.5 l in total), however important findings from turbo, IDI and medium- and heavy-duty engine research are in some cases reported. The section is sub-divided into reviewing specific classes of organics, namely PAH (Section 2.2.1), alkanes (Section 2.2.2), nitro-PAC (Section 2.2.3), and oxy-PAC (Section 2.2.4).

The majority of the reported studies utilized dilution tunnel and filter collection engine sampling. As a consequence the chapter removes the engine sampling apparatus details, unless the dilution engine sampling technique affected the results or a different engine sampling system was employed. Details of the work-up and analytical techniques are also removed unless relevant to the extent to which the profiling progressed.

### 2.2.1 PAH Emission Profiling

The early investigations into the effect of engine conditions on organic emissions focused on PAH emissions, since compounds such as benzo( $\alpha$ )pyrene, were known carcinogens. The early investigations tended to compare SI engines with diesels, and IDI with DI fuel systems. The affect of fuel and oil compositions on the exhaust make-up was largely unconsidered.

Williams & Swarin (1979) compared the benzo( $\alpha$ )pyrene emissions from diesel engines with non-catalyst petrol powered engines. The averaged value of 2.7  $\mu\text{g}/\text{mile}$  (ranging from 0.29  $\mu\text{g}/\text{mile}$  to 5.3  $\mu\text{g}/\text{mile}$  for different vehicles) from the SI engines was similar to the 2.7  $\mu\text{g}/\text{mile}$  emission rate from the diesel.

Kraft & Lies (1981) sampled four light-duty diesels (1978 Models: Rabbit & Golf, 1979 Models: Passat & Audi) over the FTP, highway fuel economy test (HWFET) and the European regulation (ECE) driving cycles. The authors found the PAH emissions were lower for the hot start HWFET cycle compared with the cold start FTP and ECE cycles.

Zierock *et al.* (1983) compared PAH emissions from a 3.8 l DI engine to those from a 1.5 l IDI engine. The authors found the two injection configurations resulted in different emission patterns over a wide range of speeds and loads (Figure 2.4). The DI engine produced peak PAH concentrations at high and low loads with low speeds, whereas emissions were elevated at high speed and across the load range for the IDI.

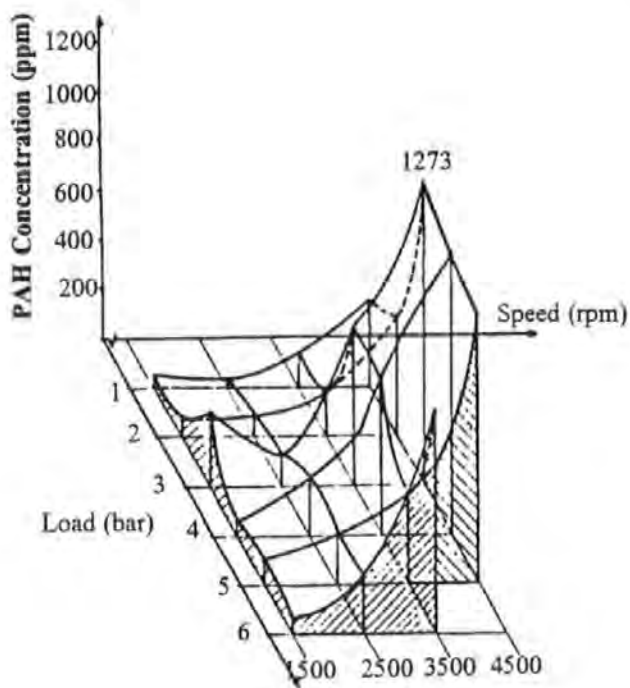
The study by Andrews *et al.* (1983) of a light-duty 2 l DI Petter AV1 diesel engine was one of the first studies to correlate the PAH in the exhaust to the PAH fuel content. The authors found that for a speed of 1500 rpm, the weight of emissions relative to the mass of fuel burned, decreased with increased load. For example, the emission of phenanthrene at low, mid, and high loads was 0.15 mg/kg, 0.06 mg/kg, and 0.04 mg/kg respectively. This suggests that the greatest combustion efficiency occurs at high loads for DI engines, and consequently that DIs are susceptible to poor combustion under low loads.

Jensen & Hites (1983) examined the effect of load (zero, half, and full) and injection timing on PAH and alkyl-PAH emissions for a Cummins single cylinder heavy-duty diesel. Injection timing did not influence the emissions; whereas load was shown to be inversely proportional to emissions. Hence, zero load produced the greatest concentration of PAH and alkyl-PAH emissions relative to the mass of particulate produced. Since the exhaust temperatures were found to be proportional to engine load, the results indicated that the emissions were greatest under low temperatures.

Mills *et al.* (1984) studied the effect of speed and load on the PAH emissions from a two cylinder light-duty Petter BA2 DI 1.2 l engine and expressed the emissions in terms of the mass of PAH emitted relative to the exhaust volume ( $\mu\text{g}/\text{m}^3$ ). The authors found at 2350 rpm the total PAH were high at low loads, reduced at mid load, and further increased once more at higher loads. Re-expressing the results relative to the fuel consumed, shows the highest PAH emissions associated with low loads.



(a) **IDI**



(b) **DI**

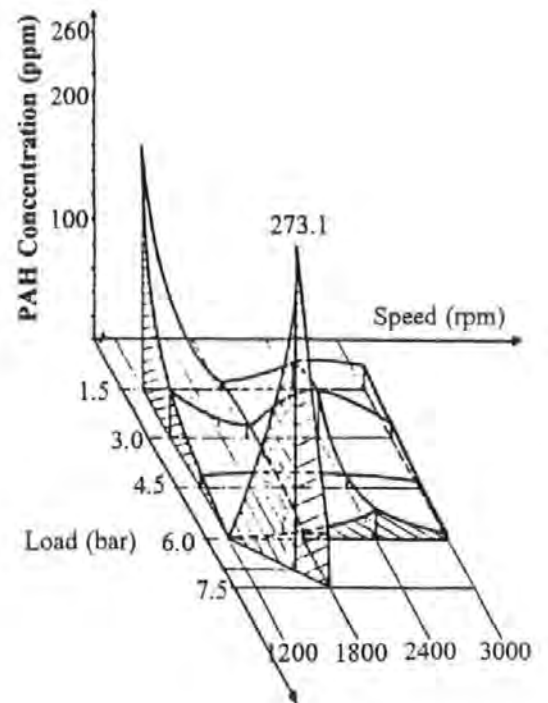


Figure 2.4 The effect of engine speed and load on the PAH emissions from IDI (a) and DI (b) diesels. (Zierock *et al.* 1983)

Shore (1984) reported that for light-duty diesels, the mass of emissions per unit time were a function of speed and load. At high and intermediate speed pyrene emissions decreased with raised loads, whereas at lower speeds, pyrene increased directly with load. Shore (1986) quantified the PAH emissions from a single cylinder Ricardo Hydra light-duty engine using DI and IDI versions, and for full and light loads with a selection of different fuel blends. For US standard diesel, the DI version emitted higher levels of benzo( $\alpha$ )pyrene at light load (5.2  $\mu\text{g}/\text{hour}$ ) compared with full load (2.4  $\mu\text{g}/\text{hour}$ ). In contrast, the IDI version produced the highest emissions at full load (4.6  $\mu\text{g}/\text{hour}$ ) relative to light load (3.3  $\mu\text{g}/\text{hour}$ ). The ratio of PAH recovered in the exhaust as a percentage of PAH in the fuel supplied to the chamber were higher for the DI at full load compared with the IDI, for the US standard fuel. For example, the recovery of chrysene with the DI was 0.36 % whilst only 0.05 % for the IDI. However, different fuels produced not only different recovery levels but also in some cases a reversal in trends for the DI and IDI comparison. The combustion of one fuel, very low in PAH, produced a exhaust recovery of 2351 % for benz( $\alpha$ )anthracene for the DI version and 5558 % for the IDI. This showed that sources other than fuel survival, most probably combustion generation, were responsible for the PAH emissions from that particular fuel blend.

Williams *et al.* (1986) sampled a Petter AV1 DI 2 l diesel at 1500 rpm for low, mid, and high loads. The reported survival of major PAH and alkyl-PAH, expressed as the percentage weight of PAC recovered in the exhaust relative to the weight of PAH supplied to the chamber, was significantly greater at low load. In contrast to Andrews *et al.* (1983), the survival of some PAH increased at high load relative to the mid-load position (Figure 2.5).

The two studies by Barbella *et al.* (1988 & 1989) investigated the effect of engine load on the PAH emissions at a speed of 2000 rpm. The emissions were expressed relative to the mass of fuel burned. The first study investigated the effect of four different fuels on the emissions from a heavy-duty turbocharged DI. For each fuel the engine was sampled at high and low air:fuel ratios ( $\alpha$ ) (Table 2.3). Generally, the PAH emissions were highest at low load (high  $\alpha$ ), except for fuels C & D, where the trend in some cases was reversed.

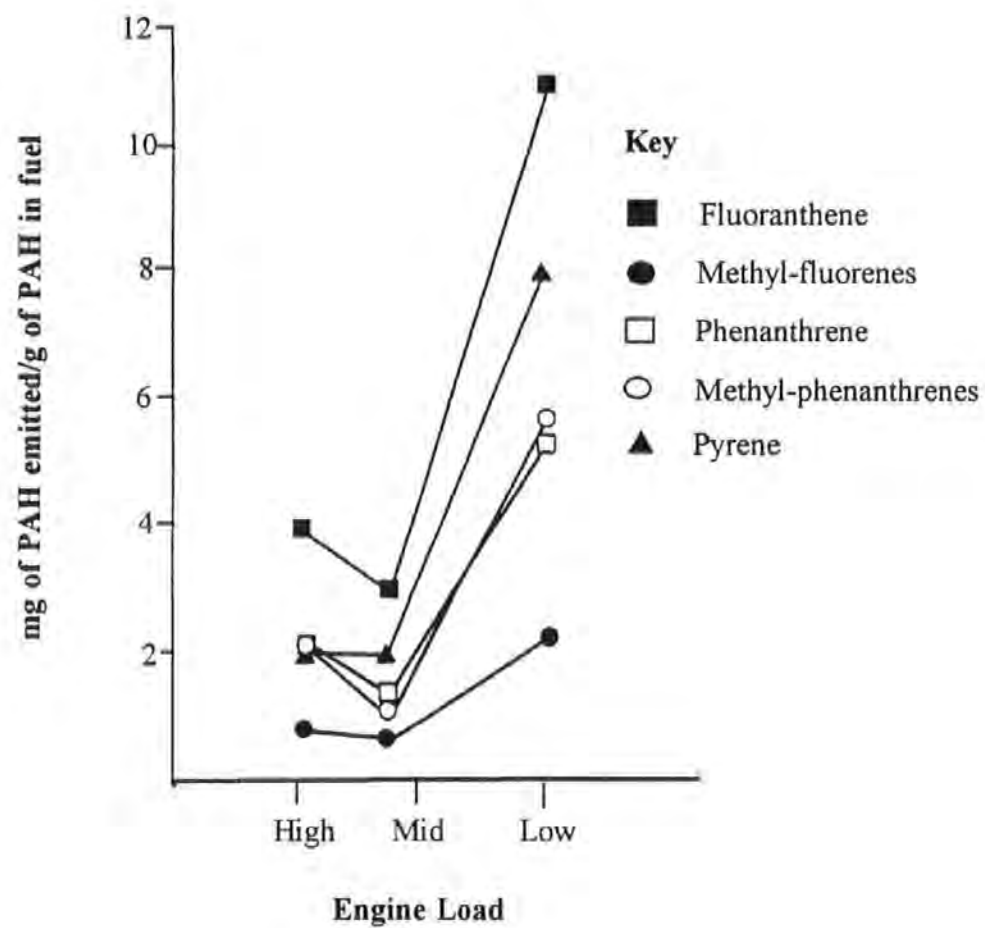


Figure 2.5 The effect of engine load on the PAH and Alkyl-PAH emissions from a light-duty DI diesel. (Williams *et al.* 1986)

Table 2.3 PAH Emission Rates (mg/kg) in DI exhausts at two different air:fuel ratios and for four fuel blends

Fuels	A		B		C		D	
Air:fuel ratio ( $\alpha$ )	$\alpha=23$	$\alpha=44$	$\alpha=2$	$\alpha=37$	$\alpha=2$	$\alpha=45$	$\alpha=23$	$\alpha=35$
Naphthalene	4.4	9.7	0.4	31.5	1.3	1.8	0.6	-
Acenaphthylene	7.0	10.0	8.5	44.6	11.4	7.5	4.3	8.3
Fluorene	2.6	4.5	1.0	14.0	2.4	1.3	8.8	0.6
Phenanthrene	7.0	19.0	3.7	42.2	6.3	3.5	2.1	3.1
Fluoranthene	0.4	0.5	0.2	0.5	4.9	-	0.1	-
Pyrene	0.6	2.5	0.3	7.6	0.5	-	0.2	-

Key to fuels (cetane No., % aromatic, full boiling point°C):

A : 35.0, 56.0, 358                      C : 49.5, 23.7, 370  
 B : 35.0, 54.5, >400    D : 51.0, 34.8, 388                      (Barbella *et al.* 1988)

In the second study Barbella *et al.* (1989) found the highest mass of PAH emissions relative to the total fuel consumed, at low loads from a light-duty 2 l DI diesel. The emission rates of fluorene and phenanthrene then decreased at mid-load, before rising once again at high load. In contrast, the emission rates for fluoranthene and benzo(e)pyrene progressively declined with increased load.

Williams *et al.* (1989) compared the organic emissions from an old Petter DI diesel to a modern medium-duty Perkins DI 4-236 4 l engine. The authors found that the superior technology incorporated into the Perkins engine corresponded to higher combustion efficiencies. In contrast to other DI studies, the survival of 2-3 ring PAH from the Perkins engine increased with elevated load at 2600 rpm. For example, the reported survival of phenanthrene at low, mid, and high load was 0.05 %, 0.03 %, and 0.58 % respectively. The different trends may reflect the larger engine size compared with the light-duty studies. The study also found survival of some PAH were greater at increased speed, whereas other PAH tended to follow a moderate decline with increased speed (Figure 2.6).

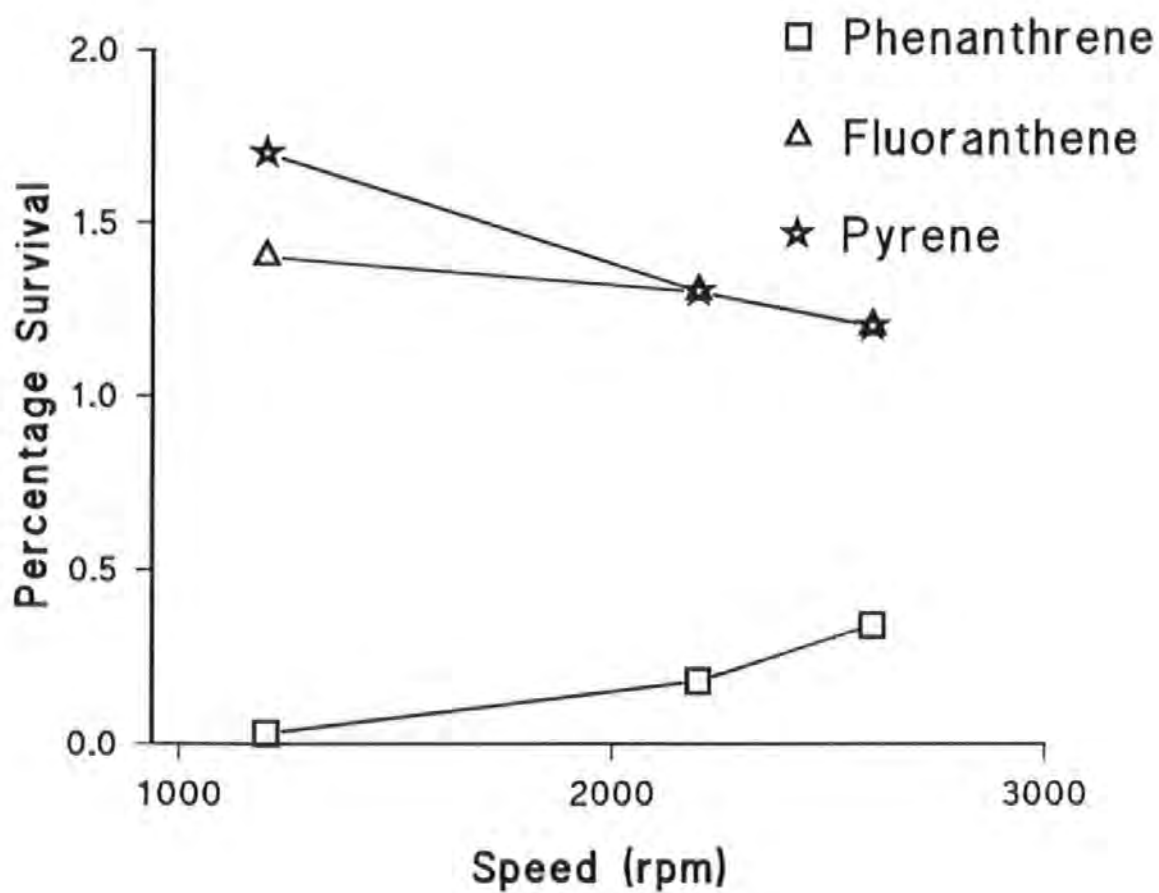


Figure 2.6 The effect of engine speed on the survival of PAH from a medium-duty DI diesel. (Williams *et al.* 1989)

As noted by the authors the higher molecular weight PAH, such as benzo( $\alpha$ )pyrene, appeared to be the result of significant combustion generation reactions, as reflected by the 60 % and 12 % 'survival' corresponding to 1200 rpm and 2600 rpm respectively.

Trier *et al.* (1990) compared the emissions from an IDI Ricardo E.6/T light-duty diesel at 2000 rpm and 3.5 kW with the emissions at 2750 rpm and 6.6 kW. The engine was sampled using the unique TESSA developed at Plymouth University (Section 2.1.1). The concentration of PAC in TES were expressed relative to those in the fuel, such that the GC/MS areas of naphthalene in TES was divided by the area of naphthalene in the fuel after correcting for injection volumes (all samples diluted to the same concentrations). In this way the dominance of fuel survival and combustion chamber contributions to TES could be assessed for the two engine powers. The results showed that the alkyl-PAC in TES relative to the alkyl-PAC in the fuel were lower compared with the corresponding unsubstituted PAC ratios (Figure 2.7). Trier *et al.* argued that the severity of the difference between the PAC and methyl derivatives at the high power (TES 2) was strong evidence for pyrosynthetic reactions by which the unsubstituted PAC were produced relative to the methyl derivatives.

Abbass *et al.* (1991a) found the mass of PAH emissions relative to the mass of fuel burned at 2200 rpm increased dramatically under high loads, for a 0.22 l IDI Petter AA1 diesel. The reported survival trend for the IDI contrast those found for light-duty DI engines, and reflects the differing engine conditions under which the two injection systems are prone to combustion problems.

Zeijewski *et al.* (1991) studied the effect of speed and load on emissions at twelve sampling points, for a light-duty 2 l DI engine. The authors determined that unburnt fuel, speed and load were the variables controlling the emissions. The highest emissions, expressed relative to the total mass of fuel consumed, corresponded to low loads. The highest recovery of exhaust PAH occurred for 1100 rpm and under idling. At 2200 rpm, the PAH survival was highest at low load, reduced at mid-load, and elevated once again at higher loads. At 3000 rpm, the survival trend with load was replicated, only with a much smaller increase in the survival at high loads relative to mid-load. The optimum speed for the greatest combustion was found to be that of 2200 rpm.

Peak area in TES/Peak area in Fuel

Peak area in TES/Peak area in Fuel

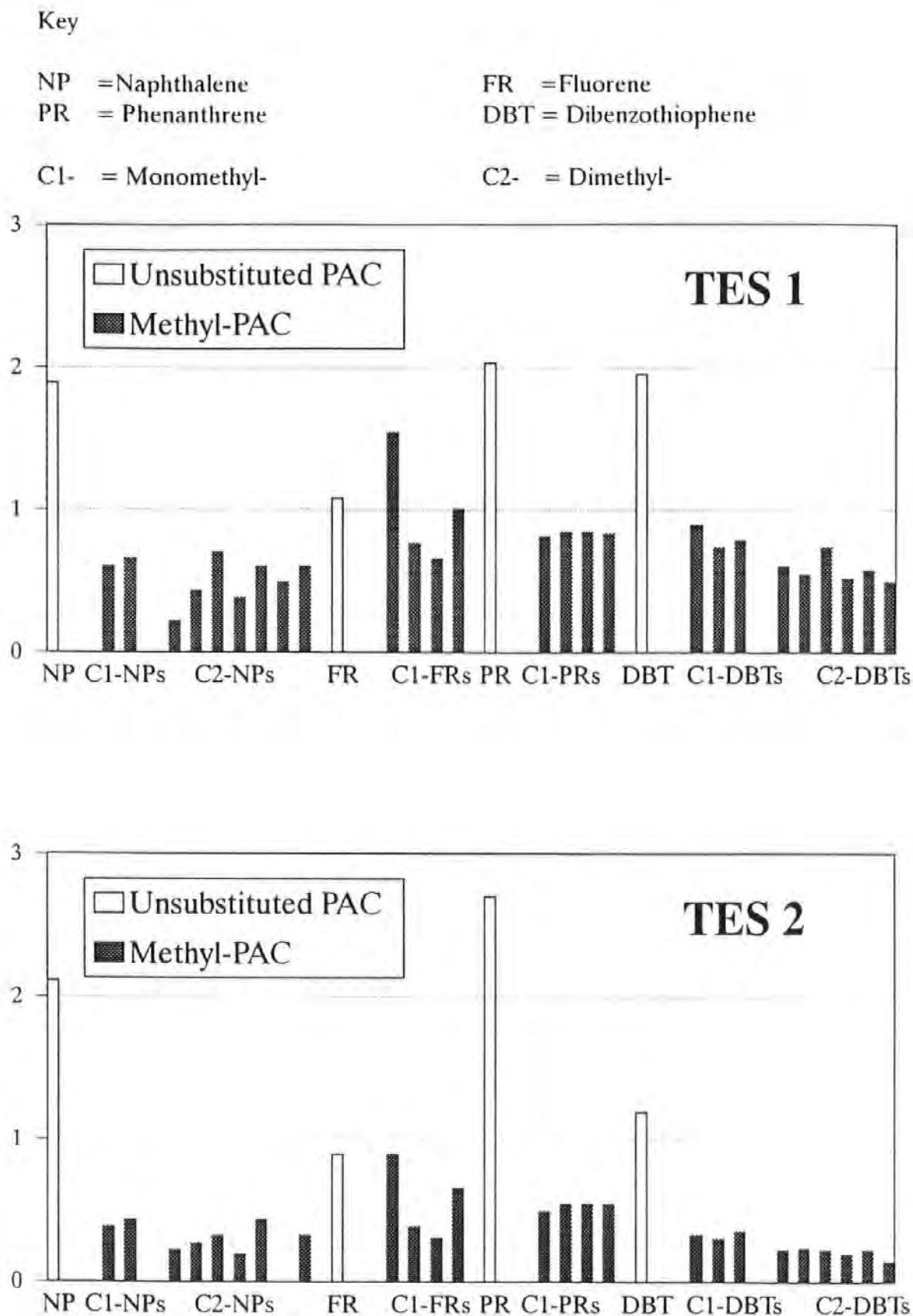


Figure 2.7 The ratio between PAC in TES relative to the PAC in the fuel for a) low engine power and b) high engine power. (Trier *et al.* 1990)

### 2.2.2 n-Alkane Emission Profiling

The low mutagenic and carcinogenic nature of n-alkane emissions has resulted in less research compared with the PAH emissions from diesel engines. The n-alkanes are also relatively unreactive in the atmosphere (Boone & Macias 1987). Where n-alkanes have been investigated, it was to assess the sources of the organic emissions over varying combustion conditions. The simple profile of the homologous series of n-alkanes present in diesel fuel enables the survival and combustion generation pathways to be investigated.

Williams *et al.* (1989) and Abbass *et al.* (1991a), reported in the PAH review (Section 2.1), also investigated the effect of engine conditions on the combustion efficiency of selected n-alkanes. In the first study, the n-alkanes survived greatest at high loads for the 4 l medium-duty DI engine, reproducing the trend found for PAH. Survival for equivalent boiling point PAH and n-alkanes, such as nonadecane relative to phenanthrene, were of similar magnitudes. The higher relative molecular mass n-alkanes survived to a greater extent than lighter n-alkanes, taken by the authors to indicate a lower combustibility associated with larger chain structures.

Abbas *et al.* (1991a) found that for the small 0.22 l IDI the highest survival of n-alkanes was, as for PAH emissions, associated with high loads (Figure 2.8). The survival comparisons of equivalent n-alkane and PAH boiling point compounds, were not as close as those found by Williams *et al.* (1989), with the PAH survival higher; especially for large PAH. The authors suggest this may be evidence for combustion chamber generation of PAH. However, as the authors note, the role of engine/exhaust deposits in producing the observed emissions could not be ruled out.



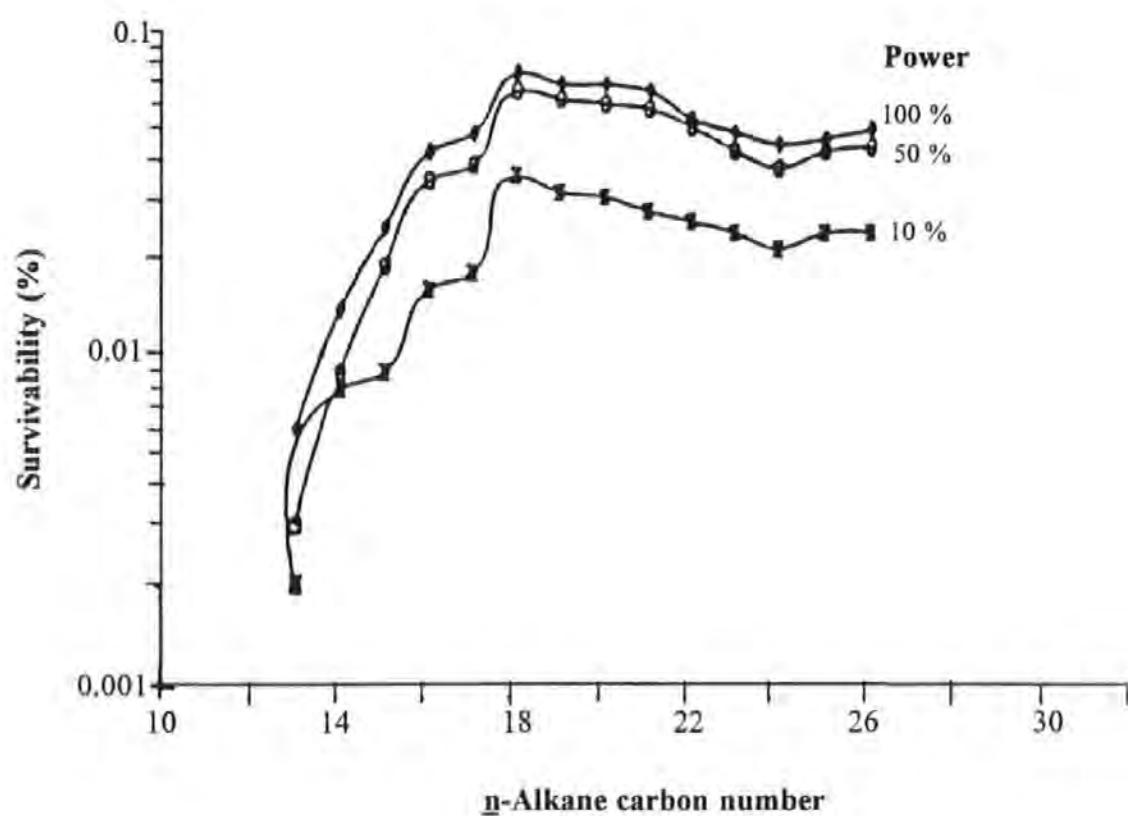


Figure 2.8 The effect of engine load on the survival of  $n$ -alkanes emissions from a light-duty IDI diesel. (Abbass *et al.* 1991a)

### 2.2.3 Nitro-PAC Emission Profiling

The discovery in the late 1970s that nitro-PAC emissions were present in diesel extracts, invoked great interest due to the high mutagenic potency of some nitro-PAC, such as 1-nitropyrene. The majority of research to date has been directed at developing fractionation and detection methods capable of detecting the trace levels of nitro-PAC in the exhaust samples (Jäger 1978, Xu *et al.* 1981 & 1982, Newton *et al.* 1982, Ramdahl & Urdal 1982, Rappaport *et al.* 1982, Hanson *et al.* 1983, Jin & Rappaport 1983, Nakagawa *et al.* 1983, Tong *et al.* 1983, Brown & Poole 1984, Chou 1984, Sigvardson & Birks 1984, Tomkins *et al.* 1984, White *et al.* 1984, Yu *et al.* 1984, Lindner *et al.* 1985, Ramdahl *et al.* 1985, Wise *et al.* 1985, Ciccioli *et al.* 1986, La Course & Jensen 1986, Robbat *et al.* 1986, Sellström *et al.* 1987, Bayona *et al.* 1988, MacCrehan *et al.* 1988, Niles & Tan 1989, Imaizumi *et al.* 1990, Schneider *et al.* 1990, Liu & Robbat 1991, Hayakawa *et al.* 1992, Fu *et al.* 1993, and Li & Westerholm 1994).

The profiling of nitro-PAC in diesel exhaust over a range of speeds and loads, resulting in the identification of engine conditions which favour nitration reactions is largely uncharted. Research so far has tended to establish the levels of selected nitro-PAC at a specific engine condition (Oehme *et al.* 1982, Schuetzle *et al.* 1982, Paputa-Peck *et al.* 1983, Campbell & Lee 1984, Hartung *et al.* 1984, and Liberti *et al.* 1984); and there has been little research aimed at sampling a range of engine conditions for a particular engine. One of the reasons for this lack of data is attributable to the technical instrumentation needed to detect the low levels of nitro-PAC in diesel exhaust. The low levels require lengthy sampling periods before the dilution tunnel and filter collection method can acquire sufficient organic material for analysis to proceed (Bechtold *et al.* 1984). The long sampling periods have in some cases resulted in artefact formation of nitro-PAC (Pitts *et al.* 1978, Gibson *et al.* 1981, Bradow *et al.* 1982, Herr *et al.* 1982, Risby & Letz 1983, Lindskog 1983, Chan & Gibson 1985, Hartung *et al.* 1984, and Lach & Winckler 1988).

Gibson *et al.* (1981) examined the emissions of 1-nitropyrene and 6-nitrobenzo( $\alpha$ )pyrene from General Motors diesel engines using the hot-start FTP. The older 1978 5.7 l engines produced significantly higher nitro-PAC emissions than did the 1980 5.7 l engines.

Tejada *et al.* (1982) determined the concentration of 1-nitropyrene in the SOF from a 1978 Volkswagen Oldsmobile diesel and a 1980 Rabbit diesel on a selection of driving cycles, such as the FTP, HWFET, and New York city cycle (NYCC). The Rabbit diesel produced less emissions than did the Oldsmobile for all driving cycles. The highest 1-nitropyrene emissions were for the NYCC, where the Rabbit produced 63.8 ppm and the Oldsmobile 111 ppm. The levels of 1-nitropyrene emitted from the diesel engines were far greater than those from SI engines tested on the same cycle. For example a Ford Mustang SI engine produced 1-nitropyrene emissions of only 12.7 ppm over the NYCC. The authors also investigated the nitration of pyrene by adding NO<sub>2</sub> to the exhaust, whereupon 1-nitropyrene increased at the expense of pyrene, as the NO<sub>2</sub> level in the exhaust was progressively increased.

Schuetzle & Perez (1983) found the concentration of 1-nitropyrene in the SOF from a heavy-duty diesel operating at 2100 rpm, initially increased with load, before decreasing with further load (Figure 2.9). For partially oxidized nitro-PAC, such as 3-nitrofluoren-9-one, the concentrations increased with load at the same speed, as did the dinitropyrenes. The highest emissions of 1-nitropyrene were found at low load and low speed, whilst the least emission variability for 1-nitropyrene was associated with 1260 rpm. The authors found the emission rate of 1-nitropyrene for light-duty diesels (4.7 µg/km) was higher compared with heavy-duty diesels (1.5 µg/km) operated over the transient FTP cycle.

Bechtold *et al.* (1984) collected the exhaust from a 1980 5.7 l eight cylinder Oldsmobile diesel over segments of the FTP cycle (total cycle time of *ca.* 23 minutes). The sampled segments included idling, accelerating periods, and steady state cruising sections. Repeated sampling was needed to gain sufficient SOF (*ca.* 200 mg) for biological and chemical analysis, especially in the case of the cold acceleration segment, where 33 consecutive cycles were combined. The authors found a strong correlation between the mutagenicity and both the exhaust temperature and gaseous exhaust NO<sub>x</sub> level. Chemical analysis indicated that 1-nitropyrene was also related to NO<sub>x</sub> and possibly temperature (Figure 2.10).

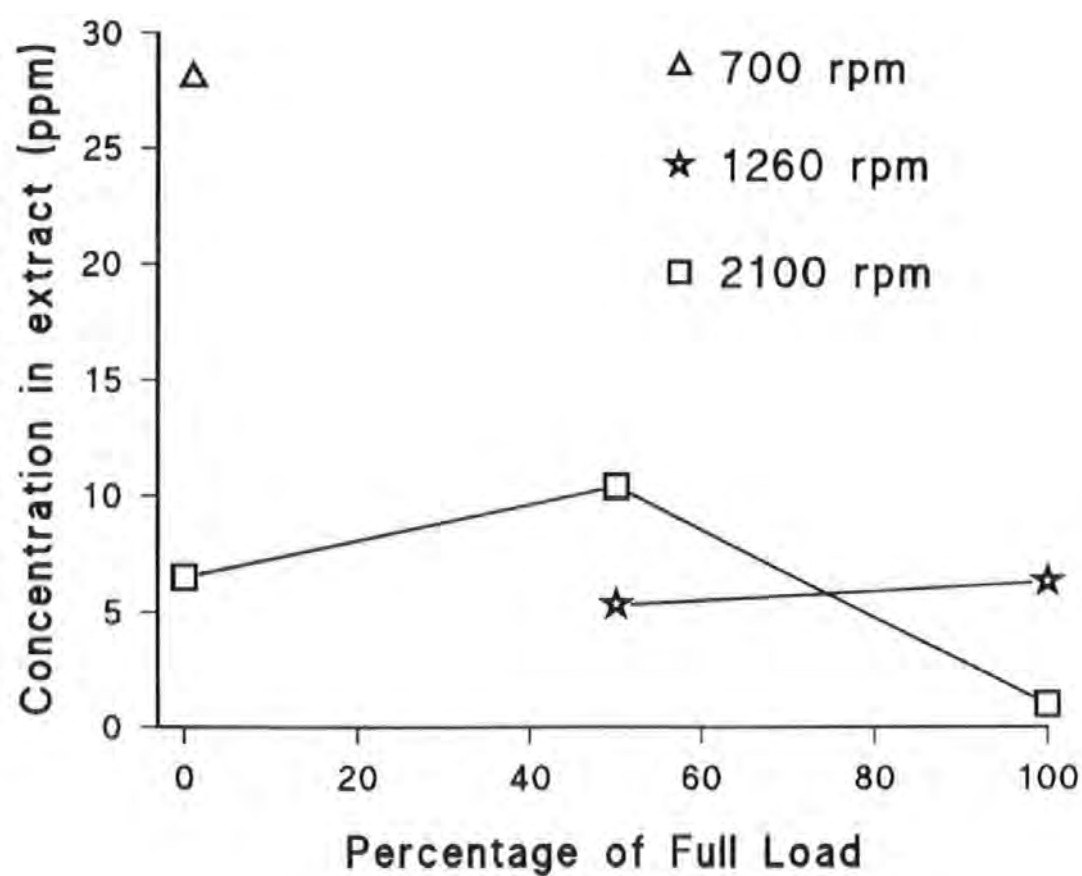


Figure 2.9 The effect of engine conditions on 1-nitropyrene emissions from a heavy-duty diesel. (Schuetzle & Perez 1983)

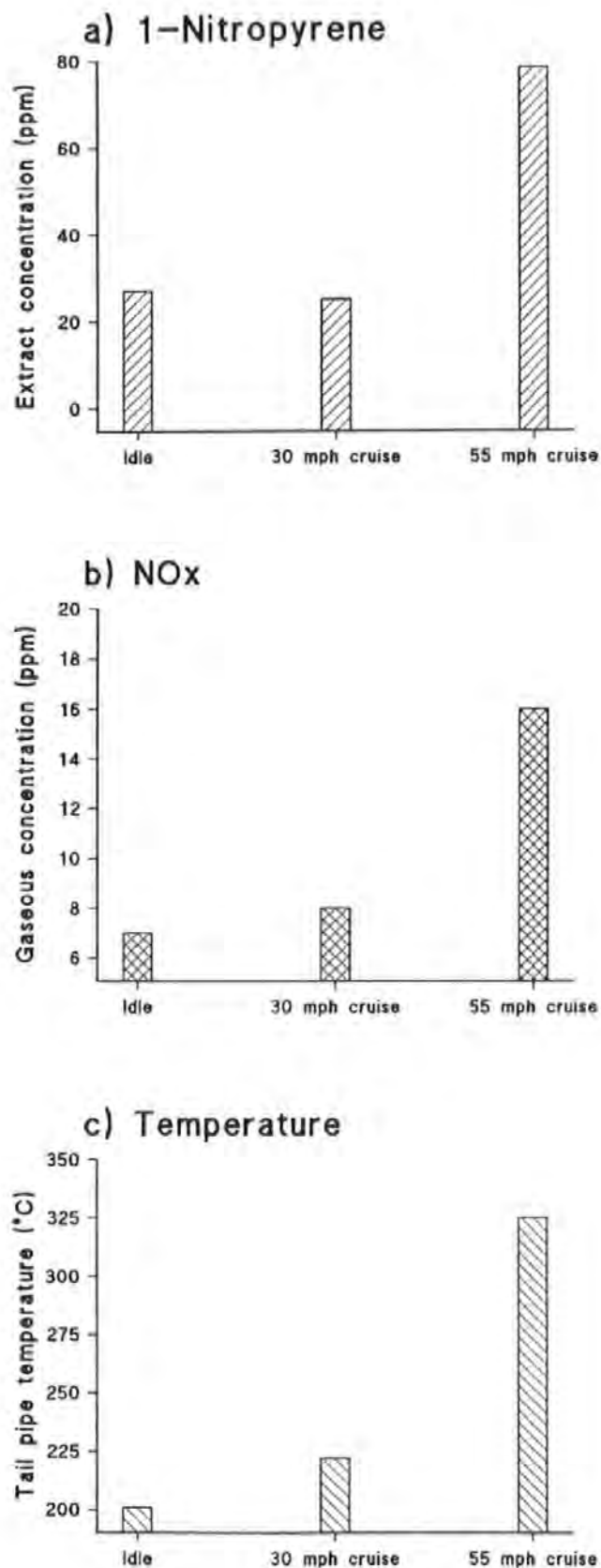


Figure 2.10 The effect of different segments of a FTP cycle on the emissions of 1-nitropyrene (a), emissions of NO<sub>x</sub> (b), and temperature (c). (Bechtold *et al.* 1984)

Handa *et al.* (1984) examined wall deposits from two tunnels for vehicle emissions, one on an ascending gradient (causing the vehicles to be under high loads) and the other on a descending gradient (vehicles subjected to a lower load burden). The vehicle flow rate was automatically recorded and the vehicle type divided into two classes according to the vehicle length: less than 6 m corresponded to mostly light-duty SI engines and greater than 6 m to heavy-duty diesel vehicles. The heavy-duty diesel contribution to 1-nitropyrene emissions at high load was 24 µg/hr compared with 6.6 µg/hr at low loads. The levels of 1-nitropyrene emitted by diesels were *ca.* ten times greater than those from SI engines. The authors found that the nitro-PAC/PAH ratio was much higher for diesels compared to SI engines, and concluded that the nitro-PAC emissions were favoured at the high NO<sub>x</sub> and temperatures associated with diesel combustion at high load.

Draper (1986) quantified the nitro-PAC emissions from a heavy-duty diesel engine at two different engine conditions. The higher relative molecular mass nitro-PAC emissions were greater at moderate load and high speed compared with high load and moderate speed (Table 2.4). The study is restricted by the limited sampling positions, and the elucidation of whether speed or load is responsible for the nitro-PAC emissions is further complicated by both variables changing for each sampling position.

Table 2.4 Effect of two different engine conditions on the Nitro-PAC Emissions from a heavy-duty diesel

Compound	High Load, Moderate Speed (µg/g)	Moderate load, High Speed (µg/g)
1-nitronaphthalene	0.77	0.47
2-nitronaphthalene	0.94	0.87
2-nitrofluorene	0.63	8.8
9-nitroanthracene	0.34	1.4
1-nitropyrene	not detected	5.0
1,3-dinitropyrene	0.52	1.6

(Draper 1986)

Shore (1986) investigated the nitro-PAC emissions from DI and IDI versions of a Ricardo Hydra diesel, operated at 2400 rpm and 7 bar. For a standard US diesel fuel the DI produced substantially higher emissions of 1-nitropyrene (11.1  $\mu\text{g}/\text{hour}$ ) compared with the IDI (0.78  $\mu\text{g}/\text{hour}$ ). The  $\text{NO}_x$  emission rate of the DI was typically three to four times that of the IDI engine. Shore could find no correlation between the 1-nitropyrene emissions and different fuel blends.

Hirakouchi, N. *et al.* (1990) analyzed the exhaust from a 6.5 l turbocharged DI diesel and a 11.2 l normally aspirated DI diesel for nitro-PAC. The turbocharged diesel, sampled over the FTP cycle, produced nitro-PAC emissions of  $1.07 \times 10^{-6}$  g/BHP-hour of 2-nitrofluorene,  $3.29 \times 10^{-6}$  g/BHP-hour of 9-nitroanthracene and  $5.90 \times 10^{-6}$  g/BHP-hour of 1-nitropyrene. The 11.2 l diesel was sampled at mid-speed for 25%, 50%, 75% and 100% of full load. The nitro-PAC emissions were expressed in terms of mass emitted per volume of gases produced (Figure 2.11). Different nitro-PAC produced different trends with respect to load. For instance 9-nitroanthracene and 2-nitrofluorene were highest at low load, reduced at mid-loads and increased at high load. The emissions of 1-nitropyrene and 3-nitrofluoranthene progressively decreased with increasing load, whereas the nitronaphthalenes were more stable across the load range. The mass of 1-nitropyrene emitted relative to the total fuel consumed was highest at low loads.

Scheepers *et al.* (1994) evaluated the 1-nitropyrene emissions from heavy-duty and light-duty diesel engines over different driving cycles (Table 2.5). There were only small differences between varying driving conditions for both engines. The oxidation catalyst fitted to the light-duty engine resulted in very low levels of 1-nitropyrene and particulates. In fact, after conducting a series of tests, 1-nitropyrene was only detectable in three out of sixteen samples. This highlights the inherent problem with dilution tunnel sampling for trace nitro-PAC analysis, namely that of lengthy sampling periods for sufficient SOF collection, which can in some cases lead to significant artefact contributions to the nitro-PAC.

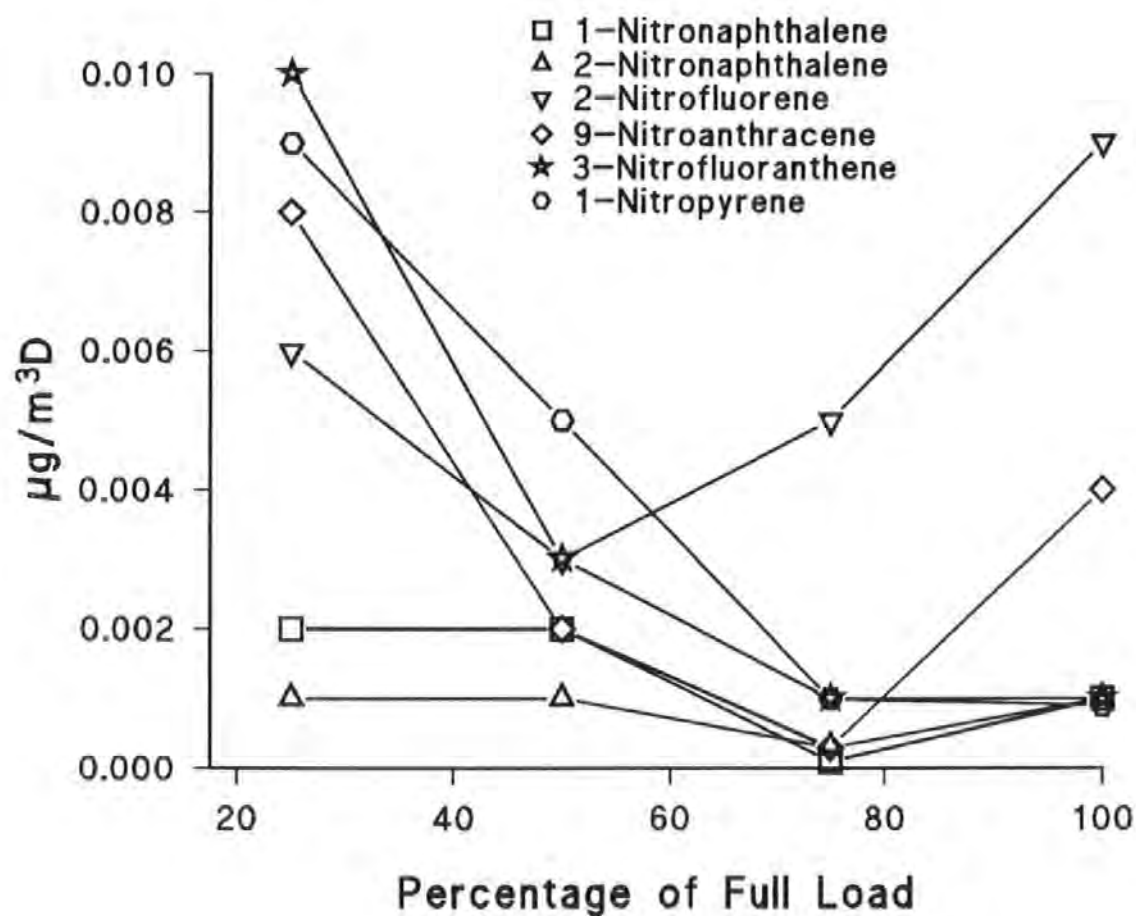


Figure 2.11 Effect of engine load on the nitro-PAC emissions from a heavy-duty turbocharged diesel. (Hirakouchi *et al.* 1990)



Table 2.5 Effect of Driving Conditions on 1-Nitropyrene emissions from Light- and Heavy-Duty diesels

Vehicle	Driving Pattern	1-nitropyrene	
		$\mu\text{g/g}$ particulate	$\mu\text{g/km}$ travelled
Heavy duty	Sub urban	1.94	2.13
	Sub urban	1.94	3.28
	Urban	3.39	6.48
	Motorway	1.94	0.87
	Motorway	2.73	1.37
Light duty <sup>1</sup>	European driving cycle (cold start)	- <sup>2</sup>	0.32
	European driving cycle (hot start)	- <sup>2</sup>	0.22
	US '75 Driving cycle	- <sup>2</sup>	0.36

<sup>1</sup> With oxidation catalyst

<sup>2</sup> Amount of particulate matter not determined

(Scheepers *et al.* 1994)

Veigl *et al.* (1994) determined the emissions of 1-nitropyrene from a 1.8 l four cylinder normal aspirated DI diesel and a 4 l four cylinder turbocharged DI diesel. The light-duty engine was tested over the US FTP and HWFET cycles. The predominately high speed HWFET cycle produced considerably higher levels of 1-nitropyrene compared with the more varied FTP cycle. The authors also found that the addition of EGR and an oxidation catalyst reduced the 1-nitropyrene emissions. The larger engine was sampled using steady state testing at 1560 rpm and across the load range. The engine was also tested at very low speed and load idling conditions (Figure 2.12). The highest 1-nitropyrene emissions for 1560 rpm were at mid-load, whilst the lowest emissions were at 600 rpm and idling. The authors also found that the addition of a fuel additive decreased the 1-nitropyrene emissions. The authors claim that since the emissions are reduced by both engineering and fuel changes, artefacts are not responsible for the results.

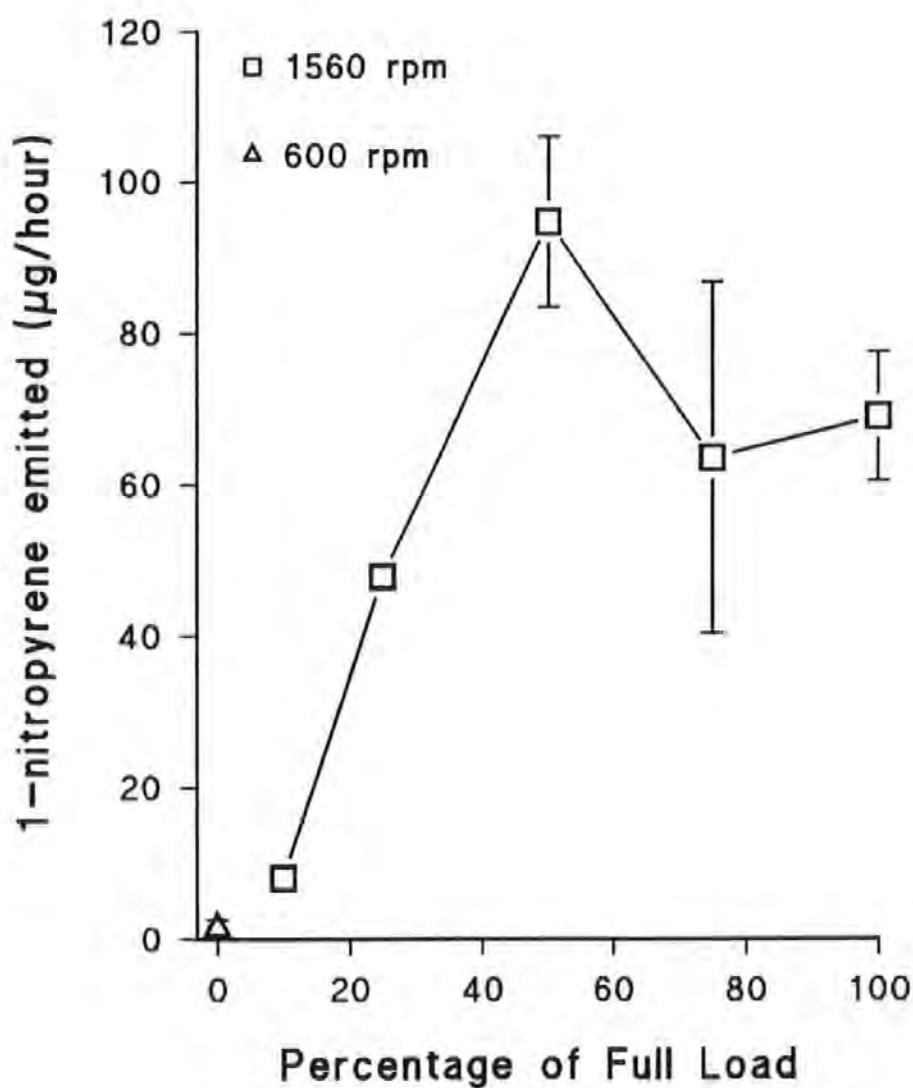


Figure 2.12 The effect of engine load on the 1-nitropyrene emissions from a medium-duty DI diesel. (Veigl *et al.* 1994)

#### 2.2.4 Oxy-PAC Emission Profiling

The realisation that nitro-PAC may not account for all of the direct acting mutagenicity of exhaust extracts led to investigation of other possible candidates. Some oxy- and polar PAC present in diesel exhaust have high mutagenic potencies (Scheepers & Bos 1992a).

The composition of the oxy- and polar PAC fractions of diesel exhaust consists of aldehyde, ketone, and quinone derivatives of PAH (Yu & Hites 1981, Choudbury 1982, Ramdahl 1983, König *et al.* 1983, and Schulze *et al.* 1984). The analysis of the polar PAC in exhaust samples by gas chromatography is hindered by the volatility problems, such as PAC carboxylic acids (Oehme 1985). The complexity of the polar derivatives of PAH necessitates techniques, such as LC/MS, to overcome the problems associated with GC analysis. As a consequence of the technical problems, the determination of the effect of engine conditions on the oxidizing potential of diesel combustion remains largely unanswered.

Jensen & Hites (1983) found the oxy-PAC emissions from a heavy-duty Cummins diesel at zero, mid, and high loads exhibited varying trends depending on the structure (Figure 2.13). For one set of oxy-PAC (naphthalenecarboxaldehydes, fluoren-9-one, and bipheylcarboxaldehydes) the emissions initially increased with engine load and then decreased thereafter. The second set (phenanthrenecarboxaldehydes and thioxanthen-9-one) decreased progressively with increased engine load and the corresponding higher exhaust temperatures.

Schuetzle & Perez (1983) showed that partial oxidation of nitro-PAC may become more active at high speeds and loads for a heavy-duty diesel. For example, the 17 ppm of 3-nitrofluoren-9-one in the extract at low load increased to 63 ppm at high load. Similarly, 3-nitro-1,8-naphthalic acid anhydride was 22 ppm and 174 ppm at low and high loads respectively.

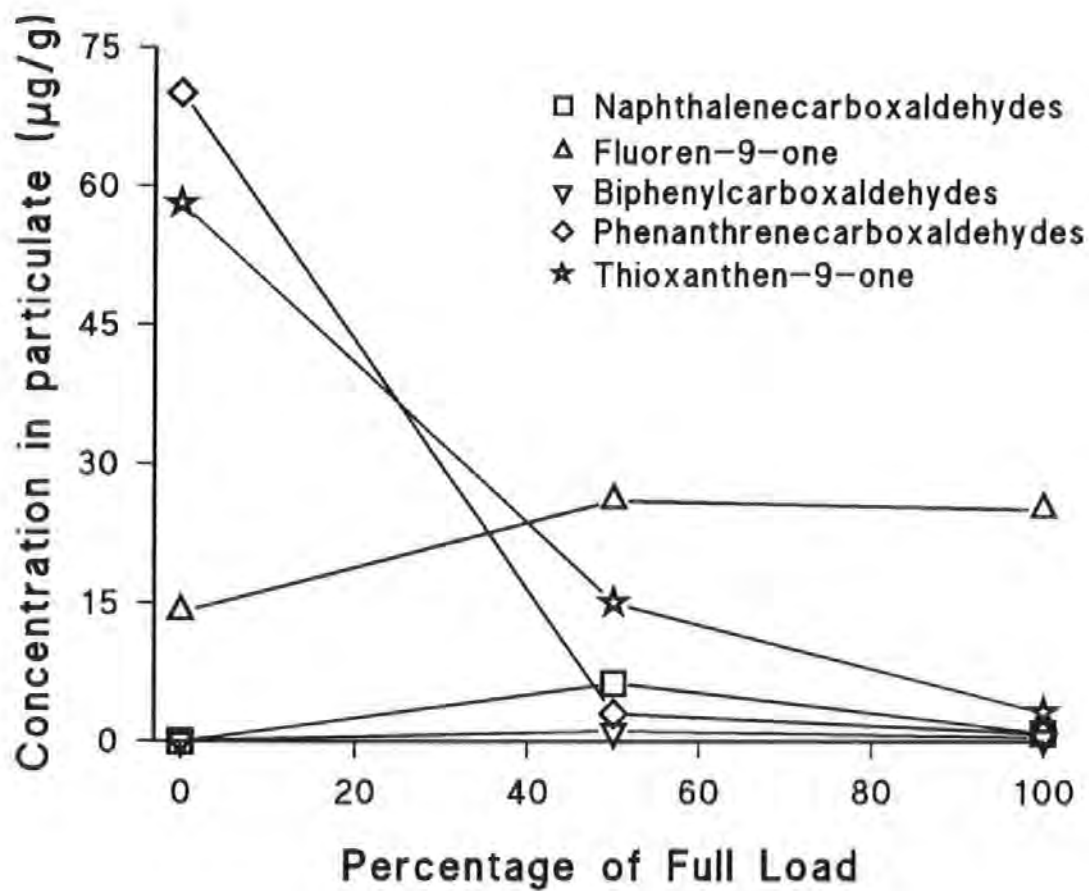


Figure 2.13 Effect of engine load on the oxy-PAC emissions from a heavy-duty diesel.  
(Jensen & Hites 1983)

The study of wall deposits on two tunnels (one inclined and the other declined with respect to the traffic flow) by Handa *et al.* (1984) showed the hourly emissions of benz( $\alpha$ )anthracene quinones, benzo( $\alpha$ )pyrene quinones, perylene quinones, and benzanthrone increased at high load. The oxy-PAC were also produced in greater quantities from the heavy-duty diesels compared with the SI light-duty vehicles.

Hirakouchi *et al.* (1990) found that the aldehyde and ketone emissions, such as formaldehyde, benzaldehyde, and acetone, relative to the total fuel consumed, were greatest under low loads for a heavy-duty diesel.

### 2.3 Summary of Emission Profiling & Aims of Investigation

In terms of the technical aspects of emission profiling, the choice of the engine sampling system is crucial to the type of profiling produced. Dilution tunnel/filter systems are not suited to sampling secondary nitro- and oxy-PAC emissions, for which extended sampling leads to high artefact contributions. The simulation of the initial atmospheric dilution of the diesel exhaust by dilution tunnels, hinders the differentiation between the role of the exhaust and combustion chamber on emissions. Sampling with TESSA allows the role of diesel combustion in the formation of primary and secondary organic emissions to be investigated; information vital to engineering and fuel companies alike. The TESSA enables large organic extracts to be rapidly collected (sampling times of the order of seconds) with minimum artefact contributions, thus allowing a wide range of speeds and loads to be profiled.

The profiling of the primary *n*-alkane and PAC emissions can be easily achieved with relatively simple work-up and detection systems. The most informative profiling units are those which relate the mass of a specific compound emitted relative to the same compound within the fuel consumed during sampling. Such units enable the combustion efficiency of different organics under varying engine conditions to be followed. The total mass of emissions collected during driving cycle simulations are not as informative as steady state tests in enabling the identification of engine conditions responsible for combustion problems. Light-duty DI diesels are prone to combustion problems at low loads. By contrast, the IDI diesel is prone to becoming inefficient at high load, as are larger DIs, emphasizing the effect of engine

design on the combustion process. There is limited evidence for the combustion efficiency of light-duty DI engines being greatest at mid-speeds. The *n*-alkane emission profiles closely resemble those found for PAH, and consequently the highest survival of *n*-alkanes occurs at engine conditions under which the greatest PAH survival occurs. To conclude, the role of the combustion chamber on the primary emissions from light-duty DI diesels over a wide range of conditions, especially speed, requires further research.

There are great sampling and analytical problems associated with profiling trace nitro- and oxy-PAC emissions. With regard to the highly mutagenic nitro-PAC, there have been few comprehensive studies on the effect of engine conditions on the nitration potential of diesel combustion. Those studies which have been conducted relied on dilution tunnel sampling systems, not suited to rapid mass sampling and prone to artefact formation of nitro-PAC. The majority of the steady state sampling studies have involved heavy-duty engines, and the similarity of heavy-duty and light-duty combustion in terms of nitro-PAC is largely unknown. Two formation theories for nitro-PAC emissions from diesel engines have been proposed:

- 1) Combustion generation involving PAH and  $\text{NO}_x$ .
- 2) Post-combustion electrophilic nitrations between PAH and  $\text{NO}_2$  (in the presence of nitric acid). (Scheepers & Bos 1992b)

The first pathway may be linked to the radical processes involved with high temperature combustion, such that PAH combine with  $\text{NO}_2$  and NO radicals, followed in the case of NO by further oxidation (Nielsen *et al.* 1983). The second route would proceed under acidic conditions, by the action of the nitronium ion ( $\text{NO}_2^+$ ), as is commonly employed in laboratory synthesis of nitro-PAC (Nielsen 1984 and Ross *et al.* 1988). It is important to stress that neither theory has been proved under specific engine conditions. This is due to dilution tunnel/filter sampling systems being unable to differentiate between the combustion and post-combustion contributions to the sample matrix. To conclude, there is insufficient information to enable elucidation of the combustion factors controlling the nitration of primary PAH emissions from light-duty DI diesel engines.

In view of the limited information on the highly hazardous secondary nitro-PAC emissions, the aim of this study was to achieve comprehensive profiling for such emissions using TESSA sampling close to the combustion chamber for a light-duty DI diesel. The objectives of the research can be summarised as follows:

- 1) To establish the relationship between the primary emissions present in the fuel, such as PAH, with engine speed and load over a range of conditions. To use the engine map to understand under which conditions the greatest fuel survival and combustion generation contributions to the emissions are favoured.
- 2) To develop and validate laboratory work-up and analytical techniques capable of detecting the secondary nitro-PAC emissions.
- 3) To employ the developed analytical routines to produce a comprehensive engine map of nitro-PAC emissions from the engine. To use the nitro-PAC map to examine the effect of speed and load on the nitration of the primary PAH emissions, and from this postulate combustion/exhaust areas to which the two proposed nitration mechanisms may be favoured.
- 4) To draw conclusions from the primary and secondary emission maps, which may be of use to both the engineer and fuel chemist, concerning the possible control strategies which could be employed, if environmental pressure resulted in PAC legislation. Finally, to indicate where further research projects could be directed.

## **Chapter 3 - Experimental Procedures & Facilities**

This chapter details the sampling and analysis procedures involved in this research programme. There are four main experimental sections, the first deals with the test facilities and the fuel/oil used throughout the study (Section 3.1). The profiling of the primary emissions (PAH and n-alkanes) over a range of speeds and loads using the initial TESSA configuration is described in Section 3.2. Following the first profiling research, TESSA was relocated, upgraded and tested (Section 3.3). The second profiling research package investigated the secondary emissions (nitro- and oxy-PAC) over a range of engine conditions using the upgraded TESSA (Section 3.4).

### **3.1 Facilities and Fuel/Oil Description**

This section covers the hardware required for engine sampling; namely the engine itself (Section 3.1.1), the engine management system (Section 3.1.2), and the engine sampling system (Section 3.1.3). The type of fuel and oil used throughout the study are detailed in Section 3.1.4.

#### **3.1.1 Engine Details**

The test engine throughout the research was that of a Perkins Prima direct injection light-duty engine. The engine is fitted with a Bosch EPVE rotary fuel injector pump along with CAV 4-hole fuel injectors. Full details are given in Table 3.1. The engine exhaust manifold had previously been modified to allow sampling from one cylinder (Rhead *et al.* 1991).

#### **3.1.2 Engine Management**

The test engine was coupled to a swinging field electric Borgi & Saveri FA1000 eddy current dynamometer managed by a Test Automation 2000 C-E compact controller, operated in the constant torque mode.

#### **3.1.3 Total Exhaust Stripping Solvent Apparatus**

This section provides technical details of the engine sampling system used for this research, termed the total exhaust solvent-stripping apparatus (TESSA). The advantages of directly sampling the exhaust close to the combustion chamber with TESSA compared with



conventional dilution and filter engine sampling are outlined in Section 2.1. This section describes the configuration of TESSA at the beginning of the research.

Table 3.1 Perkins Prima Engine Details

	Specification
Power at 4500 rpm (kW)	46
Torque at 2500 rpm (Nm)	122
Bore (mm)	84.4
Stroke (mm)	88.9
Number of cylinders	Four in-line vertical
Capacity (l)	1.993
Cycle	4 stroke
Aspiration	Natural
Combustion system	Prima one-stage direct injection
Compression Ratio	18.1:1

The system consists of a stainless steel tower into which the exhaust is fed directly from one combustion chamber of the Prima engine. The organics are removed from the tower by a downward flow of solvent mixture (DCM:methanol, 1:1). The tower is divided into three sections (Figure 3.1a). The cooled bottom section incorporates the exhaust entry point. The exhaust entry point is connected to the engine exhaust manifold by a short transfer pipe. The solvent flow is set by tap 1 and sampling of the exhaust proceeds by releasing tap 2, allowing the solvents to enter the middle section. The exhaust is directed from the main exhaust into TESSA by a slidable plate mechanism (Figure 3.1b). The middle section is filled with short sections of glass tubes. The surface of the tubing provides an interaction point for the solvent and the organics in the exhaust. The top section contains the exhaust baffles, and also provides further cooling. The entire tower length can be washed down with the solvent mixture from the entry point in the top section using tap 3.

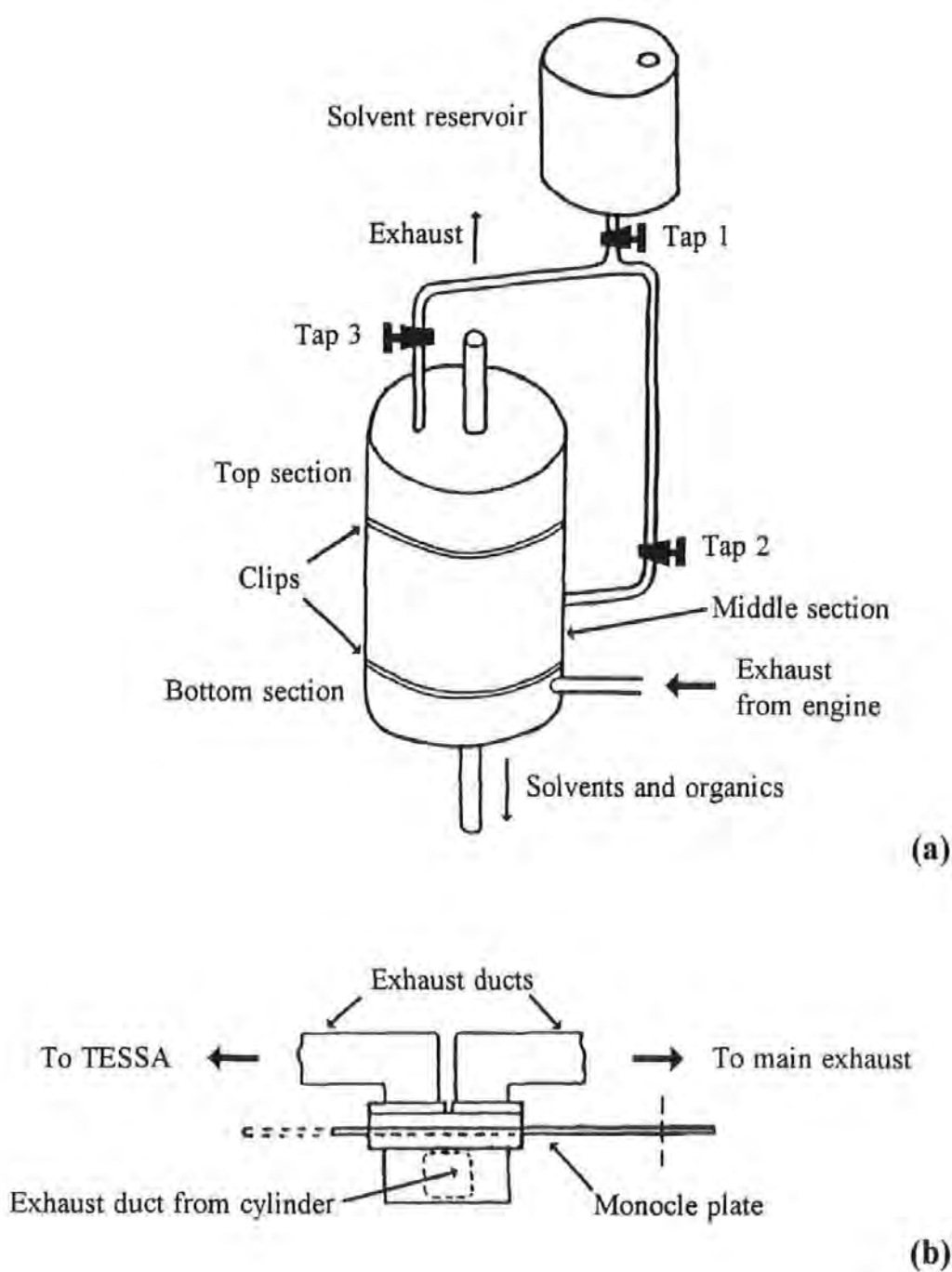


Figure 3.1 The operation of the solvent delivery system (a) and exhaust transfer mechanism (b) used for engine sampling with TESSA.

3.1.4 Fuels and Oils

Throughout the research a reliable fuel stock (1600 l) of standard No. 2 DERV (Table 3.2) was purchased and stored in eight 50 gallon (*ca.* 225 l) drums. The drums, which previously contained oil or industrial solvents, were thoroughly washed out with a portion of the standard fuel many times before the drums were filled direct from the tanker. The engine was supplied with fuel from a 10 l head tank.

The head tank output entered a fuel/water separator before entering a 400 ml fuel plinth (with measurement increments of 100 ml, 200 ml, and 400 ml). The standard return route for the fuel system was to bypass the fuel plinth. A switch mechanism was installed to allow the fuel supply to be isolated to the fuel plinth for fuel consumption measurements. The lubricating oil used throughout the study was that of Shell Heavy Duty Rimula X, grade 15/30 W.

Table 3.2      Standard No.2 Diesel Fuel Properties

	Specification
Aromatic content (IP 156)	29 %
Cetane index (IP 218) <sup>1</sup>	49
Specific gravity (@ 60°F)	0.863
Viscosity (@ 40°C)	3.58 cS
Initial boiling point	<i>ca.</i> 185°C
5 %	217°C
10 %	231°C
20 %	250°C
30 %	264°C
40 %	275°C
50 %	286°C
60 %	298°C
70 %	310°C
80 %	323°C
90 %	343°C
Final boiling point	364°C

<sup>1</sup> Based on mid-boiling point and an API gravity of 32.5

Testing carried out by Perkins Technology

### 3.2 Profiling of the Primary Emissions using the initial TESSA configuration

The profiling of the primary emissions (PAH, PASH and n-alkanes) from the Prima engine was attempted with the initial TESSA set-up. The overall procedure for the sampling, work-up of TES, and analysis of specific organic classes is shown in Figure 3.2. The sampling and the work-up details for TES are given in Sections 3.2.1 and 3.2.2 respectively. The analysis of the n-alkanes GC-FID is detailed in Section 3.2.3. The analysis of the PAH and PASH by GC/MS operated in the EI mode is described in Section 3.2.4.

#### 3.2.1 Engine Sampling for Primary Emissions

Engine sampling was performed in series, referring to sampling at a constant speed and at different percentages of full load positions. The full load for a particular speed was arrived at by increasing the load until the highest stable load was obtained. Following the acquirement of the full load position, 1 %, 25 %, 50 %, 75 % of full load were calculated.

Prior to engine sampling the chiller was filled with water/ice and circulated around the cooling coils of the tower. The engine was conditioned for one hour at 3000 rpm and 90 Nm, followed by further conditioning for fifteen minutes at the desired engine conditions. The solvent reservoir was filled with the solvent mixture (800 ml) and the reservoir opened (tap 1) to the set position. The solvent flow into the top of the middle section of the tower was started (tap 2) ten seconds before switching the exhaust from the main exhaust into the tower by the manually operated sliding plate. The exhaust was sampled for thirty seconds before switching the exhaust back to the main outlet. The solvent flow was directed to the top of the tower (tap 3), and the tower washed down with the remaining solvent.

The engine was then conditioned for the next load position, and the sampling procedure repeated until all the desired load positions had been sampled on the same day. For each engine series a fuel and sump oil sample were taken. Three engine series were completed at 1000 rpm, 2000 rpm, and 3000 rpm on different days (Tables 3.3 - 3.5).

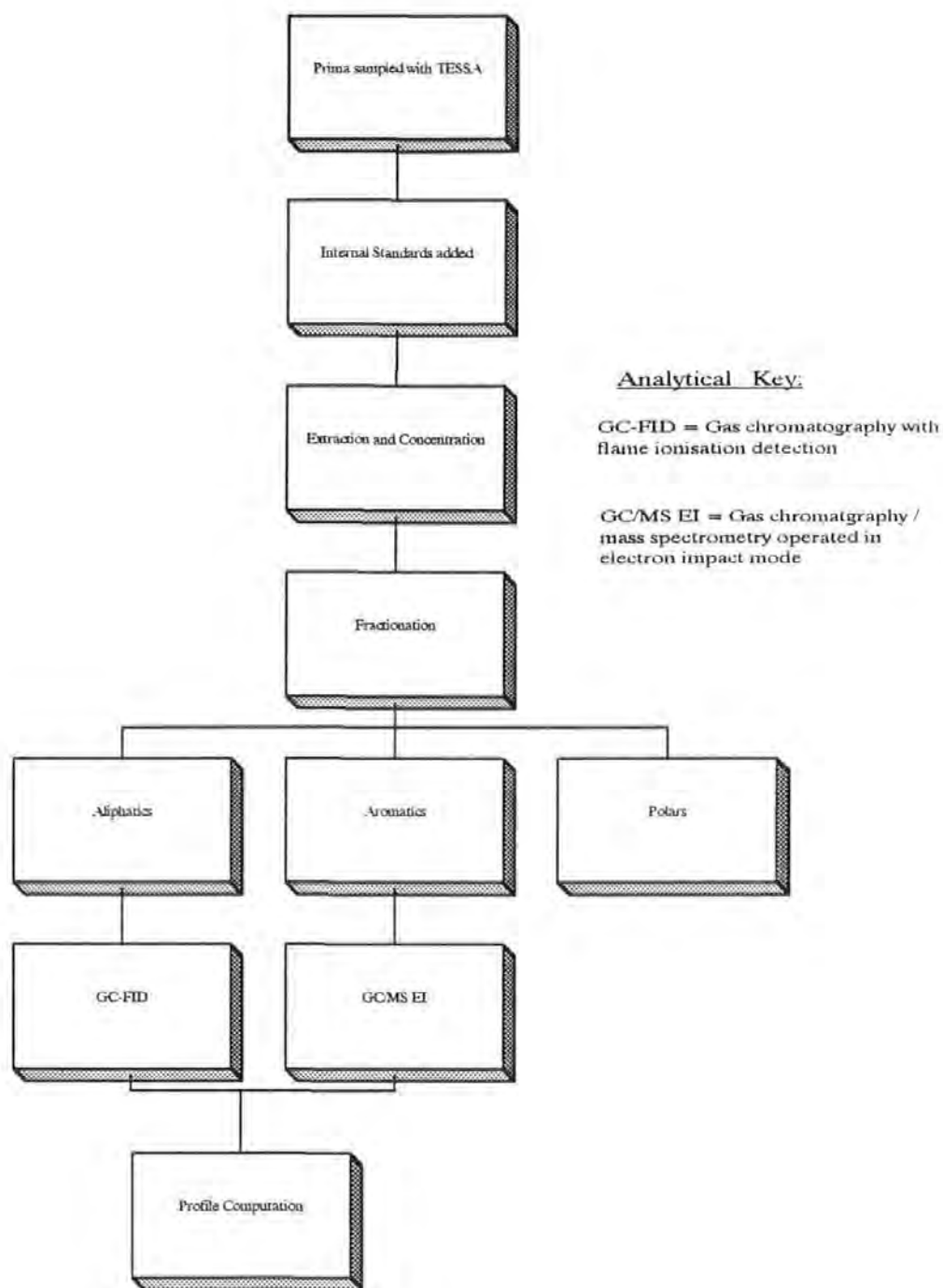


Figure 3.2 The overall experimental procedure for the profiling of primary organics.

Table 3.3 Engine sampling series at 1000 rpm

Percentage of full load	Fuel consumption (ml/min)	Sampling time (seconds)	Water temperature (°C)	Oil temperature (°C)	Coolant temperature (°C)
1	9.72	30.20	94	45	4
25	18.93	30.18	95	45	4
50	28.04	30.21	97	50	4
75	38.22	30.32	98	50	4
100	49.18	30.35	94 <sup>1</sup>	50	4

<sup>1</sup> Fans cut in

Table 3.4 Engine sampling series at 2000 rpm

Percentage of full load	Fuel consumption (ml/min)	Sampling time (seconds)	Water temperature (°C)	Oil temperature (°C)	Coolant temperature (°C)
1	20.62	30.26	92	58	4
25	37.74	30.10	93	58	4
50	58.25	30.40	93	59	4
75	76.92	30.39	93	60	4
100	92.31	29.23	95	61	4

Table 3.5 Engine sampling series at 3000 rpm

Percentage of full load	Fuel consumption (ml/min)	Sampling time (seconds)	Water temperature (°C)	Oil temperature (°C)	Coolant temperature (°C)
1	37.74	29.74	94	58	3
25	65.93	30.12	93	60	3
50	96.77	30.08	94	60	4
75	133.33	30.19	95	60	4
100	176.47	29.92	100	72	4

### 3.2.2 Sample Work-up

In order to avoid contamination, all solvents were of HPLC grade (Rathburn Chemicals) and the solvents were regularly checked for purity by GC-FID. Prior to use, all glassware was soaked in Decon-90 for 24 hours, rinsed repeatedly in tap water and then distilled water, and finally dried. The glassware was solvent washed with the appropriate solvents (normally DCM) before being used in the experiments. All filters and work-up chemicals (silica and drying agents) were soxhlet extracted with DCM (24 hours) before storing in ovens. All standard solutions (96+ % pure) and samples were stored in freezers (-20°C).

#### 3.2.2.1 Internal Standards for Aromatics

The initial validation and early experimental use of TESSA by Trier (1988), found the laboratory recovery of phenanthrene and other three to five ring PAH to be around 90%. The more volatile two ring naphthalene was recovered by 50%. Therefore, the search for internal standards for PAH relied on establishing a suitable compound to account for naphthalene and volatiles, and a more stable compound to account for the remaining more stable PAH.

Deuterated PAH standards were investigated for suitability as internal standards, since the heavier compound follows the behaviour of the native undeuterated PAH and can be easily detected by GC/MS EI (Levin *et al.* 1984). The following deuterated standards were investigated:  $d_8$ -naphthalene,  $d_{10}$ -phenanthrene, and  $d_{12}$ -chrysene (Aldrich Chemical Co.). Following the research of Williams *et al.* (1986) 9-phenylanthracene and 1,3,5-triphenylbenzene (Aldrich Chemical Co.) were also investigated as internal standards.

To verify the suitability of the internal standards, two solvent mixtures (DCM:methanol, 1:1)(800 ml) were spiked with a standard mix containing the EPA 16 priority pollutant PAH (Supelchem), dibenzothiophene (Janssen Chimica), 9-phenylanthracene, and 1,3,5-triphenylbenzene. Distilled water (800 ml) was added to the solvents and the mixture worked-up as for TES. The samples were analyzed by a Varian 6000 GC-FID fitted with a DB-5 capillary column (30 m x 0.32 mm ID, 0.25  $\mu$ m film thickness, J&W Scientific) with the detector signal recorded and integrated by a Varian 402 data system. Splitless injection at 240°C was used and the temperature program was: 40°C for 1 min., 5°C/min to 300°C, held for 15 mins. Nitrogen was used for the carrier gas.

The quantification was based on response factors to undecane (Janssen Chimica). As shown in Table 3.6 the majority of the PAH were recovered to the same high level, except naphthalene and the very high relative molecular mass PAH.

**Table 3.6      Results from Internal Standard & PAH Laboratory Recovery Experiment**

Compound	Weight of spike added (µg)	Laboratory recovery #1/%	Laboratory recovery #2/%	Average recovery /%
Naphthalene	200	21.9	14.1	18.0
Acenaphthene	200	72.1	66.8	69.5
Acenaphthylene	200	74.6	71.5	73.1
Fluorene	200	77.5	77.5	77.5
Dibenzothiophene	570	82.0	81.6	81.8
Phenanthrene	200	80.1	82.6	81.4
Anthracene	200	81.3	84.7	83.0
Fluoranthene	200	82.1	85.2	83.7
Pyrene	200	81.0	84.0	82.5
9-Phenylanthracene	210	80.0	83.3	81.7
Benz(α)anthracene	200	82.6	93.6	88.1
Chrysene	200	82.2	86.3	84.3
Benz(j&k)fluoranthene <sup>1</sup>	200 each	81.0	84.4	82.7
Benzo(α)pyrene	200	78.7	82.2	80.5
1,3,5-Triphenylbenzene	115	76.9	80.3	78.6
Indeno(1,2,3-cd)pyrene	200	81.2	85.1	83.2
Benzo(ghi)perylene	200	76.4	80.0	78.2
Dibenzo(a,h)anthracene	200	60.6	59.8	60.2

<sup>1</sup> Isomers co-eluted

A selection of different internal standards (Table 3.7) were added to TES immediately after collection and to fuel samples, allowing a comparison of the recovery of internal standards within the sample matrix with the spiked recovery experiments. The results of the review are given in Section 3.2.2.6.



Table 3.7 Internal Standards added to TES &amp; Fuel for Primary Emission Profiling

Internal Standard	1000 rpm Engine Series	2000 rpm Engine Series	3000 rpm Engine Series	Fuel samples
d <sub>8</sub> -naphthalene	✓	✓	✓	✓
d <sub>10</sub> -phenanthrene			✓	✓
d <sub>12</sub> -chrysene	✓	✓		
9-Phenylanthracene	✓		✓	✓
1,3,5-Triphenylbenzene	✓	✓		✓

Key: ✓ Internal standard added to sample

### 3.2.2.2 Extraction and Concentration of TES

The procedures developed by Trier 1988 were used for extraction and concentration of TES. Firstly, the samples were filtered under reduced pressure (Whatman GF/Fm, 5 cm). The two phases (DCM and the aqueous methanol) were separated by liquid/liquid partition. The lower DCM phase was collected in a round bottom flask (RBF, 1 l) and the remaining aqueous layer re-extracted with three aliquots of DCM (50 ml).

The DCM fraction was reduced in volume by rotary evaporation to *ca.* 250 ml before adding sodium sulphate drying agent (3 g, BDH). After a period of *ca.* 1-2 hours, the samples were filtered (Whatman A 11 cm) and reduced by rotary evaporation to leave *ca.* 0.5 ml. Samples were transferred to pre-weighed vials and the remaining solvent removed by gently passing a stream of dry nitrogen over the sample until a constant weight was recorded.

### 3.2.2.3 Open column Silica gel Fractionation

The use of gravity fed open columns packed with various stationary phases to fractionate organic samples into different polarity classes has been widely used (Snook *et al.* 1979, Lee *et al.* 1981, Robbins & McElroy 1982, Schuetzle 1983, Sorrell & Reding 1985, Liberti *et al.* 1986, and Williams *et al.* 1989). The method of Trier (1988) was modified. Difficulties in maintaining reproducibility caused by varying levels of reactive sites have been reported by Later *et al.* 1985.

To sustain the reproducibility from batch to batch and reduce irreversible adsorption, the silica (60-120 mesh, BDH) was fully activated by oven drying (24 hours, 185°C), partially deactivated to optimum activity (5% milli-Q water, w/w) and mechanically shaken for two hours.

Glass columns (200 mm x 10 mm ID, with glass frits or plugged with defatted cotton wool) were slurry packed with silica gel (3 g of silica in 20 ml hexane). A plug (*ca.* 0.5 cm in height) of sand (acid washed) was applied to the top of the silica bed. The sample (10 to 50 mg) was dissolved in hexane (*ca.* 0.5 ml) and applied to the column. The vial was rinsed thrice with hexane (*ca.* 0.5 ml) and the washings added to the column. The aliphatic class of compounds were eluted with hexane (12 ml), aromatics eluted with DCM (15 ml), and remaining polar compounds removed with methanol (25 ml). Before eluting the aromatic and polar fractions, the sample vial was rinsed with the relevant solvent thrice and washings added to the column. The different fractions collected in RBFs (50 ml) were rotary evaporated to *ca.* 0.5 ml, transferred to a pre-weighed vial, and blown down to a constant weight using a gentle stream of nitrogen. The *n*-alkanes in the aliphatic fractions and the major PAC in the aromatic fractions were analyzed by GC-FID (Section 3.2.3) and GC/MS in the EI mode (Section 3.2.4) respectively.

#### 3.2.2.4 Fuel work-up

Two fuel samples, collected during the engine sampling period, were worked-up and analyzed as follows. For each fuel sample, an aliquot of fuel (20 - 40 mg) plus a range of internal standards (Table 3.7) were fractionated by silica slurry gel adsorption chromatography (Section 3.2.2.3). The aliphatic and aromatic fractions of the fuel were analyzed by GC-FID (Section 3.2.3) and GC/MS EI (Section 3.2.4) respectively.

#### 3.2.2.5 Lubricating Oil work-up

An aliquot of fresh oil (66.3 mg) plus deuterated naphthalene (190  $\mu$ g) and deuterated phenanthrene (170  $\mu$ g) were fractionated by silica gel adsorption chromatography (Section 3.2.2.3). The aliphatic and aromatic fractions were analyzed by GC-FID (Section 3.2.3) and GC/MS EI (Section 3.2.4) respectively.

Before sump oil samples could be fractionated, the particulates in the oil had to be removed. To allow the particulates to be filtered off, the dispersants first had to be chemically broken down. This was achieved following the method of Trier (1988). Since three engine series were collected consecutively, the oil sump sample taken after the last engine series was worked-up and analyzed (corresponding to 105 hours of engine use).

An quantity of the used sump oil (0.2025 g) was placed in a conical flask. Deuterated naphthalene (200  $\mu\text{g}$ ) and deuterated phenanthrene (200  $\mu\text{g}$ ) were added. Concentrated hydrochloric acid (0.5 ml), chloroform (10 ml), and propan-2-ol (10 ml) were added, and the solution shaken. After five minutes the solution was very slowly filtered under reduced pressure (Whatman GF/F 5 cm) to remove the coagulated particulates. The filter was washed with two aliquots of chloroform (5 ml) and excess distilled water added (20 ml). The solution was then partitioned with hexane (10 ml) to extract the organics. The remaining solution was re-extracted three times with hexane (10 ml). The hexane solution was dried with sodium sulphate (3 g) and after a period of time (30 minutes) the drying agent was filtered off (Whatman A 11 cm). The hexane was reduced by rotary evaporation to *ca.* 0.5 ml. The remaining hexane was transferred to a pre-weighed vial and the hexane removed with a gentle supply of nitrogen, until a constant weight was recorded. A sub-sample (50.7 mg) of the total extract was then fractionated by silica gel adsorption chromatography (Section 3.2.2.3). The aliphatic and aromatic fractions of the sump oil were analyzed by GC-FID (Section 3.2.3) and GC/MS EI (Section 3.2.4) respectively.

#### 3.2.2.6 Recovery of Aromatic Internal Standards in TES

Table 3.8 shows the levels of the average recovery for the internal standards added to the engine series and the fuels. The samples were analyzed by GC/MS EI and the quantification was based on the response factors to undecane (Section 3.2.4). The level of recovery were high, with an average of *ca.* 86% for all the internal standards used (apart from  $\text{d}_8$ -naphthalene). The recovery results showed that future sampling could rely on  $\text{d}_8$ -naphthalene and  $\text{d}_{10}$ -phenanthrene for laboratory loss correction. The low laboratory recovery of  $\text{d}_8$ -naphthalene for some samples precluded naphthalene from the initial profiling.

Table 3.8 Laboratory Recovery for Internal Standards added to TES and Fuels

Sample	Laboratory recovery of d <sub>8</sub> -naphthalene / %	Laboratory recovery of d <sub>10</sub> -phenanthrene / %	Laboratory recovery of d <sub>12</sub> -chrysene / %	Laboratory recovery of 9-phenylanthracene / %	Laboratory recovery of 1,3,5-triphenylbenzene / %
1000 rpm	21.5	-	63.4	89.9 <sup>+</sup>	83.2
2000 rpm	5.4	-	109.0 <sup>+</sup>	-	114.8
3000 rpm	10.1	61.2 <sup>+</sup>	-	71.8	-
Fuels	49.1	84.9	-	94.1 <sup>+</sup>	89.7

Key : + indicates which internal standards used to correct the PAC quantifications for laboratory losses.

### 3.2.2.7 Laboratory Losses for n-Alkanes

The laboratory losses of selected alkanes was investigated by spiking two sets of solvent mixtures (DCM:methanol, 1:1)(800 ml) with a ten times dilution of the n-alkane standard mix (Section 3.2.3) (250 µl). The solvent mixtures were added to distilled water (800 ml) and the mixture worked-up as for TES. Following work-up, the samples were diluted with DCM to 250 µl. The areas for the alkanes from before and after work-up were compared using GC-FID (instrument details in Section 3.2.3). Table 3.9 shows that the laboratory recovery for n-alkanes of molecular weight greater than C13 are good.

Table 3.9 Laboratory Recovery of n-Alkanes from Spiking Experiment

Compound	Weight of spike added	Laboratory Recovery from Sample 1 / %	Laboratory Recovery from Sample 2 / %	Average / %
Undecane	100.0	31.7	49.0	40.4
Tetradecane	150.0	72.0	84.2	78.1
Hexadecane	87.5	86.1	93.5	89.8
Octadecane	175.0	101.8	107.9	104.9
Docosane	162.5	102.7	100.1	100.4

### 3.2.3 Quantification of n-Alkanes by Gas Chromatography with Flame Ionisation Detection

Gas chromatography with flame ionisation detection (GC-FID) is probably the most widely used GC detection system, due to the large linear range, sensitivity to virtually all organics, and stable baseline (Lee *et al.* 1981, Braithwaite & Smith 1985, Uden 1987, and Fetzer 1989).

Following the work-up and isolation of the aliphatic fraction from TES (Section 3.2), the aliphatic fraction were blow down to a constant weight. The samples (10 mg/ml in DCM) were analyzed on a Carlo Erba Mega GC fitted with a DB-5 capillary column (30 m x 0.32 mm ID, 0.25  $\mu$ m film thickness, J&W Scientific). Injection volumes were 0.5  $\mu$ l and cooled on-column injection was used. The temperature programme was: 50°C (1 min), 5°C/min to 300°C, held for 15 mins. The detector signal was recorded and integrated by a Shimadzu integrator. Hydrogen was used as the carrier gas.

The gas chromatograph was calibrated with an n-alkane standard mix (Table 3.10 & Figure 3.3). For calibration purposes the temperature ramp was increased to 10°C/minute and the top temperature reduced to 270°C without any hold time.

Table 3.10 n-Alkane standard mix used for analysis and recovery experiments

Compound	Concentration (mg/ml)
Undecane	0.40
Dodecane	0.90
Tridecane	0.35
Tetradecane	0.60
Hexadecane	0.35
Heptadecane	0.85
Octadecane	0.70
Docosane	0.65

This allowed the calibration to be rapidly checked. The quantification was based on heptadecane (Figure 3.4). The results were expressed as the weight of n-alkane emitted relative to the amount of that n-alkane in the fuel (Section 4.2.1).

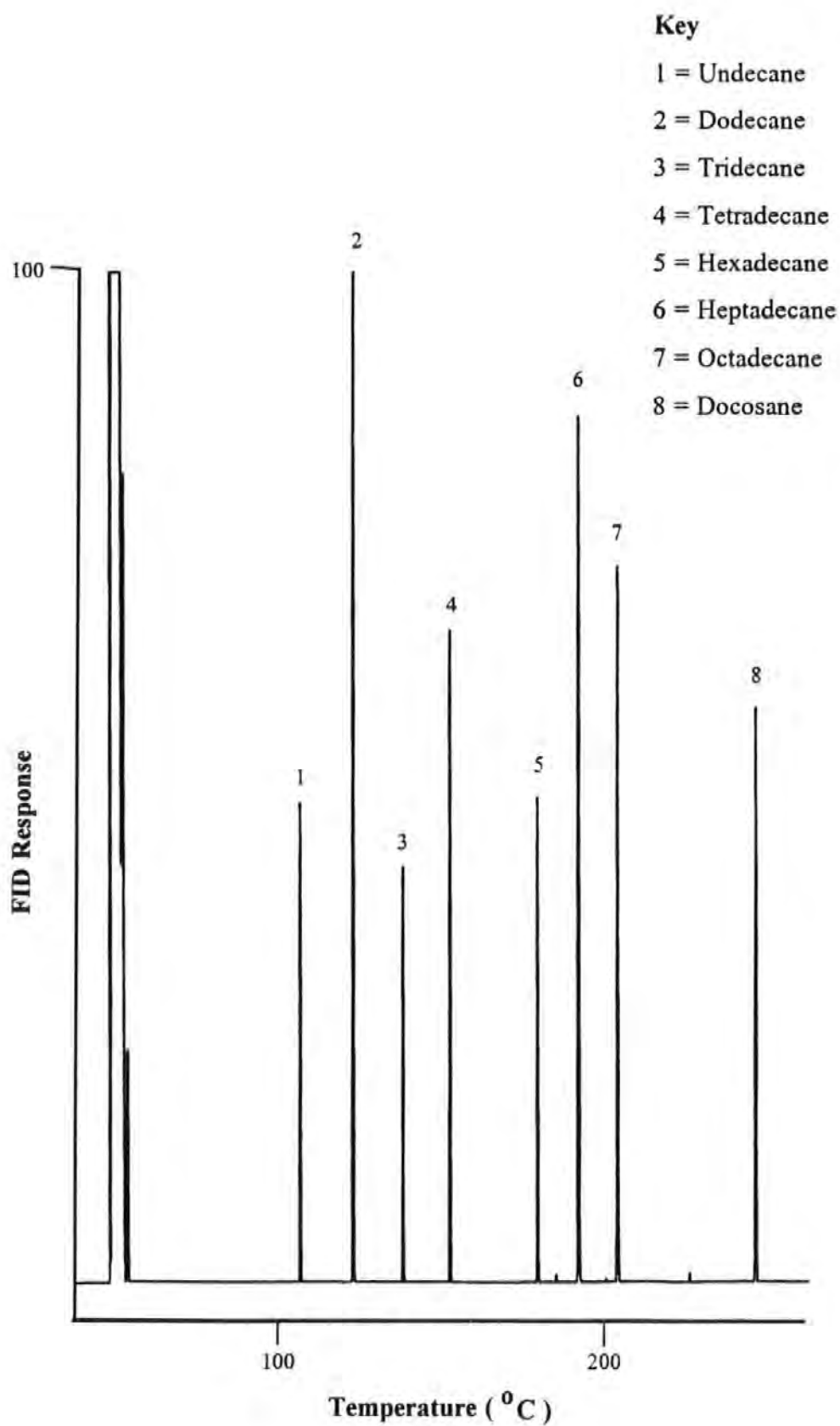
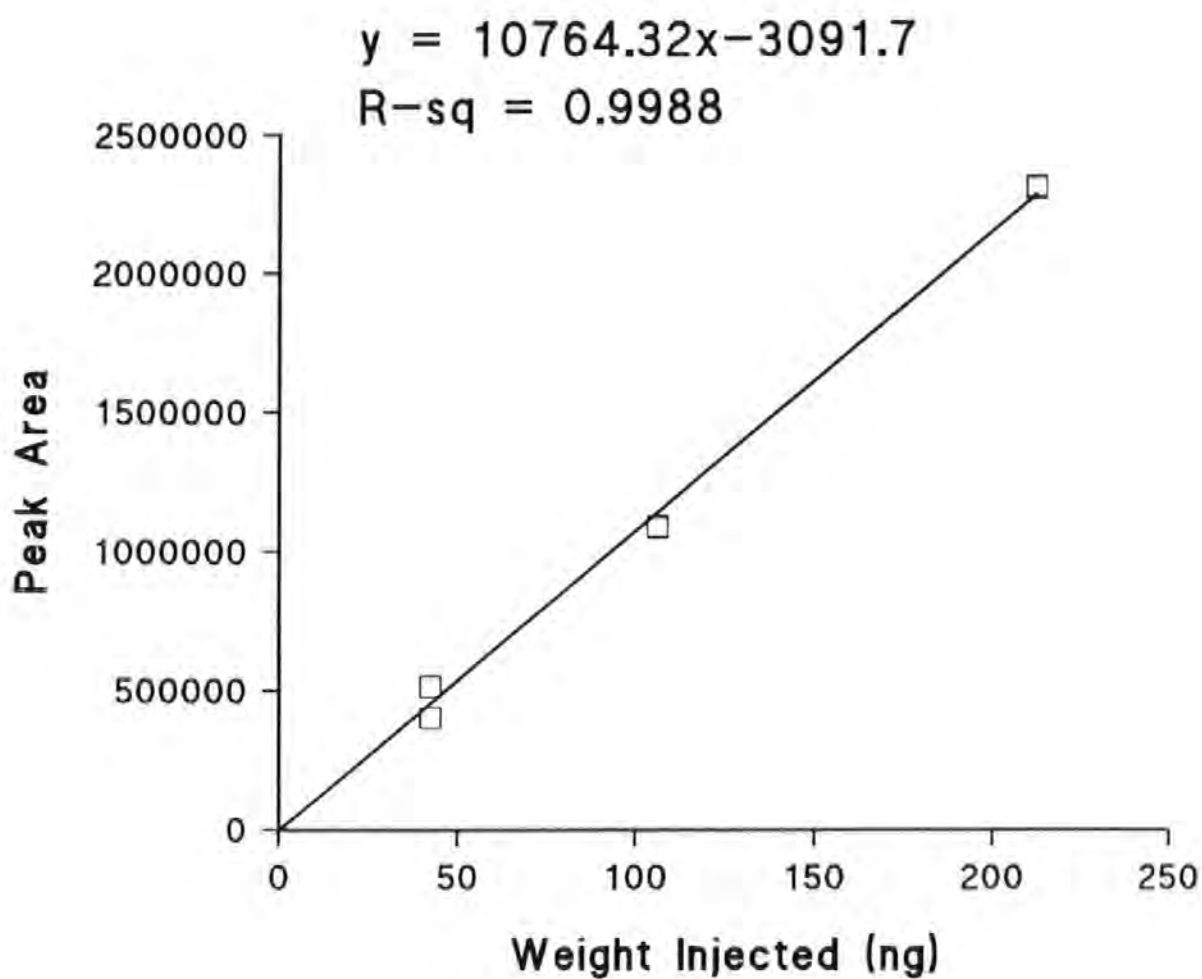


Figure 3.3 Gas Chromatogram of the n-alkane standard mix. GC conditions: DB-5 column, 50°C for 1 min, 10°C/min. upto 270°C.



*Note: Duplicate injections at each weight*

Figure 3.4 Calibration curve for heptadecane using gas chromatography with flame ionisation detection.

#### 3.2.4 Quantification of Major PAC by Gas Chromatography/Mass Spectrometry operated in the Electron Impact mode

Gas chromatography/mass spectrometry (GC/MS) operated in the electron impact (EI) mode is a powerful analytical tool for PAC analysis (Snook *et al.* 1979, Lee *et al.* 1981, Schuetzle 1983, Hites 1989, and Castello & Gerbino 1993). The mass spectrometer detector allows a far greater confirmation of compounds than GC retention data alone.

The aromatic fractions (5 mg/ml in DCM) from the silica gel clean-up were analyzed for major PAC using a Carlo Erba 5160 gas chromatograph connected to a Kratos MS25 EI mass spectrometer and managed by a Kratos DS90 computer system. A Supelchem PTE-5 fused-silica capillary column (25 m x 0.32 mm ID, film thickness of 0.25  $\mu\text{m}$ ) was used. The following chromatographic conditions were applied: 40°C (1 min.), 6°C/min. to 300°C, held for 15 mins., cooled on-column injection, detector temperature of 300°C, helium carrier gas, ionizing potential at 40 eV with scanning from 40-568 amu every 2 sec. Injection volumes were 0.5  $\mu\text{l}$ .

Under low ionisation potential the major ions for PAC are those of the molecular ion. Scanning the total ion chromatogram (TIC) for molecular ions within the retention window for compounds (derived from the standard mix) greatly aids the identification of PAC (Figure 3.5). Different compounds fragment in a unique spectra, providing more confident identifications than purely retention matches, when the spectra of peaks matches the spectra of standards (Figure 3.6). Methyl-PAC were also identified on a molecular ion basis (Figure 3.7). The peak areas were manually integrated, with each methyl-PAC separately integrated.



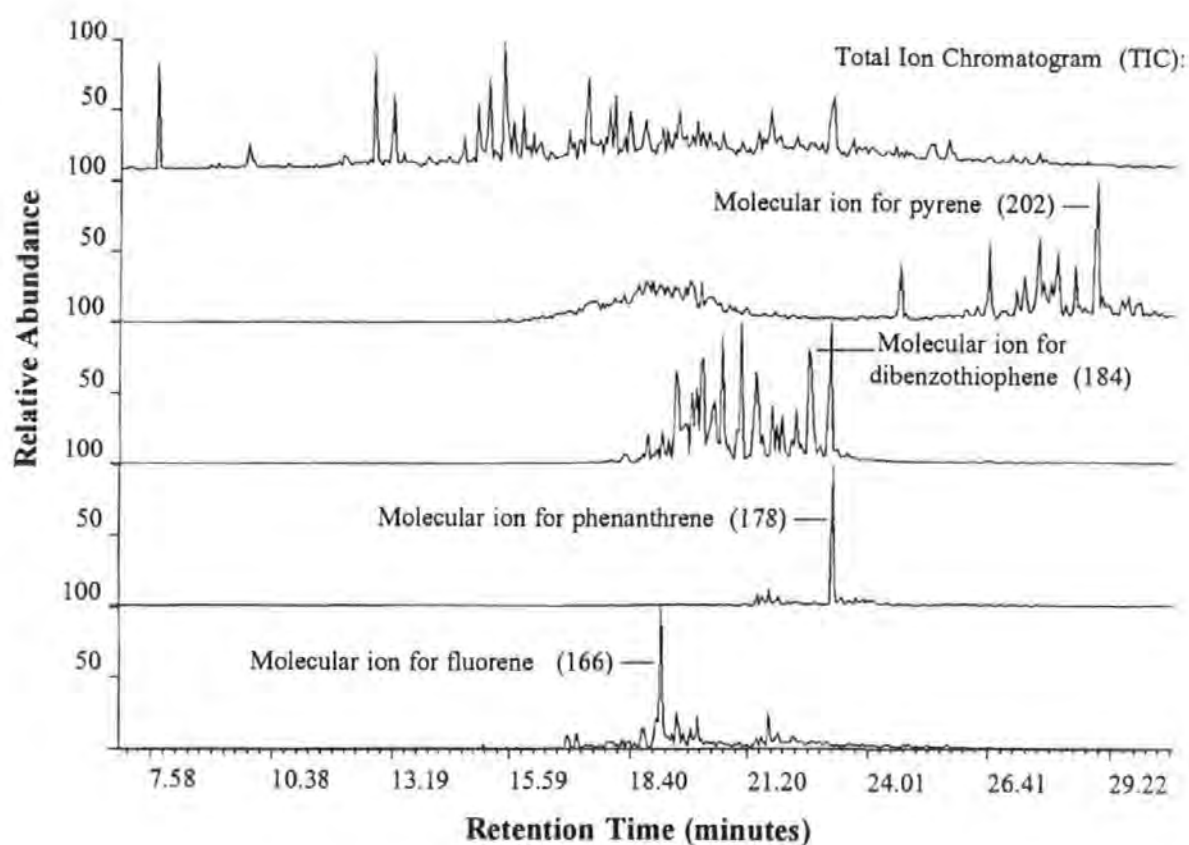


Figure 3.5 The identification of PAC on a retention and molecular ion basis. GC conditions: PTE-5 column, 40°C for 1 min., 6°C/min. upto 300°C, held for 15 mins.

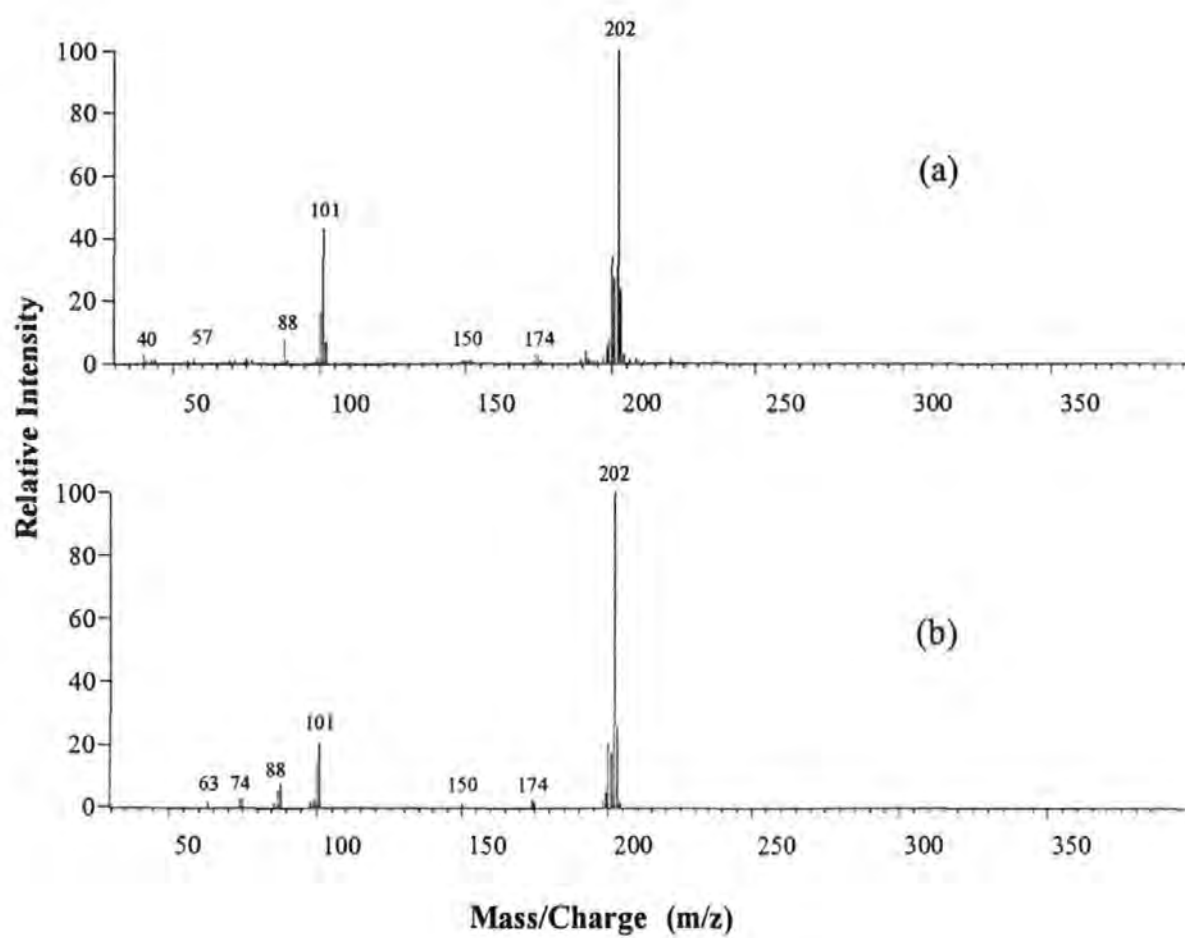


Figure 3.6 The confirmation of pyrene by matching the spectra in the sample (a) to that of the standard spectra stored in the computer library (b).

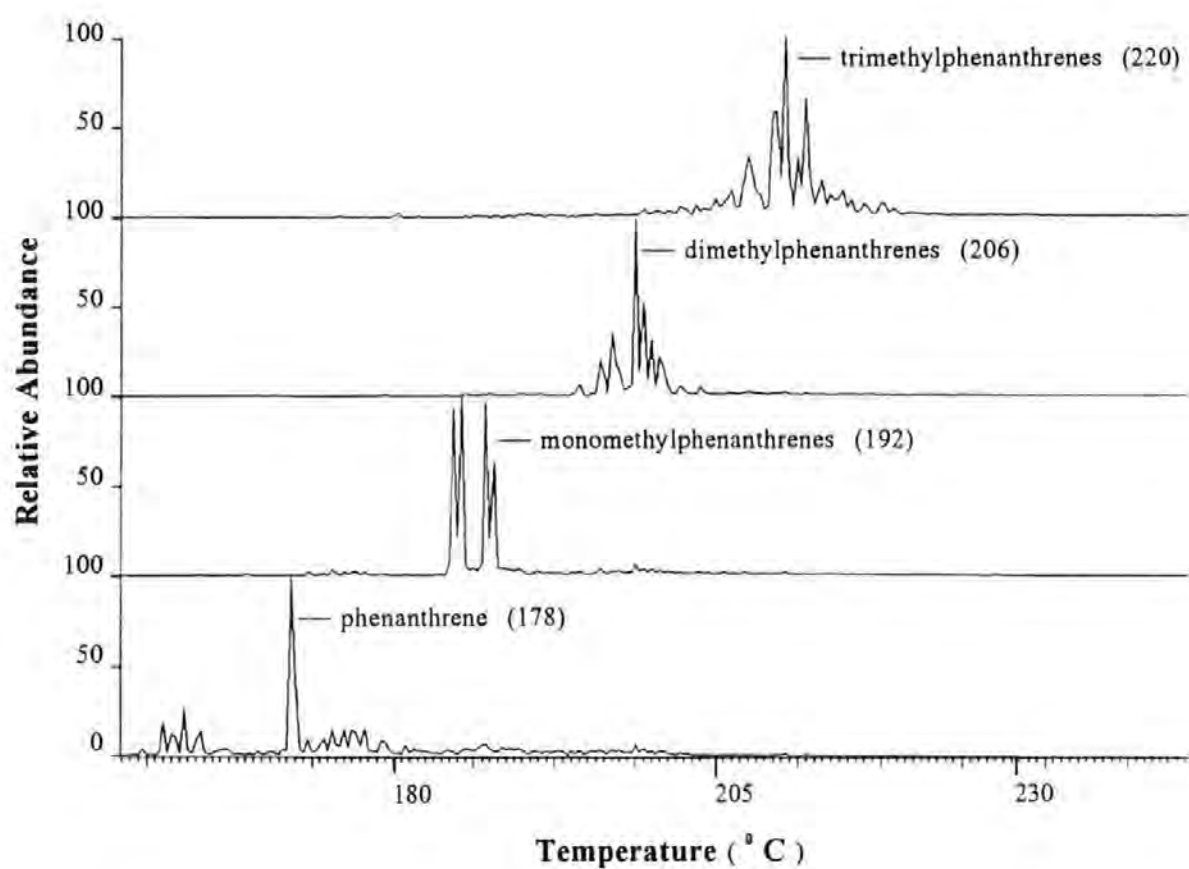


Figure 3.7 Identification of phenanthrene and methylphenanthrenes by the respective molecular ions, 178 = phenanthrene, 192 = monomethylphenanthrenes, 206 = dimethylphenanthrenes, and trimethylphenanthrenes = 220. GC conditions: PTE-5 column, 40°C for 1 min., 6°C/min. upto 300°C, held for 15 mins.

Quantification was based on response factors to a GC/MS undecane internal standard (stock concentration of 200 µg/ml) with a quarter of the 5 mg/ml sample dilution derived from the undecane solution. Internal standard quantification removes the problem of the ionisation changing for different samples, since the internal standard follows the behaviour of the compounds of interest (Reece & Scott 1987). The response factors were calculated with a standard mix containing undecane, 16 EPA PAH priority pollutants, dibenzothiophene, 9-phenylanthracene, and 1,3,5-triphenylbenzene (Table 3.11 and Figure 3.8).

The integration of undecane by the molecular ion was found to be unreliable since undecane fragments severely, and undecane was quantified using the TIC area, since there was good resolution from any interfering ions. After correcting for laboratory losses (using the internal standards identified in Table 3.8) the PAC emissions were expressed relative to the PAC in the fuel (Section 4.2.1).

Table 3.11 Response factors of PAC to Undecane

Compound	Response factor #1	Response factor #2	Average Response factor
Naphthalene	0.242	0.206	0.224
Fluorene	0.253	0.207	0.230
Dibenzothiophene	0.319	0.306	0.313
Phenanthrene	0.278	0.249	0.264
Pyrene	0.295	0.256	0.276

# Key

1 = Undecane	11 = 9-Phenylanthracene
2 = Naphthalene	12 = Benzo(a)anthracene
3 = Acenaphthene	13 = Chrysene
4 = Acenaphthylene	14 = Benzo(j&k)fluoranthene
5 = Fluorene	(not resolved)
6 = Dibenzothiophene	15 = Benzo(a)pyrene
7 = Phenanthrene	16 = 1,3,5-Triphenylbenzene
8 = Anthracene	17 = Indeno(1,2,3-cd)pyrene
9 = Fluoranthene	18 = Benzo(ghi)perylene
10 = Pyrene	19 = Dibenzo(a,h)anthracene

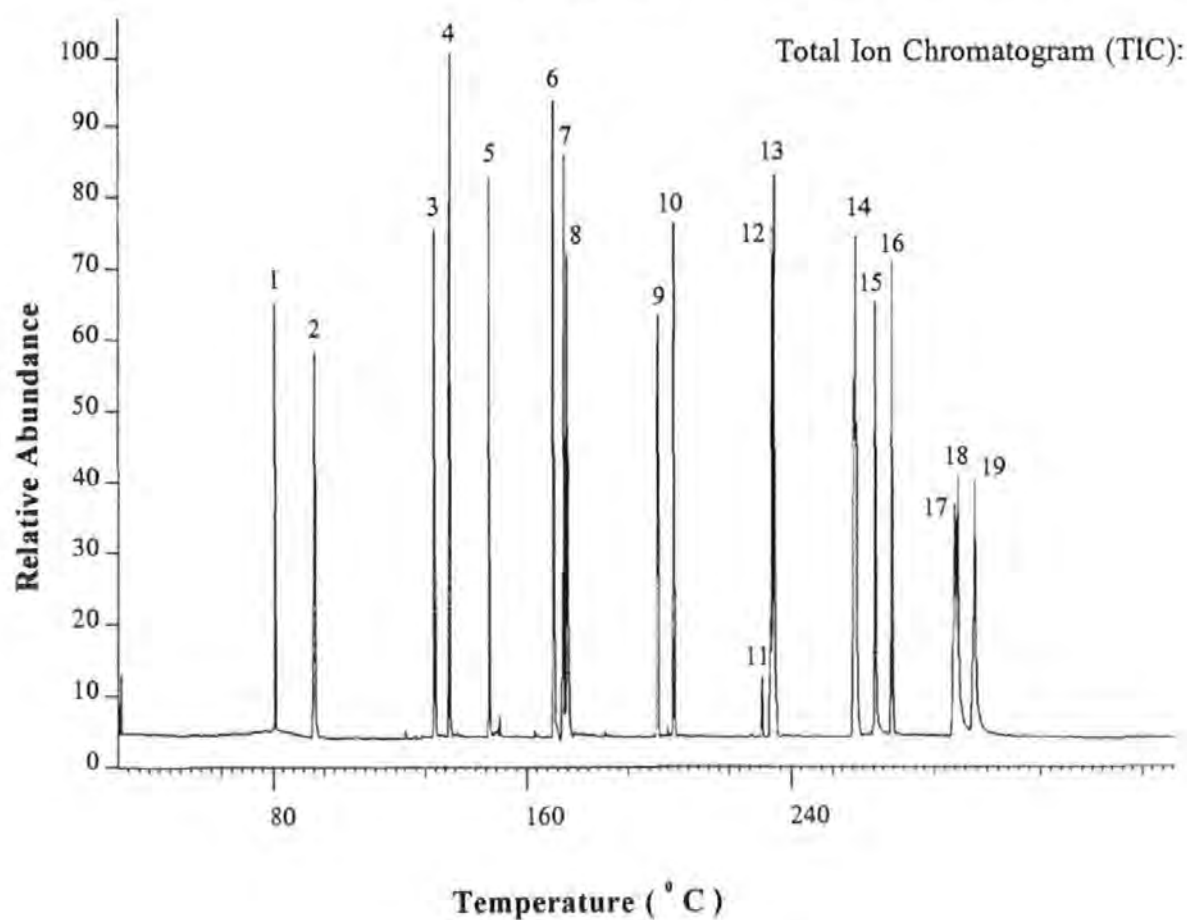


Figure 3.8 Total ion chromatogram of the standard PAC mix used for the primary PAC profiling. GC conditions: PTE-5 column, 40°C for 1 min., 6°C/min. upto 300°C, held for 15 mins.

### **3.3 Relocation and Modification of TESSA**

Following re-location of TESSA due to departmental re-arrangements, a substantial part of the research was allocated to upgrading the TESSA system. The improvements are documented in Section 3.3.1 and the initial testing of the new system is reported in Section 3.3.2.

#### **3.3.1 Improvements to the Engine Sampling Rig**

One of the first improvements to TESSA was to commission welding of stainless steel flanges to the three sections of tower; greatly improving the sealing of the tower. Polytetrafluoroethylene cord (soxhlet extracted for 24 hours with DCM) was placed between the flanges and the sections tightened with 8 self tightened screws. The flanges enable TESSA to be easily stripped down and maintained. The flange system enables the bottom section to be rotated by 180° to allow another engine to be sampled by TESSA. The new system also allows an extended transfer pipe to be installed between the engine and TESSA, enabling post-combustion reactions to be increased (Section 6.3). The dynamometer was mounted on a track, allowing a parallel future engine to be controlled.

Whilst TESSA was modified, the glass tubing normally inside the middle section of the tower were removed and thoroughly cleaned in Decon-90, as were the insides of the tower section. It was noted that the inside of TESSA and the glass tubing showed little evidence of any deposits.

One of the drawbacks of the gravity feed solvent system was that in order to maintain a constant flow rate for each sample, the solvent reservoir had to be filled for each sample. If this was not the case, the solvent flow would decrease with sampling, and could lead to differential sampling efficiencies. In an attempt to overcome the gravity feed problem, a greater head pressure was generated by forcing the solvent mixture from the reservoir using compressed air.

To improve the collection efficiencies a spray head arrangement was designed to finely disperse the solvent mixture within the oncoming exhaust (Plate 1). The plate positioned close to the exit of the tube deflects the solvents upwards, creating a fine spray. The shape of the spray was visualized using water, and the spray adjusted by altering the gap between the end of the tube and the deflector plate. The spray was set such that the solvents avoided impinging on the sides of the tower. The solvent flow rate was controlled by a precision flow controller, and solvent flow rates for varying reservoir pressures and flow controller settings were established. From these experiments it was found that a pressure of 0.6 Bar and five turns on the flow-controller would provide a flow rate of 1 l/min.

Since exhaust cooling may increase collection efficiencies (Kruzel *et al* 1991), a number of different cooling arrangements were attempted. The first method was to immerse the solvent reservoir in a mixture of ice and sodium chloride. This mixture produced temperatures as low as -20°C. However, problems were encountered with regards to achieving an even cooling of the reservoir, loading/unloading the cooling mixture and the potential for corrosion of the solvent reservoir. This led to chilling the solvent mix overnight in the freezer (-20°C), followed by filling the reservoir immediately before sampling. The cooling mixture (ice:sodium chloride) was used successfully in the chiller tank, decreasing the temperature of the cooling water around TESSA from 4°C (ice only) to between 0°C and -5°C.

The upgraded set-up enabled the tower to be wall-mounted closer to the engine exhaust manifold, allowing a shorter transfer pipe to be fitted (Plate 2). The switching system for transferring the exhaust from the main exhaust to the TESSA was upgraded to an compressed air activated device.

A thermometer was installed in-line with the engine air intake. This along with taking the humidity of the test-cell during sampling sessions allowed the effect of the test cell environment to be taken into consideration.

The overall engine test bay, showing the position of TESSA relative to the engine, is illustrated by Plate 3.



Plate 1 The spray head attachment used to evenly disperse the solvents with the oncoming exhaust.

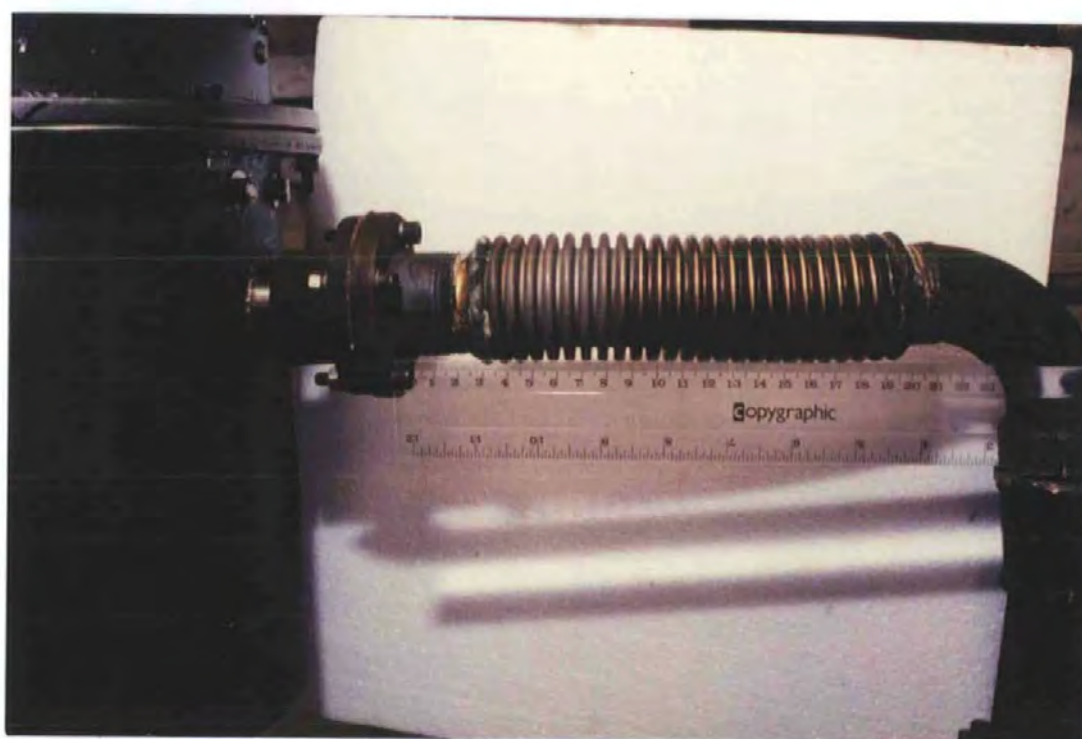


Plate 2 The transfer line from the engine to TESSA.





#### Key

- 1 = TESSA
- 2 = Engine rig
- 3 = Dynamometer controller
- 4 = Fuel tank

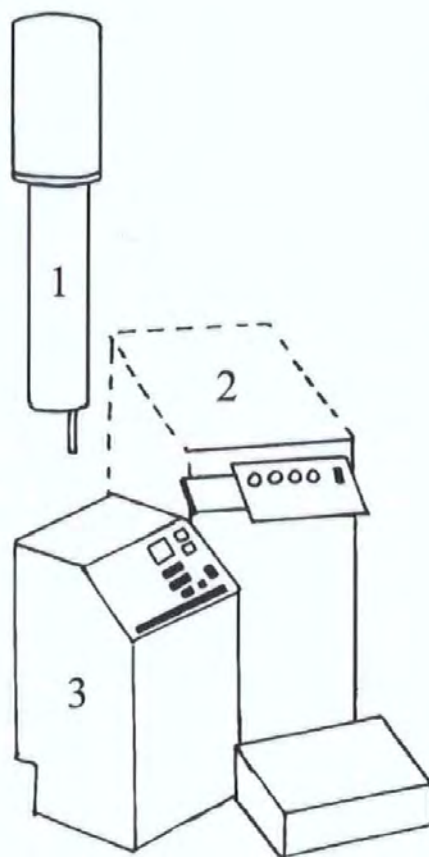


Plate 3 The overall engine test bay, showing the upgraded TESSA.

### 3.3.2 Initial Testing of the Upgraded TESSA

The introduction of a pressurized solvent feed system to TESSA was aimed at eliminating the necessity to fill the solvent reservoir for each sampling position. However, initial testing showed that the quantity of solvent collected for consecutive runs was not the same. This was due to pressurization of the solvent mix, causing the DCM component of the solvent mix to volatilise, and be lost from the solvent supply system. This volatility problem was exaggerated with the period of time the solvent was exposed to the compressed air. This necessitated a return to filling the reservoir for each sample. However, the procedure for filling the solvent reservoir was far simpler than with the initial TESSA system. The initial configuration of TESSA required raising/lowering the solvent reservoir to a mounting point above the top of TESSA.

After repeated washing of the tower with solvent mixture, through both solvent inputs, the upgraded TESSA was evaluated. Initially sampling was at 1000 rpm and at 1%, 8%, 17%, and 25% of full engine load. The solvent reservoir was filled for each sample with 600 ml of solvent mix. The solvent flow through the spray head was started 10 seconds before the exhaust was sampled for 15 seconds using TESSA. The residual solvent was used to wash the tower down. This initial testing was used to compare the extraction efficiency of the upgraded TESSA system with the initial TESSA configuration, and to investigate further the effect of low loads and speeds on the emissions. The samples were worked-up and the aromatic fractions isolated following the procedures detailed in Section 3.2.2. The aromatic fractions were analyzed by the Carlo Erba GC-FID (instrument details in Section 3.2.3) and fluorene was quantified relative to  $d_{10}$ -fluorene (98%, British Greyhound), after laboratory loss correction using  $d_{10}$ -phenanthrene (97%, Aldrich Chemical Co.). The recovery of fluorene in the exhaust relative to the fluorene in the fuel burned, was 0.91% at 1% of full load and 0.26% at 25% of full load for the initial TESSA configuration. The value for the upgraded TESSA was 0.96% at 1% of full load and 0.28% at 25% of full load. This showed that the new system was working as effectively as the old configuration. The examination of the effect of low loads at low speed on combustion characteristics, is discussed in the subsequent chapters.

### 3.4 Profiling of Secondary Emissions using the upgraded TESSA

The profiling of the secondary emissions was aimed ultimately at the highly mutagenic nitro-PAC, but some preliminary investigations into the emissions of oxy-PAC were performed. The overall procedure for the secondary emission profiling research is shown in Figure 3.9. The engine sampling for nitro-PAC, work-up, and analysis are detailed in Sections 3.4.1, 3.4.2 and 3.4.3 respectively.

#### 3.4.1 Engine Sampling for Nitro-PAC Profiling

Sampling for nitro-PAC was proposed to cover a wide range of NO<sub>x</sub> conditions, in order to examine the nitration potential of diesel combustion. As can be seen from Figure 3.10 engine load is strongly correlated with NO<sub>x</sub>, whereas engine speed has a smaller effect. As a consequence of the large variation in NO<sub>x</sub> with engine load, the initial sampling for nitro-PAC was carried out at mid-speed (2500 rpm) and low-, mid-, and high-NO<sub>x</sub> positions (Section 3.4.1.1). Later engine sampling was undertaken at 1500 rpm and 3500 rpm, and at the same NO<sub>x</sub> positions (Section 3.4.1.2).

##### 3.4.1.1 Engine Sampling for Nitro-PAC at 2500 rpm

The tower was cooled using ice and sodium chloride in the chiller. The solvents were cooled overnight in a freezer (-20°C). The engine was conditioned for one hour at 3000 rpm and 90 Nm. The load positions corresponding to low-, mid-, and high-NO<sub>x</sub> were calculated from the NO<sub>x</sub> engine map (Rhead *et al.* 1991). The engine was conditioned for 30 minutes at the chosen NO<sub>x</sub> position. The longer conditioning time, compared to that used for the primary emission profiling, was to ensure that the oxides of nitrogen had reached equilibrium (Pipho *et al.* 1991). The solvent reservoir was filled with 0.8 L of each solvent, and the solvent flow rate set to 1 l/min using the reservoir pressure and flow controller. The solvent flow was started 20 seconds before switching the exhaust into TESSA and the exhaust was sampled for 50 seconds. The remaining solvent was used to wash the tower down.

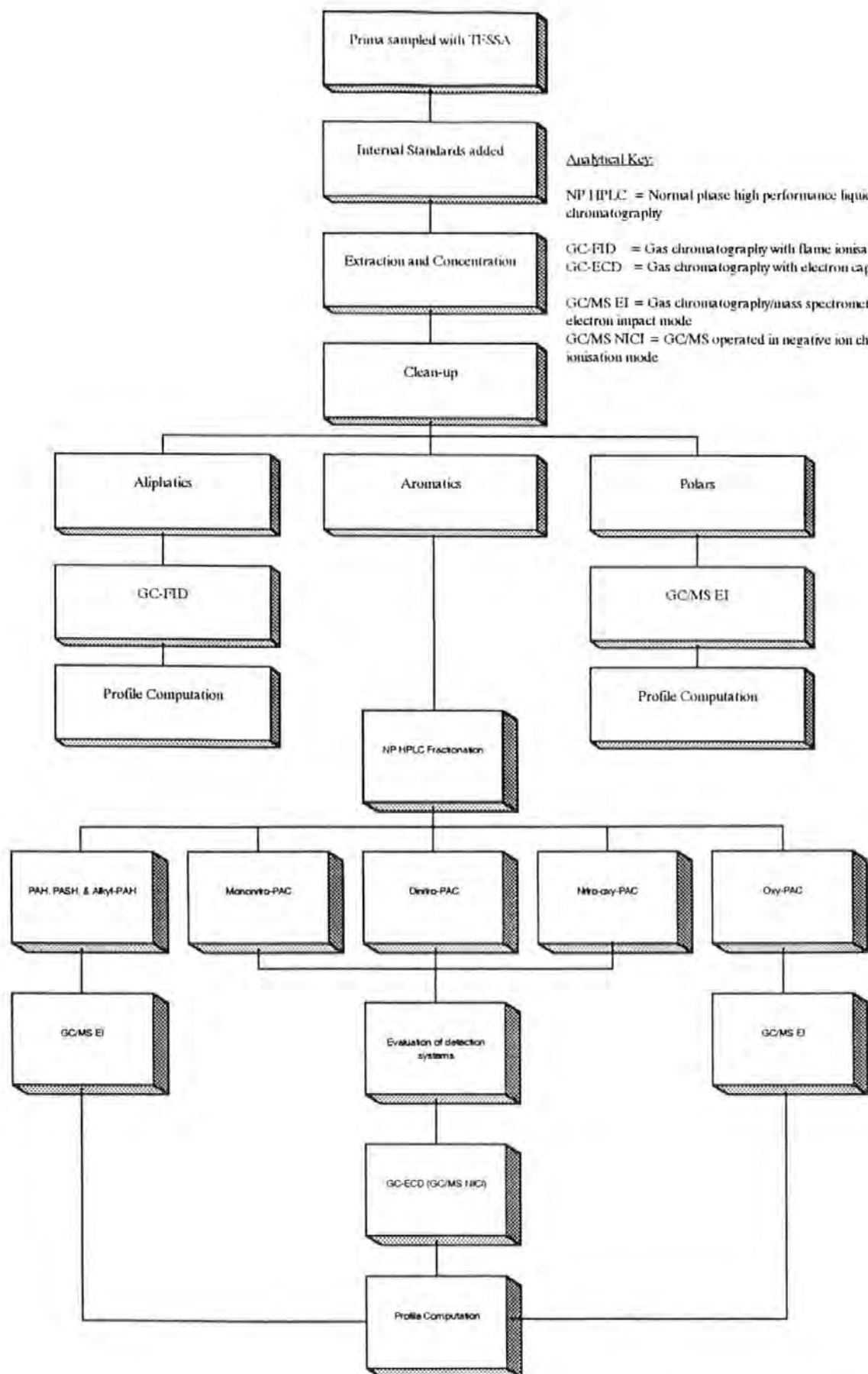


Figure 3.9 The overall experimental procedure aimed at profiling the secondary nitro- and oxy-PAC.

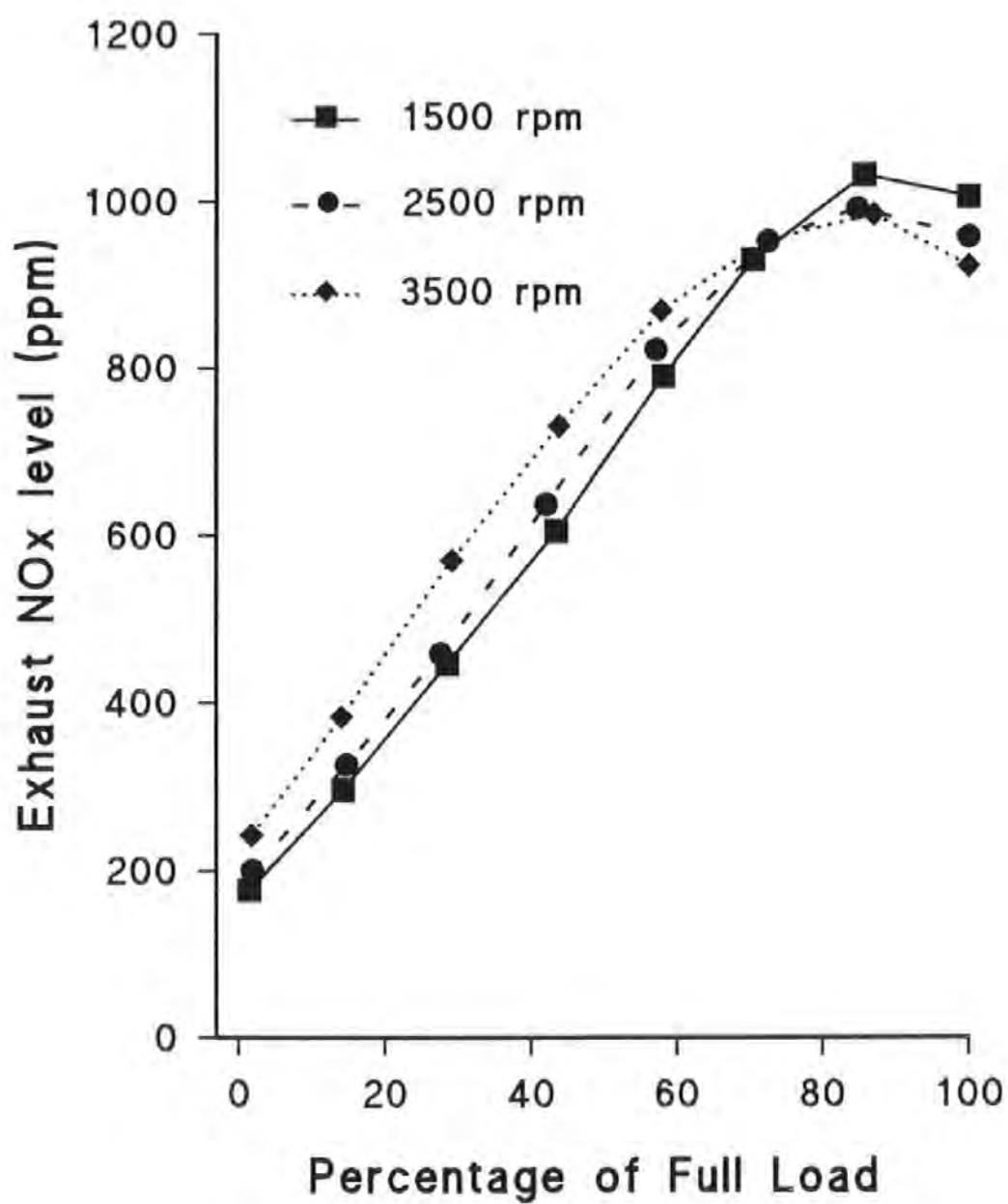


Figure 3.10 The effect of engine speed and load on the gaseous oxides of nitrogen,  $\text{NO}_x$ .

Following the addition of  $d_8$ -naphthalene and  $d_{10}$ -phenanthrene internal standards for the laboratory loss correction of major PAC, the samples were worked-up following the procedures detailed in Section 3.4.2. For each set of duplicate engine samples, fuel, sump oil and bosch samples were taken. Full details of sampling at 2500 rpm are given in Table 3.12.

Table 3.12 Engine sampling for nitro-PAC at 2500 rpm

	Low- NO <sub>x</sub> #1	Low- NO <sub>x</sub> #2	Mid- NO <sub>x</sub> #1	Mid- NO <sub>x</sub> #2	High- NO <sub>x</sub> #1	High- NO <sub>x</sub> #2
Percentage of full load	1.4	1.4	50	50	85	85
Fuel consumption (ml/min)	30.73	31.10	74.07	73.17	111.61	110.38
Air intake temperature °C	17	18	16	16	22.5	23.0
Chiller temperature °C	-5.0	-4.0	-5.4	-5.2	0.3	0.3
Water temperature °C	96	97	96	95	100	100
Oil temperature °C	54	56	52	53	62	62
Bosch No.	1.35		0.98		2.59	
Humidity %	62.9	63.1	44.3	45.2	36.5	36.7
Weight of $d_8$ -naphthalene added (µg)	220	220	220	220	540	540
Weight of $d_{10}$ -phenanthrene added (µg)	165	165	165	165	420	420

### 3.4.1.2 Engine Sampling for Nitro-PAC at 1500 rpm & 3500 rpm

The sampling procedure at 1500 rpm and 3500 rpm was the same as used for 2500 rpm, with the following exceptions. Firstly, fresh oil was used before sampling at 1500 rpm. Secondly, at 1500 rpm, exhaust samples were taken at low-NO<sub>x</sub> and mid-NO<sub>x</sub> on the same day. The next sampling session at 3500 rpm also sampled low-NO<sub>x</sub> and mid-NO<sub>x</sub> sampling positions on the same day. Thirdly, the high-NO<sub>x</sub> samples at 1500 rpm and 3500 rpm were taken on the same day. Following the addition of  $d_8$ -naphthalene and  $d_{10}$ -phenanthrene internal standards for major PAC laboratory loss correction, the samples were worked up as documented in Section 3.4.2. Fuel, sump oil, and bosch samples were taken on each sampling day (full sampling details given in Tables 3.13 & 3.14).

Table 3.13 Engine sampling for nitro-PAC at 1500 rpm

	Low- <sup>†</sup> NO <sub>x</sub> #1	Low- <sup>†</sup> NO <sub>x</sub> #2	Mid- <sup>†</sup> NO <sub>x</sub> #1	Mid- <sup>†</sup> NO <sub>x</sub> #2	High- NO <sub>x</sub> #1	High- NO <sub>x</sub> #2
Percentage of full load	1.8	1.8	50	50	85.6	85.6
Fuel consumption (ml/min)	16.42	16.68	39.28	38.94	62.11	62.42
Air intake temperature °C	22	23	22	23	24	23
Chiller temperature °C	-1.1	2.4	4	3.9	-0.5	-0.1
Water temperature °C	95	95	98	97	100	98
Oil temperature °C	48	47	50	52	50	51
Bosch No.	0.93		1.24		3.27	
Humidity %	33.4	33.5	32.2	31.4	50.1	51.5
Weight of d <sub>8</sub> -naphthalene added (µg)	110	110	270	270	460	460
Weight of d <sub>10</sub> -phenanthrene added (µg)	112	112	210	210	303	303

<sup>†</sup>Collected on same day

Table 3.14 Engine sampling for nitro-PAC at 3500 rpm

	Low- <sup>‡</sup> NO <sub>x</sub> #1	Low- <sup>‡</sup> NO <sub>x</sub> #2	Mid- <sup>‡</sup> NO <sub>x</sub> #1	Mid- <sup>‡</sup> NO <sub>x</sub> #2	High- <sup>*</sup> NO <sub>x</sub> #1	High- <sup>*</sup> NO <sub>x</sub> #2
Percentage of full load	1.6	1.6	29	29	87	87
Fuel consumption (ml/min)	49.78	50.86	85.11	86.51	172.21	173.31
Air intake temperature °C	23	24	24	24	28	27
Chiller temperature °C	-1.0	-1.0	-0.8	-0.9	1.3	1.8
Water temperature °C	100	100	100	100	110	115
Oil temperature °C	72	70	70	70	90	92
Bosch No.	2.70		2.06		5.75	
Humidity %	33.5	32.5	31.4	31.2	50.0	49.0
Weight of d <sub>8</sub> -naphthalene added (µg)	416	416	624	624	819	819
Weight of d <sub>10</sub> -phenanthrene added (µg)	418	418	543	543	707	707

<sup>†</sup>Collected on same day for that speed

<sup>‡</sup>Collected on same day for that speed

<sup>\*</sup>Collected on same day as the high-NO<sub>x</sub> samples at 1500 rpm



### 3.4.2 Sample Work-up for Nitro-PAC

The sample work-up for the secondary emission samples followed all the preparation measures employed for the primary emission profiling. Due to the nitro-PAC being photo sensitive (Stärk *et al.* 1985), all work-up was carried out under red light, or alternatively, all apparatus wrapped in foil. All nitro- and oxy-PAC standards were obtained from Aldrich Chemical Co. and were greater than 97% in purity.

The work-up procedure for exhaust samples consisted of a modified extraction and concentration procedure to reduce the possibility of nitrating the samples (Section 3.4.2.1). The samples taken at 2500 rpm were subjected to a simple cartridge clean-up to remove the aliphatics; whereas the silica gel clean-up for the samples at 1500 rpm and 3500 rpm removed the aliphatics and polars (Section 3.4.2.2). The aromatic fractions containing the nitro-PAC were further fractionated using normal-phase HPLC to isolate specific PAC classes (Section 3.4.2.3). The work-up procedures for fuel and oil samples are given in Section 3.4.2.4. The estimation of laboratory losses for nitro-PAC during the exhaust work-up procedure is detailed in Section 3.4.2.5.

#### 3.4.2.1 Extraction and Concentration of Exhaust Samples for Nitro-PAC Profiling

The potential of the aqueous methanol phase to nitrate the organics presence in the DCM fraction was considered a possibility, since the aqueous phase may contain nitric acid, a powerful nitration agent (Nielsen 1984). With the aim of reducing the nitration possibility, the samples were partitioned first and filtered second. This was the opposite way to the profiling of the primary organics. The reversal of the steps meant that the organics could be rapidly removed from the aqueous phase. The concentration and drying procedures were as for the primary organics work-up (Section 3.2.2.2).

The nitration potential of the methanol phase was checked for engine samples taken at 1500 rpm and 3500 rpm. After completing removing the DCM fractions, an aliquot (20 - 40 ml) of the aqueous methanol layer was removed for pH testing. The pH varied between 3.15 and 4.13 for samples.



The remaining aqueous methanol was spiked with the standard PAH mix (100  $\mu$ l) used for GC/MS analysis of major PAH and PASH (Section 3.2.4). The solution was vigorously shaken and left for 24 hours. The aqueous methanol fraction was then extracted three times with DCM (20 ml). The solvent was dried with sodium sulphate (1 g, BDH), filtered (Whatman A 11 cm), and reduced by rotary evaporation to *ca.* 0.5 ml. After transferring to a pre-weighed vial the remaining solvent was removed with a gentle flow of nitrogen. The total extracts were cleaned-up using glass columns packed with silica gel (Section 3.4.2.2.2) and the mononitro-PAC fraction isolated by normal-phase HPLC (Section 3.4.2.3). After removing the solvent from the HPLC fractionation and diluting with acetonitrile (50  $\mu$ l), the nitration check was examined by GC-ECD (refer to Section 3.4.3.1.4 for full details of GC-ECD). The presence of nitro-PAC was checked by co-injection of the nitration check with the mononitro-PAC standard mix. The results were compared with the solvent blank (Figures 3.11 & 3.12). There was no evidence for any nitro-PAC being formed from the aqueous methanol fraction.

#### 3.4.2.2 Clean-up of TES

To aid the detection of the trace nitro-PAC, a greater isolation and concentration step of the nitro-PAC was required than was needed for the detection of major aromatics. The desired fractionation scheme was for a simple cleanup step to remove the aliphatics, and then apply the aromatics to HPLC fractionation to isolate the nitro-PAC fractions of interest. Initially a simple cartridge clean-up step was used (Section 3.4.2.2.1). However, interference problems associated with aliphatic compounds were later found for the analysis of the mononitro-PAC HPLC fractions by GC-ECD. This led to reverting back to the silica gel glass column clean-up method with modified solvent elution volumes (Section 3.4.2.2.2).

##### 3.4.2.2.1 Octadecylsilane Cartridge Clean-up

One method of achieving the desired clean-up was previously used by Obuchi *et al.* (1984). This method used octadecylsilane (ODS) cartridges to retain the aliphatic components of crude oils, whilst eluting the aromatics. This method was tested using ODS Sep-Pak cartridges (Millipore, sorbent mass of 360 mg) attached to a 20 ml glass syringe and using diesel fuel as a test sample. Diesel fuel (48.7 mg) was applied to the column and the vial washed with acetonitrile (0.5 ml), and the washings applied to the cartridge.

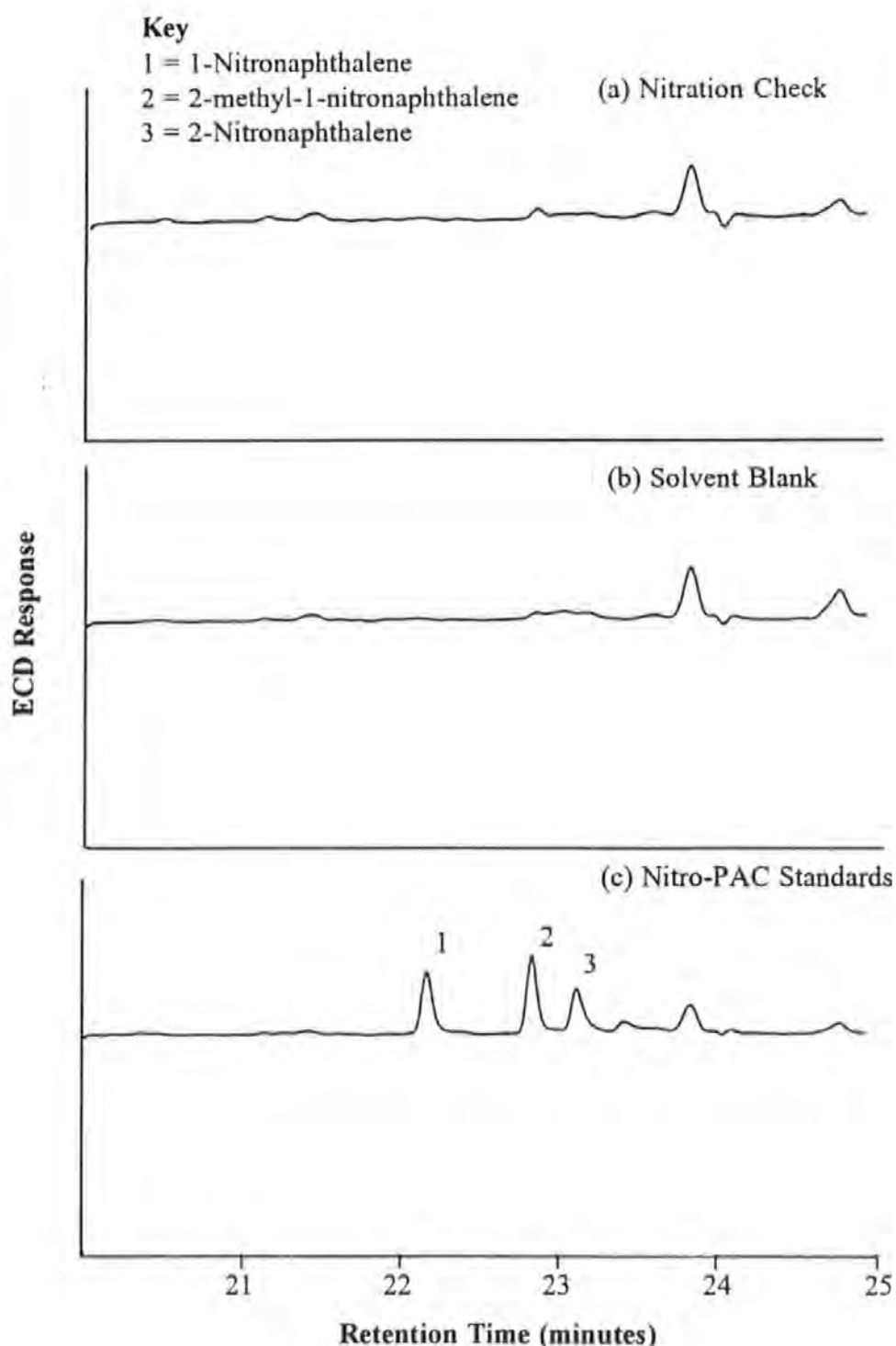


Figure 3.11 The evaluation of the acidic aqueous methanol phase for the formation of nitronaphthalenes. The comparison of the nitration check phase (a) to both the solvent blank (b) and the mononitro-PAC standard mix (c) proved there was no such nitration occurring. (Chromatographic conditions given in Section 3.4.3.1.4.1).

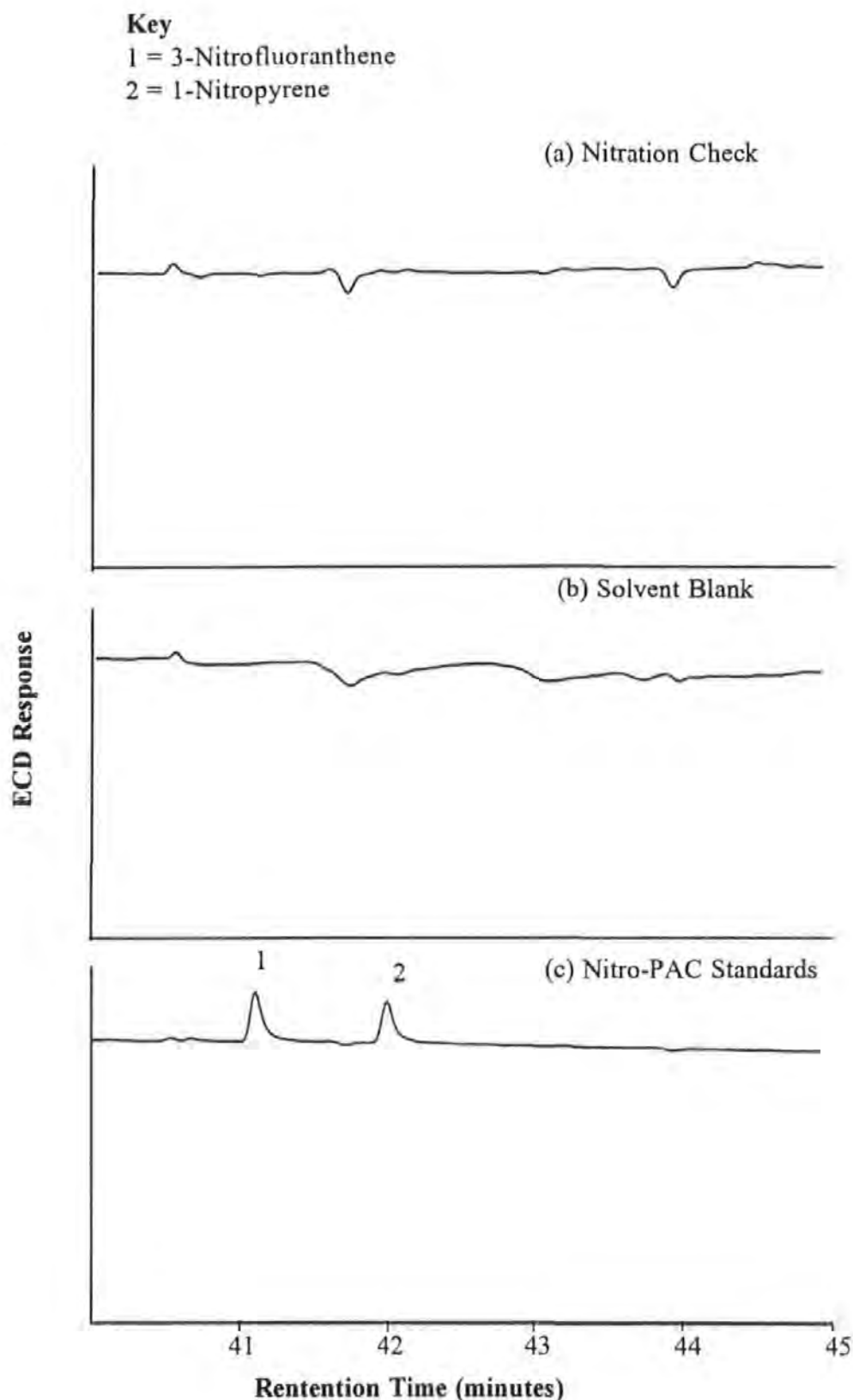


Figure 3.12 The evaluation of the acidic aqueous methanol phase for the formation of 3-nitrofluoranthene and 1-nitropyrene. The comparison of the nitration check (a) to both the solvent blank (b) and the mononitro-PAC standard mix (c) proved there was no such nitration occurring. (Chromatographic conditions given in Section 3.4.3.1.4.1).

The cartridge was slowly eluted with 0.5 ml increments of acetonitrile and the fractions collected. The results shown that as little as 1 to 2 ml of acetonitrile was sufficient to co-elute the aliphatics with aromatics.

However, when a TES was used a far greater separation was achieved after 5 - 6 ml of acetonitrile. A similar effect was found by Obuchi *et al* (1984). The eventual procedure for the ODS clean-up was to apply the exhaust sample (ca. 25 - 48 mg) dissolved in acetonitrile to a pre-rinsed cartridge (20 ml of hexane, followed by 20 ml of DCM, and finally 20 ml of acetonitrile). The sample was then pushed onto the cartridge and the aromatics eluted with acetonitrile (6 ml). There was some breakthrough of some lower molecular weight *n*-alkanes. It was envisaged that the small breakthrough of aliphatics would be removed with the major PAH fraction from the HPLC fractionation, and the small aliphatic co-elution would not hinder the identification of major aromatics by GC/MS.

However, the analysis of one from each of the duplicate HPLC mononitro-PAC fractions from the 2500 rpm sampling, by GC-ECD (refer to Sections 3.4.2.3 and 3.4.3.1.4 for details of HPLC fractionation and GC-ECD respectively) showed, in some cases, the presence of aliphatics. The negative spiking of the baseline, caused by aliphatics quenching the ECD, upset the baseline integration markers. The presence of trace aliphatics in the mononitro-PAC fractions from 2500 rpm was confirmed by GC-FID analysis.

The co-elution of aliphatics with the aromatic fraction of TES and the subsequent GC-ECD baseline disturbances led to increasing the hexane segment of the solvent HPLC fractionation programme (Section 3.4.2.3). This increased the likelihood of eluting the aliphatics in the major PAH HPLC fraction and not the later mononitro-PAC HPLC fraction. However, the analysis of the remaining 2500 rpm samples by GC-ECD also found aliphatic interferences in the mononitro-PAC HPLC fractions.

#### 3.4.2.2.2 Silica gel Clean-up

The aliphatic co-elution problem associated with the ODS cartridges, led to the samples from 1500 rpm and 3500 rpm being subjected to gravity fed open column silica gel adsorption clean-up (Section 3.2.2.3). The volumes of hexane used for the removal of the aliphatics was

increased to 25 ml, and the volume of DCM used to remove the nitro-PAC was increased to 35 ml. This clean-up step also helped to reduce the accumulation of polar material on the HPLC fractionation column.

#### 3.4.2.3 High Performance Liquid Chromatography Fractionation

Normal phase (NP) high performance liquid chromatography (HPLC) employing different stationary phases and solvents has been used extensively for isolation of nitro-PAC from diesel extracts (Levine & Skewes 1982, Paputa-Peck *et al.* 1983, Schuetzle *et al.* 1982, Nielsen 1983, Tomkins *et al.* 1984, Tong *et al.* 1984, and Draper 1986). Out of all the commercially available stationary phases, the most widely used is that of silica. HPLC fractionation with a silica stationary phase allows the retention windows for chemical classes of differing polarity to be established by standards. One of the problems with silica columns is the irreversible adsorption of material and water, producing inconsistent retention times. To counter this a guard column was used and the solvents were stored with calcium hydride (3 g) (40 mesh, 95+ %, Aldrich Chemical Co.). The solvents were filtered prior to use (Whatman 0.5  $\mu\text{m}$ ).

A Perkin Elmer series 410 LC pump connected to a Perkin Elmer LC-235 diode array UV detector was used, with the data recorded on a Perkin Elmer GP-100 chart recorder. The detector signal was also transferred to an IBM PC using a PE Nelson 900 series interface and processed by PE Nelson associated software. The monitoring wavelength was set at 254 nm. A 10  $\mu\text{m}$  semi-preparative Spherisorb silica (HPLC Technology) guard column (5 cm x 10 mm ID) and fractionation column (25 cm x 10 mm ID), using the same stationary material, were used with an 100  $\mu\text{l}$  sample loop fitted to a Rheodyne 7125 injector.

There were two solvent programmes used in this study. The initial solvent programme was used for the fractionation of the samples collected at 2500 rpm (Section 3.4.2.3.1). The initial solvent programme was modified in an attempt to eliminate aliphatic co-elutions. The modified programme also separated the dinitro- and nitro-oxy-PAC compounds. The fractionation of the aromatic fraction of exhaust samples from 1500 & 3500 rpm by the revised HPLC method is detailed in Section 3.4.2.3.2.

### 3.4.2.3.1 Initial HPLC Fractionations and Method Development

The initial solvent programme was aimed at isolating the mononitro-PAC from the aromatic/polar fraction eluted from the ODS cartridges. The gradient elution programme was based on the work of Tong *et al.* (1984). It consisted of 100% hexane for 5 min; programmed to 100% DCM over 20 min, held for 10 min, programmed to 100% acetonitrile over 10 min, held for 10 min; programmed back to 100% DCM in 5 min and finally to 100% hexane in further 5 min. The flow-rate was 4 ml/min. Standard mixes (Table 3.15) were used to establish the retention windows for the fractions to be collected (Figure 3.13), with the retention times being reproducible (Table 3.16).

Table 3.15 HPLC fractionation standard mix

Mix	Compounds
PAH	Naphthalene, fluorene, & phenanthrene
PANH	Quinoline, indole, 1,4-naphthaquinone, & carbazole
Mononitro-PAC	1-Nitronaphthalene, 2-nitronaphthalene, 2-methyl-1-nitronaphthalene, 2-nitrofluorene, 9-nitroanthracene, 3-nitrofluoranthene, & 1-nitropyrene
Dinitro-PAC	1,5-Dinitronaphthalene, 1,8-dinitronaphthalene, 2,7-dinitronaphthalene, & 1,6-dinitropyrene
Nitro-oxy-PAC	3-nitrofluoren-9-one, 2,7-dinitrofluoren-9-one, & 2,5,7-trinitrofluoren-9-one

Table 3.16 Reproducibility of Retention Times ( $R_t$ ) for NP HPLC Fractionation

Injection #	$R_t$ for 1-nitronaphthalene (minutes)	$R_t$ for 1,8 dinitro-naphthalene (minutes)	$R_t$ for 3-nitro-fluoren-9-one (minutes)
1	17.31	25.07	31.40
2	17.31	25.61	31.56
3	17.64	26.00	31.40
4	17.59	25.89	31.24
5	17.26	25.34	31.40
6	17.64	25.95	31.35
Average (minutes)	17.46	25.64	31.39
Standard Deviation	0.167	0.343	0.0942

**Key**

A = PAH standards

B = Mononitro-PAC standards

C = Dinitro-PAC & Nitro-oxy-PAC standards

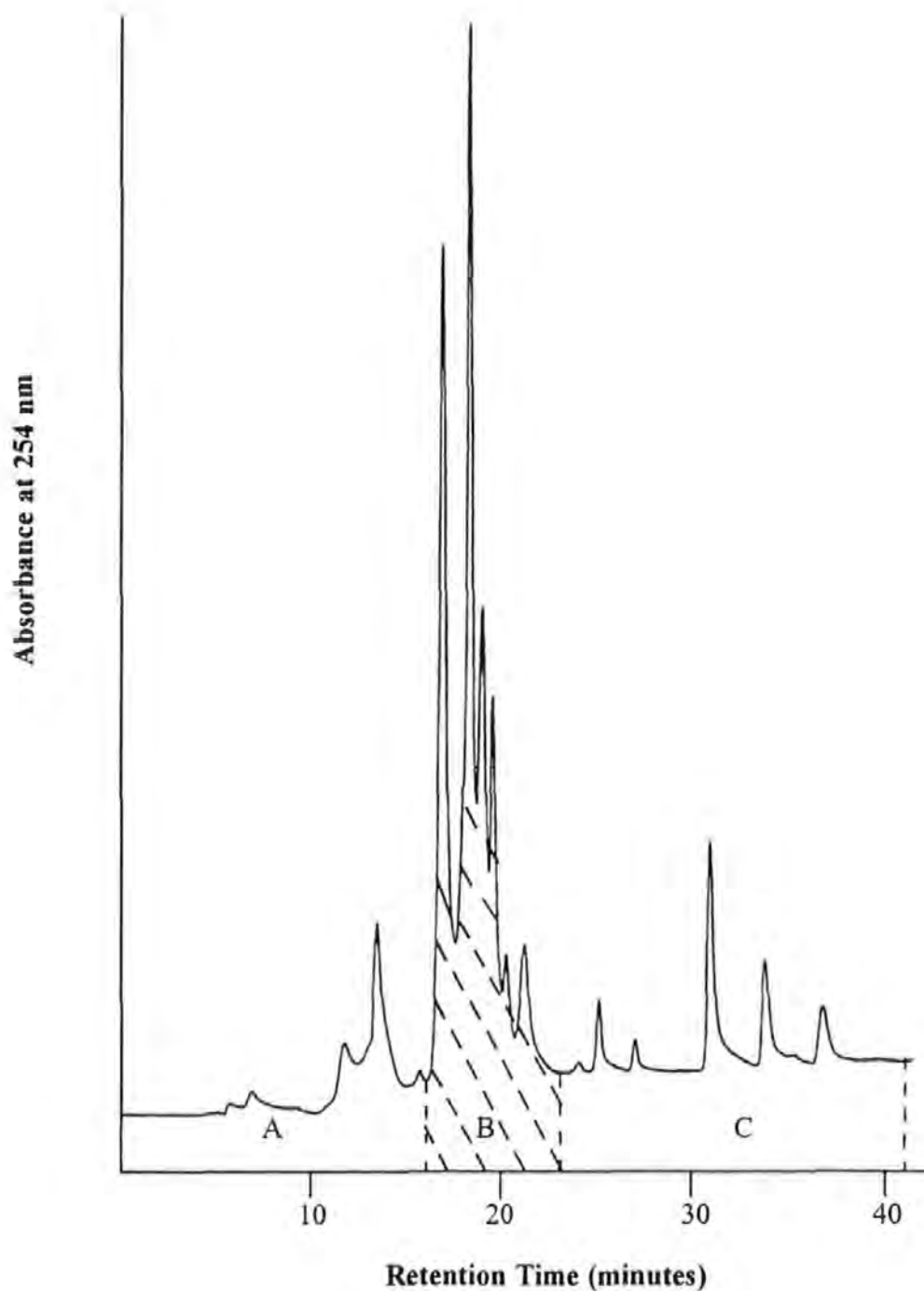


Figure 3.13 The chromatogram of the HPLC fractionation standard mix and the establishment of the initial HPLC fraction elution windows. HPLC conditions: Spherisorb silica column, 100% hexane (5 min.), increased to 100% DCM (20 min.), held 10 min., increased to 100% acetonitrile (10 min), and held for 10 min. Flowrate of 4ml/min.

The aromatic fractions from the ODS cartridge clean-up of one from each duplicate obtained at 2500 rpm were injected (100 µl, 100 mg/ml). Initially four fractions were collected in RBFs (100 ml) (Figure 3.14). Preliminary analysis of the HPLC fractionations by GC-ECD, indicated that a small proportion of aliphatics had broken through on the ODS cartridges. As previously explained (Section 3.4.2.2.1), the aliphatics had the effect of producing negative peaks on the GC-ECD. In an attempt to eliminate the aliphatic interferences the hexane part of the solvent programme was increased to 15 minutes. Preliminary analysis of the third HPLC fraction (which may have contained dinitro-PAC, nitro-oxy-PAC, and some oxy-PAC) showed the fractions to contain many compounds. Hence, fraction three of the initial solvent programme was further fractionated in an attempt to concentrate further the dinitro-PAC. There were now five HPLC fractions. The modified procedure failed to elute the aliphatics prior to the mononitro-PAC.

#### 3.4.2.3.2 HPLC fractionations of TES collected at 1500 rpm & 3500 rpm

To remove the aliphatic co-elution problem the TES collected at 1500 rpm and 3500 rpm were cleaned-up using glass columns packed with silica gel (Section 3.4.2.2.2.). The aromatic fractions from the clean-up were further fractionated by NP HPLC using the revised solvent programme. There was no problem with aliphatic carry over for these samples and five fractions were collected in RBFs (50 ml and 100 ml).

#### 3.4.2.4 Fuel and Oil Work-up

Following silica gel fractionation (Section 3.4.2.2.2) one fuel sample was subjected to NP HPLC fractionation, using the revised procedure, for investigation of nitro-PAC in the fuel. Following the removal of particulates (Section 3.2.2.5) and the silica gel clean-up (Section 3.4.2.2.2) of sump oil (obtained after last sample for nitro- & oxy-PAC profiling was taken, and corresponding to 50 hours of use), the aromatic fraction was subjected to NP HPLC fractionation, using the revised procedure, to examine the nitro-PAC content of the oil.



# Key

- A = PAH, PASH, and alkyl-derivatives
- B = Mononitro-PAC
- C = Dinitro-PAC & Nitro-oxy-PAC
- D = Polar PAC

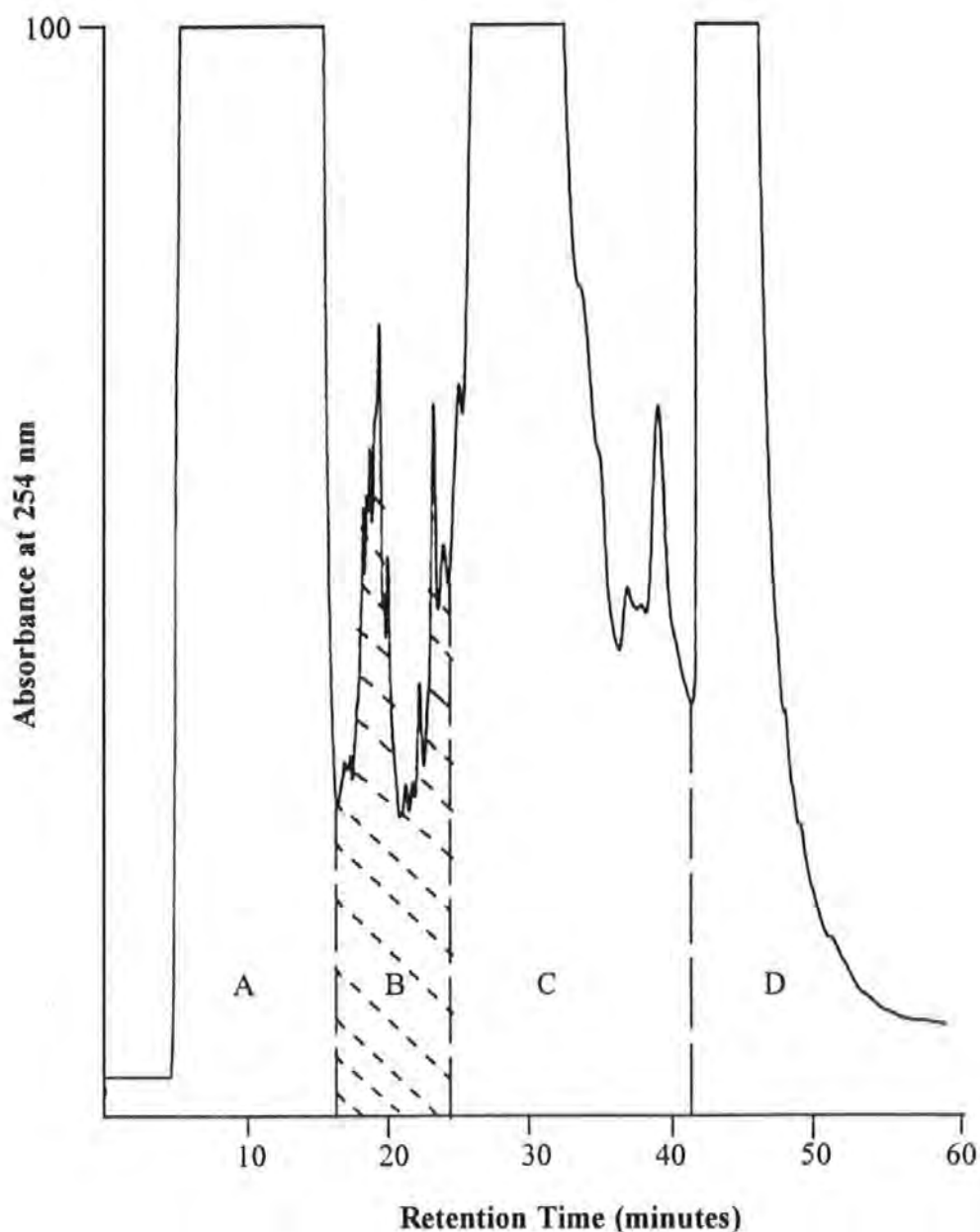


Figure 3.14 The HPLC fractionation of the aromatic fraction from the ODS clean-up of TES collected at 2500 rpm and low load. HPLC conditions: Spherisorb column, 100% hexane (5 min.), increased to 100% DCM (20 min.), held 10 min., increased to 100% acetonitrile (10 min), and held for 10 min. Flowrate of 4 ml/min.

#### 3.4.2.5 Recovery of Nitro-PAC for Laboratory Work-Up

The recovery of nitro-PAC for the entire work-up procedure was divided into three stages, with each stage being carried out in duplicate. Firstly, the HPLC fractionation mix (50 µl) was added to the solvent mixture (DCM:methanol, 1:1, 800 ml total) plus distilled water (800 ml). The mixture was worked-up to the total extract stage. Similarly in the second stage, the HPLC mix (50 µl) was applied to silica gel columns or ODS cartridges and the samples worked-up. In the last stage, the HPLC mix was injected (10 µl) on the NP-HPLC system and the different fractions worked-up. At each stage, the recoveries (Table 3.17) were calculated by comparing areas of compounds in the recovery standard mix before and after work-up by the Carlo Erba GC-FID (instrument details in Section 3.2.3, with nitrogen instead of hydrogen used for the carrier gas).

Table 3.17 Laboratory recovery of nitro-PAC

Compound	Laboratory recovery after total extract work-up %	Laboratory recovery after ODS clean-up %	Laboratory recovery after silica gel clean-up %	Laboratory recovery after HPLC fractionation %	Laboratory recovery for total procedure (using silica clean-up) %
1-nitronaphthalene	95.7	97.6	101.6	92.8	90.1
2-nitronaphthalene	94.6	98.1	101.2	94.5	90.3
2-nitrofluorene	95.7	99.2	100.7	94.2	90.6
1-nitropyrene	97.0	92.6	101.2	79.2	77.4
1,8-dinitronaphthalene	97.4	99.9	99.1	72.2	68.7
2,7-dinitronaphthalene	96.8	94.2	93.0	70.4	60.2
3-nitro-fluoren-9-one	102.8	96.0	88.5	84.3	75.6

#### 3.4.3 Analysis of Nitro- and Oxy-PAC

The analysis of nitro-PAC explored several detection systems and established GC-ECD as the best system, with GC/MS NICI used as a back-up technique (Section 3.4.3.1). The oxy-PAC were analyzed by GC/MS EI (Section 3.4.3.2). The *n*-alkanes and the major PAH were analyzed by GC-FID (Section 3.4.3.3) and GC/MS EI respectively (Section 3.4.3.4).

### 3.4.3.1 Evaluation and establishment of detection systems for Nitro-PAC analysis

The following detection systems were evaluated with a mononitro-PAC standard mix (Table 3.18) and in some cases with samples for the analysis of nitro-PAC:

- 1) Gas chromatography with nitrogen-phosphorous detection (GC-NPD) (Section 3.4.3.1.1)
- 2) Reverse phase HPLC with fluorescence/chemiluminescence detection (Section 3.4.3.1.2)
- 3) Gas chromatography (GC/MS) operated in electron impact (EI) mode (Section 3.4.3.1.3)
- 4) Gas chromatography with electron capture detection (GC-ECD) (Section 3.4.3.1.4)
- 5) GC/MS operated in the negative ion chemical ionisation (NICI) mode (Section 3.4.3.1.5)

Table 3.18 Mononitro-PAC standard mix

Compound	Stock Concentration (mg/ml)
1-nitronaphthalene	0.10
2-nitro-1-methyl-naphthalene	0.10
2-nitronaphthalene	0.10
6-nitroquinoline	0.10
2-nitrofluorene	0.10
9-nitroanthracene	0.16
3-nitrofluoranthene	0.13
1-nitropyrene	0.10

#### 3.4.3.1.1 Gas Chromatography with Nitrogen-Phosphorous Detection

Gas chromatography with nitrogen-phosphorous detection (GC-NPD) is a selective detector for nitrogen and phosphorous compounds, and has been employed for the analysis of nitro-PAC in diesel extracts and environmental samples (Oehme *et al.* 1982, Nielsen 1983, Paputa-Peck *et al.* 1983 and Campbell & Lee 1984). The technique is reviewed by White *et al.* (1984). The evaluation was performed on a Carlo Erba Mega series GC with a NPD-40 detector fitted. A Supelchem PTE-5 (25 m x 0.32 ID, 0.25  $\mu$ m film thickness) capillary column was used with cooled on-column injector. The output of the gas chromatograph was recorded by a Shimadzu integrator. After trying several different bead heights the sensitivity was low and the chromatography unstable; leading to GC-NPD being dismissed for nitro-PAC analysis.

#### 3.4.3.1.2 Reverse Phase HPLC with Fluorescence/Chemiluminescence Detection

Reverse phase HPLC with fluorescence/chemiluminescence detection is a sensitive technique for nitro-PAC, and in the case of chemiluminescence very selective as well. As a consequence of the greater selectivity, the chemiluminescence technique has been gaining popularity in recent years (Sigvardson & Birks 1984, Imaizumi *et al.* 1990, Liu & Robbat 1991, and Li & Westerholm 1994). Chemiluminescence detection is reviewed by Robards & Worsfold (1992) and Kwakman & Brinkman (1992).

For evaluation of fluorescence, a Merck Hitachi system equipped with a L-6000 two pump system connected to an F-1050 fluorescence detector and linked to a D-2500 integrator was used. A PE Nelson data computer system was also used to collect and process the data. Sample injection were made using a Rheodyne 7125 injector with a 20  $\mu$ l loop. A Spherisorb-2 ODS 5  $\mu$ m (HPLC Technology) column (25 cm x 4.6 mm ID) was used. The evaluation was performed using 1-aminopyrene and 1-nitropyrene. The method of Liu & Robbat (1991) was used, with the excitation ( $ex_{\lambda}$ ) and emission ( $em_{\lambda}$ ) wavelengths were 260 nm and 430 nm respectively.

The detection limits for nitro-PAC can be significantly increased if the nitro group is reduced to the amino derivative (Sigvardson & Birks 1984, MacCrehan *et al.* 1988, and Liu & Robbat 1991). This can be achieved on or off-line. In this research the on-line reduction adopted method of Liu & Robbat (1991) was used. The reductive columns were made by packing stainless steel columns (4 cm x 2 mm id) with zinc (99.998%, Aldrich Chemical Co.). In order for the reduction mechanism to proceed an ammonium acetate buffer was used. Isocratic elution with acetonitrile-water (80:20, v/v) with ammonium acetate buffer (30 mM, 99%, Aldrich Chemical Co.) was used to evaluate the system. Figure 3.15 shows the high sensitivity of the system for detection of 1-nitropyrene in the reduced amino- form. The peak shape was acceptable, indicating that the reductive column was not causing excessive peak broadening.

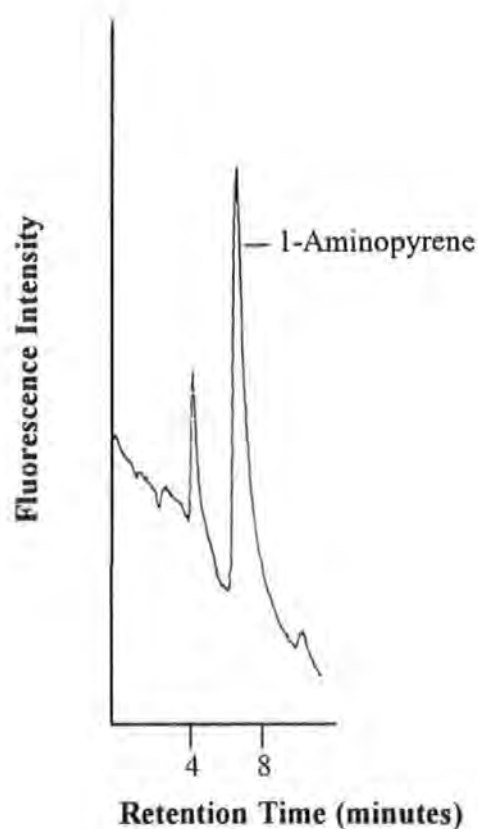


Figure 3.15 The sensitivity of fluorescence detection with on-line pre-column reduction for the determination of 1-nitropyrene (2.5 pg injected) in the reduced form of 1-aminopyrene. HPLC conditions: Spherisorb ODS-2 column, isocratic elution with acetonitrile:water (80:20), and ammonium acetate buffer (30 mM).  $Ex_{\lambda} = 260 \text{ nm}$  and  $Em_{\lambda} = 430 \text{ nm}$ , Flowrate of 1 ml/min.

The evaluation of chemiluminescence detection was performed in conjunction with the development and testing of a purpose built chemiluminescence detector (CamSpec) by Gachanja (1994), at the University of Plymouth. The chemiluminescence reaction involved with bis (2,4-dinitrophenyl)oxalate (DNPO) (1.45 mg/ml, in acetonitrile) and hydrogen peroxide (40% H<sub>2</sub>O<sub>2</sub> in acetonitrile, v/v) was initially tested. Flow injection analysis was used, with the two reagent streams (controlled by peristaltic pumps) mixed prior to meeting the eluent flow. Flow rates of 0.5 ml/min for each reagent stream was used, and the flow rate for the mobile phase (100% acetonitrile) was 1 ml/min. The sensitivity of the system was investigated with 1-aminopyrene (Figure 3.16). However, when the chemiluminescence reagents were combined with the ammonium acetate buffer used for the on-line reduction of the nitro-PAC, the chemiluminescence reaction did not work. This was a consequence of the buffer pH of 7.4 inhibiting the chemiluminescence. The incompatibility of the DNPO reaction with the on-line reduction of nitro-PAC, led to investigating bis (2,4,6- trichlorophenyl)oxalate (TCPO) as an alternative chemiluminescence reagent. The TCPO reaction is less rapid than DNPO but has the advantage of optimum sensitivity at a pH of around 7.0 (Imaizumi *et al.* 1989, Robards & Worsfold 1992, and Gachanja 1994). The same chromatographic conditions as used for DNPO were employed with the TCPO appraisal. The TCPO system gave similar sensitivities to 1-aminopyrene as achieved with DNPO and the system was compatible with the on-reductive HPLC system.

On a routine basis, the analysis suffered greatly from the short lifetime of the zinc reductive columns, resulting in unacceptable peak broadening. This resulted in no TES being analyzed. Future reliability could be improved by using a heated rhodium/platinum reduction column (Tejada *et al.* 1982 & 1986).

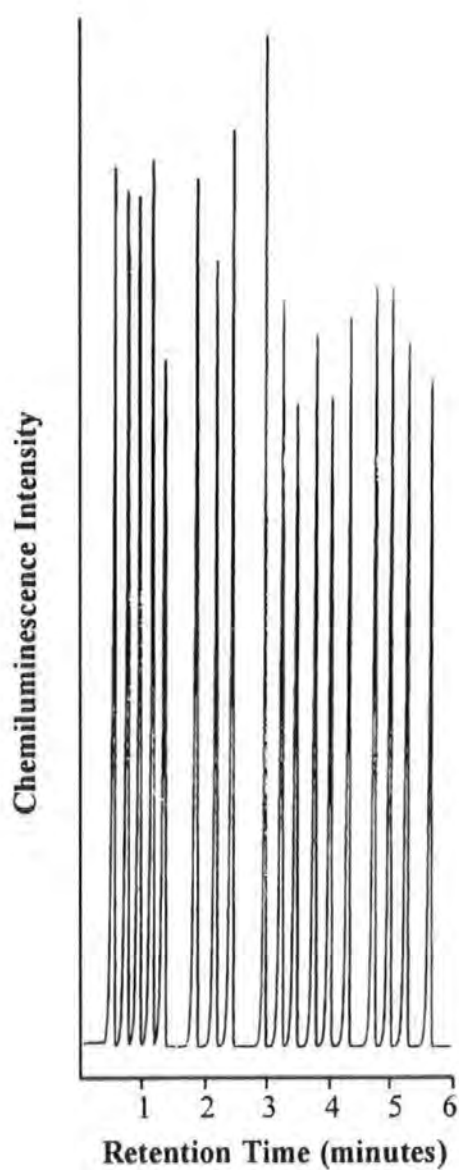


Figure 3.16 The sensitivity of the bis (2,4-dinitrophenyl)oxalate (DNPO) chemiluminescence reaction to the detection of 1-aminopyrene (20 ng injected each time) using flow-injection analysis. Flow rate of 1 ml/min for mobile phase (100% acetonitrile) and 0.5 ml/min for each reagent stream (DNPO and  $\text{H}_2\text{O}_2$ ).

nitro-PAC and has been used to confirm prominent nitro-PAC in some diesel studies (Schuetzle *et al.* 1983 and Bayona *et al.* 1988).

The evaluation of GC/MS in EI mode was performed on a Carlo Erba 5160 GC linked to a Kratos MS25 mass spectrometer. The ionisation was set at 40 eV, and 40-528 amu were scanned every 2 seconds. A Rt<sub>x</sub>-5 (25 m x 0.32 ID, 0.25 µm film thickness) capillary column was used with cooled on-column injector. The temperature program consisted of 60°C for 1 minute, 5°C/min temperature ramp up to 300°C, held for 10 minutes. Helium was used for the carrier gas. The output of the mass spectrometer was managed by a Kratos DS90 data system. The detection limits were of the order of 0.5 - 1.0 ng per injection for some nitro-PAC, such as 1-nitronaphthalene (signal/noise, S/N, 3:1) (Figure 3.17). Injection of mononitro-PAC HPLC fractions could not detect any nitro-PAC.

#### 3.4.3.1.4 Gas Chromatography with Electron Capture Detection

Gas chromatography with electron capture detection (GC-ECD) is very sensitive towards electrophilic compounds and has been used for the analysis of nitro-PAC (Oehme *et al.* 1982, Campbell & Lee 1984, and Draper *et al.* 1986). The technique is reviewed by Poole (1982).

The evaluation of GC-ECD was performed on a Perkin Elmer 8600 GC with ECD fitted. A Supelchem PTE-5 (25 m x 0.32 ID, 0.25 µm film thickness) capillary column was used with a programmable temperature (PTV) injector. The output of the gas chromatograph was recorded by a GP-100 Perkin Elmer chart recorder. The output was also linked to an IBM compatible PC by a Perkin Elmer Series 900 data capture unit before sending to the PE Nelson integration package. The computer system enabled a backup of runs to be made and allowed reprocessing of data at a later date.

The oven temperature and other parameters were initially based on the work of Oehme *et al.* (1982): 1 minute at 40°C, 30°C/min to 140°C, 5°C/min to 300°C, detector temperature 320°C, injection volumes of 0.5 µl, nitrogen as the carrier gas. The initial analysis was severely hindered by the detector cell rapidly becoming contaminated.



**Key**

- 1 = 1.0 ng of 1-Nitronaphthalene
- 2 = 1.0 ng of 2-Methyl-1-nitronaphthalene
- 3 = 1.0 ng of 2-Nitronaphthalene
- 4 = 1.0 ng of 6-Nitroquinoline
- 5 = 1.0 ng of 2-Nitrofluorene
- 6 = 1.6 ng of 9-Nitroanthracene
- 7 = 1.3 ng of 3-Nitrofluoranthene
- 8 = 1.0 ng of 1-Nitropyrene

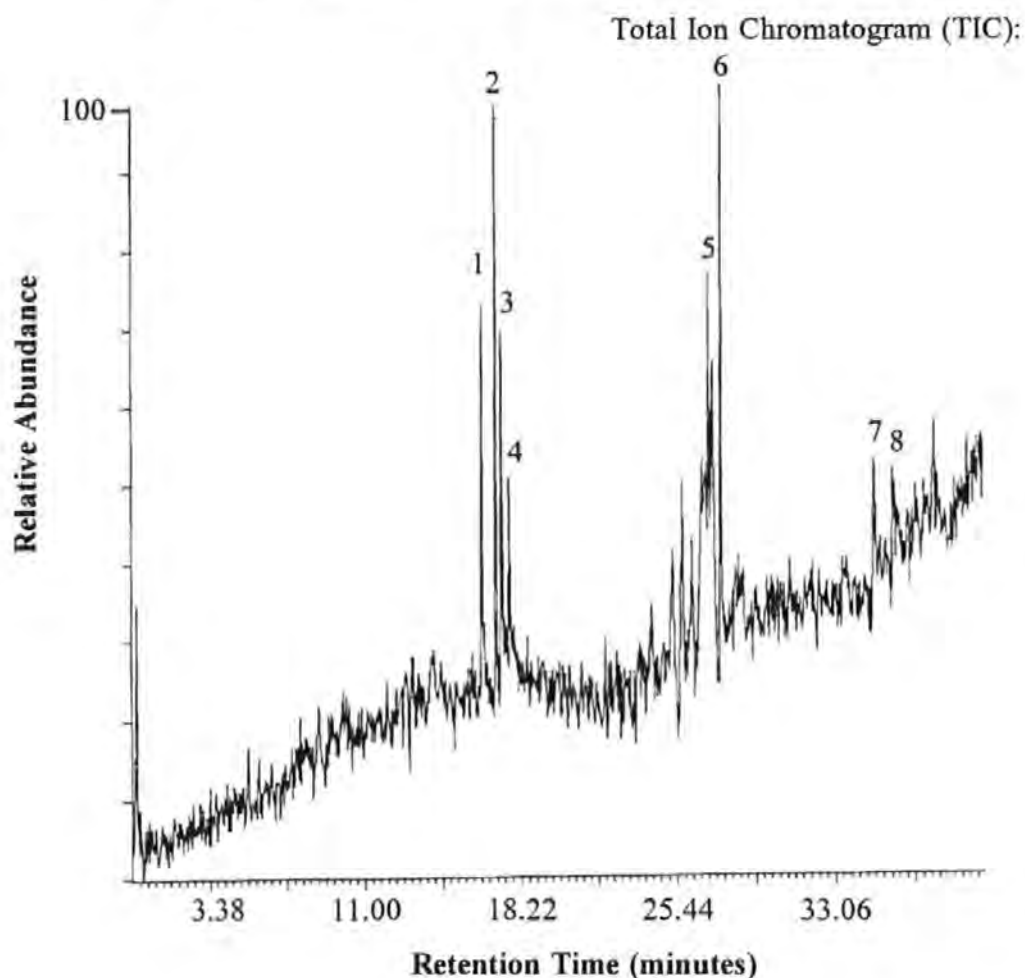


Figure 3.17 The low sensitivity of gas chromatography/mass spectrometry operated in the electron impact mode to the mononitro-PAC standard mix. GC conditions: Rt<sub>x</sub>-5 column, 60°C for 1 min., 5°C/min to 300°C, held for 10 min.

The contamination affected the saturation levels and consequently the sensitivity. The contamination problem was greatly reduced by adding a piece of deactivated silica tubing (1 m x 0.32 mm ID, Jones Chromatography) to the detector end of the analytical column. The columns were connected using a glass column connector (Jones Chromatography). The deactivated silica column enabled the temperature of the detector to be increased to 350°C, without significant increase in column bleed. The higher detector temperature reduced the accumulation of material and thus a lower (and hence more sensitive) saturation level could be maintained.

The detection limits were of the order of *ca.* 50 pg per mononitro-PAC injected (S/N of 3/1) (Figure 3.18). The linear ranged from the detection limits to *ca.* 2 ng. The reproducibility of both the retention times and integrations was good. For example, five replicate injections of 1-nitropyrene (50 pg) gave a standard deviation of 0.0964 for the retention times and 0.549 for the integrations respectively. The excellent GC resolution, high sensitivity, and access to instrument resulted in GC-ECD being used extensively for the detection of nitro-PAC in the HPLC fractions. The GC-ECD analysis is divided into the mononitro-PAC HPLC fractions (Section 3.4.3.1.4.1), dinitro-PAC HPLC fractions (Section 3.4.3.1.4.2), and nitro-oxy-PAC HPLC fractions (3.4.3.1.4.3).

#### 3.4.3.1.4.1 Analysis of Mononitro-PAC HPLC Fractions by GC-ECD

This section describes the analysis of the mononitro-PAC HPLC fractions by GC-ECD. The final temperature programme was 60°C for 1 min., 5°C/min. to 300°C, held for 10 mins.. Nitrogen was used as the carrier gas. The PTV injector was programmed as follows: 0.01 minutes after injection temperature increased from under 50°C to 300°C, 2.49 minutes later purge vent opened, and 1.51 minutes later the PTV injector was cooled back to under 50°C using compressed air.

Integration of peaks within the retention windows established by the mononitro-PAC standard mix (Figure 3.19) were between 20-25 minutes for nitronaphthalenes, 30-35 minutes for nitroanthracenes and nitrofluorenes, and 40-45 minutes for nitropyrenes and nitrofluoranthenes. These windows were used to mark the baseline start and stop positions. In doing this, the baseline was forced to follow directly underneath the peaks of interest.

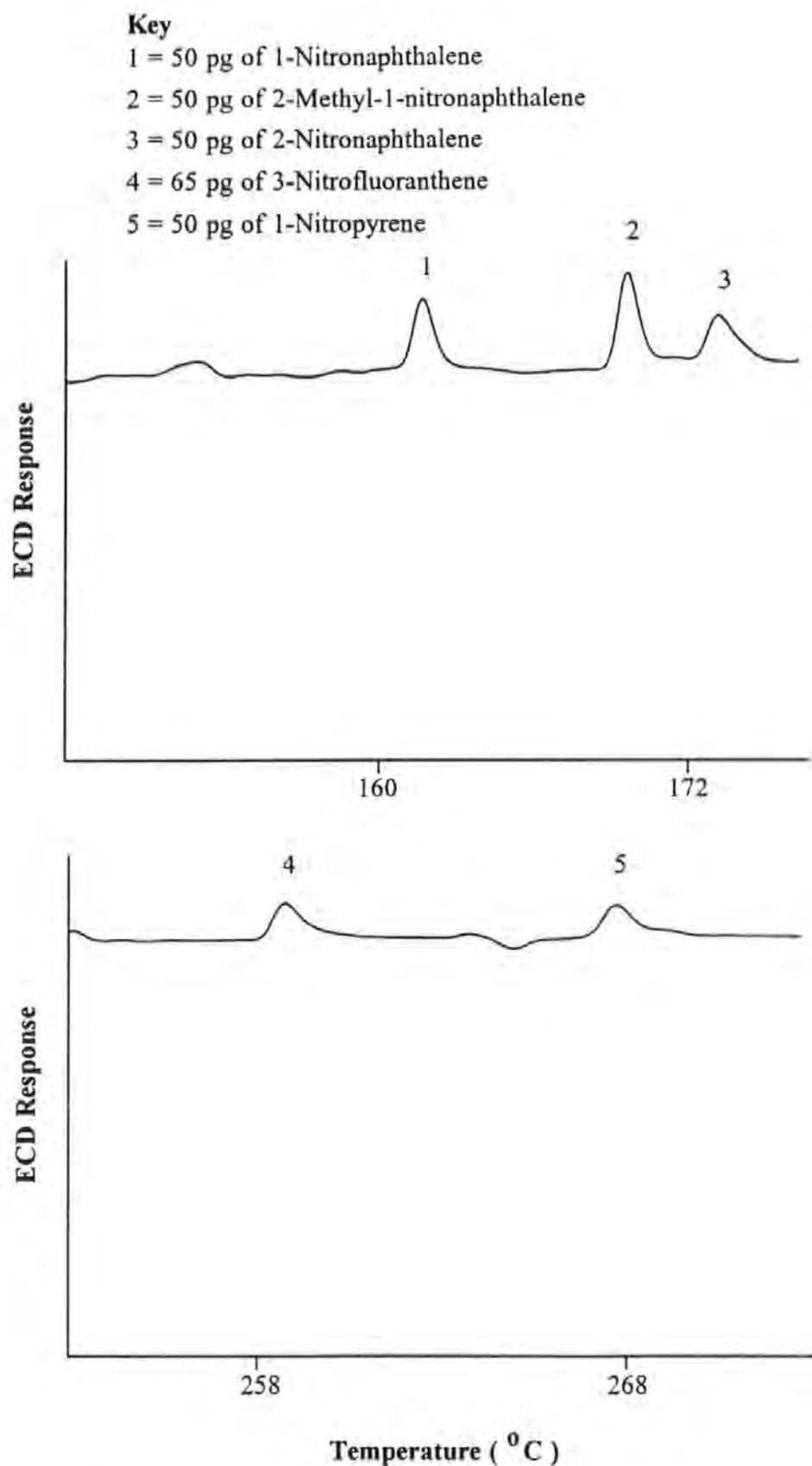


Figure 3.18 The high sensitivity of gas chromatography with electron capture detection to a) the nitronaphthalenes, and b) 3-nitrofluoranthene and 1-nitropyrene. GC conditions: Supelchem PTE-5 column, 60°C for 1 min., 5°C/min to 300°C, held for 10 min.

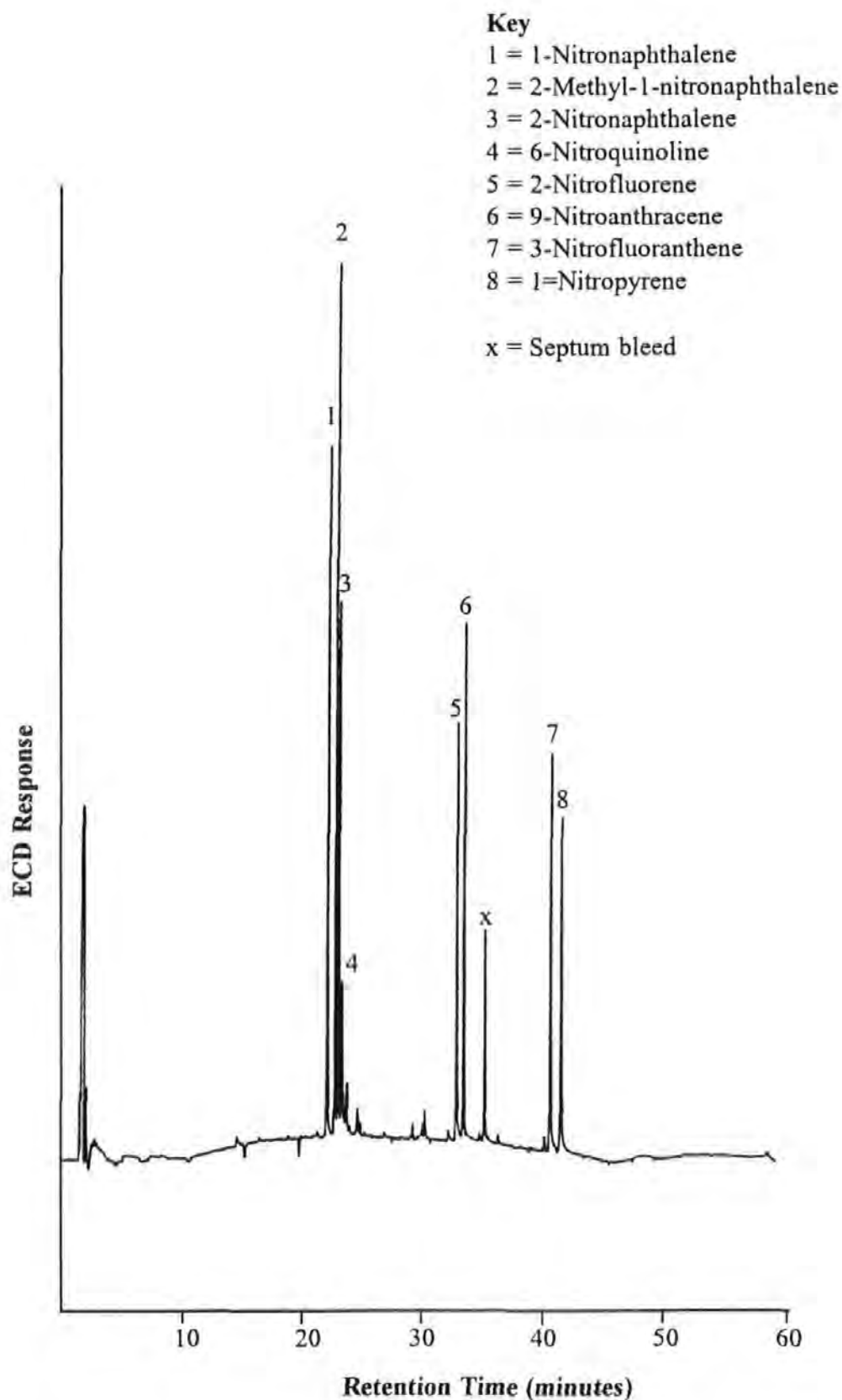


Figure 3.19 The establishment of the integration temperature windows for nitro-PAC using the mononitro-PAC standard mix. GC conditions: Supelchem PTE-5 column, 60°C for 1 min., 5°C/min to 300°C, held for 10 min.

Mononitro-PAC HPLC fractions were blown down to constant weight under a gentle stream of nitrogen. The weights were low for all samples; less than 0.2 mg. Sample dilutions were made with 100 µl of acetonitrile. Mononitro-PAC were identified by co-injecting the sample with the mononitro-PAC standard mix. The increase of peak areas with respect to the sample injection only, confirmed the presence of compounds. Co-injections were performed with different concentrations of the standard mix. In this way the possibility of the standard mix masking several peaks was eliminated as the concentration of the mix was progressively reduced. Figure 3.20 shows the confirmation of the nitronaphthalenes by co-injection techniques. Positive co-injection confirmations were achieved for 1-nitronaphthalene, 2-nitronaphthalene, 2-methyl-1-nitronaphthalene, and 1-nitropyrene for all samples. The confirmation of the presence of nitro-PAC was backed-up by retention indices based on 1-nitropyrene (Table 3.19).

Table 3.19      Retention Index (RI) based on 1-nitropyrene

Sample	RI for 1-nitronaphthalene	RI for 2-methyl-1-nitronaphthalene	RI for 2-nitronaphthalene
Standard Mix	0.528	0.545	0.551
LS & L-NO <sub>x</sub>	0.528	0.543	0.551
LS & M-NO <sub>x</sub>	0.529	0.544	0.552
LS & H-NO <sub>x</sub>	0.528	0.543	0.551
MS & L-NO <sub>x</sub>	0.530	0.546	0.552
MS & M-NO <sub>x</sub>	0.528	0.545	0.551
MS & H-NO <sub>x</sub>	0.528	0.544	0.551
HS & L-NO <sub>x</sub>	0.529	0.544	0.552
HS & M-NO <sub>x</sub>	0.528	0.544	0.551
HS & H-NO <sub>x</sub>	0.528	0.543	0.551

Key:    L = low    M = medium    H = high    S = speed  
(RI taken from 1 injection of one of each duplicates)

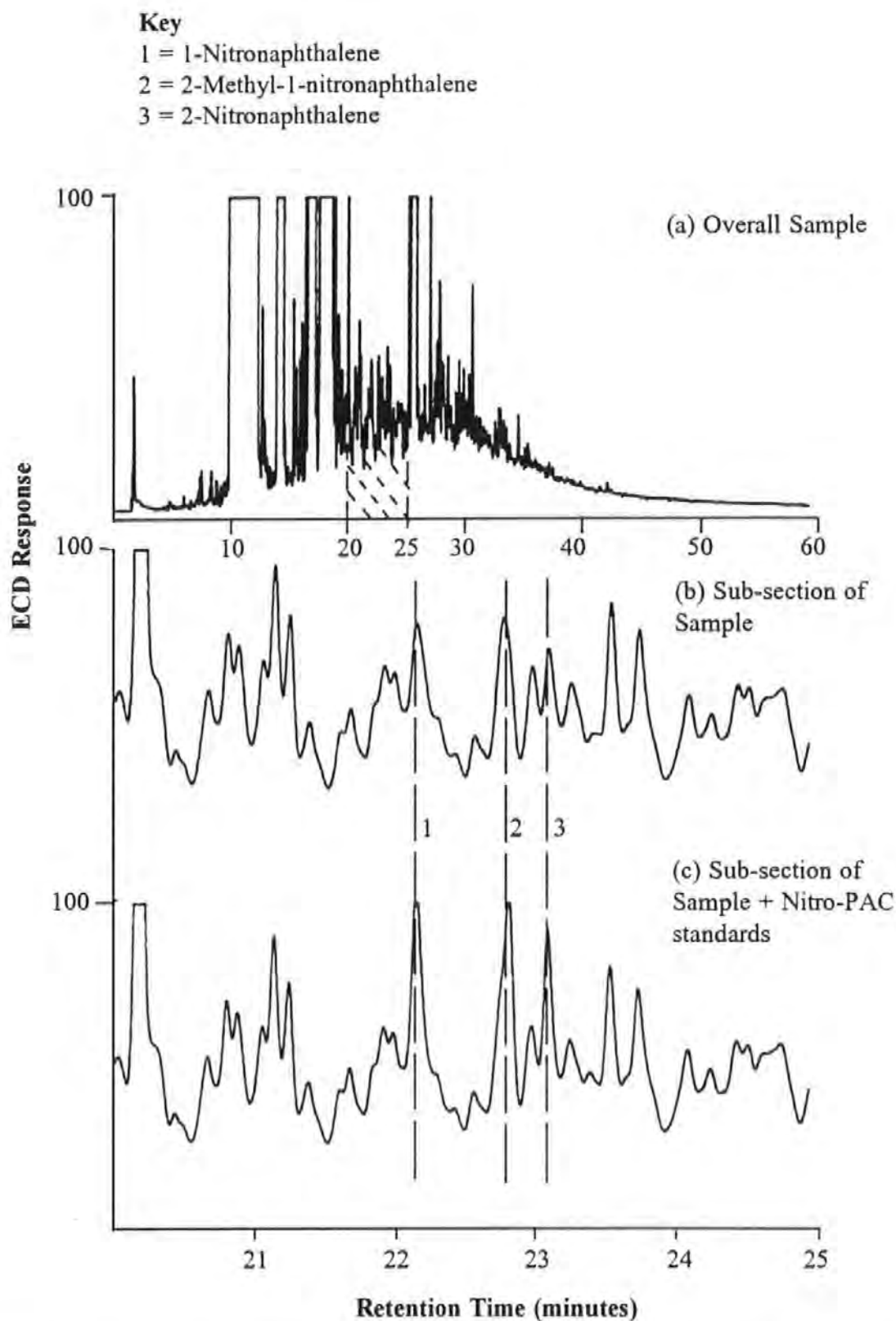


Figure 3.20 The confirmation of the nitronaphthalenes in the mononitro-PAC HPLC fraction collected at high load and 1500 rpm (a) by comparing the nitronaphthalene temperature window (b) with that of the same sample co-injected with the mononitro-PAC standard mix (c) (Chromatographic conditions given in Section 3.4.3.1.4.1).

Quantification was based on external calibration using the mononitro-PAC mix. Figure 3.21 shows the calibration curve for 1-nitronaphthalene and 1-nitropyrene. Each mononitro-PAC HPLC fraction was then injected twice (0.5 µl). The calibration was checked following completion of the injection of samples from 1500 rpm and 2500 rpm. The mononitro-PAC emissions were calculated in terms of the weight of nitro-PAC emitted divided by the TES weight collected and relative to the total fuel consumed during sampling.

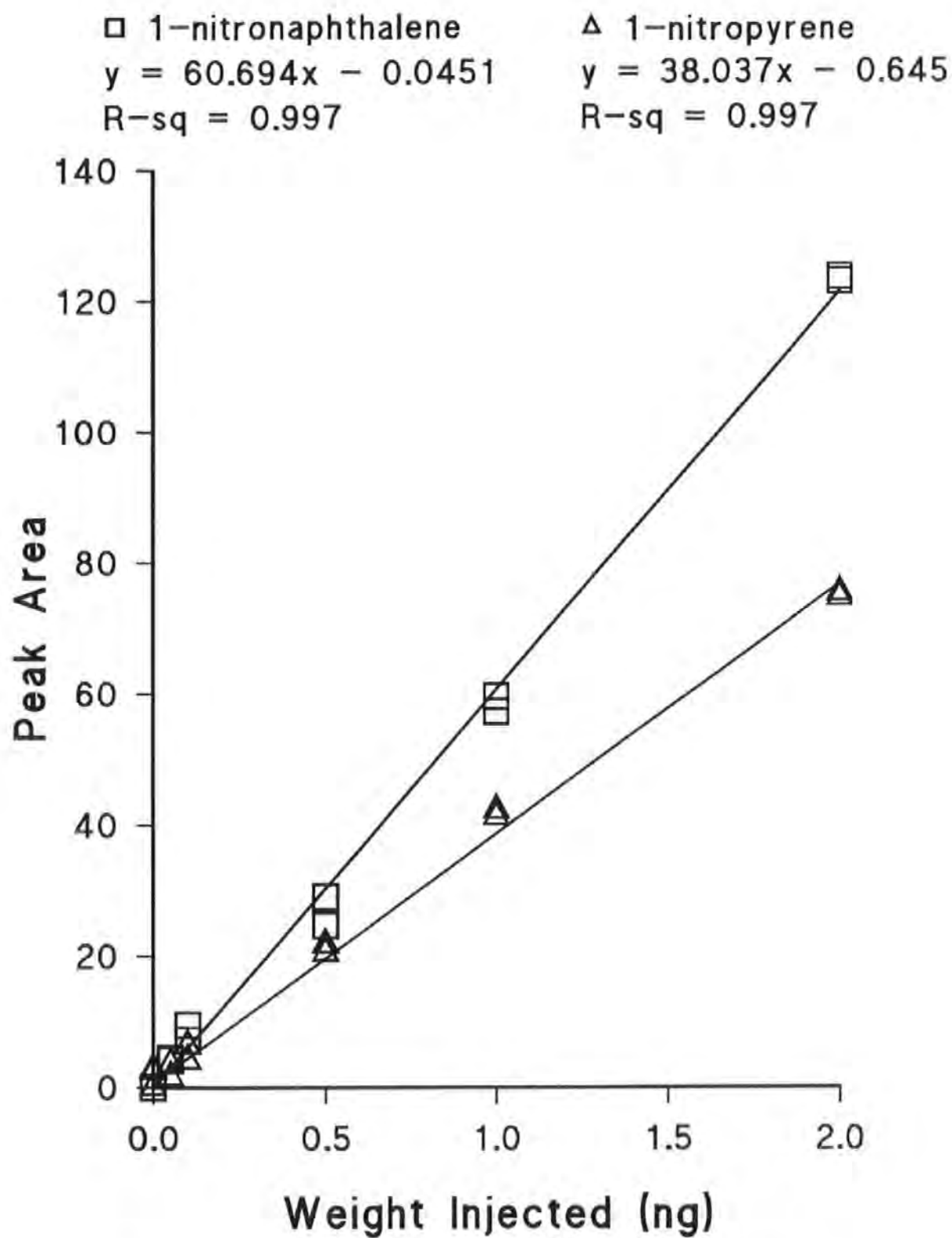
#### 3.4.3.1.4.2 Analysis of Dinitro-PAC HPLC Fractions by GC-ECD

This section describes the analysis of the dinitro-PAC HPLC fractions by GC-ECD. The instrumentation and set-up parameters were as for those used for the analysis of the mononitro-PAC HPLC fractions (Section 3.4.3.1.4.1), with the following exceptions. The temperature programme was initially 60°C held for 1 min, temperature ramp of 10°C/min to 180°C, then a temperature ramp of 5°C/min to 300°C, held for 10 minutes. The integration areas were defined by the standard dinitro-PAC mix: 17-23 minutes for 1,5-dinitronaphthalene and 1,8-dinitronaphthalene, 28-30 minutes for 2,7-dinitrofluorene, and finally 32-36 minutes for the dinitropyrenes (Figure 3.22).

The detection limits were: 94 pg for 1,8-dinitronaphthalene, 660 pg, for 2,7-dinitrofluorene, and 1.2 ng for 1,8-dinitropyrene (S/N of 3/1). The analysis concentrated on the duplicate samples taken at 3500 rpm. Samples were blown down to a constant weight under a gentle stream of nitrogen. Samples were diluted to a concentration of 2.5 mg/ml and injection volumes were 0.5 µl. Identifications were attempted by co-injection with the dinitro-PAC standard mix.

#### 3.4.3.1.4.3 Analysis of Nitro-oxy-PAC HPLC Fractions by GC-ECD

This section describes the analysis of the nitro-oxy-PAC HPLC fractions by GC-ECD. The instrumentation and set-up parameters were as for those used for the analysis of the mononitro-PAC HPLC fractions (Section 3.4.3.1.4.1), with the following exceptions. The temperature programme was initially 60°C held for 1 min, temperature ramp of 10°C/min to 200°C, then a temperature ramp of 5°C/min to 300°C, held for 10 minutes.



*Note: Duplicate injections at each weight*

Figure 3.21 The calibration curves for 1-nitronaphthalene and 1-nitropyrene using gas chromatography with electron capture detection.



**Key**

- 1 = 1,5-Dinitronaphthalene
- 2 = 1,8-Dinitronaphthalene
- 3 = 2,7-Dinitrofluorene
- 4 = 1,3-Dinitropyrene
- 5 = 1,6-Dinitropyrene
- 6 = 1,8-Dinitropyrene

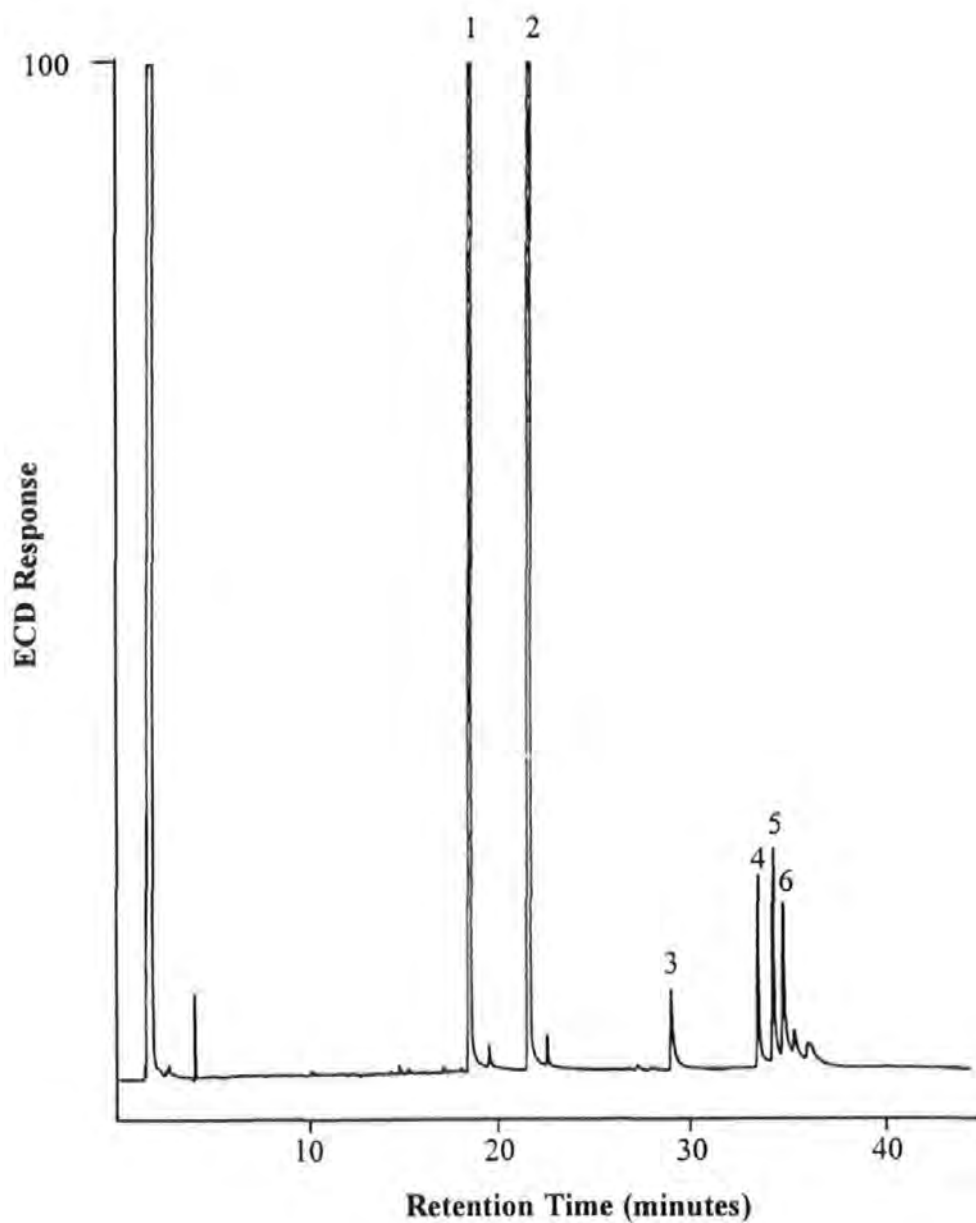


Figure 3.22 The gas chromatogram of the dinitro-PAC standard mix. GC conditions: Supelchem PTE-5 column, 60°C for 1 min., 10°C/min to 180°C, 5°C/min to 300°C, held for 10 min.

The detection limits (S/N, 3/1) were: 312.5 pg for 2-nitrofluoren-9-one and 2.5 ng for 2,4,7-trinitrofluoren-9-one. Samples were blown down to a constant weight under a gentle stream of nitrogen. Samples were diluted to a concentration of 2.5 mg/ml and injection volumes were 0.5 µl. The integration areas were defined by the standard nitro-oxy-PAC mix : 20-23 minutes for 2-nitrofluoren-9-one, and 30-35 minutes for 2,7-dinitrofluoren-9-one and 2,4,7-trinitrofluoren-9-one (Figure 3.23). It was found that the injection of the nitro-oxy-PAC HPLC fractions rapidly caused the detector cell to become contaminated. For this reason, one of each of the duplicates from the samples at 3500 rpm were injected. Identifications were attempted by co-injection with the nitro-oxy-PAC standard mix.

#### 3.4.3.1.5 Gas Chromatography/Mass Spectrometry operated in the Negative Ion Chemical Ionisation mode

Gas chromatograph/mass spectrometry operated in the negative chemical ionization mode (GC/MS NCI) is very sensitive to electrophilic compounds such as nitro-PAC (Tong *et al.* 1984, Ramdahl & Urdal 1982, Sellström *et al.* 1987, and Bayona *et al.* 1988).

The evaluation of GC/MS in NCI mode was performed on a Carlo Erba 5160 GC linked to a Finnigan 4500 EI - CI mass spectrometer. Isobutane was used as the reagent gas. The source temperature was 150°C, electron beam set at 45 eV, source pressure at 0.4 Torr, vacuum at  $2.4 - 2.8 \times 10^{-5}$  Torr. The Supelchem PTE-5 capillary column (25 m x 0.32 I.D., 0.25 µm film thickness) with cooled on-column injector were used with the same temperature program as used for the GC-ECD analysis. The output of the mass spectrometer was managed by a Data General Nova/4 and INCOS computer.

Initially, the system was used in the full scan mode, however large source interferences were evident, and the mode was switched to selective ion monitoring for specific molecular ions of nitro-PAC. This also greatly increased the sensitivity, resulting in detection limits in excess of those obtained with GC-ECD (Figure 3.24). The mononitro-PAC HPLC fraction from TES collected at high load and 3500 rpm was analysed and the presence of nitro-PAC was confirmed by molecular ion and RI on 1-nitropyrene (Figure 3.25).

**Key**

1 = 2-Nitrofluoren-9-one

2 = 2,7-Dinitrofluoren-9-one

3 = 2,4,7-Trinitrofluoren-9-one

x = Septum bleed

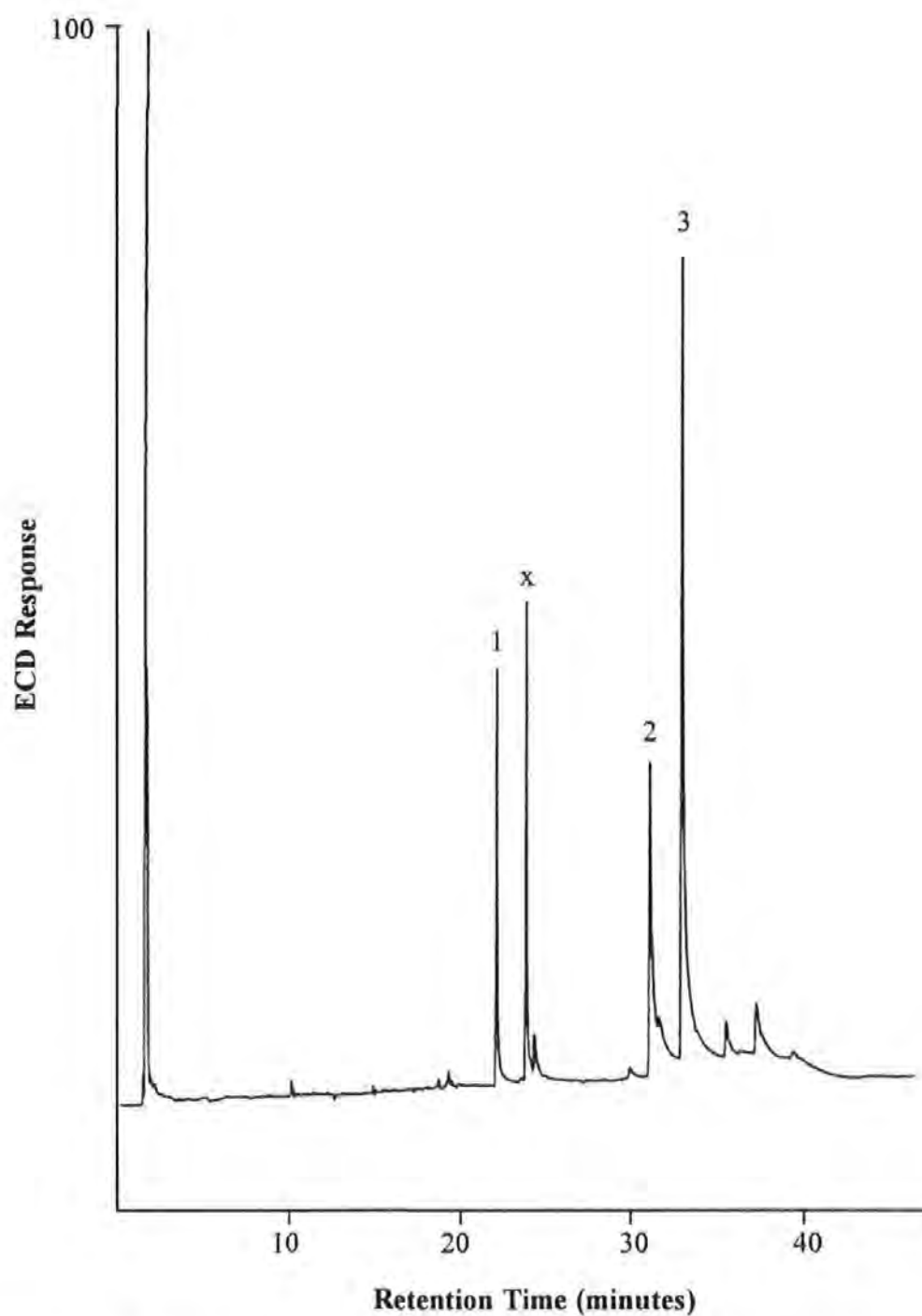


Figure 3.23 The gas chromatogram of the nitro-oxy-PAC standard mix. GC conditions: Supelchem PTE-5 column, 60°C for 1 min., 10°C/min to 200°C, 5°C/min to 300°C, held for 10 min.

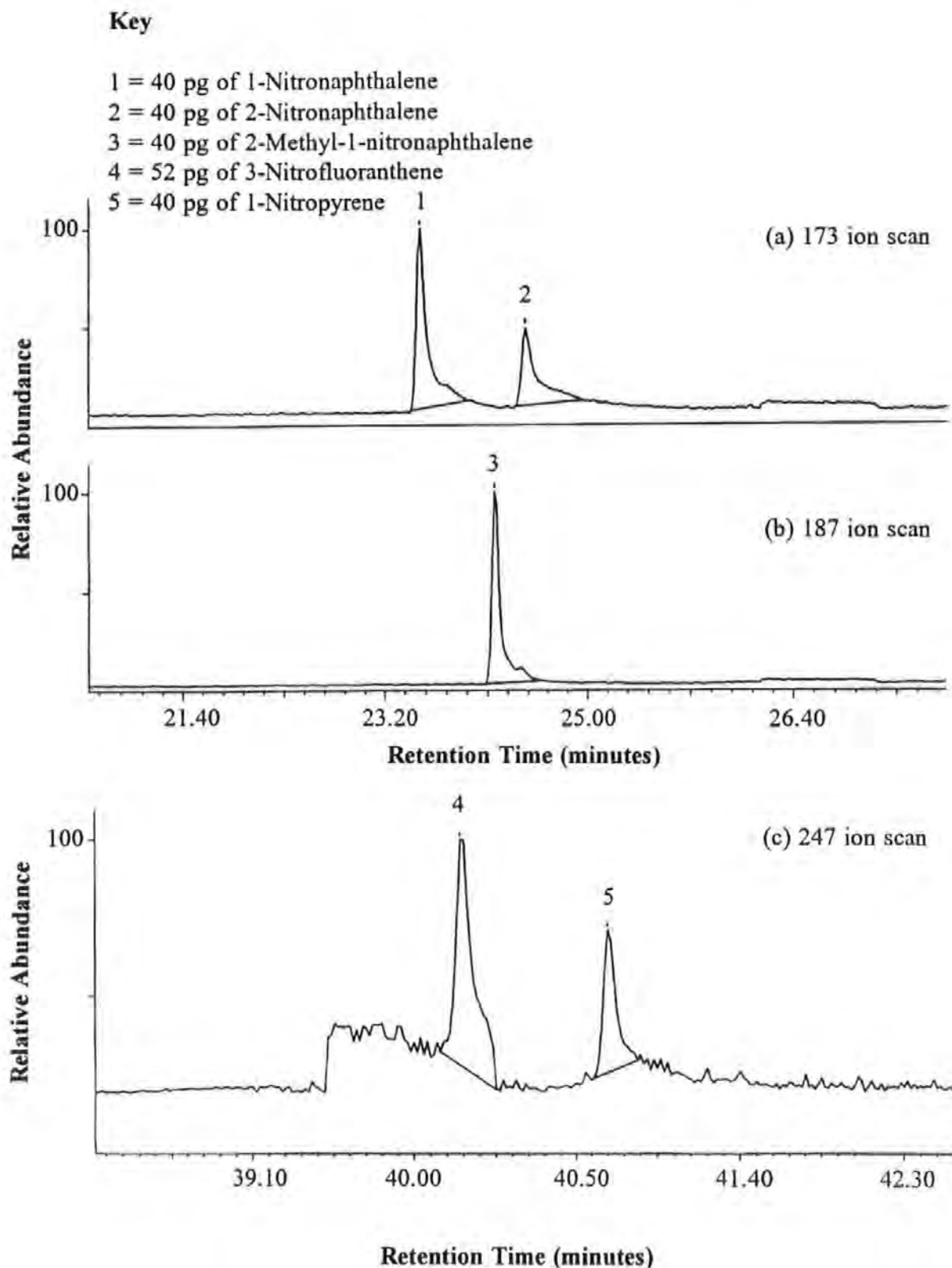


Figure 3.24 The sensitivity of gas chromatography/mass spectrometry operated in the negative ion chemical ionisation and selective ion modes to a) 1- & 2-nitronaphthalene, b) 2-methyl-1-nitronaphthalene, and c) 3-nitrofluoranthene and 1-nitropyrene. GC conditions: Supelchem PTE-5 column, 60°C for 1 min., 5°C/min to 300°C, held for 10 min.

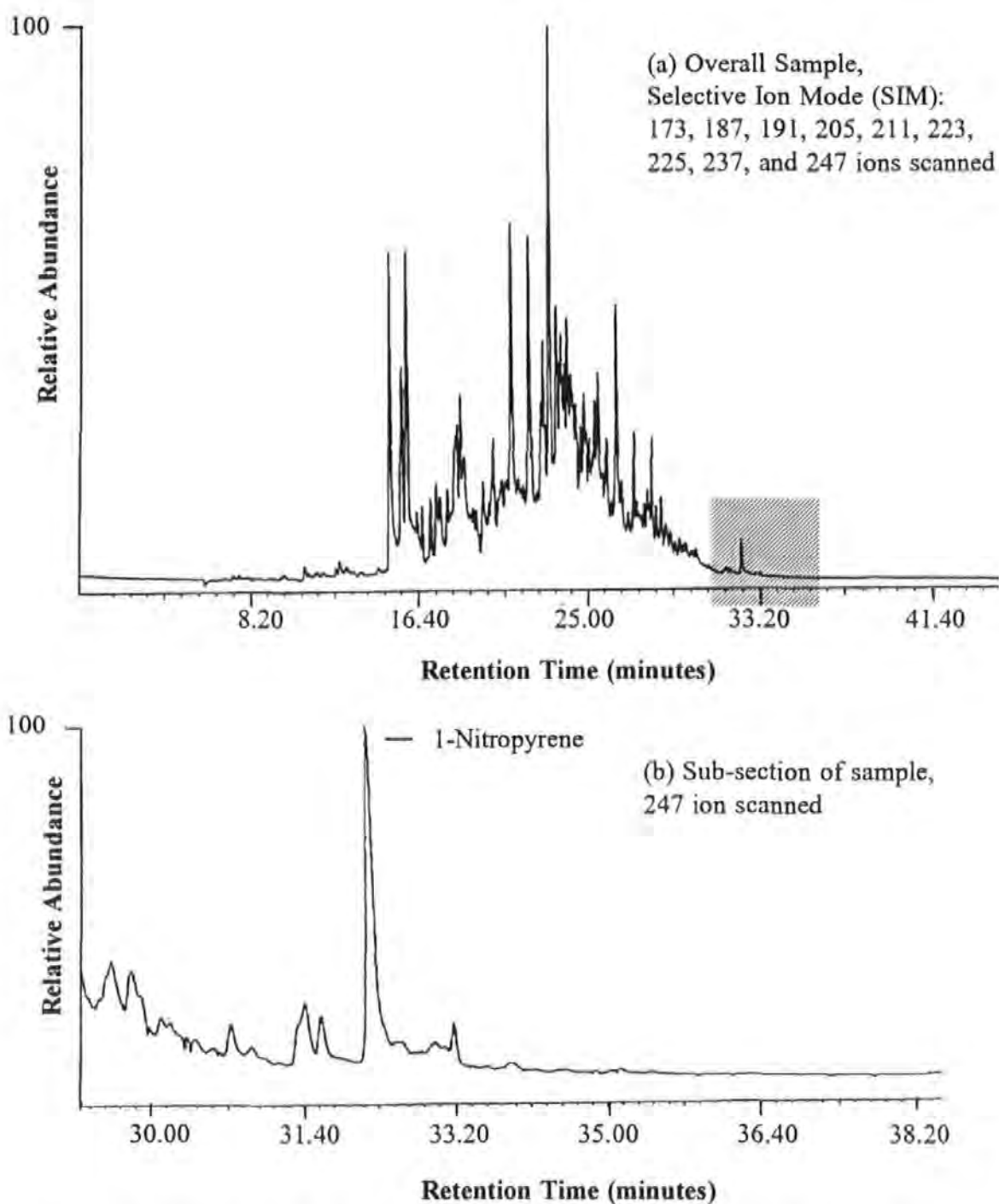


Figure 3.25 The analysis of the mononitro-PAC HPLC fraction obtained at 3500 rpm and high load by gas chromatography/mass spectrometry operated in negative ion chemical ionisation mode, using selective ion monitoring (a) and the confirmation of 1-nitropyrene by scanning for the 247 molecular ion (b). GC conditions: Supelchem PTE-5 column, 60°C for 1 min., 5°C/min to 300°C, held for 10 min.

#### 3.4.3.2 Gas Chromatography/Mass Spectrometry operated in Electron Impact mode for Oxy-PAC

Several researchers have utilized GC/MS in the EI mode for identifying prominent oxy-PAC in diesel extracts (Ramdahl 1983, König *et al.* 1983, and Schulze *et al.* 1984).

The HPLC fractions corresponding to the retention windows for dinitro-PAC, nitro-oxy-PAC, and polar oxy-PAC were investigated for the presence of oxy-PAC by GC/MS in EI mode. The polar fractions from the silica gel chromatography from exhaust samples were also analyzed by GC/MS EI.

A Rt<sub>x</sub>-5 (25 m x 0.32 ID, 0.25 µm film thickness) capillary column was used with cooled on-column injector and helium carrier gas. The temperature programme was 60°C for 1 min., 5°C/min to 300°C, held for 10 mins. The ionisation was 40 eV, with 40-544 amu scanned every 2 seconds. The dinitro-PAC and nitro-oxy-PAC HPLC fractions had previously been diluted and injection volumes were 1.0 µl. The polar fractions from the silica gel clean-up were diluted with acetonitrile to 5 mg/ml and 0.5 µl injections were made. The samples were co-injected with a PAH retention index (0.3 µl injected) containing naphthalene, phenanthrene, chrysene, and benzo(ghi)perylene. The oxy-PAC standard mix was also co-injected with the PAH retention index (Figure 3.26). The retention index was used to aid identification of compounds.

#### 3.4.3.3 Analysis of n-Alkanes by Gas Chromatography with Flame Ionisation Detection

This section details the analysis of the aliphatic fractions collected at 1500 rpm and 3500 rpm by GC-FID. The ODS clean-up of the samples collected at 2500 rpm resulted in retaining the aliphatic fractions on the cartridges. Following the work-up and isolation of the aliphatic fraction from TES (Section 3.4.2), the aliphatic fractions were blown down to a constant weight. The samples (10 mg/ml in DCM) were analyzed on the Carlo Erba Mega GC-FID fitted with a DB-5 capillary column (30 m x 0.32 mm, 0.25 µm film thickness, J&W Scientific), with hydrogen as the carrier gas. Injection volumes were 0.5 µl and cooled on-column injection was used. Integration was by a Shimadzu integrator. The analysis and calibration procedures correspond to those used for the aliphatic fractions from 1000 rpm, 2000 rpm, and 3000 rpm (Section 3.2.3).

**Key**

**Retention Index:**

A = Naphthalene  
B = Phenanthrene  
C = Chrsyene  
D = Benzo(ghi)perylene

**Oxy-PAC:**

1 = Naphthaldehyde  
2 = 9-Hydroxyfluorene  
3 = Xanthone  
4 = Anthrone  
5 = Phenanthrene-9-carboxaldehyde  
6 = 9-Phenanthrol  
7 = 9-Fluorene-9-carboxylic acid  
8 = Benzo(a)anthracene-7,12-dione

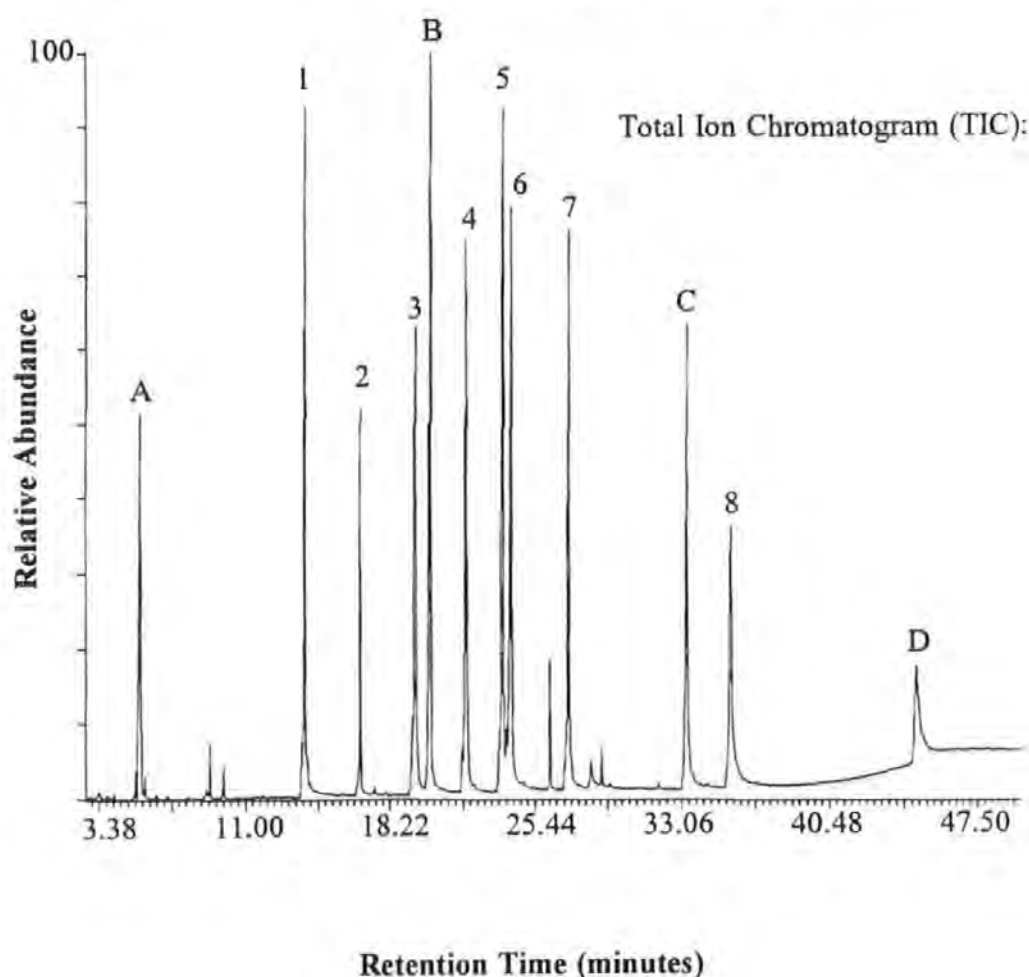


Figure 3.26 Total ion chromatogram of the oxy-PAC standard mix. GC conditions: Rt-5 column, 60°C for 1 min., 5°C/min to 300°C, held for 10 min.

The *n*-alkane quantifications were based on heptadecane ( $R\text{-sq} = 0.9997$ ). The stability of the calibration was confirmed after the 1500 rpm samples. Results were calculated relative to the fuel (Section 4.2.1). The aliphatic fractions from the fresh oil and sump oils were also analyzed.

3.4.3.4 Analysis of Major PAC by Gas Chromatography/Mass Spectrometry operated in the Electron Impact mode

Prior to analysis the engine samples collected at 1500 rpm, 2500 rpm, and 3500 rpm were concentrated, cleaned-up (Section 3.4.2) and the major PAH were isolated by HPLC fractionation (Section 3.4.3). An aliquot of fuel (20.6 mg), taken during the nitro-PAC profiling sampling sessions, plus  $d_8$ -naphthalene (110  $\mu\text{g}$ , 98+%, Aldrich Chemical Co.) and  $d_{10}$ -phenanthrene (86  $\mu\text{g}$ , 97%, Aldrich Chemical Co.) was subjected to silica gel clean-up (Section 3.4.2.2.2).

The analysis and identification of major PAH in the exhaust and fuel samples followed the same instrument and set-up conditions as used for the major organics profiling session (Section 3.2.4), with the following exceptions. Quantification was based on the response to deuterated fluorene (0.228 mg/ml, Janssen Chimica), added as a quarter of the GC/MS dilution concentration (5 mg/ml) to all the samples (Table 3.20). Thus for a 0.5  $\mu\text{l}$  injection 28.5 ng of deuterated fluorene was injected. Results were calculated relative to the fuel (Sections 4.2.1 & 5.2.1.6). The aromatic fractions from the fresh oil and sump oils were also analyzed.

Table 3.20 Response factors ( $R_f$ ) for PAC based on  $d_{10}$ -Fluorene

Compound	$R_f\#1$	$R_f\#2$	$R_f\#3$	Average $R_f$
Naphthalene	0.80	0.755	0.790	0.784
Dibenzothiophene	1.062	1.025	1.022	1.036
Phenanthrene	0.836	0.710	0.716	0.721
Pyrene	0.706	0.721	0.685	0.704



## **Chapter 4 - Primary Organic Emissions**

This chapter examines the primary emissions from diesel combustion for a variety of engine speeds and loads. The primary emissions are defined as being straight chain  $n$ -alkanes in the aliphatic fraction and the major PAC, such as 2-4 ring PAH, in the aromatic fraction.

The establishment of the parameters controlling the primary organic emissions is vital in relation to the improvement of diesel combustion with an aim of meeting proposed future particulate limits and possible future PAH legislation. The origins of the organic emissions is also fundamental to the elucidation of the formation processes resulting in secondary emissions of highly mutagenic nitro-PAC.

The chapter is divided into four parts. Section 4.1 examines the relevant contributions of fuel and oil survival to the Prima emissions. The results from samples collected with the initial and upgraded TESSA configurations are presented and discussed in Sections 4.2 & 4.3 respectively. Finally, the combustion parameters responsible for the primary emissions are summarized in Section 4.4.

### **4.1 The Contributions of Fuel and Oil Survival to the Emissions**

Many diesel exhaust studies have shown that survival of lubricating oil and fuel occurs to different degrees depending on the engine running conditions (Mayer *et al.* 1980, Cartellieri & Tritthart 1984, and Cuthbertson *et al.* 1987). This section examines the relative contributions of unburnt fuel and oil to the Prima emissions over a range of speeds and loads. Figure 4.1a shows a typical chromatogram of the aliphatic fraction of the standard diesel fuel. The fuel is dominated by an homologous series of  $n$ -alkanes ranging from C9 to C28, with the maximum  $n$ -alkane concentration associated with hexadecane (Table 4.1). The aliphatic fraction of lubricating oil consists largely of an unresolved complex mixture (UCM) eluting at high temperatures, with a series of high boiling  $n$ -alkanes superimposed on the UCM hump (Figure 4.1b).

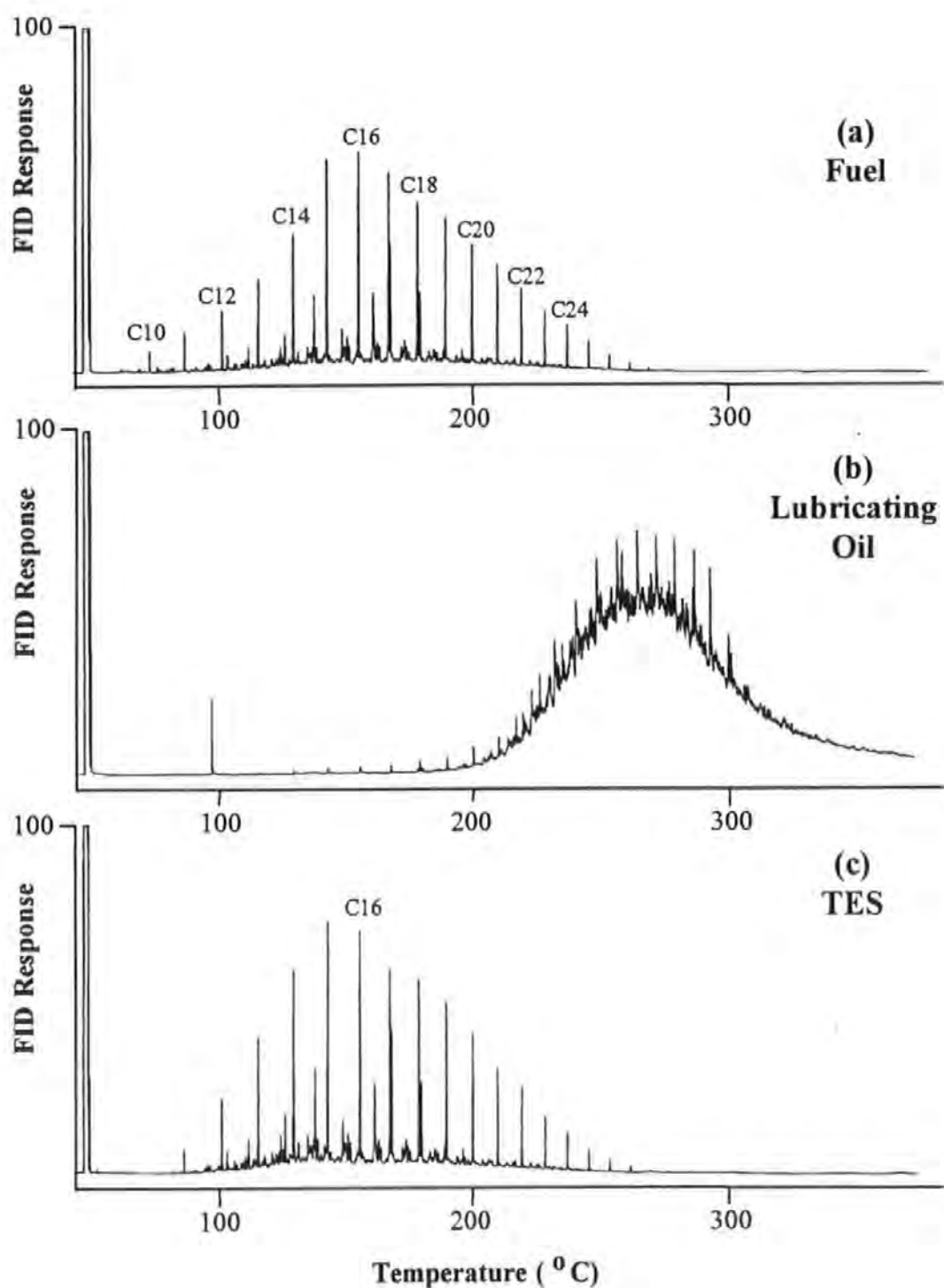


Figure 4.1 Comparison of the aliphatic fractions of diesel fuel (a) and lubricating oil (b), with the TESSA extracted sample (TES) at 1% of full load and 1000 rpm (c) (Chromatographic conditions given in Section 3.2.3).

A comparison of the fuel and oil with the aliphatic fraction of a TES collected at low speed and low load is shown in Figure 4.1c. The compounds associated with the fuel temperature region are clearly visible, whereas the lubricating oil hump is indiscernible.

Table 4.1 Concentration of Selected *n*-alkanes in the A2 Fuel

Compound	Relative molecular mass	Melting point (°C), Boiling point (°C) <sup>1</sup>	Concentration (ppm)
Decane (C10)	142	-29.7, 174.1	1578
Dodecane (C12)	170	-9.6, 216.3	3924
Tetradecane (C14)	198	5.9, 253.7	8855
Hexadecane (C16)	226	18.2, 287.0	14529
Octadecane (C18)	254	28.2, 316.1	10369
Eicosane (C20)	282	36.8, 343.0	7542
Docosane (C22)	310	44.4, 386.6	4702
Tetracosane (C24)	338	54.0, 391.3	2697
Hexacosane (C26)	366	56.4, 412.2	1030
Octacosane (C28)	394	64.5, 431.6	244

<sup>1</sup> Weast & Astle (1985)

After enlarging the lubricating oil temperature window there is evidence of a small oil hump eluting between 275°C and 300°C (Figure 4.2). This hump does not cover the entire range of the lubricating oil UCM (165°C to 300°C), suggesting that only the very high molecular weight constituents of oil leakages survive unchanged. The great majority of any lubricating oil leakages are combusted. There does appear to be some peak matching of the exhaust to the lubricating oil throughout the lubricating oil range. This shows that specific components of the oil may have sufficient resistance to combustion, allowing these compounds to survive unchanged. The absence of a significant oil UCM in the aliphatic fraction of the exhaust at low load and low speed, indicates that even at the engine conditions known to favour oil survival (Williams *et al.* 1987), there are only minor oil survival contributions to the Prima exhaust. The oil contributions remained low for increased loads and speeds (Figure 4.3). For all the engine samples collected, no significant oil UCM could be detected, even after reducing the chart recorder attenuation within the oil temperature zone.

**Key**

+ = matching of compounds in both samples

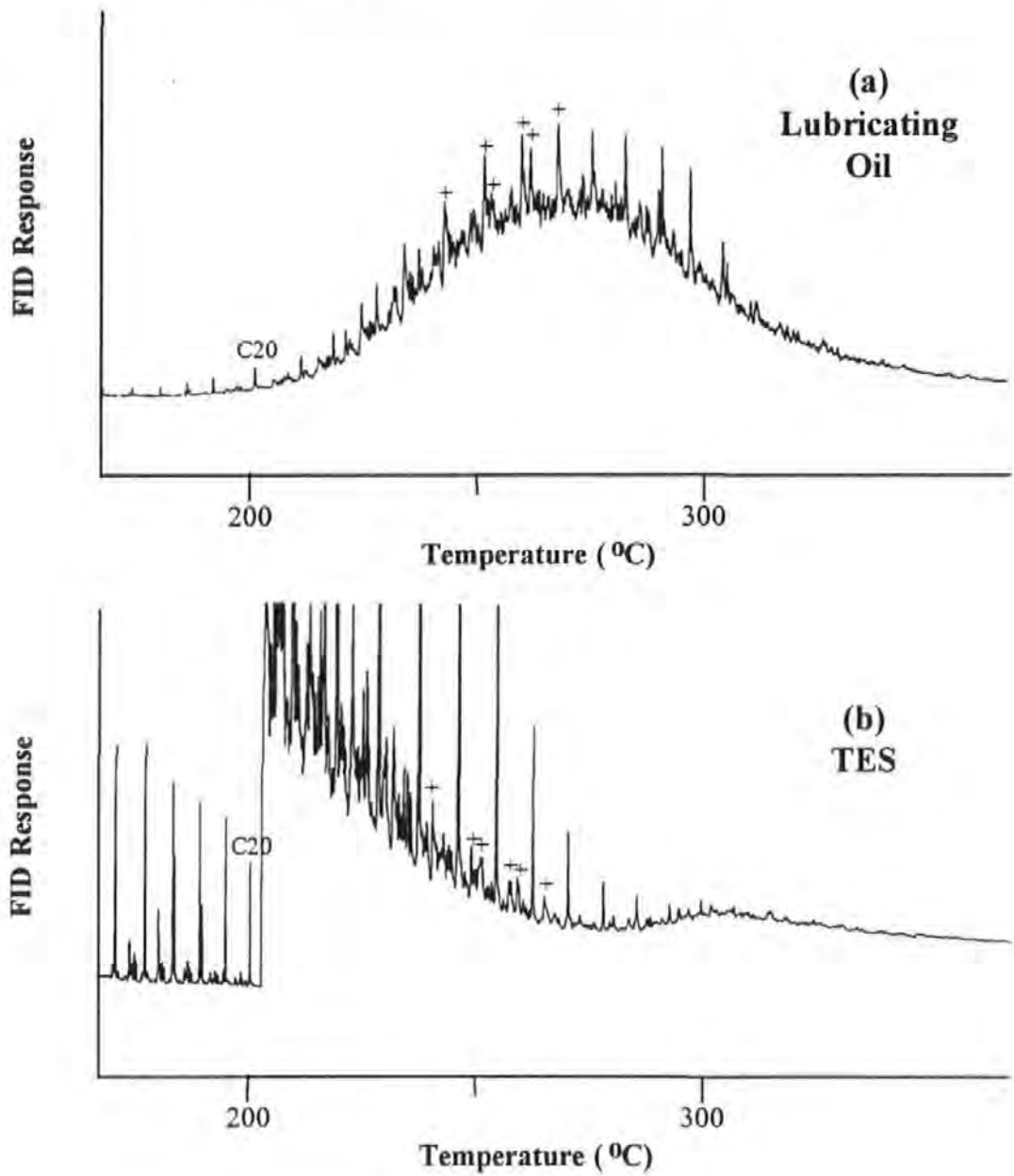


Figure 4.2 Close examination of the oil hump temperature window (a) to the same temperature range of the TESSA extracted sample (TES) at 1% of full load and 1000 rpm (b) (Chromatographic conditions given in Section 3.2.3).

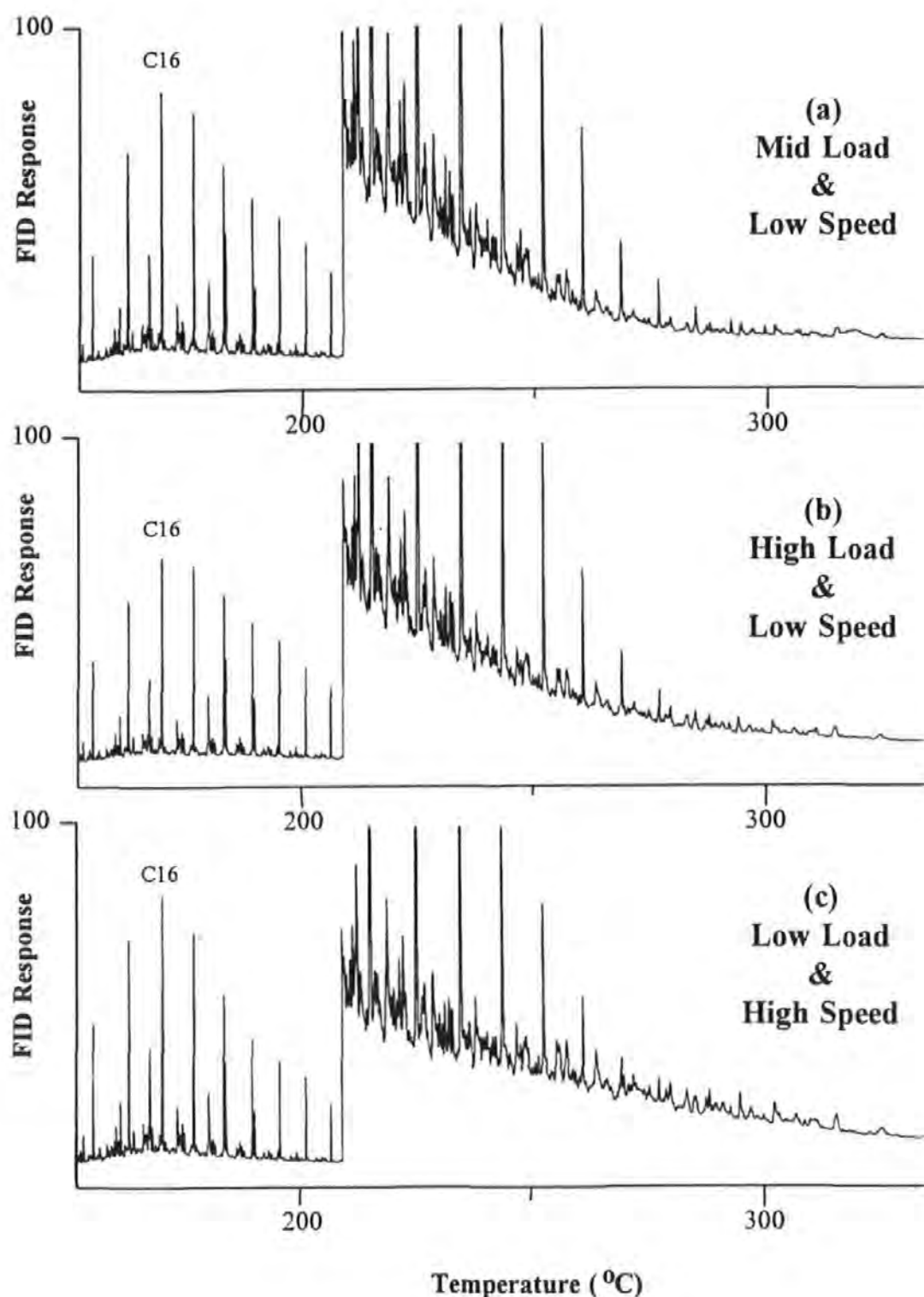


Figure 4.3 Examination of the aliphatic fractions of TESSA extracted samples (TES) for evidence of oil contributions at three power settings: 50% of full load & 1000 rpm (a), full load and 1000 rpm (b), and 1% of full load and 3000 rpm (c) (Chromatographic conditions given in Section 3.2.3).

Figure 4.4 shows the gas chromatographic traces of the aromatic fractions of the A2 fuel, lubricating oil, and exhaust at low speed and load. Figure 4.4a and Table 4.2 indicate that the fuel is dominated by the smaller 2-3 ring PAH and the corresponding methyl derivatives. Further evidence that fuel survival is the dominant source is shown by the close chemical resemblance of the fuel and emissions character. The high boiling aromatic constituents of the oil are not recovered at significant levels in TES.

Table 4.2 Concentration of Selected PAC in the A2 fuel

Compound	PAC class	Relative molecular mass	Melting point (°C), Boiling point (°C) <sup>1</sup>	Concentration (ppm)
Naphthalene	PAH	128	81, 218	2593
Methylnaphthalenes	PAH	142	22-35, 245-251	8632
Dimethylnaphthalenes	PAH	156	1.6-108, 262-276	18432
Fluorene	PAH	166	115-116, 294	831
Methylfluorenes	PAH	180	46-87, 302-318	2116
Dibenzothiophene	PASH	184	97, 332 <sup>2</sup>	296
Methyldibenzothiophenes	PASH	198	66-85, -	634
Phenanthrene	PAH	178	101, 338	1631
Methylphenanthrenes	PAH	192	52-123, 352-359	3980
Pyrene	PAH	202	151, 393	151
Chrysene	PAH	228	254, 431	31

<sup>1</sup> Karcher *et al.* (1985)

<sup>2</sup> Weast & Astle (1985)

Although the contributions of oil survival to TES were low, the accumulation of unburnt fuel components in the sump was investigated. Figure 4.5 shows there was no or very little build up of the lighter fuel aliphatics in the sump oil after 50 and 105 hours of usage. Survival of used oil is not responsible for aliphatic emissions eluted within the fuel hump retention zone. The accumulation of aromatics in the sump oil was also examined (Figure 4.6). There was a moderate build-up of PAH as can be seen by the appearance of phenanthrene and the methyl-phenanthrenes in used sump oil. After adjusting for laboratory losses it can be shown that the level of PAH in the oil increased with oil usage (Figure 4.7).

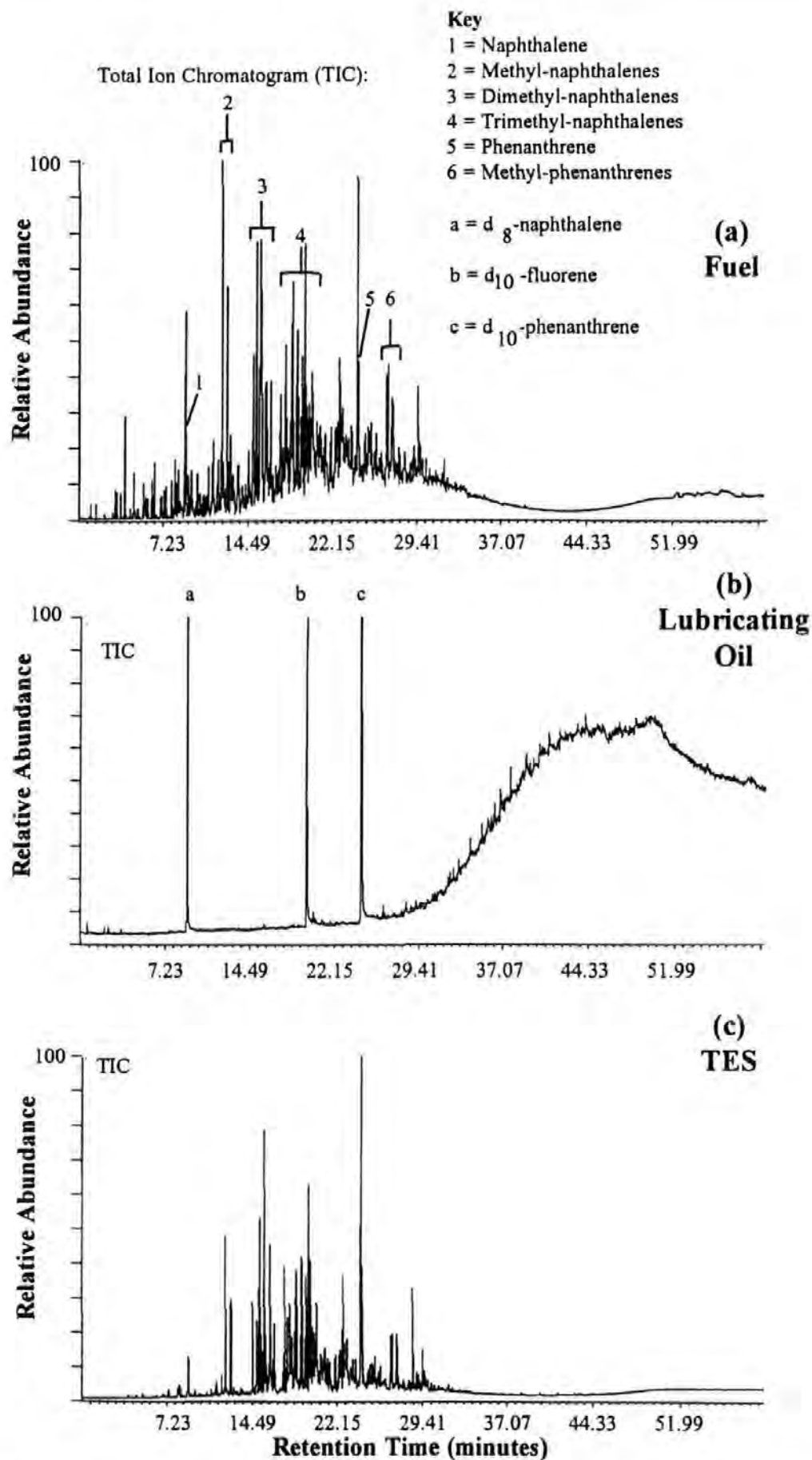


Figure 4.4 Comparison of the aromatic fractions of fuel (a) and lubricating oil (b), with the TESSA extracted sample (TES) at 1% of full load and 1500 rpm (c) (Chromatographic conditions given in Section 3.2.4).

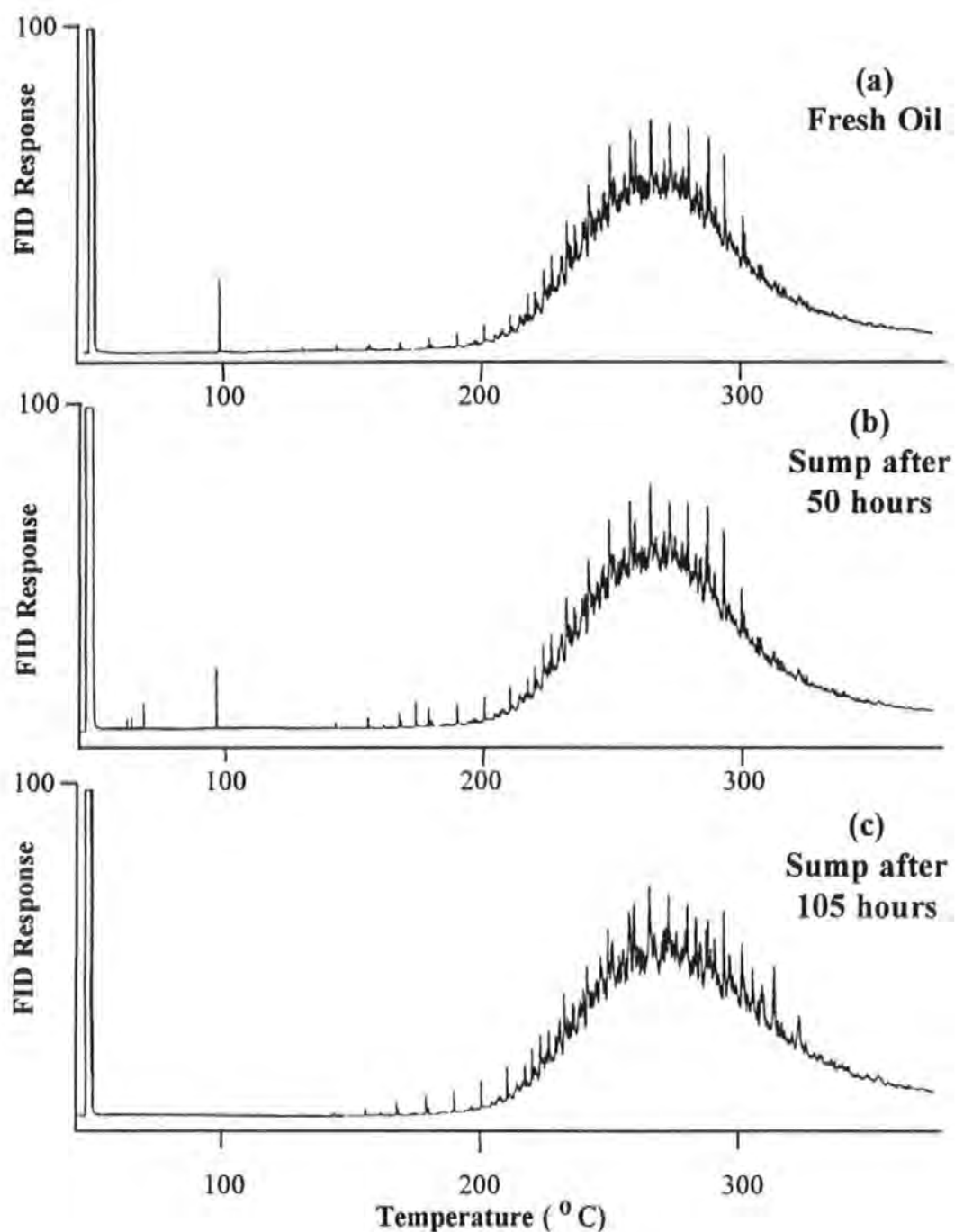


Figure 4.5 Examination of the aliphatic fractions of sump oils for accumulation of unburnt fuel. Fresh oil (a), sump after 50 hours use (b), and sump after 105 hours use (c) (Chromatographic conditions given in Section 3.2.3).



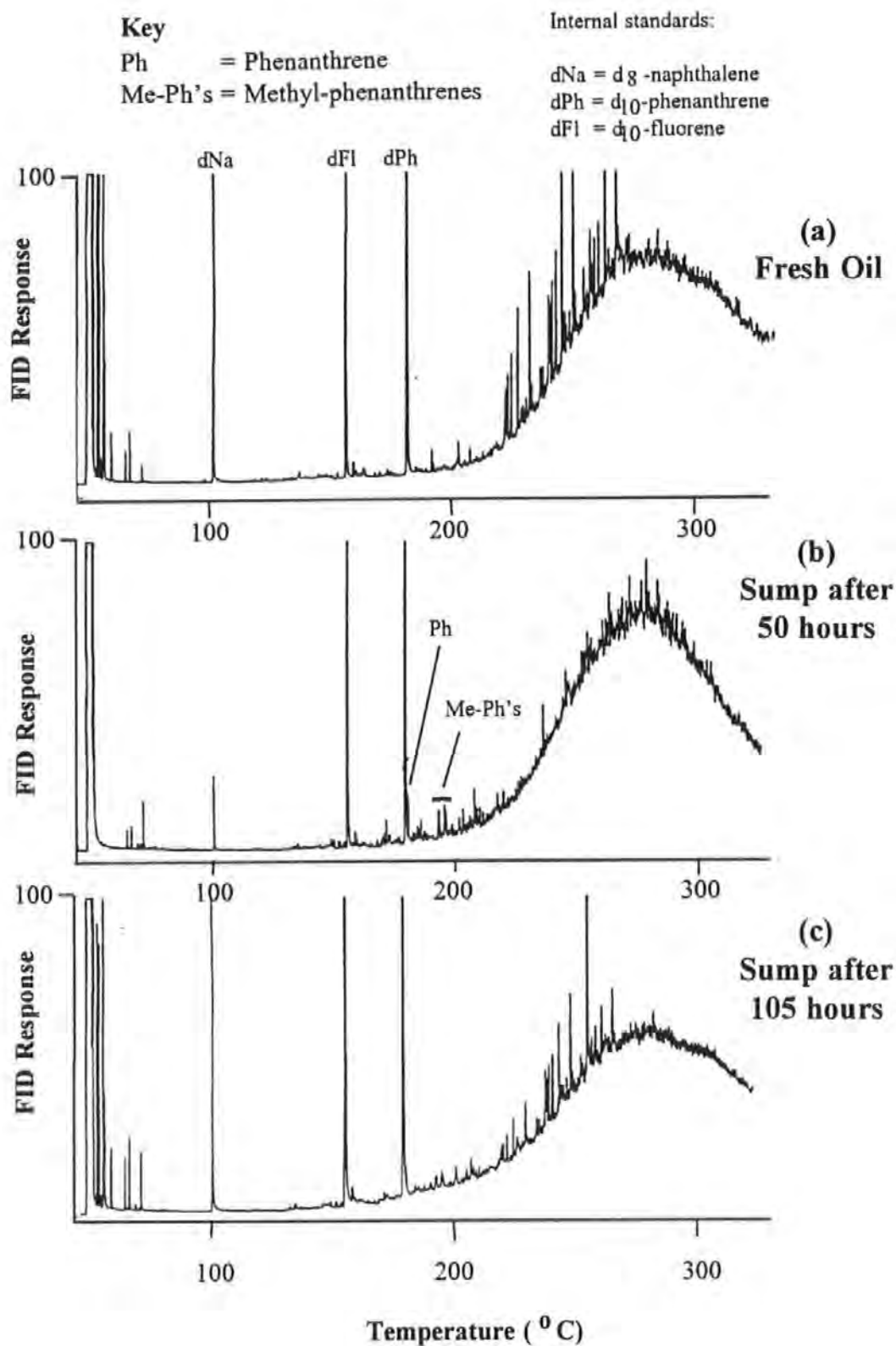


Figure 4.6 Examination of the aromatic fractions of sump oils for accumulation of unburnt fuel. Fresh oil (a), sump after 50 hours use (b), and sump after 105 hours use (c) (Chromatographic conditions given in Section 3.2.4).

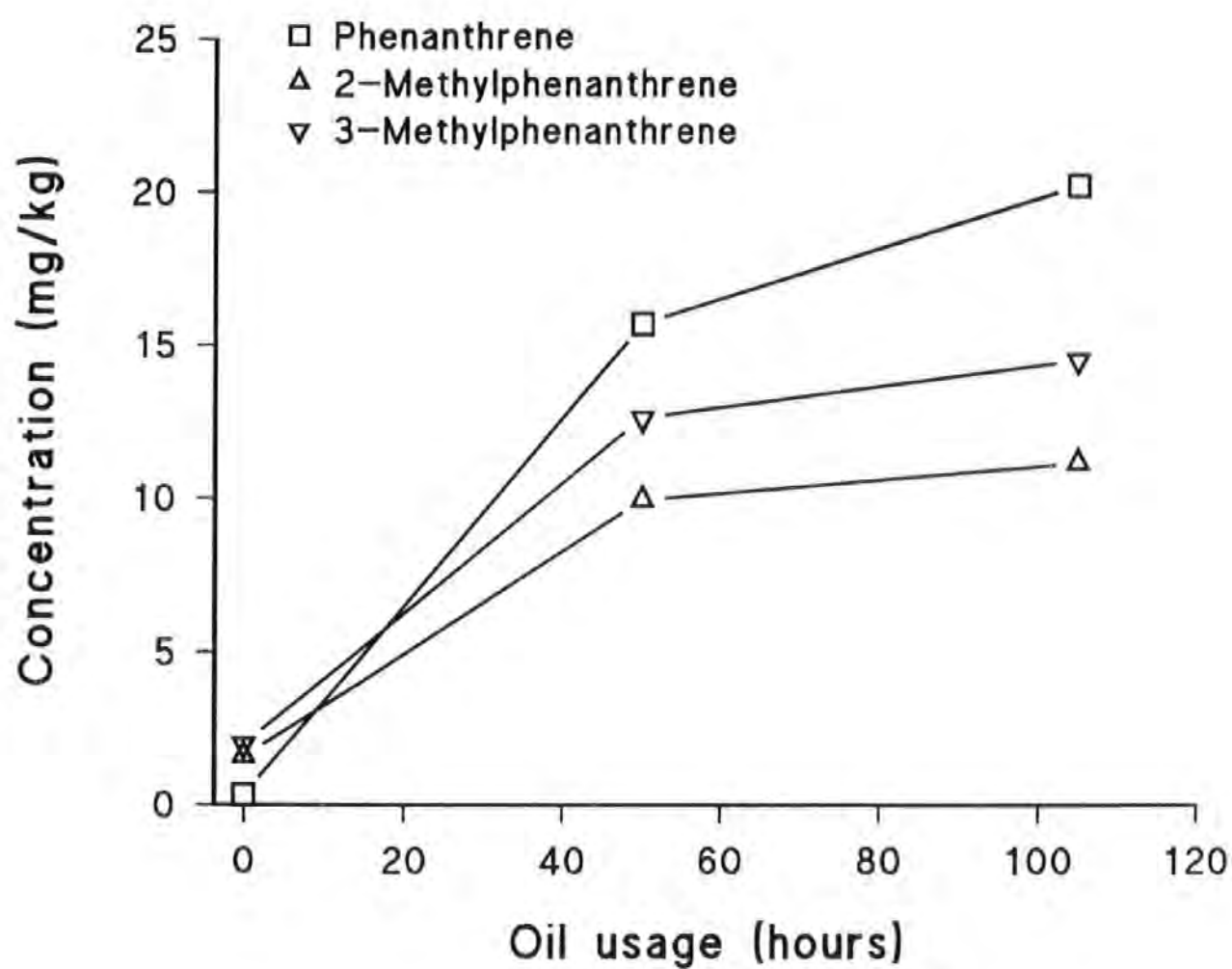


Figure 4.7 Accumulation of phenanthrene and methyl derivatives in sump oil over time.

Previous studies have shown an accumulation of both lower *n*-alkane and PAC in the sump oil over a period of time (Abbass *et al.* 1987). Abbass and co-researchers found 30 mg of phenanthrene/kg of oil had accumulated after 106 hours for a 4 l Perkins DI engine. The authors found the accumulation levels reached an maximum after 120 hours of oil use. Compared with the study by Abbass *et al.* (1987), the accumulation of phenanthrene in the sump oil for the Prima engine was lower, corresponding to *ca.* 20 mg/kg after 105 hours of oil use.

The lack of prominent peaks present in the aromatic fraction of the oil sump, collected after 50 hours of use, is of interest. Compared with the other two oil samples, the sump sample collected after 50 hours of use was subjected to HPLC fractionation to examine the nitro- and oxy-PAC content (Section 3.4.2.3). Absence of prominent peaks indicates that there are more polar constituents in the oil which elute after the PAH fraction. The composition of the more polars fractions of the oil are discussed in Chapter 5.

An examination of the relative contributions of fuel and oil at varying engine conditions, reveals that fuel survival is by far the dominant survival source. The results presented later in this chapter were derived from two sampling sessions. For both sessions the oil usage over the sampling periods was low, and as a result the accumulation of organics is correspondingly low. This allows emissions from the earlier samples to be directly compared to the later samples. Finally, the minor contribution of lubricating oil to TES means that the limited accumulation of *n*-alkane and PAC which does occur will not add significantly to the Prima exhaust.

#### 4.2 Profiling of the Primary Organics using the initial TESSA configuration

Engine emissions are strongly influenced by driving conditions and cycles, for example the combustion environment at high speed motorway driving will be different from that evolved at urban congested driving. The contribution of survival and pyrosynthesis/pyrolysis to emissions may also be affected by differing engine conditions. Engine sampling under different conditions followed by comparing the chemical profiles or 'fingerprints' produced at the different conditions, allows an estimation of both the effect of engine conditions on the emission levels and also the dominant emission pathways.

The results in this section were obtained by sampling at 1000 rpm, 2000 rpm, and 3000 rpm using the initial TESSA set-up (Section 3.2.1). The samples were then extracted, concentrated, and fractionated by silica gel open column gravity fed chromatography (Section 3.2.2). The *n*-alkanes and PAH were quantified by GC-FID (Section 3.2.3) and GC/MS EI (Section 3.2.4) respectively.

#### 4.2.1 The Concept of Percentage Recoveries

The major pathways for the source of the primary organic emissions, ie. compounds present in the fuel and/or oil, in the Prima exhaust are:

- a) survival of the compound from the fuel/lube oil unchanged
- b) combustion reactions in which fragments of fuel/lube oil pyrosynthesize, resulting in partially combusted products.
- c) transformation reactions in the exhaust pipe.

In (a) the carbon skeleton of the compound remains unchanged, while in (b) the carbon skeleton of the compound is altered/newly formed in the combustion chamber. The results presented in Section 4.1 identified that lubricating oil contributions to TES are minimal in comparison to those derived from fuel survival. The close proximity of TESSA to the engine will reduce the opportunities for post-combustion exhaust reactions (c). Therefore, the following results and discussions are focused on the survival and combustion products of diesel fuel.

For different compounds in the emissions, the relative contributions by mechanism (a) may vary. This will reflect the different combustion efficiencies that occur for differing organic structures under different combustion conditions. The similarity in ratios of compounds in the fuel and the emissions may thus be a measure of the conditions which favour similar combustion efficiencies, so that they survive to similar degrees. By contrast, very different ratios in emissions compared with the fuel, may indicate conditions which favour differences in degree of destruction of structures. Interpretation here is made more complicated because different ratios may also indicate a significant contribution from pyrosynthetic reactions (ie. mechanism (b)).

The degree of combustion for a compound is related to a number of factors in the combustion chamber, eg. temperature, oxidant concentration, air motion, and kinetics of reaction (Campbell *et al.* 1981, Scheepers & Bos 1992b). For a molecule within the combustion chamber to react, it may be necessary for it to experience a sufficiently high temperature to break bonds, sufficient oxidant and a sufficient length of time to allow the reaction to be completed. The extent of reaction that occurs in the combustion chamber will depend especially on temperatures and the kinetics of the reaction.

In an attempt to evaluate the relative contributions of the emission pathways, namely survival and pyrosynthesis/pyrolysis, at varying engine conditions, the recovery of primary emissions as a percentage of the corresponding fuel compound supplied to the combustion chamber were calculated. An example of the percentage recovery of pyrene at 1% of full load and 1000 rpm is given below:

$$PY_{PR} = \frac{PY_{ex}}{PY_{fu}} \times 100$$

$$= \frac{0.0018}{0.155} \times 100 = 1.16\%$$

where  $PY_{PR}$  = percentage recovery of pyrene

$PY_{ex}$  = pyrene in exhaust sample collected (mg)

$PY_{fu}$  = pyrene in fuel consumed during sampling period (mg)

The comparison of the percentage recovery of different compounds at a particular engine condition enables an insight into the source of the emissions. Figure 4.8 uses a theoretical model to demonstrate the interpretation of the percentage recoveries. If all compounds (A, B, and C) are recovered by the same amount, then the ratio of these compounds in the exhaust matches that in the fuel, ie. fuel survival unchanged. Differing percentage recoveries may indicate that the structure of compound C results in a greater combustion compared with compound A. On the other hand, a proportion of compound A may be added to by pyrosynthetic reactions, such as compound C being transformed into compound A.

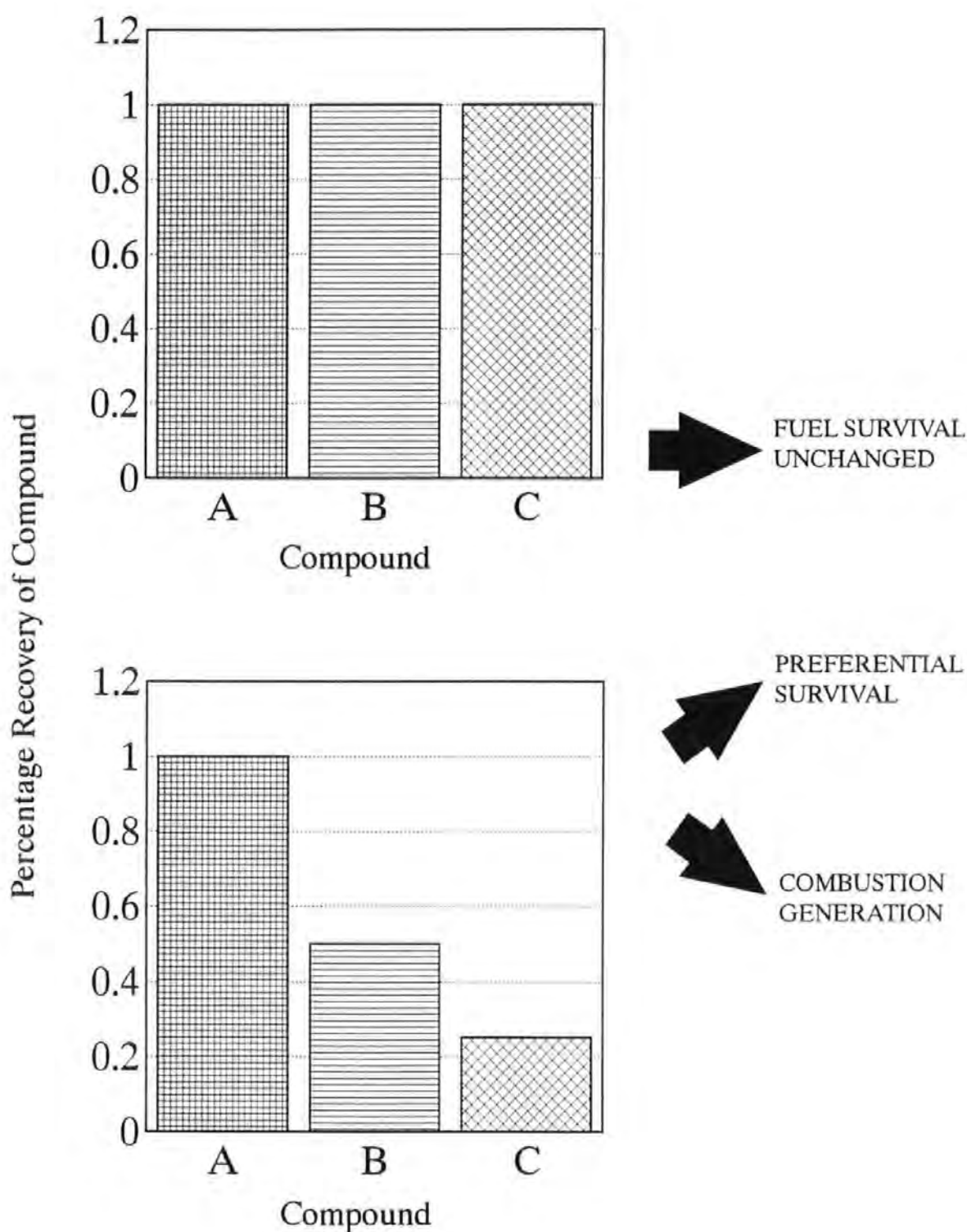


Figure 4.8 Interpretation of percentage recoveries for identification of the source of emissions.

The percentage recovery for selected PAC and *n*-alkanes for a range of speeds and loads are shown in Tables 4.3 and 4.4 respectively. To aid the comparison of the results to other combustion studies, the data is also presented in terms of the amount of compound emitted relative to the total amount of fuel consumed (units of mg/kg).

Table 4.3 The Exhaust PAC emissions relative to the corresponding fuel PAC consumed during sampling

Engine Speed (rpm)	Percentage of Full Load	Fluorene	Dibenzothiophene	Phenanthrene	Pyrene
1000	1	0.91 (6.83)	0.88 (3.28)	0.86 (14.28)	1.16 (1.79)
	25	0.26 (1.95)	0.20 (0.76)	0.20 (3.31)	0.14 (0.22)
	50	0.19 (1.45)	0.17 (0.63)	0.16 (2.72)	0.13 (0.21)
	75	0.20 (1.50)	0.18 (0.65)	0.17 (2.75)	0.15 (0.23)
	100	0.21 (1.57)	0.20 (0.75)	0.21 (3.49)	0.19 (0.31)
2000	1	0.36 (2.70)	0.31 (1.14)	0.29 (4.80)	0.30 (0.47)
	25	0.32 (2.44)	0.23 (0.86)	0.18 (3.60)	0.14 (0.21)
	50	0.21 (1.55)	0.16 (0.59)	0.16 (2.67)	0.11 (0.16)
	75	0.22 (1.65)	0.18 (0.68)	0.16 (2.70)	0.10 (0.15)
	100	0.16 (1.19)	0.15 (0.56)	0.15 (2.56)	0.08 (0.12)
3000	1	0.63 (4.72)	0.49 (1.83)	0.45 (7.52)	0.29 (0.44)
	25	0.46 (3.44)	0.35 (1.29)	0.26 (4.38)	0.19 (0.30)
	50	0.31 (2.31)	0.28 (1.06)	0.23 (3.82)	0.13 (0.20)
	75	0.17 (1.25)	0.19 (0.70)	0.16 (2.71)	0.09 (0.14)
	100	0.13 (0.99)	0.17 (0.64)	0.13 (2.19)	0.08 (0.12)

Figures in brackets expressed as compound (mg) recovered per kg of fuel consumed (mg/kg).

Emissions expressed relative to the total fuel consumed take no account of the varied concentrations of compounds in the fuel itself. This can translate to compounds having the same percentage recovery at specific conditions but different values when expressed relative to the total fuel burned. For example fluorene and phenanthrene are both recovered by 0.21% at 1000 rpm and full load. However, the greater phenanthrene compared with fluorene in the

fuel, results in higher emissions relative to the total fuel consumed for phenanthrene. Expressing the emissions as a percentage recovery allows the combustion of compounds at differing fuel concentrations to be directly compared.

Table 4.4 The Exhaust n-alkane emissions relative to the corresponding fuel n-alkane consumed during sampling

Speed (rpm)	Percentage of Full Load	C14	C15	C16	C18	C20
1000	1	0.55 (46.0)	0.51 (61.0)	0.39 (57.5)	0.43 (43.3)	0.50 (33.6)
	25	0.17 (13.9)	0.14 (16.8)	0.1 (14.7)	0.09 (8.7)	0.09 (6.6)
	50	0.11 (9.5)	0.10 (12.6)	0.08 (11.6)	0.07 (7.3)	0.07 (5.0)
	75	0.12 (10.2)	0.11 (13.4)	0.08 (11.9)	0.08 (7.7)	0.07 (4.9)
	100	0.10 (8.5)	0.10 (11.4)	0.07 (10.6)	0.08 (7.5)	0.07 (5.2)
2000	1	0.15 (13.0)	0.18 (21.8)	0.12 (17.9)	0.09 (9.2)	0.08 (5.4)
	25	0.10 (8.3)	0.05 (5.7)	0.07 (9.6)	0.04 (4.3)	0.04 (2.5)
	50	0.11 (9.3)	0.11 (12.9)	0.07 (10.5)	0.05 (4.9)	0.04 (2.9)
	75	0.06 (5.2)	0.06 (7.2)	0.04 (6.1)	0.03 (2.8)	0.02 (1.5)
	100	0.09 (7.4)	0.10 (12.2)	0.07 (9.8)	0.05 (4.7)	0.03 (2.3)
3000	1	0.31 (25.7)	0.29 (35.1)	0.18 (26.8)	0.14 (13.6)	0.13 (9.3)
	25	0.19 (15.8)	0.18 (21.2)	0.11 (16.2)	0.07 (7.3)	0.06 (4.4)
	50	0.19 (15.5)	0.19 (22.5)	0.13 (19.1)	0.08 (8.2)	0.06 (4.1)
	75	0.12 (9.7)	0.13 (15.6)	0.10 (14.6)	0.08 (7.5)	0.05 (3.6)
	100	0.03 (2.3)	0.04 (4.2)	0.03 (4.8)	0.03 (3.2)	0.02 (1.7)

Figures in brackets expressed as compound (mg) recovered per kg of fuel consumed (mg/kg).



#### 4.2.2 The Effect of Engine Load on the Percentage Recovery of Primary Organics

This section examines the effect of engine load on the combustion efficiency of specific components of diesel fuel, namely those of selected *n*-alkanes and 2-4 ring PAC. Combustion efficiency is thermodynamically defined as the actual energy produced from the fuel:air charge relative to the theoretical maximum. Calculation of combustion efficiency defined then requires complicated temperature measurements, which are particularly difficult with the heterogenous nature of diesel combustion. Combustion efficiency can also be defined as the mass of fuel emitted from the cylinder relative to the mass of fuel injected, ie. in the form of percentage recovery. Whenever the term combustion efficiency is used in this study for a specific compound it is expressed as the level of its percentage recovery. For example, a 0.1% recovery is equivalent to 99.9% combustion efficiency.

Figure 4.9a illustrates the recovery of selected PAC in the emissions from an engine run at 1000 rpm and varying loads. For a specific load the closeness of the points for the different PAC, indicates ratios of PAC content similar in the emissions to those in the fuel. This is strong evidence for survival of the PAC unchanged (mechanism (a)). It is also apparent from Figure 4.9a that the individual recoveries of PAC are lower at higher loads compared to the lowest load. At the lowest load the total yield of PAC in the emissions is at its maximum and the ratios are observed to be much more variable than at all other loads for this speed (pyrene especially appears to be atypical at low load). The *n*-alkane molecules exhibit a similar relationship with engine load as for the PAC emissions at low engine speed (Figure 4.9b). The greatest recoveries are, as for the aromatics, associated with low loads. The closeness of the percentage recovery of different *n*-alkanes at each load position again suggests that the organic emissions are derived from fuel surviving combustion unchanged.

Further evidence for the PAC and *n*-alkane emissions being derived from fuel survival at low speed is indicated by the decline of total unburnt hydrocarbon (UHC) and TES emissions with engine load (Figure 4.10a & b). The UHC and TES emissions relative to the total fuel consumed both decrease with increased load. The aromatic and *n*-alkane emissions follow the main emission pathway of the UHC and TES emissions, namely survival.

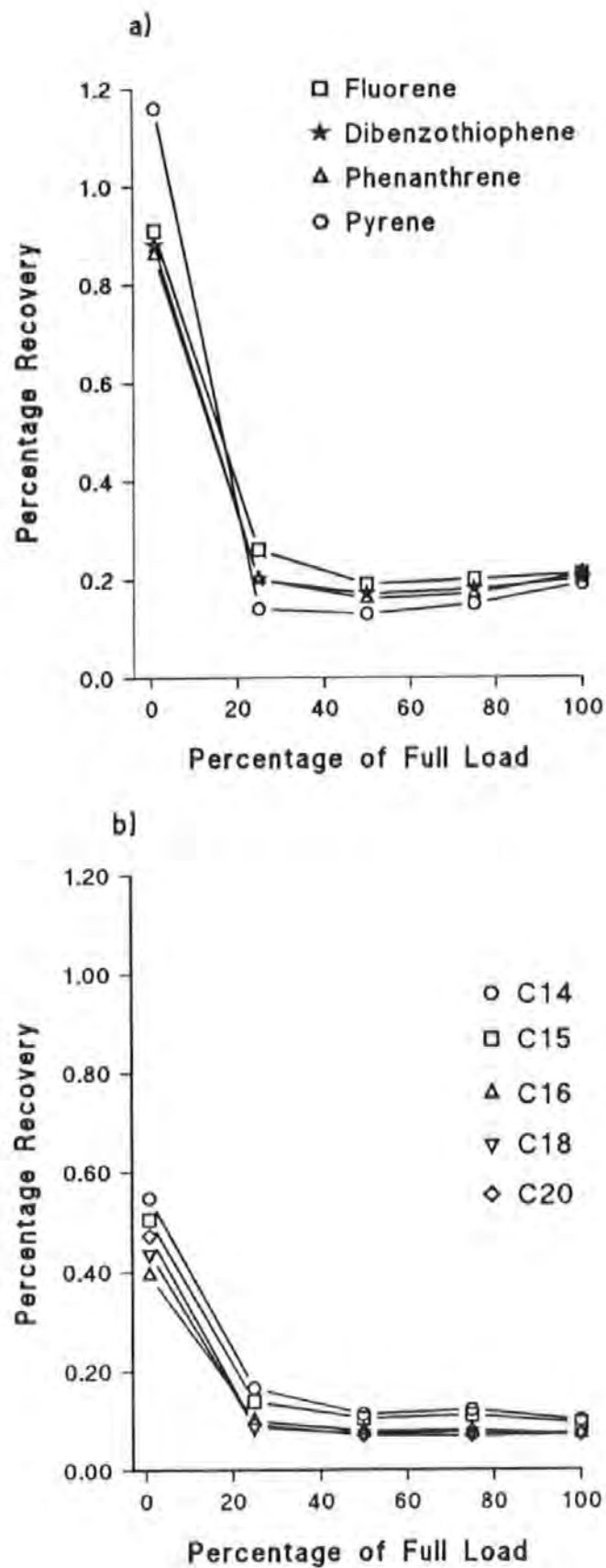


Figure 4.9 Effect of engine load on the percentage recovery of selected PAC (a) and n-alkanes (b) at 1000 rpm.

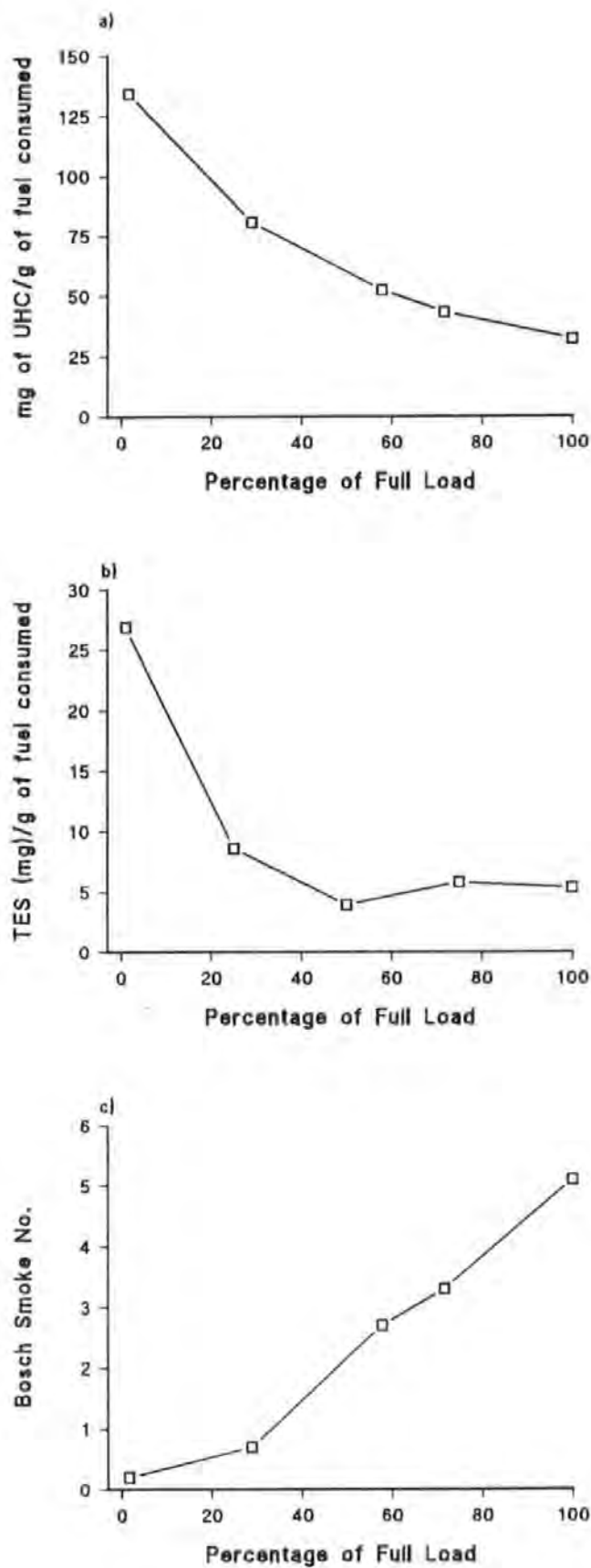


Figure 4.10 Effect of engine load on the emissions of unburnt hydrocarbons (UHC) (a), TESSA extracted sample (TES) (b), and bosch smoke (c) at 1000 rpm

Figure 4.10c shows the trend of smoke, measured by a Bosch smoke meter, relative to the engine load. The Bosch smoke measurements can be equated to the dry soot composition of particulates, since the technique relies on the absorption of light by the carbon nuclei, rather than a weight determination (Alkidas 1984). A weight determination would include both 'dry' and 'wet' organics. The trend for the smoke is the opposite to the organic emissions, such that the soot output increases with increased load. This indicates that the exhaust composition at low loads is enriched in organics whereas the dry soot contribution to total particulates dominates at high loads. This agrees with the findings of Iida *et al.* 1986, who studied the particulate and SOF emissions from a single cylinder 0.9 l DI diesel engine. These authors found that at full load, 95% of the total mass of particulates was dry particulate, whereas at zero load 100% of the particulate was SOF based. Draper (1986) also found that under full load the particulate collected was less than 3% SOF, whereas under reduced load the exhaust particulate was 29% SOF. A similar finding was found by Gomes & Yates (1992) for a single cylinder 0.6 l Hydra engine, for which the SOF contribution at low loads was between 80% to 90%, whilst much reduced at high loads.

The average fuel survival for the selected PAC decreased from 0.95% at low load to 0.2% at full load. The average fuel survival for selected *n*-alkanes ranged from 0.48% at low load to 0.084% at high load. This shows that fuel survival exhibited a negative association with engine load. This finding is in agreement with previous studies (Table 4.5), which also suggested fuel survival was highest at low engine loads. Other studies, such as that by Assaumi *et al.* 1992, have found that combustion conditions deteriorated badly at low loads and led to greater SOF emissions. Mills *et al.* (1984) also found the total PAH emissions were highest at low loads for a light-duty DI diesel, suggesting inefficient fuel combustion under these conditions. Barbella *et al.* (1989) also found that PAH emissions relative to the fuel consumed were highest at low loads. The authors showed that different PAH exhibited varying trends across the load range, such that fluorene and phenanthrene initially decreased at mid-load before rising again at higher loads. By contrast, fluoranthene and benzo(e)pyrene progressively declined with increased load. The size of the engine and the configuration of the combustion chamber may be significant factors in the emission trends. For example, the study of a medium-duty Perkins DI 4-236 4 l diesel engine by Williams *et al.* (1989) found opposite

trends to the earlier study of a smaller 0.5 l per cylinder DI engine. For example the recovery of phenanthrene at low, mid, and high load was 0.05 %, 0.03 %, and 0.58 % respectively for the 4 l diesel (Williams *et al.* 1989). The PAH emissions from IDI diesel engines are also highest at high load (Zierock *et al.* 1983 and Abbass *et al.* 1991a). It is important to note, that even within the same fuel injector type and engine capacity range, the combustion efficiencies are greatly influenced by the actual design used (Kamimoto & Kobayashi 1991). Overall, the limited studies of the primary organic emissions, relative to the fuel consumed, from light-duty DI diesels suggest that the lowest combustion efficiencies are generally associated with low loads.

Table 4.5 Previous Studies on Fuel Survival for Diesel Engines

Engine Type	Speed (rpm)	Load	Emission Levels	Reference
DI 2 l	1500	Low Mid High	phenanthrene emitted/total fuel burned: 0.15 mg/kg 0.06 mg/kg 0.04 mg/kg	Andrews <i>et al.</i> 1983
DI 1 cylinder 0.5 l	1500	Low Mid High	Recovery of Pyrene: 0.8 % 0.2 % 0.2 %	Williams <i>et al.</i> 1986
Heavy-duty DI turbocharged run on high aromatic fuel	2000	air:fuel ratios: 23 44	Pyrene emitted/total fuel burned: 0.6 mg/kg 2.5 mg/kg	Barbella <i>et al.</i> 1988
DI 1 cylinder 0.5 l	3600	% of full load: 1 25 50 75 100	Total PAH emitted $\mu\text{g/g}$ of fuel: 3.17 2.22 0.38 0.22 0.81	Ziejewski <i>et al.</i> 1991

Engine load is strongly correlated with combustion chamber and exhaust temperatures (Table 4.6). Since engine oil and water remove heat from the engine, the values of these two solutions can be used to follow the temperature of the Prima engine. Referring to sampling details tabulated in Section 3.2.1 indicates temperatures of both oil and water, and hence combustion temperatures, rise with engine loads.

Table 4.6 The effect of engine load on the combustion and exhaust temperatures

Engine Type	Speed	Load	Combustion chamber temperature (°C)	Exhaust temperature (°C)	References
1 cylinder	-	Zero Half Full	-	190 470 590	Jensen & Hites 1983
1.2 l 2 cylinder DI	2350 rpm	Zero Quarter Mid Three quarters Full	-	178 232 302 408 533	Mills & Howarth 1984
0.87 l 1 cylinder DI	2400 rpm	Low Mid High	-	500 600 900	Iida <i>et al.</i> 1986
0.5 l DI	1500 rpm	Low Mid High	-	146 208 371	Andrews <i>et al.</i> 1987
0.7 l 1 cylinder DI	1500 rpm	Low Mid High	-	80 300 430	Pipho <i>et al.</i> 1991
0.5 l 1 cylinder	-	Zero Full	250 to 300 <sup>a</sup> 450 to 500	-	Chang <i>et al.</i> 1993

<sup>a</sup> Temperatures taken 38° after TDC

The peak gas temperatures in the combustion chamber are much higher than the exhaust, with typical combustion temperatures near TDC between 1000 to 2000°C (Chang *et al.* 1993). The higher combustion temperatures associated with full loads increase the likelihood that an organic compound will be completely combusted. It is important to note that the heterogeneous nature of diesel combustion will result in a range of temperatures for any given engine speed and load. For example, Li 1982 found the temperatures (between 232°C and 252°C) in the space between the top ring liner and piston head, termed the crevice volume, lower than the temperatures encountered in the piston bowl (*ca* 280°C). Saito *et al.* 1986 showed that the temperature of the top-edge of the combustion bowl wall was 237°C whilst only 215°C at the bottom of the chamber. Signer & Steinke (1987) also found lower temperatures in the crevice volume associated with the oil liner zone compared with the bowl edge, and that the higher the top ring the less space available for the flame to penetrate, and hence lower temperatures.

A temperature gradient or profile, as used by Schmeltz & Hoffmann (1976) to describe the different temperatures in cigarette combustion, can also be envisaged to describe the range of temperatures at a particular engine condition. The overall temperature for the temperature gradient will be lowest at low loads, and the average temperature within the gradient will increase with engine load.

One of the largest contributors to UHC at light loads arises from excessive air:fuel ratios taking the fuel from the spray edge beyond the lean flammability limit (Greeves 1979, Yu 1980, Campbell *et al.* 1981, Wheeler 1984, Gomes & Yates 1992, and Stone 1992). Low engine load also gives rise to hydrocarbon emissions via 'quenching' of the flame front in the clearance between the piston top and the cylinder head near TDC (Laity *et al.* 1973, Matsui & Sugihara 1986, Kobayashi *et al.* 1992, and Horrocks 1993). The crevice volume also gives rise to high UHC emissions, since the trapped gases at around TDC cannot be reached by the flame during compression, and consequently the unburnt fuel is emitted during the expansion stroke (Ferguson 1986 and Horrocks 1993).

Low combustion temperatures associated with low loads allows fuel impinged on the chamber walls to survive combustion later in the cycle and become emitted (Yu *et al.* 1980, Haupais 1982, Lilly 1984, Andoh & Shiraish 1986, Tsunemoto *et al.* 1986, Gomes & Yates 1992, Tanabe *et al.* 1992, and Cossali *et al.* 1993). A study of a Ricardo Hydra 0.6 l per cylinder engine found fuel impingement on the bowl walls occurred under all loads (Rao *et al.* 1993), as did the 4 l diesel studied using high-speed photography by Karimi (1989). It follows that the small Prima engine may also encounter fuel impingement over a range of loads. The fuel impingement would be greatest at high loads, since more fuel is injected later in the cycle. However, the higher chamber temperatures and greater turbulence mixing at high loads may account for a greater combustion of the fuel deposited on the walls. In some cases, fuel impingement can increase turbulence and further promote the combustion of the fuel (Kamimoto & Yagita 1989, Matsuoka 1990, and Kamimoto & Kobayashi 1991), especially for engines specifically designed to utilize impingement (Lilly 1984 and Akaska & Tamanouchi 1992).

A major source of UHC is derived from the fuel contained within the residual sac volume (RSV) of injectors and the fuel spray tail injected late in the cycle surviving combustion (Henein 1973, Greeves 1979, Campbell *et al.* 1981, Kowalewicz 1984, Lilly 1984, Wheeler 1984, Andoh & Shiraish 1986, Beck *et al.* 1988, Gomes & Yates 1992, and Horrocks 1993). The survival of the RSV and the spray tail will be increased by lower cylinder temperatures. Similarly, uncontrolled fuel releases such as those associated with injector dribble and secondary stage injection enter late in the combustion cycle and survive under low temperatures (Henein 1973 and Stone 1992).

Iida & Sato 1988 studied the UHC and SOF emissions from 1 cylinder of a DI diesel engine, and found that the emissions (units of g emitted/kg of fuel) correlated negatively with temperature at low loads. As the temperature decreased a linear increase in the SOF and UHC was found.

Overall, the mixing beyond the lean flammability limit and low combustion temperatures associated with low loads, favour condensation and adsorption of unburnt fuel from the outlined sources onto soot particulates, resulting in large SOF contributions to total particulates.

Figures 4.9a & b may be used to show the extremes of conditions related to temperature. At high load the higher temperatures in the combustion chamber result in greater combustion efficiencies for the selected compounds. The molecules of organics which are collected in the emissions represent those which have escaped totally the combustion temperatures as indicated by the closeness of their recoveries (similar ratios to fuel ratios). By contrast, at low load the inefficient combustion results in lower temperatures and the local temperature gradients may become more pronounced. The greater heterogenous temperature zones occurring at lower loads may lead to a greater variation in the combustion efficiencies for different organic compounds. At high load the temperature gradient may be narrower, as a consequence of greater combustion turbulence, mixing the chamber temperatures to a greater extent than at low loads (Shiozaki *et al.* 1980).



#### 4.2.3 Effect of Engine Speed on the Percentage Recovery of Primary Organics

Figure 4.11a showing the full range of load at 3000 rpm indicates a wider separation of PAC emissions/fuel ratios compared with lower speed runs. The average recovery at low load was 0.47% and this value declined progressively with increased load to 0.13% at full load. Increased speed leads to increasing average efficiency of combustion of the PAC. The wider range of ratios for a specific load, suggest differing combustion efficiencies between the PAC at all loads, or alternatively combustion generation reactions have become more prominent. The greatest variation between the PAC recoveries is again associated with the lowest load.

The percentage recoveries of the  $n$ -alkanes at high speed also decrease with increased engine load (Figure 4.11b). The  $n$ -alkane percentage recovery are again lower than those of the aromatics, with the average recovery decreased from 0.21% to 0.03% at full load. The wide variations between different  $n$ -alkane percentage recoveries at low load is similar to the aromatic emissions at low load. For both classes of organics the percentage recoveries converge at high load, providing further evidence for fuel survival unchanged at high loads and speeds. The closeness of the trends for the  $n$ -alkanes and PAC at all conditions suggests the aromatic and  $n$ -alkane emissions are derived from the same sources.

The selected PAC and  $n$ -alkane emissions follow the TES and UHC trends with load at high speed (Fig 4.12). The soot emission follows the same trend as for the lower speed, i.e. increased emissions with increased loads. All three types of emissions are at lower levels than at the lower speed, showing the improved combustion at higher speeds.

Engine speed effects the air motion (swirl, squish, and turbulence) characteristics, injection timing, and combustion temperatures of the engine (Jensen & Hites 1983, and Rao *et al.* 1993). The effect of air swirl, the dominant air motion parameter, is to increase the rate of air entrainment into the fuel jet (Campbell *et al.* 1981, Cossali *et al.* 1993, and Singal *et al.* 1993). The tangential motion of the swirl tends to deflect the spray penetration of the chamber, whilst improving the atomization and vaporization. Increased swirl may also further the turbulence and thereby promote fuel-air mixing in the later stages of combustion (Shioji *et al.* 1989).

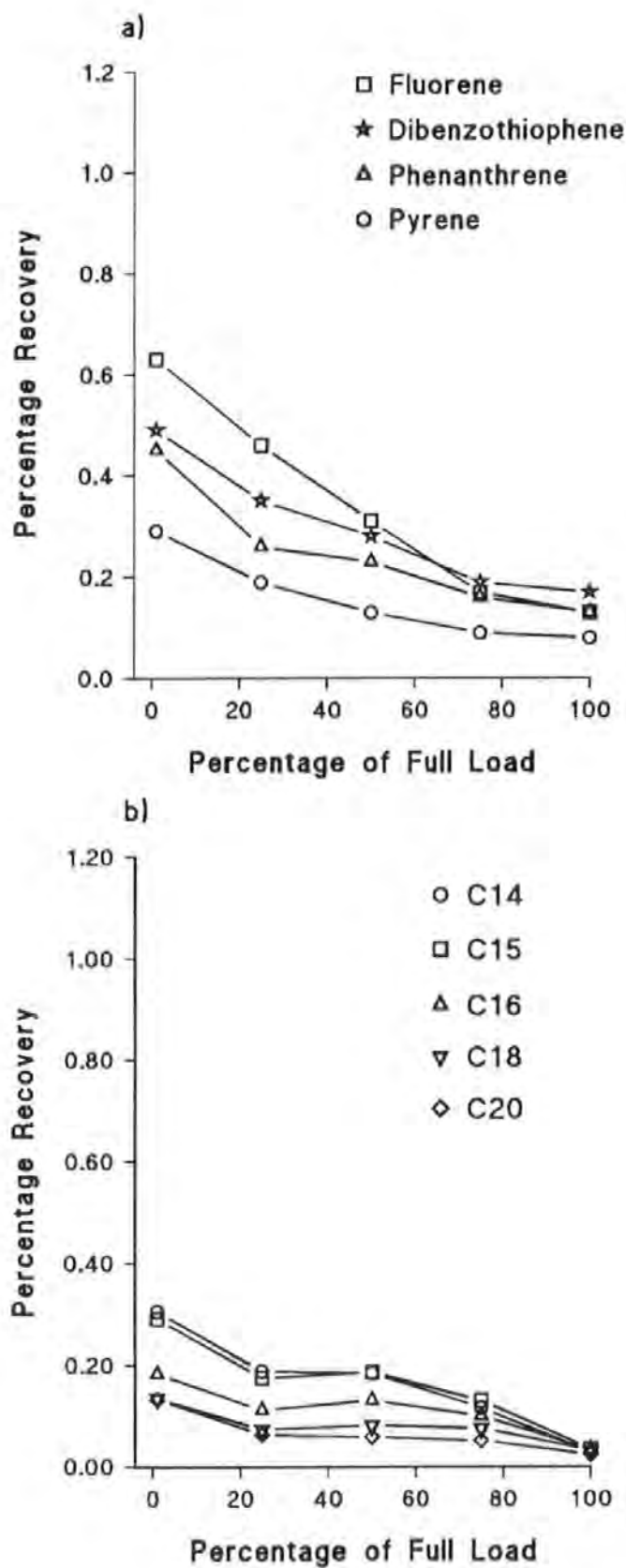


Figure 4.11 Effect of engine load on the percentage recovery of selected PAC (a) and n-alkanes (b) at 3000 rpm.

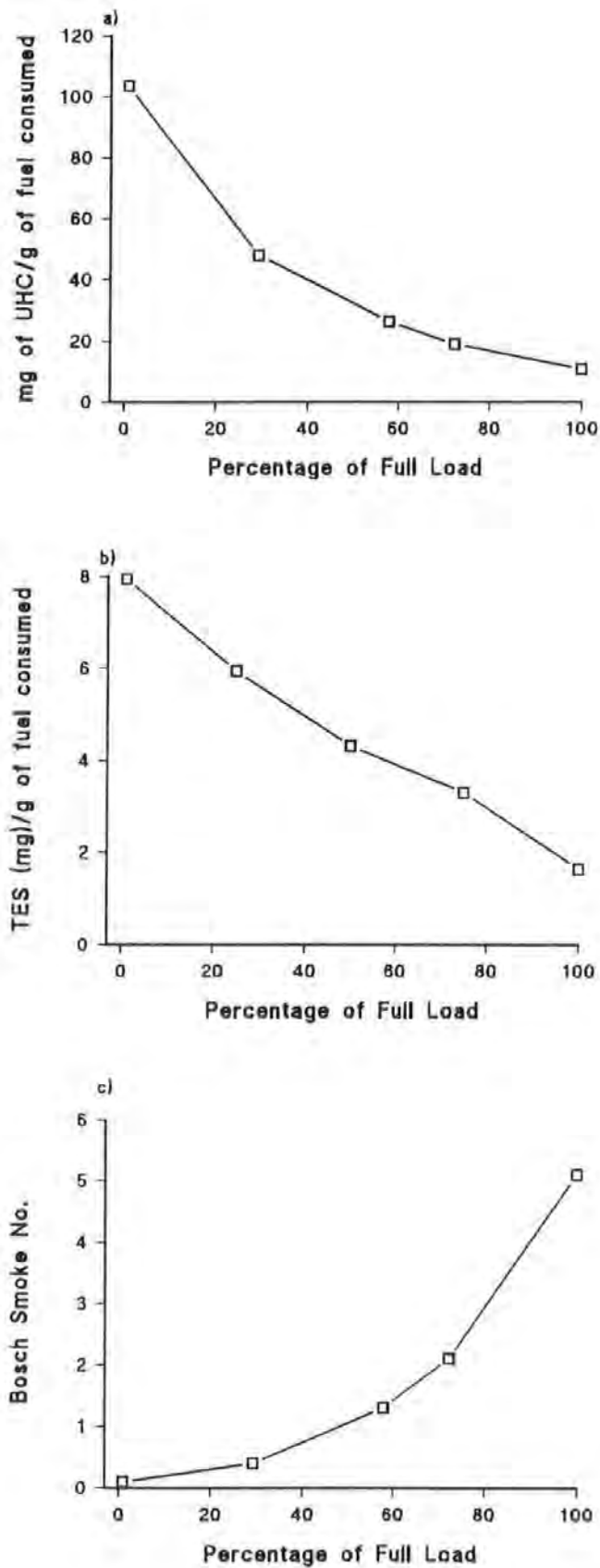


Figure 4.12 Effect of engine load on the emissions of unburnt hydrocarbons (UHC)(a), TESSA extracted sample (TES) (b), and bosch smoke (c) at 3000 rpm.

At low speed, the associated low swirl has little effect on the fuel sprays, except to carry the fuel vapour from the spray boundaries beyond the limit of combustion (Rao *et al.* 1993). At mid-speed the optimum swirl dynamics and timing enable efficient combustion to develop, resulting in the maximum power band for small high-speed DI engines. At high engine speeds, high swirl causes the spray tip to become unstable, resulting in wall jet break down and over mixing (Rao *et al.* 1993). Over swirl combined with the limited time for combustion, leads to increased SOF emissions (Shiozaki *et al.* 1980, Jensen & Hites 1983, and Ziejewski *et al.* 1991).

As engine speed is increased, cycle time decreases, leading to increased wall temperature and reducing time for heat loss; thus increasing air temperature (Campbell *et al.* 1981 and Li 1982). Bechtold *et al.* (1984) found that the exhaust temperatures for a 5.7 l eight cylinder diesel increased from 222°C at 30 mph to 325°C at 55 mph. The overall effect of increased engine speed is to shorten ignition delays, increase reaction rates, and reduce time for reaction to occur (Campbell *et al.* 1981).

The differences between the emissions at low and high speeds may be explained in terms of varying rates of combustion (kinetics of the reactions) for the compounds. Hence, increased speed limits the combustion process reactions allowing some organic molecules to react whilst allowing insufficient time for others to burn to the same extent. In this way, a wider range of combustion efficiencies may occur. Alternatively, the increased range of recoveries may indicate that some compounds are produced as a consequence of specific pyrosynthetic/pyrolysis reactions. The results obtained do not allow survival derived from varying combustion efficiencies to be distinguished from pyrosynthetic/pyrolysis contributions.

#### 4.2.4 Combined Effect of Engine Speed and Load on Primary Emissions

Figure 4.13 shows the combined effect of speed and load on the recovery of PAC. This clearly shows the area of greatest emission variability is associated with low load for the three speeds. Figure 4.13 indicates that for low load there is an optimum speed of 2000 rpm at which combustion efficiencies are greatest.

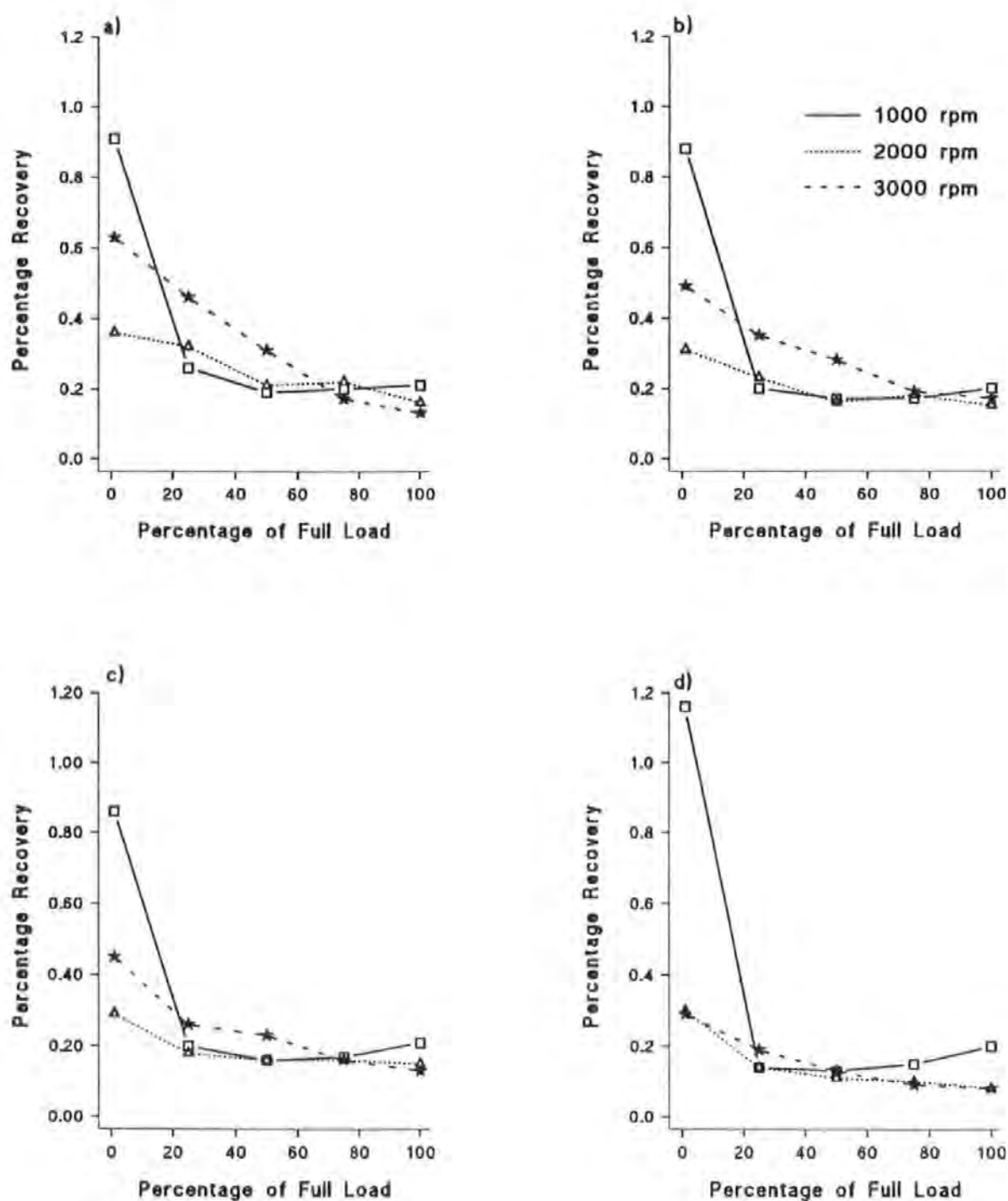


Figure 4.13 Effect of engine speed and load on the percentage recovery of fluorene (a), dibenzothiophene (b), phenanthrene (c), and pyrene (d).

Table 4.7 also correlates mid-speed with optimum combustion, as indicated by the smallest decrease in percentage recoveries, when increasing load. At higher loads the difference between different engine speeds diminishes.

Table 4.7 Effect of Speed on the Percentage Recovery (PR) of PAC between 1 % and 25 % of Full Load

Speed (rpm)	Difference in PR of fluorene at 1 % and 25 % of full Load	Difference in PR of dibenzothiophene at 1 % and 25 % of full Load	Difference in PR of phenanthrene at 1 % and 25 % of full Load	Difference in PR of pyrene at 1 % and 25 % of full Load
1000	0.65	0.66	0.66	1.02
2000	0.04	0.08	0.11	0.16
3000	0.18	0.14	0.19	0.10

Similar trends with engine speed and load were found for selected  $n$ -alkanes (Figure 4.14 and Table 4.8). The difference between the combustion efficiency at low speed and low loads was not as great as for the PAC.

Table 4.8 Effect of Speed on the Percentage Recovery (PR) of  $n$ -alkanes between 1 % and 25 % of Full Load

Speed (rpm)	Difference in PR of C14 at 1 % and 25 % of full Load	Difference in PR of C16 at 1 % and 25 % of full Load	Difference in PR of C18 at 1 % and 25 % of full Load	Difference in PR of C20 at 1 % and 25 % of full Load
1000	0.38	0.29	0.35	0.38
2000	0.06	0.06	0.05	0.04
3000	0.12	0.07	0.06	0.07

The greatest decline in the percentage recoveries induced by increasing the load at low speed, indicates that the low swirl and low temperature conditions at low engine power result in the lowest combustion efficiencies. The results agree with the those of Bazari & French 1993 who found a significant reduction in the UHC emissions could be achieved by increasing the swirl at low loads. At high loads the authors found swirl led to over mixing and increased UHC emissions.

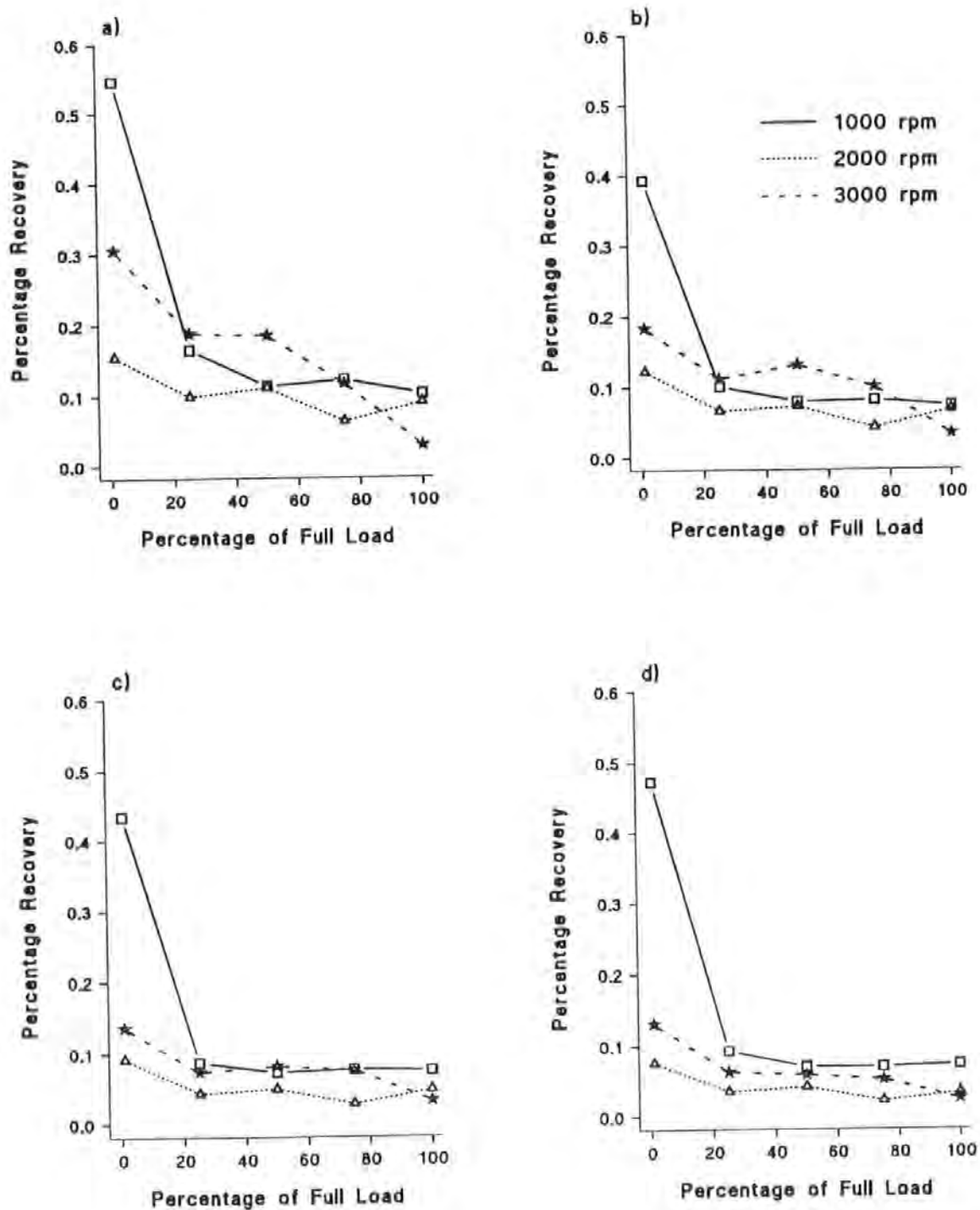


Figure 4.14 Effect of engine speed and load on the percentage recovery of tetradecane (a), hexadecane (b), octadecane (c), and eicosane (d).

With regards to the Prima exhaust, higher speeds resulted in the greatest combustion efficiencies at full load, indicating that the higher temperatures associated with elevated speeds may have countered any over-mixing effects. The increase in emissions at low load and high speed compared with those at mid-speed, may result from increased bulking quenching of the combustion process due to the volume expansion occurring in the expansion stroke (Yu *et al.* 1980).

The majority of previous investigations into selected organic emissions have concentrated on the effect of engine load. However, Zeijewski *et al.* 1991 also found the highest combustion efficiencies for PAH were associated with a mid-speed of 2200 rpm.

#### 4.2.5 Comparison of the n-Alkanes with the Major PAC emissions

Comparing the aromatic with the n-alkane emissions (Tables 4.3 & 4.4), reveals that for all exhaust samples, the combustion efficiencies for n-alkanes are greater than those for PAC. For example, the comparison of similar boiling point compounds, such as fluorene with hexadecane and phenanthrene with nonadecane, shows higher percentage recoveries for the PAH at all engine conditions (Figures 4.15 & 4.16).

It is important to note that unlike the aromatics, the n-alkane emissions have not been corrected with internal standards. However, spiking of solvent mixes with n-alkane standards and then working up the mixture as for TES showed that laboratory losses for the n-alkanes with a higher relative molecular mass than C13 were minimal (Section 3.2.2.7). For example, the laboratory losses for C14 and C16 were *ca.* 22% and *ca.* 10% respectively. Comparing the n-alkane laboratory losses with the averaged loss of *ca.* 14 % of the aromatic internal standards shows that the difference in emission levels is not a consequence of laboratory losses.

This may indicate that at the temperatures and pressures associated with diesel combustion, the aromatic structures survive relative to the n-alkane structures. The other possibility is that pyrosynthetic reactions favour the production of the aromatics compared with the n-alkanes. The study by Abbass (1991a) on a 4 l DI engine using dilution tunnel and filter collection, also found higher survivals for the PAC in comparison with the n-alkanes.



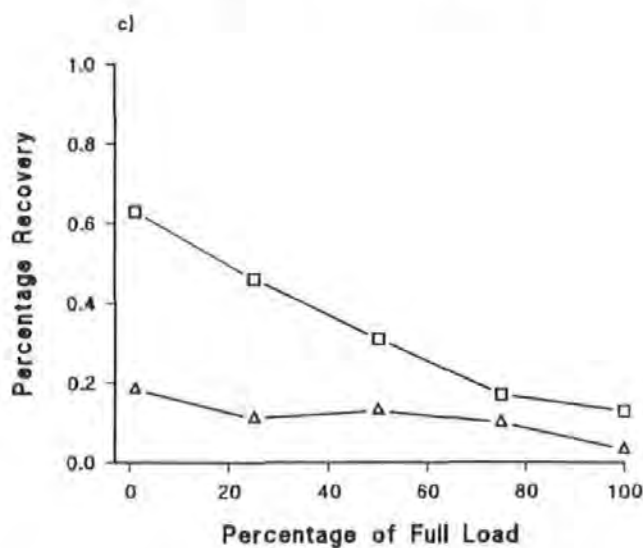
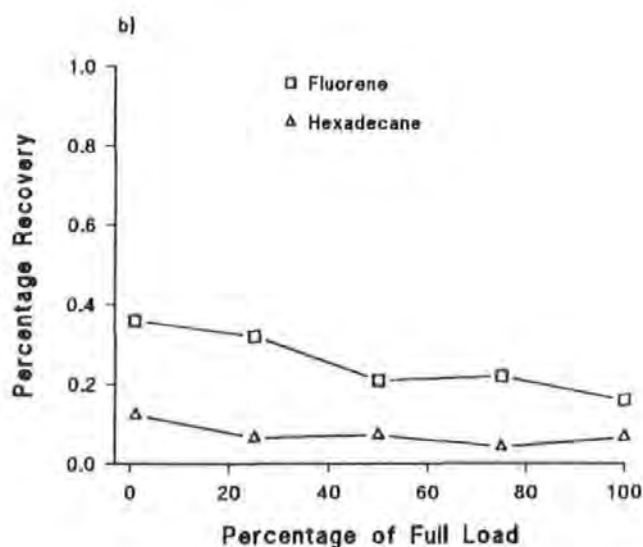
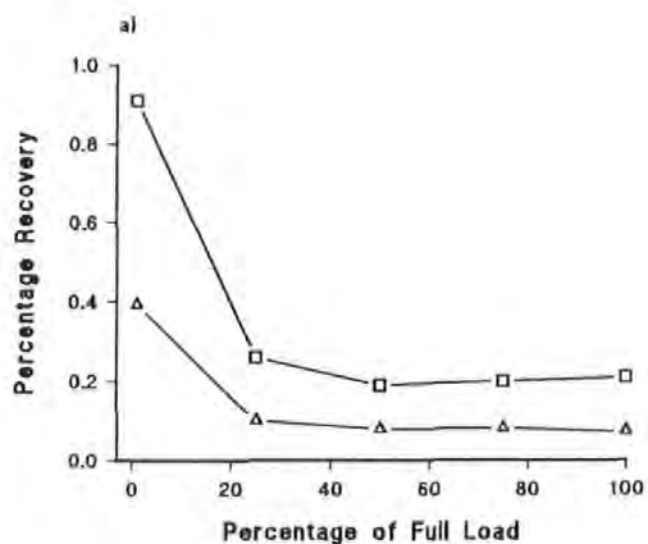


Figure 4.15 Comparison of the percentage recovery of fluorene compared with hexadecane at 1000 rpm (a), 2000 rpm (b), and 3000 rpm (c).

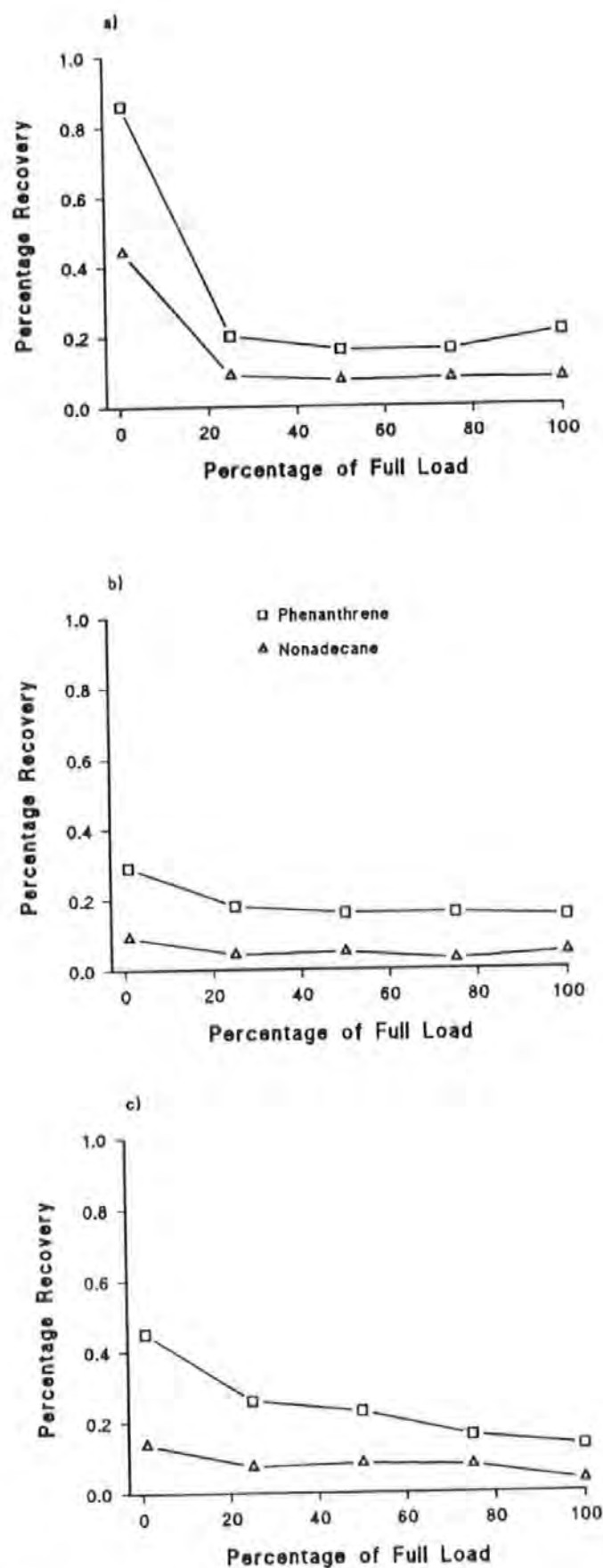


Figure 4.16 Comparison of the percentage recovery of phenanthrene compared with nonadecane at 1000 rpm (a), 2000 rpm (b), and 3000 rpm (c).

However, the authors, due to exhaust deposits and oil survival, were unable to attribute the greater PAC emissions to pyrosynthesis. The pyrosynthetic possibility is studied further in section 4.2.6.

The highest percentage recovery for aromatics were obtained for the lighter PAC, especially at high speed and low loads (Figure 4.17a). The results agree with the concurrent research of Tancell 1995 at the University of Plymouth. Tancell proposes a link between the reactivity of the PAC and the survival of the compound, such that the greater reactivity of pyrene compared to fluorene results in a greater survival of fluorene. The  $n$ -alkane percentage recovery also decreased with increased molecular weight at low load and high speed (Figure 4.17b). As the chain length of the  $n$ -alkanes is increased the percentage recovery decrease, showing that fuel survival unchanged cannot account for all the  $n$ -alkane emissions. If fuel survival unchanged was solely responsible for the  $n$ -alkane emissions at low load and high speed, the percentage recovery would be similar for all  $n$ -alkanes, i.e. similar exhaust to fuel ratios. This is indeed the case at high load and high speed, showing once again that the combustion environment at this condition supports fuel survival unchanged.

#### 4.2.6 The contribution of combustion generation to the organic emissions

The main source of the major exhaust organics has been shown to be from fuel survival, with minimal oil contributions. However, as explained in the previous sections the wide variation in the percentage recovery at low loads may indicate combustion chamber reactions, such as pyrosynthesis, involved with both  $n$ -alkane and aromatic structures.

The combustion chamber generation contribution to the aromatic emissions was further investigated by comparing the percentage recovery of unsubstituted PAC with the methyl-PAC derivatives. Figure 4.18a compares the percentage recovery of dibenzothiophene with three methyl-dibenzothiophene isomers at low engine speed. The numbering of the isomers is purely arbitrary and does not refer to the position of the methyl- moiety. There are very close percentage recoveries for both unsubstituted PAC and methyl-PAC. The close ratios at all loads suggest that dibenzothiophene and the methyl derivatives survive combustion unchanged, providing further evidence for fuel survival unchanged at 1000 rpm.

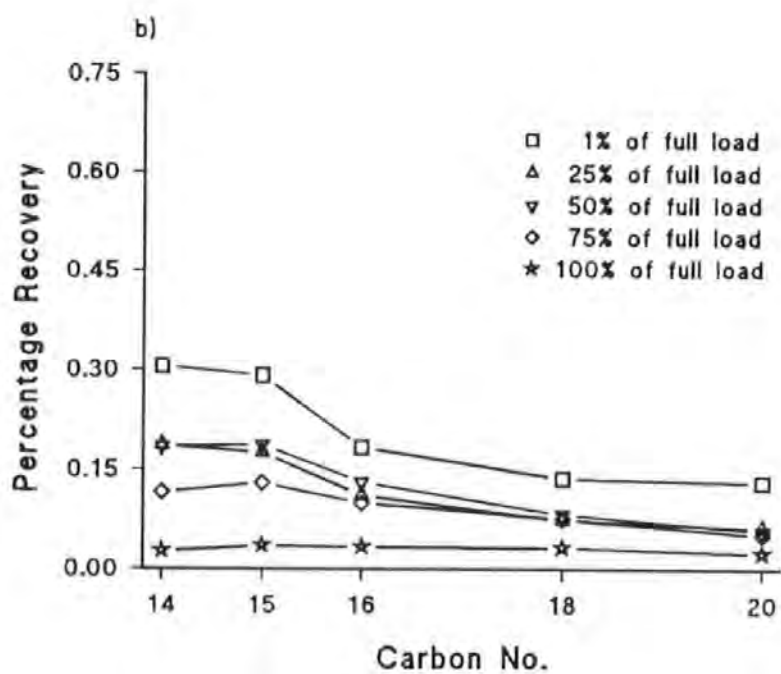
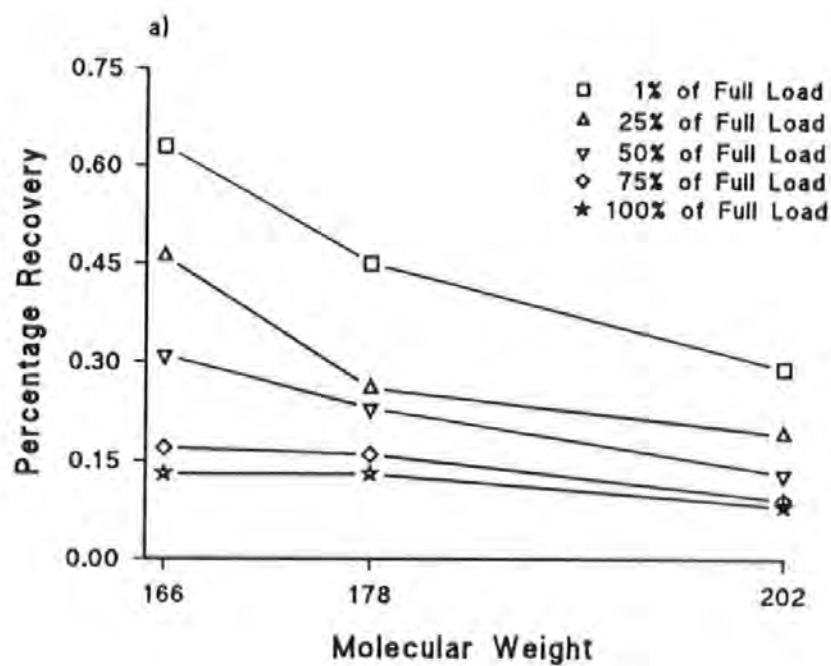


Figure 4.17 Effect of molecular weight on the percentage recovery of PAH (a) and n-alkanes (b).

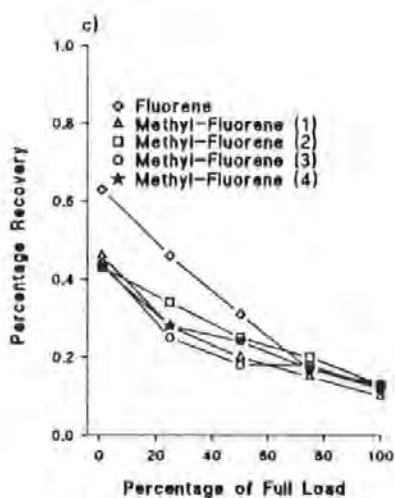
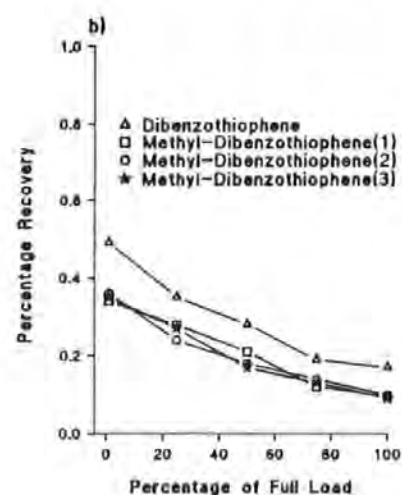
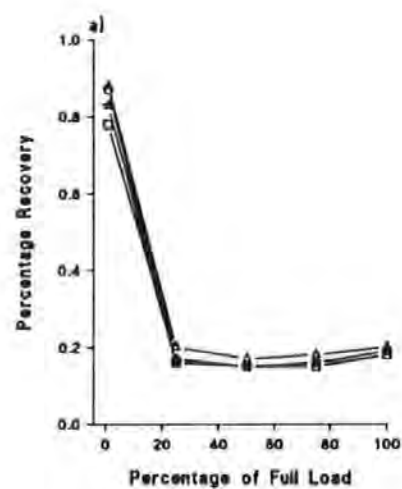


Figure 4.18 Comparison of dibenzothiophene with methyl-dibenzothiophenes at 1000 rpm (a) and 3000 rpm (b). Comparison of fluorene with methyl-derivatives at 3000 rpm (c).

Figure 4.18b shows the same comparison but for the higher engine speed of 3000 rpm. The recovery of dibenzothiophene is consistently higher than the methyl derivatives at each load sampled. The greatest recovery difference was 0.14% at the lowest load, decreasing to 0.075% at full load. This indicates that the combustion environment at 3000 rpm may cause dibenzothiophene to survive to a greater extent relative to its methyl derivatives, especially at low loads. Alternatively, pyrosynthetic/pyrolytic reactions resulting in the dibenzothiophene recovery being higher than that of the methyl derivatives may be favoured at low loads and high speed. Figure 4.18c indicates that a similar process may be involved with fluorene at high speed. Again, the recovery of the methyl derivatives at low load are much less than the recovery of fluorene. The difference in recovery decreases as the load is increased, resulting in near equal recoveries for fluorene and its methyl derivatives at high loads. This further reinforces the suggestion that conditions of high speed and low load give rise to variations in PAC recoveries.

In a similar study using GC/MS operated in EI mode, the concentrations of the unsubstituted parent PAC compound to the alkyl derivatives was described by Trier *et al.* 1990 for a light-duty IDI engine. The study using TESSA showed that in contrast to the fuel, the PAC concentration in the exhaust samples were greater than the alkyl derivatives, indicating pyrosynthetic reactions may have been involved.

The study of the recovery of PAH in the exhaust from DI and IDI engines operated on a variety of fuel blends by Shore (1986) found evidence for pyrosynthetic reactions occurring for fuels virtually free of PAH. The pyrosynthetic activity was evident from the large percentage recovery of PAH, for example 2351% of benz( $\alpha$ )anthracene was recovered in the exhaust of the DI engine. Clearly, the source of the PAH emissions was derived from sources other than fuel survival.

There are three possible combustion generation routes which could account for the observed recovery of the PAC relative to corresponding methyl derivatives. Firstly, the methyl- group may have been cleaved resulting in the formation of the parent PAC. Secondly, the parent PAC may be derived from aromatic species other than the methyl derivative, and thirdly, the parent PAC may be derived from aliphatic precursors.

Recent radiolabelled research has shown that at 2500 rpm and mid-load, proportions of 1-methylnaphthalene and 2-methylnaphthalene are converted into naphthalene during combustion (Pemberton 1995). Further radiolabelled experiments with larger ring PAC methyl derivatives, such as methyl-fluorene would be needed to establish whether methyl group cleavage occurs for other PAC. Spiking of fuels with ethyl-phenanthrene and butyl-naphthalene showed that the formation of vinyl-PAC were favoured for combustion of PAH with larger alkyl side chains (Pemberton 1995 and Tancell *et al* 1995b). In the ethyl-phenanthrene experiment, the formation of the vinyl-phenanthrenes occurred at 3000 rpm and low load, an engine region identified as a possible pyrosynthetic/pyrolytic area by this study.

The combustion generation reactions involving the  $n$ -alkanes were examined by visually comparing the distributions of the  $n$ -alkanes in the fuel with the corresponding distribution in the aliphatic fraction derived from high speed and low load (Figure 4.19). The same series of  $n$ -alkanes are present in both samples, but the maximum  $n$ -alkane component has shifted from C16 in the fuel to C15 in TES. Compared with the fuel, the lower carbon numbers in the exhaust are also relatively higher compared with the higher molecular weight  $n$ -alkanes. For example, the abundance of C14 is greater than C17 in TES, whereas in the fuel C14 is lower in abundance than C19. The skew to the lower volatile carbon numbers, cannot be accounted for by laboratory losses. Laboratory losses would tend to have the opposite effect, and decrease the abundance of the lower more volatile molecular  $n$ -alkanes relative to the more stable higher molecular  $n$ -alkanes. This suggests that the lighter  $n$ -alkanes are to some extent being derived from pyrosynthetic/pyrolytic reactions, or are less prone to destruction. This finding contrasts the study by Williams *et al.* (1989) on a medium-duty 4 l Perkins DI engine, for which the higher relative molecular mass  $n$ -alkanes were shown to survive to a greater extent than the lighter  $n$ -alkanes. The authors propose that this indicates a relatively greater difficulty for complete combustion of the larger  $n$ -alkane structures. The differences between the two studies may be a consequence of the two differing engine sampling systems used. The TESSA used in this study has been shown to collect more of the volatile gas components of diesel exhaust compared to the dilution tunnel/filter collection used by Williams *et al.* (1989) (Trier *et al.* 1988). Hence, the lower survival attributed to the more volatile  $n$ -alkanes may be a result of a relatively lower collection efficiencies with respect to the larger less volatile  $n$ -alkanes.

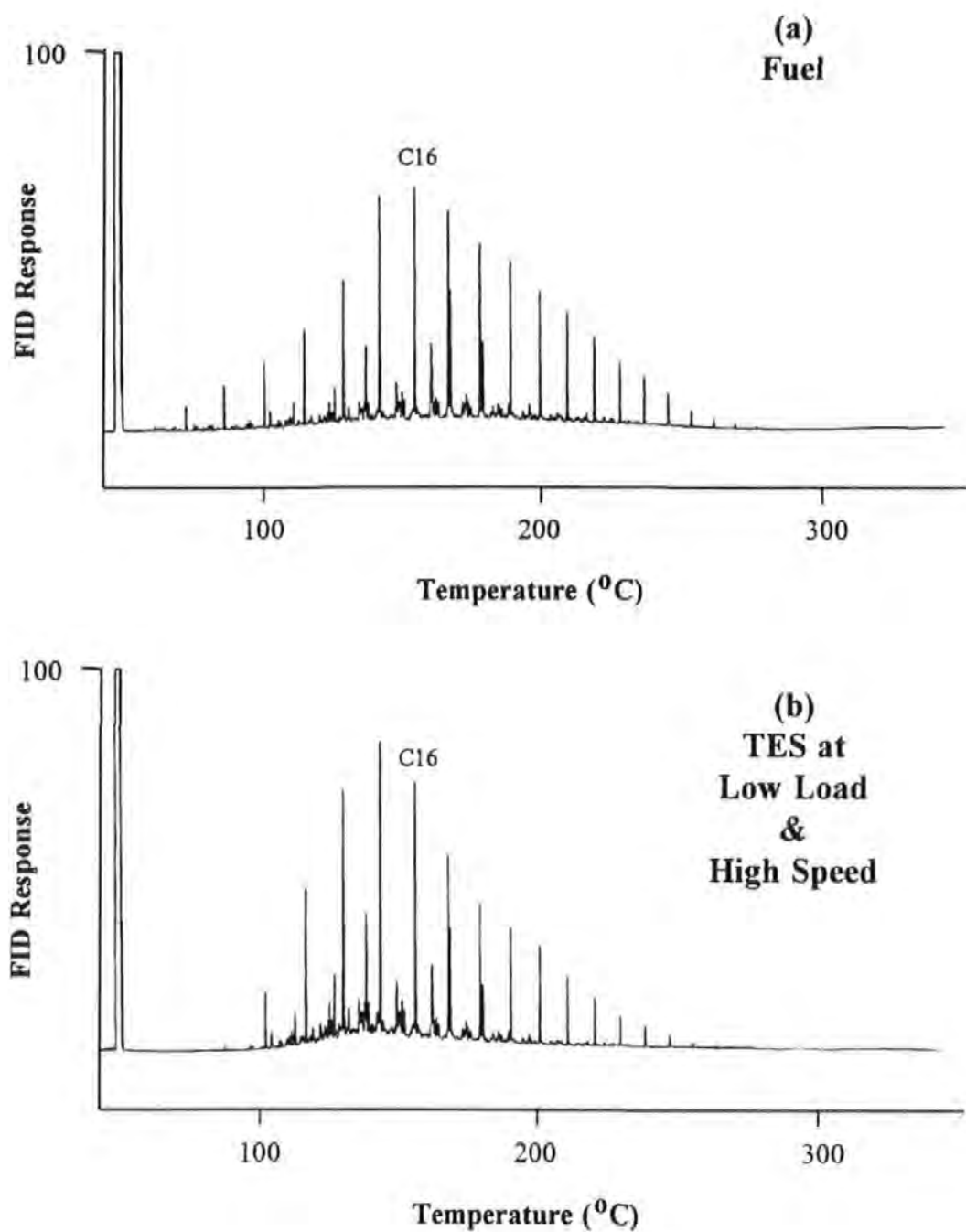


Figure 4.19 Comparison of the *n*-alkane distribution in diesel fuel (a) with the TESSA extracted sample (TES) at 1% of full load & 3000 rpm (b).



The TESSA arrangement also precludes post-combustion reactions to a large extent, and in so doing, quenches further reactions of the smaller carbon units that may normally occur in the exhaust pipe. Within the dilution tunnel assembly, there would be a greater opportunity for reaction and removal of such species. The other possibility is that the engine and the conditions at which the engines are sampled at, are critical to the  $n$ -alkane profiles. Indeed, in this study the profile of selected  $n$ -alkanes at 3000 rpm and high load is different to that at the same speed and low load. At the high load, the  $n$ -alkane recoveries are much closer compared with at the low load, and the skew to more volatile  $n$ -alkanes found at low load is not present at the high load.

The ratios of selected  $n$ -alkanes relative to hexadecane for fuel and exhaust samples are given in Table 4.9. For low speed, the normalised ratios for C18 and C20 in the exhaust are close to those in the fuel, whereas those for C14 and C15 are higher in exhaust. At mid-speed, the lighter  $n$ -alkanes compared with C16 increase in the exhaust whereas the heavy  $n$ -alkanes decrease with respect to C16. At high speed, the greatest difference between the fuel and exhaust are apparent at low loads. As the load is increased the ratios in the fuel and exhaust become closer, confirming earlier findings that the emissions at high load are derived from fuel survival unchanged.

The skewing effect of the carbon number distribution was also found by Nelson 1989 for the emissions from a 3 l IDI diesel truck engine. The maximum  $n$ -alkane in the exhaust distribution was C14 compared with C15 - C17 in the fuel. Nelson suggested that gas phase cracking reactions of the higher  $n$ -alkanes may have occurred. In the study significant quantities of styrene, indene, and naphthalene were found in the exhaust. These compounds were not present in the fuel. Nelson suggests that a significant proportion of the one- to three-ring aromatics are formed by pyrosynthetic addition of aromatic radicals to unsaturated aliphatics. Other studies have indicated that simple aliphatic fuels lead to the combustion formation of PAC (Crittenden & Long 1973, Cole *et al.* 1984, Henderson *et al.* 1984, Abbass *et al.* 1988, and Barbella *et al.* 1989). However, synthetic fuels are not accurate representatives, since the complex combustion reactions which occur with standard diesel fuel would be distorted if a simplex mixture was used.

Table 4.9 n-Alkane areas normalised to Hexadecane for a range of Speeds and Loads

		C14/C16	C15/C16	C18/C16	C20/C16
	Fuel	0.57	0.82	0.68	0.49
Speed (rpm)	Percentage of Full Load				
1000	1	0.80	1.06	0.75	0.58
	25	0.95	1.14	0.59	0.45
	50	0.82	1.09	0.63	0.43
	75	0.86	1.13	0.65	0.41
	100	0.80	1.08	0.70	0.49
2000	1	0.72	1.22	0.51	0.30
	25	0.87	0.59	0.45	0.26
	50	0.88	1.23	0.46	0.28
	75	0.86	1.18	0.46	0.24
	100	0.76	1.25	0.48	0.24
3000	1	0.96	1.31	0.51	0.35
	25	0.97	1.31	0.45	0.27
	50	0.81	1.18	0.43	0.22
	75	0.67	1.07	0.52	0.25
	100	0.47	0.87	0.66	0.35

Tancell (1994) used  $^{14}\text{C}$ -hexadecane to investigate the pyrosynthetic contribution to the n-alkane emissions for the Prima engine at 2500 rpm and mid-load. He showed that a significant proportion of the hexadecane (66 %) in the emissions was derived from combustion generation. Tancell also found that the n-alkane distribution in the exhaust was skewed in favour of the lower relative molecular mass n-alkanes compared with the fuel distribution, confirming the findings from this study at a particular engine condition. This may, as Nelson (1989) proposed, indicate pyrolytic cracking of aliphatic compounds into smaller units.

### 4.3 Comparison of Primary Emissions collected using Initial & Upgraded TESSA

This section examines the effect of engine conditions on the *n*-alkane and PAC emissions obtained using the upgraded TESSA (Sections 3.3 & 3.4) and compares the results to those found from the first sampling session using the initial TESSA (Section 3.1). Section 4.3.1 examines more closely the effect of low loads on the combustion of fluorene at low engine speed. The effect of engine load at 1500 rpm, 2500 rpm, and 3500 rpm for selected *n*-alkanes and PAH is presented in Section 4.3.2. Finally, the results from the sampling sets obtained with the initial and upgraded TESSA configurations are combined at low load in Section 4.3.3.

#### 4.3.1 Combustion of Fluorene at low loads and low speed

The greatest percentage recoveries, and hence lowest combustion efficiencies, for both PAC and *n*-alkanes were found at low loads from the profiling obtained with initial TESSA configuration (Section 3.1). For this reason, the initial testing of the upgraded TESSA examined the effect of low loads more closely. Loads corresponding to 1% (cold and hot start), 8%, 17%, and 25% were sampled (Section 3.3.2), aromatic fractions isolated by silica gel clean-up (section 3.4.2.2.2) and fluorene quantified using GC-FID.

Figure 4.20 shows the effect of the incremental increases in engine load at 1000 rpm, and also compares the findings to those obtained from the first sampling session. The 0.91% recovery of fluorene at 1% of full load from the initial TESSA sampling compared with the upgraded TESSA result (0.96%) is good, as is the 0.26% and 0.28% recovery at 25% of full load for the initial and upgraded systems respectively. This shows the reproducibility of both the engine combustion and the sampling system on different days. Increasing the engine load from 1% to 8% of full load resulted in a much greater combustion efficiency of fluorene. Hence, the large increase in combustion efficiency observed when the load was increased from 1% to 25% is in fact due to *ca.* the first 30% of the rise. Since temperature was identified as a key factor in determining the emissions, one of the samples collected at 1% of full load was taken without conditioning, ie. cold start (conditioning consists of 1 hour at 3000 rpm and 90 Nm, followed by 15 minutes at the chosen engine condition). As indicated the lack of conditioning increased the percentage recovery of fluorene from 0.96% to 1.31%.

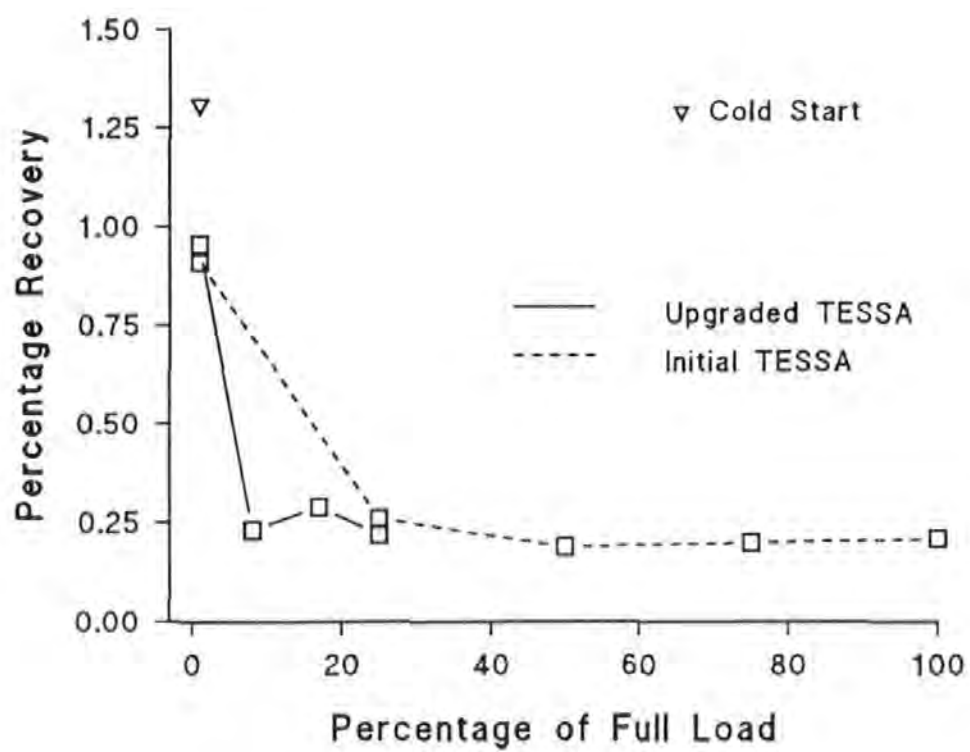


Figure 4.20 Effect of low loads on the percentage recovery of fluorene.

Kraft & Lies (1981) also found higher PAH emissions from light-duty diesel engines from the cold start FTP transient test cycle compared to the hot start for the same cycle. The degree to which fuel is mixed beyond the lean flammability limit should be the same for both conditioned and unconditioned engines, since the air:fuel ratio remains the same. Thus, the decrease in the combustion efficiency provides further proof that low combustion chamber temperatures causes greater fuel survival.

#### 4.3.2 Effect of Engine Load on the Percentage Recovery of Primary Emissions

The same negative relationship of engine load with percentage recoveries and the associated increased combustion efficiencies as found for 1000 rpm, 2000 rpm, and 3000 rpm was replicated by 1500 rpm, 2500 rpm, and 3500 rpm (Figures 4.21 & 4.22). The lower laboratory losses incurred for naphthalene (calculated from  $d_8$ -naphthalene) enabled the percentage recoveries of naphthalene to be calculated. The laboratory losses were still high, owing to the increased hexane volume used in the revised silica gel clean-up (Section 3.4.2.2.2), removing a large proportion of naphthalene into the aliphatic fraction. The effect of load on the recovery of naphthalene was the same as for other PAC at 1500 rpm and 3500 rpm, whilst at 2500 rpm the recovery was markedly increased at mid-loads compared with other PAC. For all PAC, the reproducibility of the percentage recoveries are generally good, with a few exceptions.

Fuel surviving unchanged remains the dominant process at high loads, shown by the convergence of the percentage recoveries, most noticeably for the  $n$ -alkanes at 3500 rpm (Figure 4.22b). Of interest is the distinct increase in the percentage recovery of pyrene at high load and 3500 rpm relative to the other PAC (Figure 4.21c). The fact that the remaining PAC converge at high load whilst pyrene increases suggest that a proportion of the emitted pyrene was derived from pyrosynthesis, rather than as a result of differing combustion efficiencies. Tancell (1995) using radiolabelled experiments on the Prima engine, found that pyrene was especially prone to pyrosynthesis compared to other PAC. For example, Tancell calculated that of the pyrene recovered in the exhaust, 70% was pyrosynthesized compared with less than 20% for benz( $\alpha$ )pyrene under the same engine conditions.

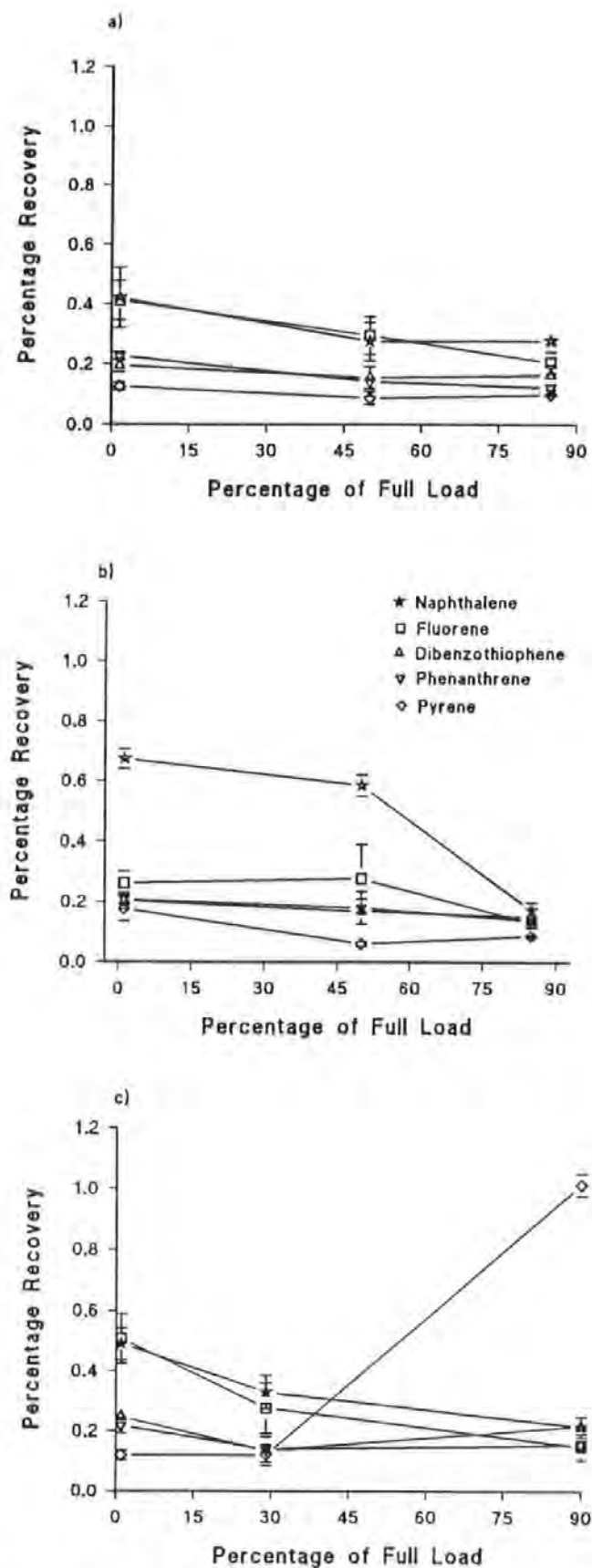


Figure 4.21 Effect of engine load on the percentage recovery of selected PAC at 1500 rpm (a), 2500 rpm (b), and 3500 rpm (c).

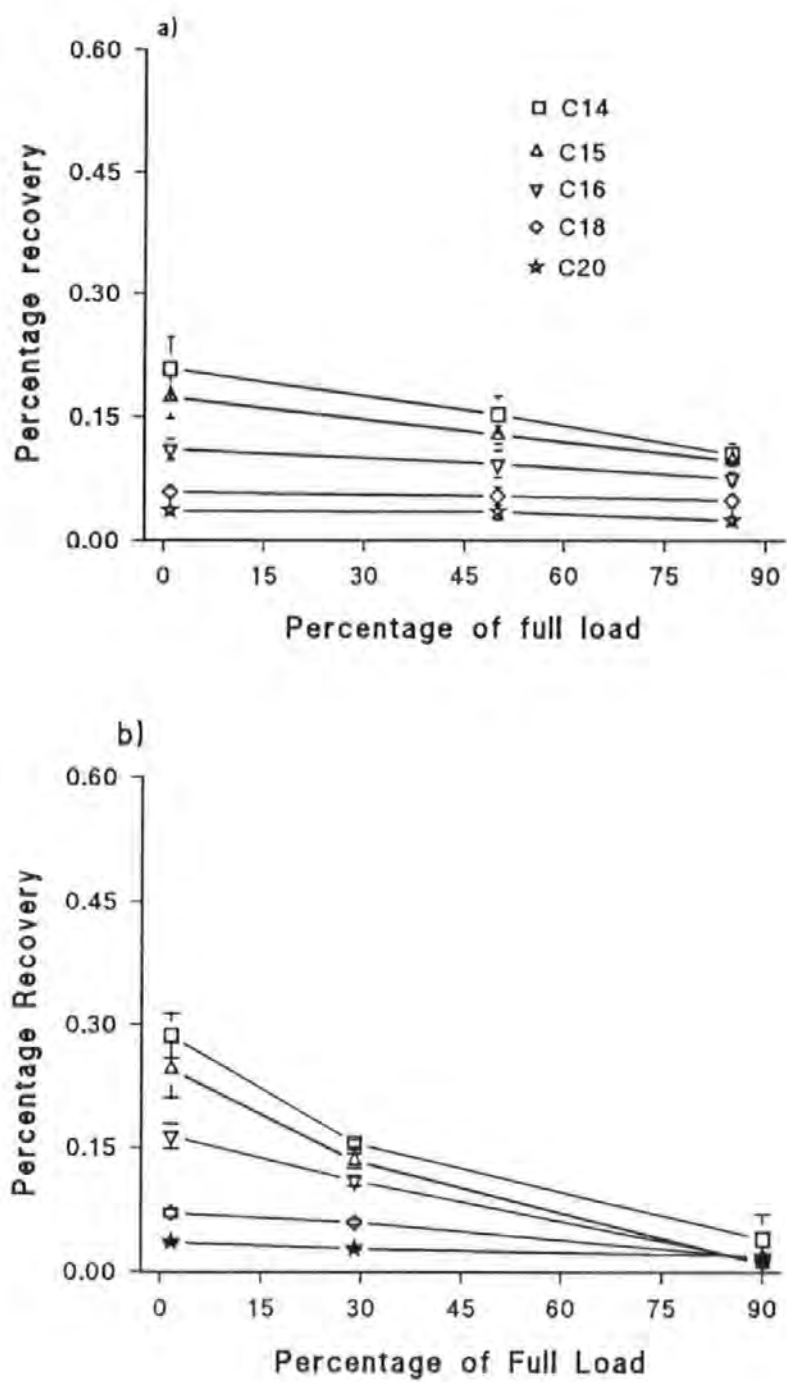


Figure 4.22 Effect of engine load on the percentage recovery of selected  $n$ -alkanes at 1500 rpm (a) and 3500 rpm (b).

The *n*-alkane recovery follow the PAC trends, with the recovery remaining lower than those of equivalent boiling point PAC. The highest recoveries are, as before, associated with the lighter *n*-alkanes and PAC.

#### 4.3.3 Effect of Engine Speed for the Combined Sampling Sets

The combination of the sampling sessions at 1 % of full load for all speeds on the emissions of fluorene and hexadecane is shown in Figure 4.23. The data for hexadecane at 2500 rpm is missing due to the ODS cartridge clean-up method being employed. Taking into consideration the error bars, the recovery of both compounds is highest at low load and low speed. The greatest combustion efficiencies occur at mid-speeds, with the recovery increasing with further speeds. These trends confirm the findings from the sampling sessions carried out with the initial TESSA. Hence, the organics survive at low speeds and low loads due to the limited temperatures and insufficient air motion, whereas at high speed the combustion is restricted by the limited reaction time and over-swirl. The recovery of hexadecane, whose volatility is similar to fluorene, is always lower than that of the latter, and as discussed may mean that the structure of fluorene is more resistant to combustion than that of hexadecane. Alternatively, the combustion chamber generation of fluorene may be relatively higher than that of hexadecane.



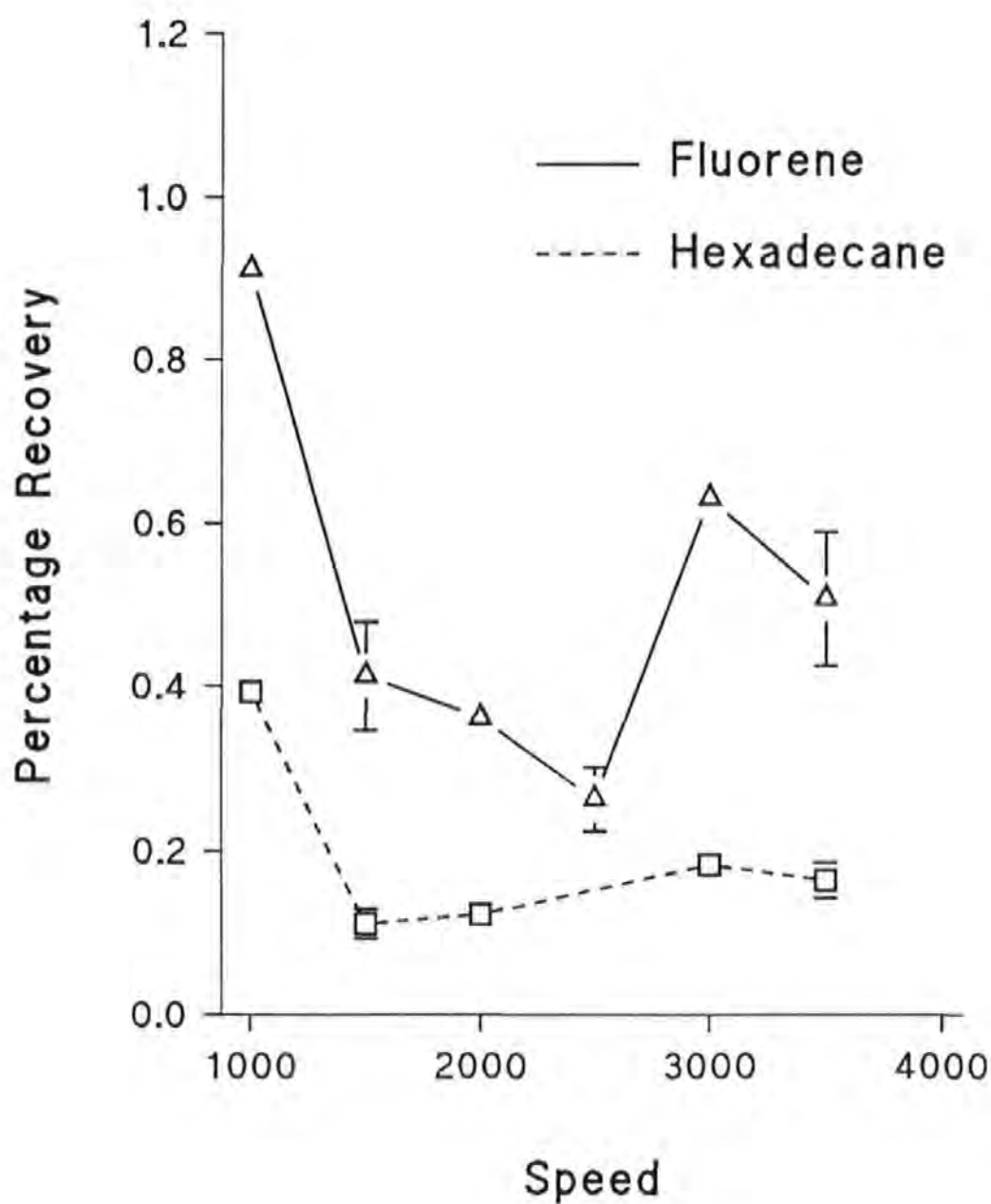


Figure 4.23 Effect of speed on the percentage recovery of fluorene and hexadecane at low load.

#### 4.4 Summary of Major Organic Emissions

- 1) Fuel survival is dominant over lubricating oil survival for the selected organic compounds studied.
- 2) Combustion efficiencies (as defined by percentage recoveries) are lowest at low loads, and increase with load. The highest emissions at 1% of full load and 1000 rpm are a consequence of the low temperatures and the fuel:air mixture being beyond the lean flammability limit.
- 3) The  $n$ -alkane emissions produce the same trends as for the PAC emissions, indicating that the  $n$ -alkanes and aromatics are derived primarily from the same source. The selected organic emissions agree with the overall unburnt hydrocarbon and TES emissions. The dominant source for such emissions is *via* fuel survival.
- 4) The convergence of the percentage recovery at high load indicates that the combustion environment at these conditions favours fuel survival unchanged. The combustion environment at high load results in the greatest temperatures with the smallest range or gradient.
- 5) The poor mixing at low loads results in lower overall temperatures with a larger temperature gradient than at high load. This may result in a greater range of combustion efficiencies. Low load combined with high speed may restrict the kinetics of the reaction and result in a wider range of combustion efficiencies than at lower speeds. Alternatively, the combustion environment at low loads and high speed (defined by a wider range of temperatures) may favour greater combustion generation, such as the cleavage of methyl- groups from PAC.
- 6) The optimum swirl, time and combustion chamber temperatures associated with mid-speed results in greatest combustion efficiencies at low loads. The higher temperatures at high load results in speed having a smaller effect at high loads.

7) The percentage recovery of the PAC were significantly higher than those of equivalent boiling point  $n$ -alkane molecules. The difference may arise from the PAC structures being more stable than the straight chain  $n$ -alkanes, resulting in greater survival of the PAC. Alternatively, the pyrosynthetic formation of PAC may be favoured.

8) The emissions of some PAC are more likely to be derived from pyrosynthesis than others. Pyrene especially, appears atypical in behaviour compared to other PAH and seems to be more readily pyrosynthesized.

9) The skewing of  $n$ -alkane profile suggest combustion generation is involved at specific engine conditions, possibly resulting from the breakdown of higher molecular compounds into smaller  $n$ -alkane molecules.

## **Chapter 5 - Secondary Nitro- & Oxy-PAC Emissions**

This chapter examines the effect of engine speed and load on the secondary nitro- and oxy-PAC emissions from the Prima engine. These PAC are formed from conversion of primary PAH, such as pyrene, during the combustion and exhaust stages. The results presented in this chapter were derived from sampling the exhaust stream of the Prima as it leaves the combustion chamber by using TESSA. In this way, the potential of the combustion chamber to form nitro- and oxy-PAC can be assessed, and the artefact problems associated with the dilution tunnel/filter sampling systems avoided. The main part of the chapter is focused on the nitro-PAC, since some members of this PAC class have been found to be highly mutagenic and carcinogenic to mammalian biological systems.

A comparison of HPLC fractionations in Section 5.1, evaluates the overall chemical composition of the exhaust as it leaves the chamber, along with the effect of speed and load on the relative contributions of different chemical classes. The results from the nitro-PAC profiling are reported and discussed in Section 5.2, as are those regarding oxy-PAC in Section 5.3. The major findings from both nitro- and oxy-PAC profiling are listed in Section 5.4.

### **5.1 The Contribution of Different PAC classes to the Emissions**

Fractionation of diesel combustion samples provides information on the relevant contributions of different chemical classes present in the sample. The elution times of specific classes of compounds are established by analyses of standards, using semi-preparative normal phase HPLC (Section 3.4.2.3). The contribution of specific PAC classes, such as nitro-PAC, to the overall composition can then be investigated.

The overall composition of TES under different speeds and loads showed a regular pattern or profile (Figure 5.1). The first and largest class of PAC to be eluted (0-26 mins.) corresponds to the non polar PAH, PASH, and alkyl-derivatives. The source for these compounds is predominately from unburnt fuel surviving combustion (Chapter 4). By contrast, the mononitro-PAC HPLC fraction (26-33 mins.) is much reduced in concentrations.

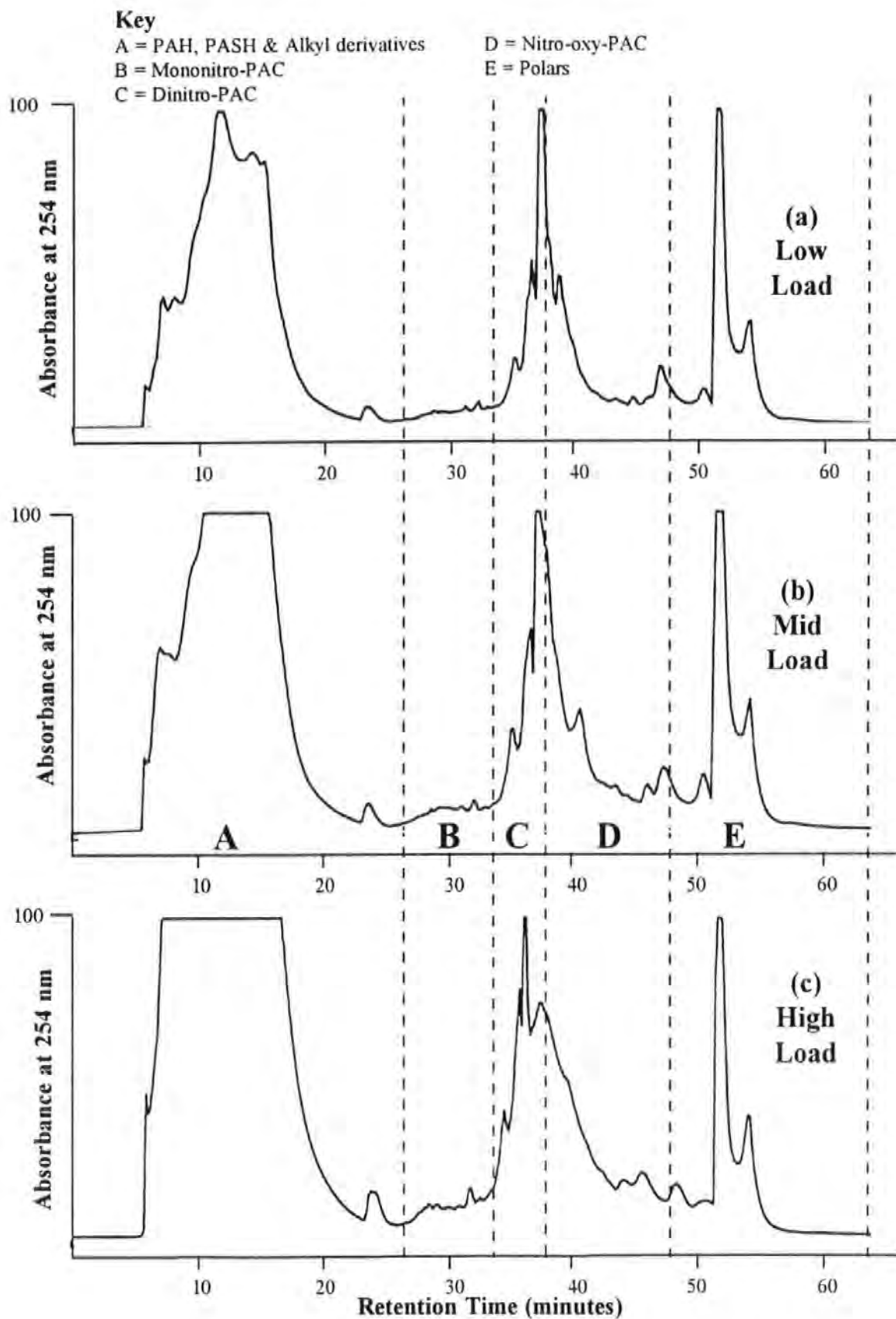


Figure 5.1 Overall chemical composition of the aromatic fractions of TES at 1500 rpm and a) low load, b) mid load, and c) high load, determined using normal-phase high-performance liquid chromatography (Chromatographic conditions given in Section 3.4.2.3.2).

The second large group of PAC eluted was divided into the dinitro-PAC (33-38 mins.) and nitro-oxy-PAC (38-48 mins.). Oxy-PAC, such as the ketone and aldehyde PAC derivatives co-eluted with the dinitro- and nitro-oxy PAC fractions, whereas the more polar carboxylic acids elute in the final large band (48-63 mins.). Engine load seems to have little effect on the relevant distribution of chemical classes at low engine speed. A similar regular trend was repeated for higher speeds.

The regular emission pattern generated for a wide variation of engine conditions suggest similar combustion reactions had occurred across the load and speed ranges. Hence, a proportion of the fuel input to the cylinder has been transformed into the secondary nitro- and oxy-PAC. Due to the complexity of the HPLC fractions, it is necessary to chemically characterise each HPLC fraction (Sections 5.2 & 5.3). Individual species can then be followed over varying speeds and loads, and the factors giving rise to their formation investigated.

## 5.2 Nitro-PAC Emissions

The high mutagenicity and carcinogenicity of some nitro-PAC (Tokiwa *et al.* 1981 & 1986, Rosenkranz & Mermelstein 1983, and Beland *et al.* 1985) has been central to health concerns related to diesel emissions (IARC 1989 & QUARG 1993). Research has shown that 1-nitropyrene, a powerful mutagen, can contribute between 10 to 40% of the total mutagenicity of diesel particulate extracts (Schuetzle *et al.* 1981, Nakagawa *et al.* 1983, Schuetzle & Frazier 1986, and Veigl *et al.* 1994). The health concerns in relation to nitro-PAC emissions, makes elucidation of the engine processes controlling their formation highly desirable.

The formation of nitro-PAC result from the nitration of PAH, such as pyrene. The nitrating species, termed  $\text{NO}_x$ , are generated from the thermal decomposition of nitrogen and air in the combustion chamber (Scheepers & Bos 1992b). The  $\text{NO}_x$  may then react with PAH to form nitro-PAC *via* free radical processes (Nielsen *et al.* 1983, and Scheepers & Bos 1992b). Nitration may also occur by electrophilic substitution of the PAH ring by nitrogen dioxide,  $\text{NO}_2$ , in the presence of nitric acid *via* the nitronium ion (Nielsen 1984, Ross *et al.* 1988, and Scheepers & Bos 1992b). The nitro-PAC emissions are limited by competitive removal of PAH by combustion, in which case nitration cannot occur. Similarly, nitro-PAC may react

further, for example further oxygenation may give rise to nitro-oxy-PAC (Schuetzle & Perez 1983). Research to date has provided little information on which nitration reactions are favoured under different engine conditions.

This section details the emissions of nitro-PAC from the Prima engine and compares the results with those in the literature. Three types of nitro-PAC are considered, namely, mononitro-PAC, dinitro-PAC, and nitro-oxy-PAC. The aim of the nitro-PAC profiling was to correlate the abundance of nitro-PAC emissions with the nitration potential of the combustion chamber. The short transfer line between the engine and TESSA enables the combustion products as they leave the chamber to be characterised. Post-combustion reactions are significantly reduced for sample collection using TESSA.

Samples were derived from three speeds and at three loads for each speed (Section 3.4.1). The samples were extracted, concentrated, cleaned-up, and fractionated by normal-phase HPLC (Section 3.4.2). Section 5.2.1 reports and discusses the identification and levels of mononitro-PAC in the fuel, oil, and emission samples collected using TESSA and analyzed by the selected detection systems. The search for the dinitro-PAC and nitro-oxy-PAC in the Prima emissions is detailed in Section 5.2.2.

#### 5.2.1 Analysis of the Mononitro-PAC HPLC fractions by Gas Chromatography with Electron Capture Detection

The mononitro-PAC from the TES, fuel and oil sump samples were identified (by co-injections with a standard mix and by RI) and quantified (external calibration) by GC-ECD (Section 3.4.3.1.4). The GC-ECD system provided the greatest detection, resolution, and access needed for resolving the complex mononitro-PAC HPLC fractions. Figure 5.2 shows the analysis of three mononitro-HPLC fractions sampled at 1500 rpm and for three load positions. As for the overall HPLC fractionation profiles, the chemical distribution of the mononitro-PAC HPLC fractions were found to be similar for varying loads and speeds.

The GC-ECD analysis revealed 1-nitronaphthalene, 2-methyl-1-nitronaphthalene, 2-nitronaphthalene, and 1-nitropyrene present in all TES. Figure 5.3 focuses on the temperature elution zone associated with the nitronaphthalenes for the TES collected at 1500 rpm.

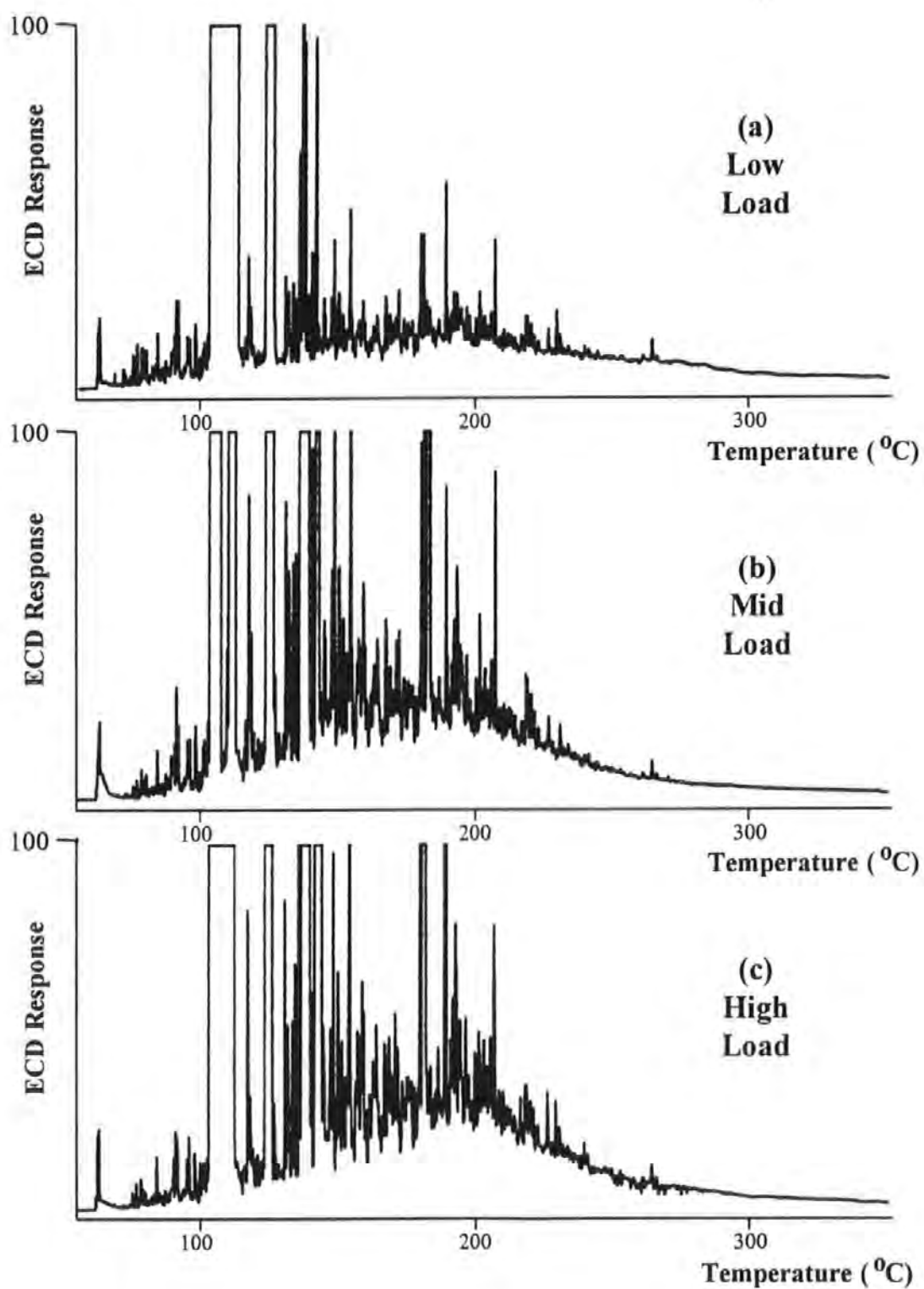


Figure 5.2 The analysis of the mononitro-PAC HPLC fractions derived from sampling at 1500 rpm and across the load range, by gas chromatography with electron capture detection (Chromatographic conditions given in Section 3.4.3.1.4.1).



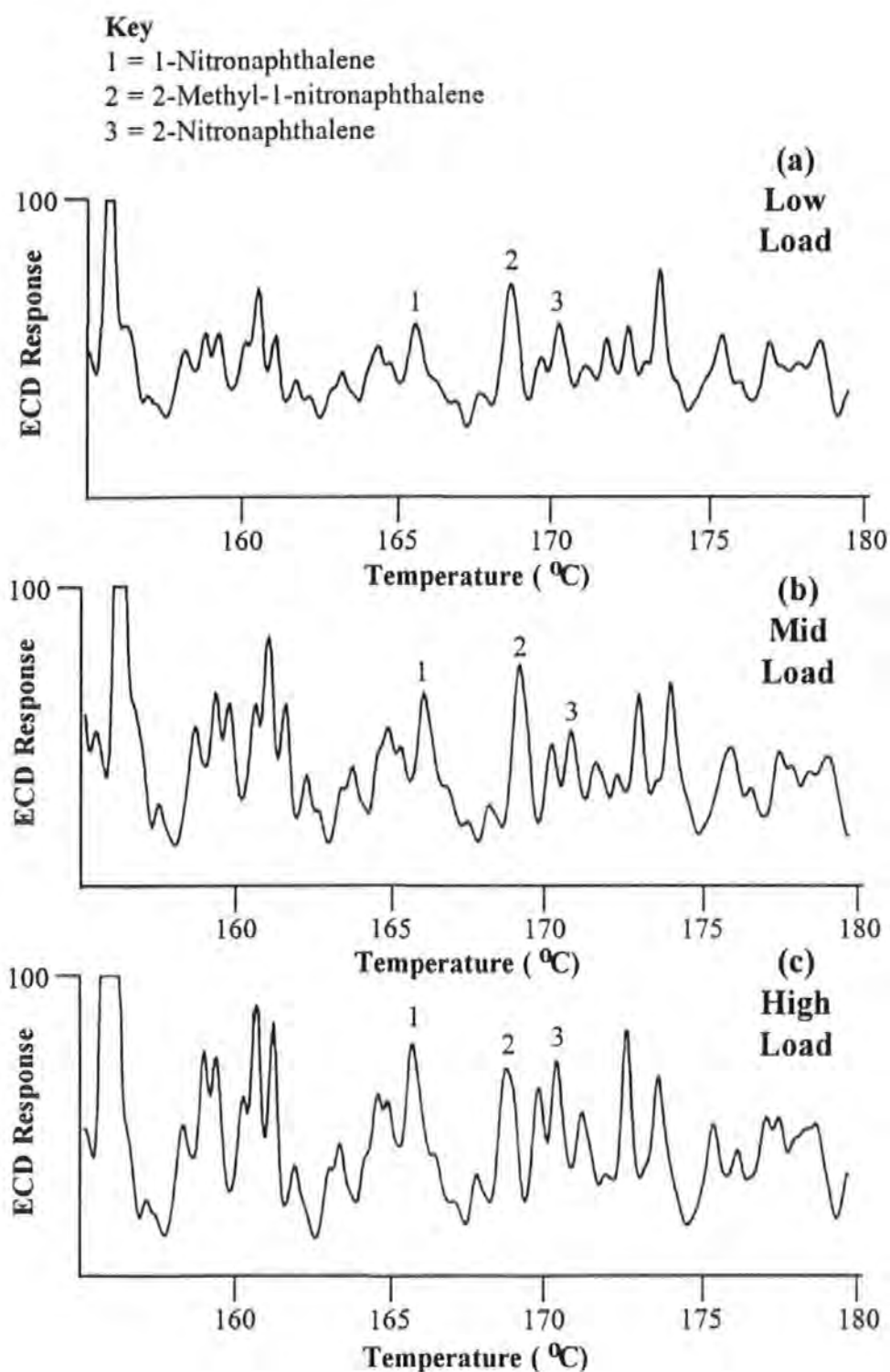


Figure 5.3 The profile of the nitronaphthalenes at 1500 rpm and across the load range, determined using gas chromatography with electron capture detection (Chromatographic conditions given in Section 3.4.3.1.4.1).

The regular pattern of the nitronaphthalenes is replicated at each load position. The regularity of the profiles suggests that a common formation pathway for nitro-PAC is operating.

Figure 5.4a shows the analysis of the mononitro-PAC HPLC fraction of the fuel by GC-ECD. There are very few positive peaks, and during the middle section of the GC temperature programme some non-electrophilic compounds are evident, as indicated by the negative peaks (between 30 and 35 minutes). Figure 5.4b&c shows the delimited retention windows of the fuel analysis, for the retention times associated with mononitro-PAC standards. Since there are no peaks evident between 22-23.5 minutes (nitronaphthalene standards elution window, Section 3.4.3.1.4.1) nor between 42.0-42.3 minutes (1-nitropyrene retention time, Section 3.4.3.1.4.1), there are no mononitro-PAC in the fuel. Figure 5.5a shows the analysis of the mononitro-PAC HPLC fraction of sump oil. There are a number of prominent peaks, however, as for the fuel no mononitro-PAC could be found (Figure 5.5b&c). The absence of nitro-PAC in the fuel and oil was verified by co-injection techniques.

The lack of mononitro-PAC in the fuel and sump oil showed that specific nitro-PAC were formed as a result of combustion reactions, rather than as a consequence of nitro-PAC surviving combustion. Previous studies by Jensen *et al.* (1986) found that sump oil accumulated 1-nitropyrene to a small degree, but could find no evidence for oil survival contributions to nitro-PAC emissions. The results from this study were expressed as the weight of nitro-PAC emitted relative to the total TES weight collected (Table 5.1). The laboratory losses were found to be minimum for the engine sample work-up and fractionation procedures, for example *ca.* 10 % of 1-nitronaphthalene was lost (Section 3.4.2.5).

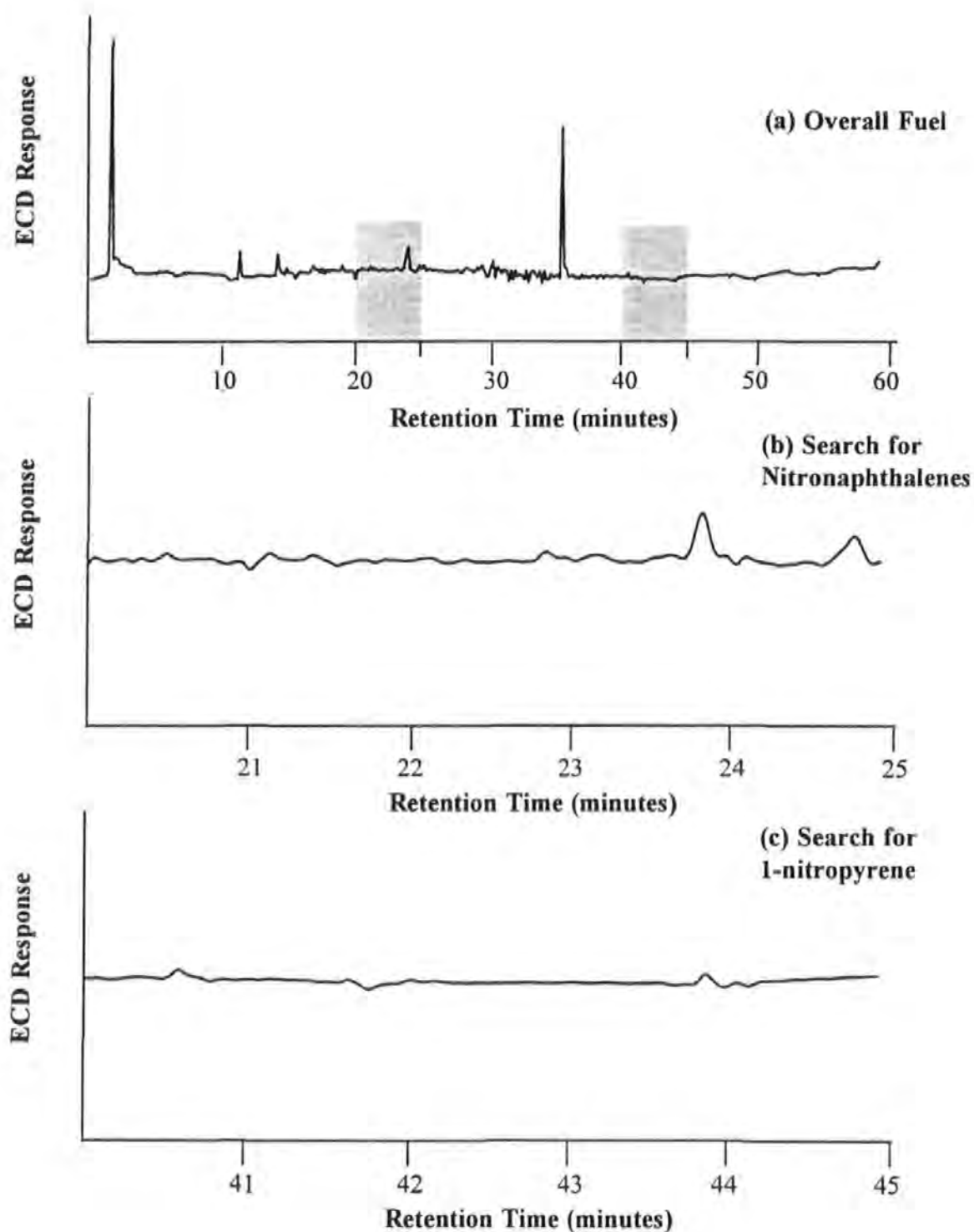


Figure 5.4 The analysis of the mononitro-PAC HPLC fraction of diesel fuel by gas chromatography with electron capture detection (a), and the verification of the lack of nitro-PAC in the fuel (b&c). Retention times for nitro-PAC standards: 1-nitronaphthalene (22.237 mins.), 2-methyl-1-nitronaphthalene (22.919 mins.), 2-nitronaphthalene (23.487 mins.), and 1-nitropyrene (42.054 mins.) (Chromatographic conditions given in Section 3.4.3.1.4.1).

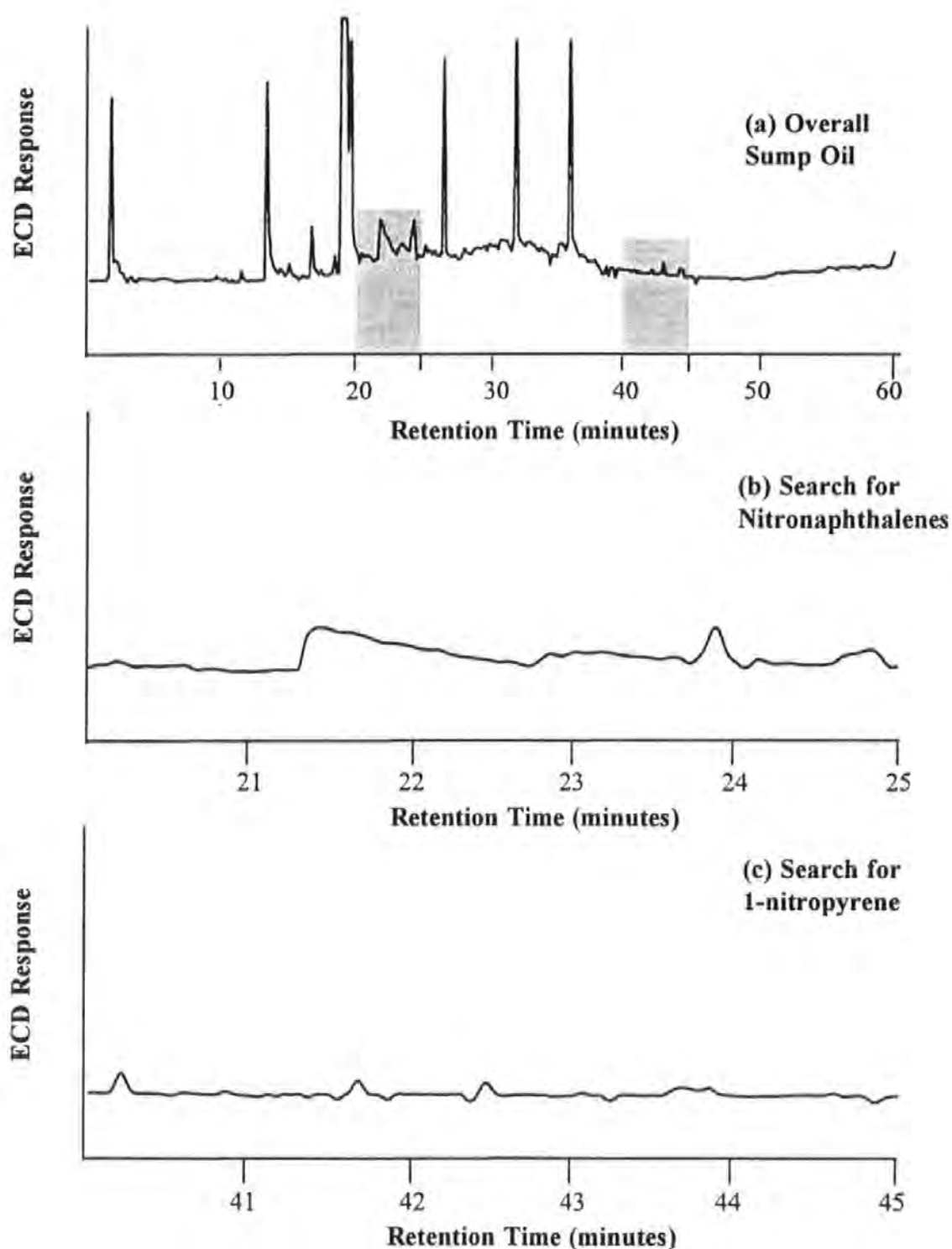


Figure 5.5 The analysis of the mononitro-PAC HPLC fraction of sump oil (after 50 hours use) by gas chromatography with electron capture detection (a), and the verification of the lack of nitro-PAC in the fuel (b&c). Retention times for nitro-PAC standards: 1-nitronaphthalene (22.237 mins.), 2-methyl-1-nitronaphthalene (22.919 mins.), 2-nitronaphthalene (23.487 mins.), and 1-nitropyrene (42.054 mins.) (Chromatographic conditions given in Section 3.4.3.1.4.1).

Table 5.1 Nitro-PAC emitted from the Prima Engine at different engine conditions

Speed (rpm)	% of Full Load	1-Nitropyrene in TES  (ppm)	1-Nitronaphthalene in TES  (ppm)	2-Nitronaphthalene in TES  (ppm)	2-Methyl-1- nitronaphthalene in TES  (ppm)
1500	1	1.6	9.3	7.1	8.2
	50	1.1	11.9	6.1	10.2
	85	1.3	10.6	7.5	7.7
2500	1	1.0	-	-	-
	50	2.6	-	-	-
	85	2.2	-	-	-
3500	1	0.6	13.3	7.0	7.8
	29	0.6	20.9	7.9	11.7
	90	5.3	35.1	18.9	18.5

Notes: 1) Averaged results from duplicate samples  
 2) Results expressed as  $\mu\text{g}$  of nitro-PAC emitted/g of TES collected  
 3) Quantification of nitronaphthalenes at 2500 rpm not possible as a result of negative peaks, from aliphatic compounds, interfering with the baseline position.

#### 5.2.1.2 Analysis of the Mononitro-PAC HPLC fraction derived from High Speed and High Load by Gas Chromatography/Mass Spectrometry operated in Negative Ion Chemical Ionisation Mode.

Analysis of nitro-PAC by GC/MS operated in the NICI mode results in very little fragmentation (Newton *et al.* 1982, Oehme *et al.* 1982, Ramdahl & Urdal 1982, & Bayona *et al.* 1988), and for this reason, selective ion monitoring (SIM) of the molecular ion of nitro-PAC was utilized in this study. The SIM mode greatly enhanced the sensitivity, resulting in the same order of sensitivity as that of GC-ECD (Section 3.4.3.1.5). Matching of peaks on a molecular ion basis and retention indices provides strong evidence for the presence of nitro-PAC, since the compound under question not only elutes at the precise time of the proposed nitro-PAC but also the main ion for the compound matches that of the nitro-PAC standard.

Selective ion monitoring combined with a retention index based on 1-nitropyrene confirmed the GC-ECD identifications of the nitronaphthalenes. Based on the comparison of the areas of 1-nitropyrene in the sample with that in the standard, the concentration of 1-nitropyrene in TES at high speed and high load was calculated to be 1.78 ppm. Considering the crude GC/MS NICI quantification and that the analysis was performed several months later than the

GC-ECD analysis, this figure agrees favourably with that of 5.75 ppm obtained using GC-ECD.

The GC/MS NICI was then used to search for other nitro-PAC in the sample. This was achieved by calculating the molecular ions for the nitrated form of major PAH and alkyl derivatives. Scanning for mono-, di-, and trimethylnitronaphthalenes revealed a series of peaks, similar to the distribution of naphthalene and methylnaphthalenes in the fuel (Figure 5.6). The spread of the retention times for the methylnitro-PAC is greater than the methyl-PAH due to the greater isomer possibilities.

Similarly, scanning for the molecular ions of nitrofluorene (211) and nitroanthracene (223) as well as the methylnitro- derivatives indicated a number of compounds present (Figures 5.7 & 5.8). Investigating the peaks corresponding to ions of molecular weight 211 (by co-injection), showed no presence of 2-nitrofluorene. The GC-ECD analysis could also find no evidence for 2-nitrofluorene in the exhaust. This is interesting, considering the levels of fluorene present in the fuel (Section 4.1). The 9-nitroanthracene isomer was not present among the 223 ions. However, it is phenanthrene rather than anthracene which is present at elevated levels in the fuel (Section 4.1). This suggests that the 223 and 237 ion distributions may refer to nitrophenanthrenes and methyl-nitrophenanthrenes. Even though the exact structures of the scanned molecular ions have not been elucidated by GC/MS, the analysis has shown a similarity between the fuel distribution and the secondary emission profiles, ie. a proportion of the fuel has undergone transformation into nitro-PAC. However, the lack of 2-nitrofluorene in the emissions suggests that certain elements of the fuel are more susceptible to transformations than others.

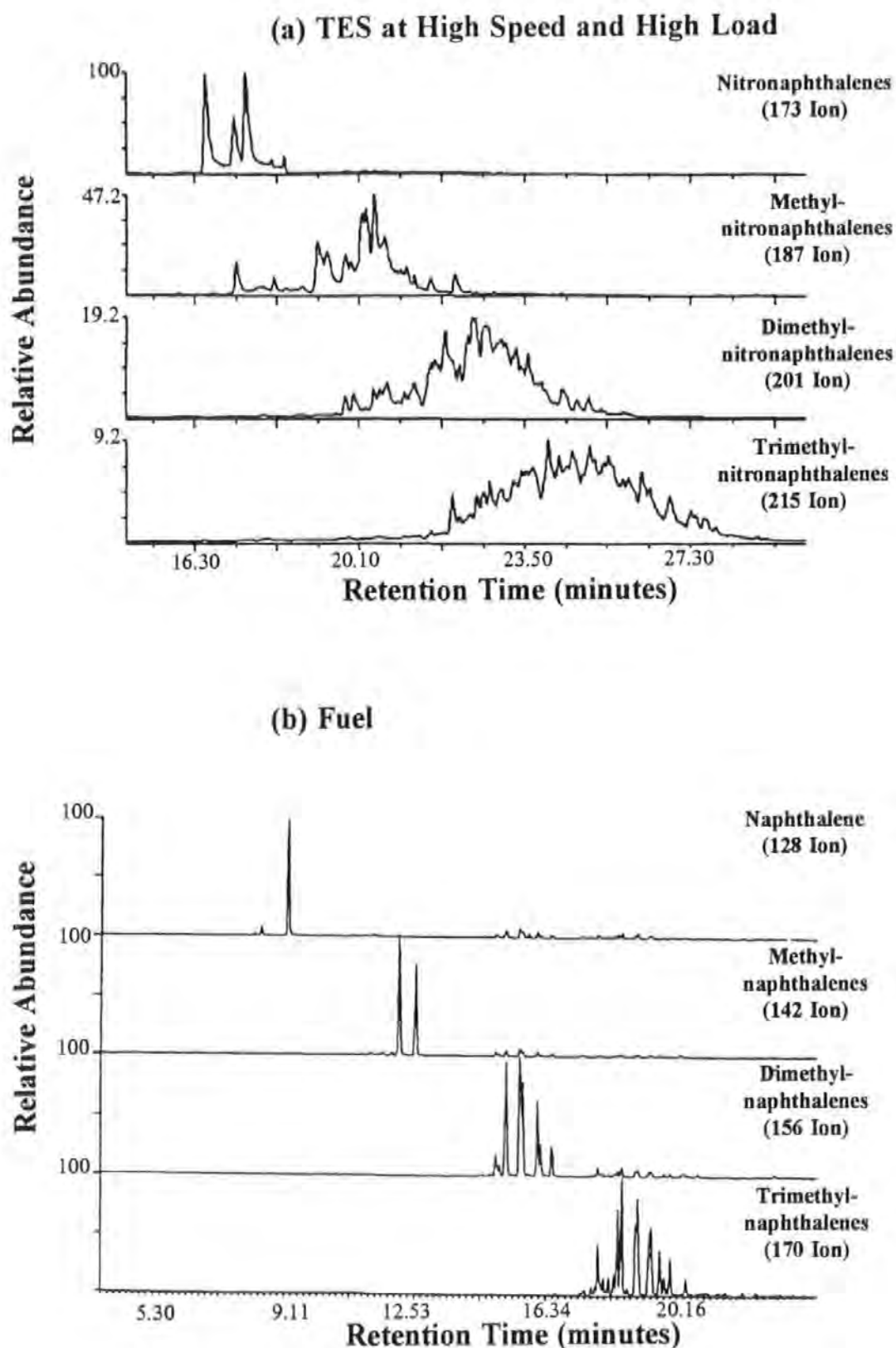


Figure 5.6 Distribution of the nitronaphthalenes in TES collected at 3500 rpm and high load, determined by gas chromatography/mass spectrometry (GC/MS) operated in the negative ion chemical ionisation mode (a) compared with the distribution of naphthalenes in the fuel, as determined by GC/MS in the electron impact mode (b) (Chromatographic conditions given in Sections 3.4.3.1.5 and 3.2.4 respectively).

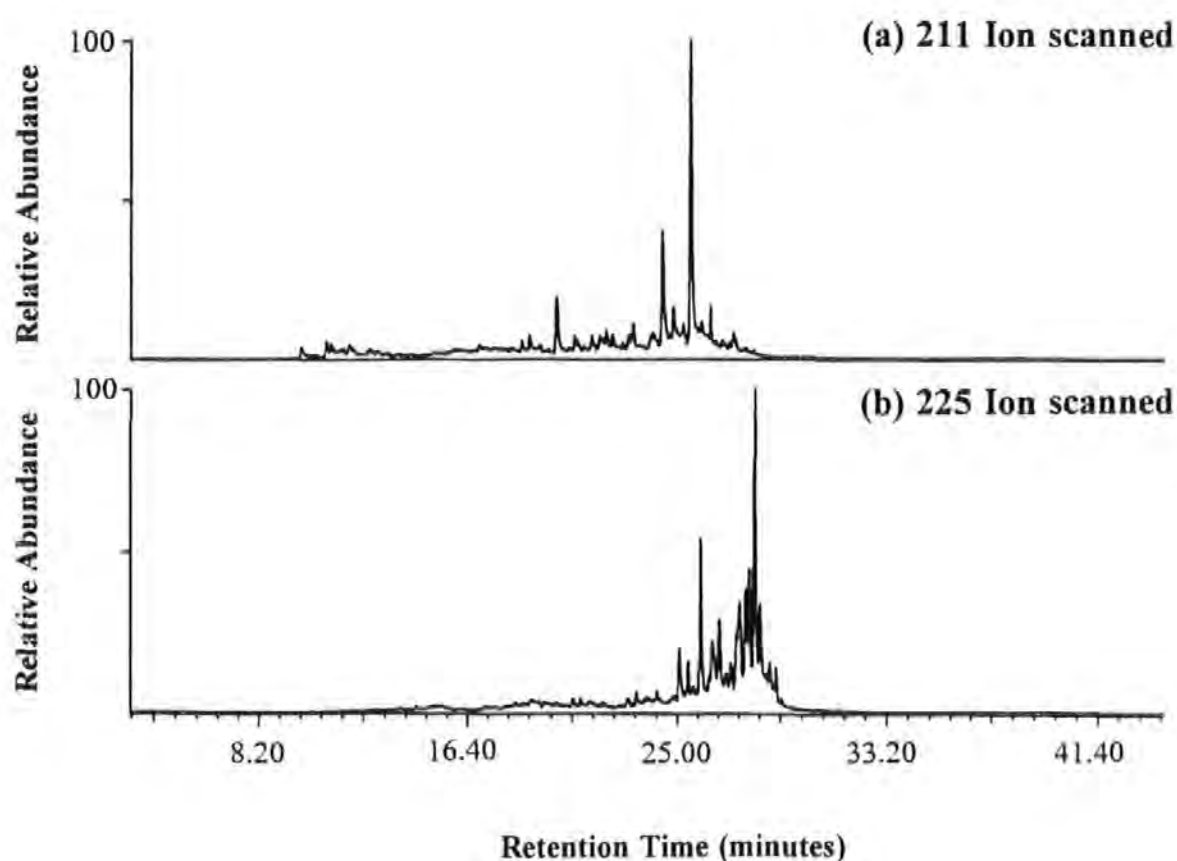


Figure 5.7 Distribution of molecular ions 211 and 225 in the mononitro-PAC HPLC fraction collected at 3500 rpm and high load. Determined using gas chromatography/mass spectrometry operated in the negative ion chemical ionisation mode (Chromatographic conditions given in Section 3.4.3.1.5).



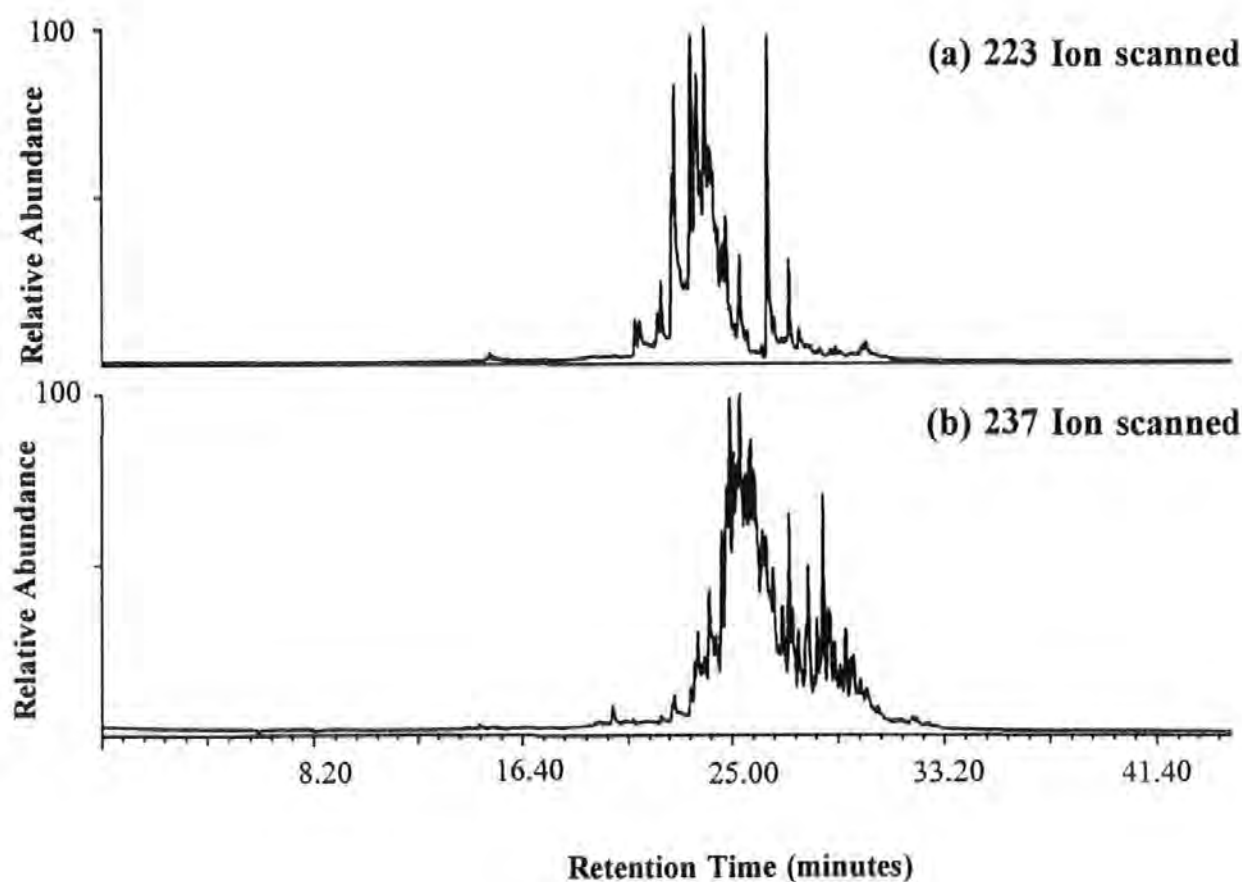


Figure 5.8 Distribution of molecular ions 223 and 237 in the mononitro-PAC HPLC fraction collected at 3500 rpm and high load. Determined by gas chromatography/mass spectrometry operated in the negative ion chemical ionisation mode (Chromatographic conditions given in Section 3.4.3.1.5).

### 5.2.1.3 Comparison of the levels and distribution of Nitro-PAC found using TESSA with Previous Studies

The levels of nitro-PAC found in this study (Table 5.1) are significantly lower than the levels found by previous studies of light-duty engines collected with dilution tunnel/filter sampling systems (Table 5.2).

Table 5.2 Previous Nitro-PAC levels from Light-Duty Diesel Engines

Reference	Sample Details	1-Nitropyrene
Li & Westerholm 1994	Light-duty diesel engine sampled with cyclone particulate separator	4.5 $\mu\text{g/g}$ of extract
Veigl <i>et al.</i> 1994	1.8 l normal aspirated DI diesel operated on transient cycles: HWFET FTP	854 ng/filter 69 ng/filter
Imaizumi <i>et al.</i> 1990	Diesel exhaust	50 ng/g of particulate
Williams <i>et al.</i> 1986	Light-duty Oldsmobile on HWFET (48 mph steady speed) sampled with dilution tunnel	107 ppm in extract
Brown & Poole 1984	Diesel exhaust sampled with dilution tunnel	165 $\pm$ 15 $\mu\text{g/g}$ of extract
Schuetzle <i>et al.</i> 1982	Four light-diesel engines sampled using dilution/filter sampling	ranged from 55 $\pm$ 11 to 2280 $\pm$ $\mu\text{g/g}$ of extract
Campbell & Lee 1984	Light-duty diesel sampled with dilution tunnel	43 $\mu\text{g/g}$ of extract
Paputa-Peck <i>et al.</i> 1983	Light-duty diesel sampled with dilution tunnel	75 $\pm$ 10 ppm of extract
Tejada <i>et al.</i> 1982	Two light-duty diesels sampled on FTP using dilution tunnel: 1978 Oldsmobile 1980 Volkswagen Rabbit	$\mu\text{g/g}$ of extract: 100.0 58.5

The study by Li & Westerholm (1994) using a cyclone particulate sampling system, found levels of 1-nitropyrene comparable with this study. There is a large degree of variation in the levels between different studies and engines. The levels of 1-nitropyrene found in this study are more in line with some of the 1-nitropyrene emissions from medium- and heavy-duty engines (Table 5.3).

Table 5.3 Previous Nitro-PAC Emissions from Medium- &amp; Heavy-Duty Engines

Source	Sample Details	1-Nitropyrene
Draper 1986	Caterpillar 3304 NA sampled using dilution tunnel at 2 conditions: high load and moderate speed low load and high speed	$\mu\text{g/g}$ of particulate: 5.0 not detected
Bechtold <i>et al.</i> 1984	Oldsmobile 5.7 L 8 cylinders. Four cycles of Federal Test Procedure using dilution tunnel sampling	81 ppm in particulate
Jin & Rappaport 1983	Dilution tunnel sampling of four heavy duty diesels:  Cummins VTB-903 International Harvester DT-466 Volvo TD-100 Caterpillar 3046 DITA	ng/mg of extract: 0.7 28.0 9.2 142.0
Nakagawa <i>et al.</i> 1983	1970 Isuzu BY 30 Bus 4 l diesel sampled at idling and 1200 rpm at the end of exhaust with condensation trap followed by filter collection	70.5 ppm in the extract
Schuetzle & Perez 1983	Heavy-duty engine sampled with dilution tunnel at 2 conditions: idle 2100 rpm & full load	ppm in extract: 28.0 1.0
Rappaport <i>et al.</i> 1982	Dilution tunnel sampling of 2 diesels:  medium-duty DSR-46 heavy-duty 1980 Mack	ng/mg of extract: 8 20

Previous studies which relied on dilution and filter collection may have included significant artefact contributions to the nitro-PAC quantifications. Several experimental studies have investigated the possibility of artefact formation of nitro-PAC during sampling.

Pitts *et al.* (1978) found that PAH on glass filters were transformed into nitro derivatives. Tokiwa *et al.* 1981 exposed pyrene to 10 ppm of  $\text{NO}_2$  and found the formation of 1-nitropyrene. This level of  $\text{NO}_2$  could be found in diluted exhaust (Gaddo *et al.* 1984). Gibson *et al.* (1981) found that increasing the sampling time increased both the 1-nitropyrene emissions and mutagenicity whereas the pyrene concentrations decreased. Bradow *et al.* (1982) concluded that above 5 ppm  $\text{NO}_2$  the dilution tunnel system would generate artefacts.

Lindskog *et al.* (1983) found that exposure of pyrene to 1 ppm NO<sub>2</sub> on filters caused degradation. The degradation was greatly enhanced by nitric acid. Risby & Lestz (1983) used a theoretical model for pyrene based on the synthetic fuel and oil study by Herr *et al.* (1982). Risby & Lestz (1983) concluded that the activation energies for surface reactions on filters were lower than the gas-phase reactions, hence artefacts reactions were favoured. Schuetzle & Perez (1983) estimated an average of 12.5% of the nitro-PAC in diesel particles collected in dilution tunnels resulted from artefact formations.

Gaddo *et al.* (1984) showed that 1-nitropyrene concentrations increased dramatically with sampling time for collection on fibre glass filters. For example, the 1-nitropyrene concentration after 5 minutes of sampling was  $24 \pm 7 \mu\text{g/g}$  compared to  $74 \pm 7 \mu\text{g/g}$  after 10 minutes. The authors claimed that after one hour of engine sampling, somewhere between 50 to 90% of the nitro derivatives could be formed as a consequence of the sampling process itself. Hartung *et al.* (1984) found that 18% of nitro-PAC were derived from artefact reactions on the filters used with the dilution tunnel system. The authors also found electrostatic precipitator sampling to have a greater tendency for artefact formations. Chan & Gibson (1985) found that increasing the NO<sub>2</sub> concentration from 2 to 4 ppm in diluted exhaust for a 23 minute FTP sampling cycle resulted in a 60-160% increase in the level of 1-nitropyrene emitted.

Care should be taken when interpreting some of the early artefact studies, such as the initial work of Pitts *et al.* (1978). Grosjean *et al.* (1983) point out that such studies tended to employed high flow rates through the filters and spiked the filters with large doping masses of PAH, such as pyrene. On-road measurement of 1-nitropyrene in the Allegheny tunnel by Gorse *et al.* (1983) found significantly lower emissions compared to dilution tunnel studies. The authors note that the higher acidity of dilution tunnels compared with the more neutral environment in the road favoured nitration reactions within the dilution tunnels. Similarly, the higher levels of NO<sub>2</sub> encountered in dilution tunnels (2-4 ppm) compared with only 0.04-0.16 ppm in the road tunnel may also favour nitration in the confined dilution tunnel arrangement. However, significant degradation of nitro-PAC may have occurred in the environment, accounting for the lower nitro-PAC in the road tunnel study (Stärk *et al.* 1985).

The concept of the TESSA results in the minimum opportunity for artefact formation. This is due to the extremely fast sampling times (order of seconds) and the corresponding rapid removal of the sample from the incoming exhaust. Artefact formation is an inherent problem with the dilution tunnel design, since the sample is held on the filter whilst gaseous reactive species are passed through for lengthy periods (23 minutes for FTP cycle). The filter provides a condensation point for nitric acid which greatly enhances the artefact nitration. Sasaki *et al.* (1980) found that dilution tunnels progressively convert NO into NO<sub>2</sub> with sampling time, creating a greater nitration potential with extending sampling.

One area of concern involved with the work-up of TES samples, was with the separation of the extracted organics into the aqueous methanol phase and the DCM phase containing the PAC of interest. This partition, achieved immediately as the solvent mixture flows from the tower into distilled water, was introduced by Trier (1988) to quench any post-combustion reactions. Concern was raised that there may be some interaction of PAH in the DCM with the acidic aqueous methanol, resulting in nitration of PAH. The possibility that nitro-PAC were formed from the interaction of the acidic aqueous methanol phase and the DCM organic phase was examined (Section 3.4.2.1). This was achieved by adding an aliquot of a standard PAH mix (with each PAH weight added equivalent to that present in a TES) to a pre-extracted aqueous phase from an engine run. The solution was left for 24 hours. Since, the normal work-up procedure would be to rapidly separate the aqueous methanol and DCM phases (less than 30 minutes per sample), any nitration that may have occurred would be detectable in the nitration check. Following the extraction of the PAH from the aqueous phase and isolation of the fraction corresponding to the nitro-PAC elution window by NP HPLC, the sample was analyzed by GC-ECD. The analysis, shown in Figure 3.11 (Section 3.4.2.1), could find no evidence for any formation of nitro-PAC.

If it is assumed that the careful use of filters and dilution sampling techniques result in artefact contributions to the nitro-PAC emissions of the order of 10 to 30%, there still exists a significant difference between the highest 1-nitropyrene emissions from the Prima engine (5.3 ppm) sampled with TESSA, compared with the majority of the light-duty engines sampled with

dilution tunnel/filter systems. Some of the previous studies on light-duty diesels, such as that by Campbell & Lee (1984), are closer to this study (assuming 30% artefact derived, the Campbell & Lee study gives a concentration of 12.9 ppm of 1-nitropyrene in the extract).

More importantly the dilution tunnel samples are typically derived from engine conditions less extreme than 3500 rpm and high load, conditions which in this study resulted in the highest 1-nitropyrene levels. The average of the remaining 1-nitropyrene emissions from this study gives an average of 1.4 ppm in the extract. Even after correcting for severe artefact contributions these 1-nitropyrene emissions are significantly lower than any of the previous studies on light-duty engines, sampled using dilution tunnels.

The difference between the levels found in this study and previous ones may be a reflection of the type of sampling system used. In this study the samples are derived primarily from the combustion chamber with the minimum of exhaust contributions, whereas dilution tunnel systems are designed to simulate exhaust and environmental effects. Hence, the difference in 1-nitropyrene emissions obtained from this study compared with the dilution tunnel studies may be due to the limited dilution allowed by the engine and TESSA arrangement. This suggests that increased dilution may increase the nitro-PAC emissions, possibly by increasing reaction time between PAH and nitrogen dioxide in the diluted exhaust stream. Li & Westerholm (1994) collected emissions using a particulate cyclone without any additional exhaust dilution. The levels of 1-nitropyrene emitted were comparable with those in this study, supporting the theory that increased dilution increases nitro-PAC emissions, possibly as a consequence of artefact formations.

Another reason for the different emission levels may result from the engine technology available at the time of the studies. The early engines would not have been as efficient as the more modern Prima engine. Consequently, the emissions from the older engines may have been relatively higher than the Prima design. The comparison of 1978 diesel engines to the later 1980 models for 1-nitropyrene emissions by both Gibson *et al.* (1981) and Tejada *et al.* (1982) did in fact show a marked reduction for the newer engines.

Many dilution tunnel studies have found between 60 to 200 different nitro-PAC in the exhaust extracts, with the most abundant nitro-PAC in most cases being 1-nitropyrene (Schuetzle *et al.* 1982, Paputa-Peck *et al.* 1983, and Williams *et al.* 1986b). In this study, analysis of the sample collected at high speed and high load by GC/MS NICI also indicated that many nitro-PAC were present in TES at low levels (Section 5.2.1.2). The GC/MS results indicate that a proportion of the fuel PAC undergoes nitration to form nitro- derivatives with a similar distribution to the fuel. A series of studies by Henderson *et al.* (1982, 1983, & 1984) also found that a fraction of fuel underwent nitration, resulting in the exhaust nitro-PAC composition being similar in distribution to the PAH in the fuel.

By contrast to other light-duty diesel engine studies, the nitronaphthalenes were in greater abundance than 1-nitropyrene. The study of diesel nitro-PAC emissions by Williams *et al.* (1986b) found much lower levels of 1-nitronaphthalene (0.3 ppm of extract) compared with 1-nitropyrene (107 ppm of extract). Heavy-duty diesel studies have in some cases found higher 1-nitronaphthalene emissions, for example Draper (1986) could not detect 1-nitropyrene at high load and moderate speed whilst 1-nitronaphthalene was emitted at 0.77  $\mu\text{g/g}$  particulate. However, at a higher speed and lower load, the situation reversed, with 1-nitropyrene emissions of 5.0  $\mu\text{g/g}$  particulate compared with 1-nitronaphthalene emissions of only 0.47  $\mu\text{g/g}$  particulate. The greater nitronaphthalene levels compared with 1-nitropyrene found by this study may to a limited extent be a result of higher laboratory losses of *ca.* 30% for 1-nitropyrene compared with the nitronaphthalenes (for example *ca.* 10% of 1-nitronaphthalene lost). However, taking this into consideration still leaves the nitronaphthalene levels higher than those of 1-nitropyrene. The different distribution of the nitro-PAC in the Prima emissions may indicate different nitro-PAC formation processes may have been involved. This may again reflect the decreased potential for post-combustion reactions, including artefact contributions, using TESSA. Alternatively, some of the dilutions tunnel studies may not have collected the more volatile nitronaphthalenes to the same extent as 1-nitropyrene. The PAH content of the fuel may also have varied significantly between the different studies, and it may be that in this study there were greater levels of naphthalene compared with pyrene than there were in other studies, or alternatively other studies had relatively higher pyrene levels.

#### 5.2.1.4 The Effect of Engine Speed and Load on the Mononitro-PAC Emissions

The rapid sampling and low artefact potential of TESSA enables the effect of engine speed and load to be examined. Nitro-PAC profiling over a wide range of speeds and loads is best suited to TESSA, which outperforms other engine sampling techniques in terms of mass sampling.

Figure 5.9 shows the effect of engine load on the identified nitro-PAC emissions at the lowest speed of 1500 rpm. The nitro-PAC levels for each set of duplicate samples show good overall reproducibility, with some exceptions. The effect of engine load on the nitro-PAC extract concentrations is not repeated for different nitro-PAC. Within the indicated range of error bars, 2-methyl-1-nitronaphthalene increases in concentration at mid load and thereafter decreases at higher loads. In contrast, the concentrations of 1-nitronaphthalene, 2-nitronaphthalene and 1-nitropyrene are more constant across the load range.

Figure 5.10 shows the effect of load on the 1-nitropyrene emissions at the mid-speed of 2500 rpm. The reproducibility is very good and 1-nitropyrene increases up to mid load and then decreases slightly at high load. Figure 5.11 shows the emissions of nitro-PAC at the highest speed of 3500 rpm and the three load positions. The nitro-PAC emissions at this high speed are significantly different with respect to the nitro-PAC emission trends at the lower speeds, with all nitro-PAC increasing with engine load. The nitronaphthalenes progressively increase with engine load, whilst 1-nitropyrene is initially stable and then rapidly increases at high load.

Figure 5.12 shows the combined effect of engine speed and load on the emissions of 1-nitronaphthalene and 1-nitropyrene. The emissions of 1-nitronaphthalene are more stable across the load range at 1500 rpm, whereas at the higher speed the 1-nitronaphthalene increased with engine load (Figure 5.12a). Figure 5.12b shows that the greatest variation in the 1-nitropyrene emissions occurs at high load and for the three speeds.

After establishing the effect of speed and load on the nitro-PAC emissions from the Prima combustion chamber it is now possible to compare the findings with those from previous studies, concentrating on 1-nitropyrene. The majority of previous studies have concentrated on heavy-duty emissions and used dilution tunnel and filter collection.



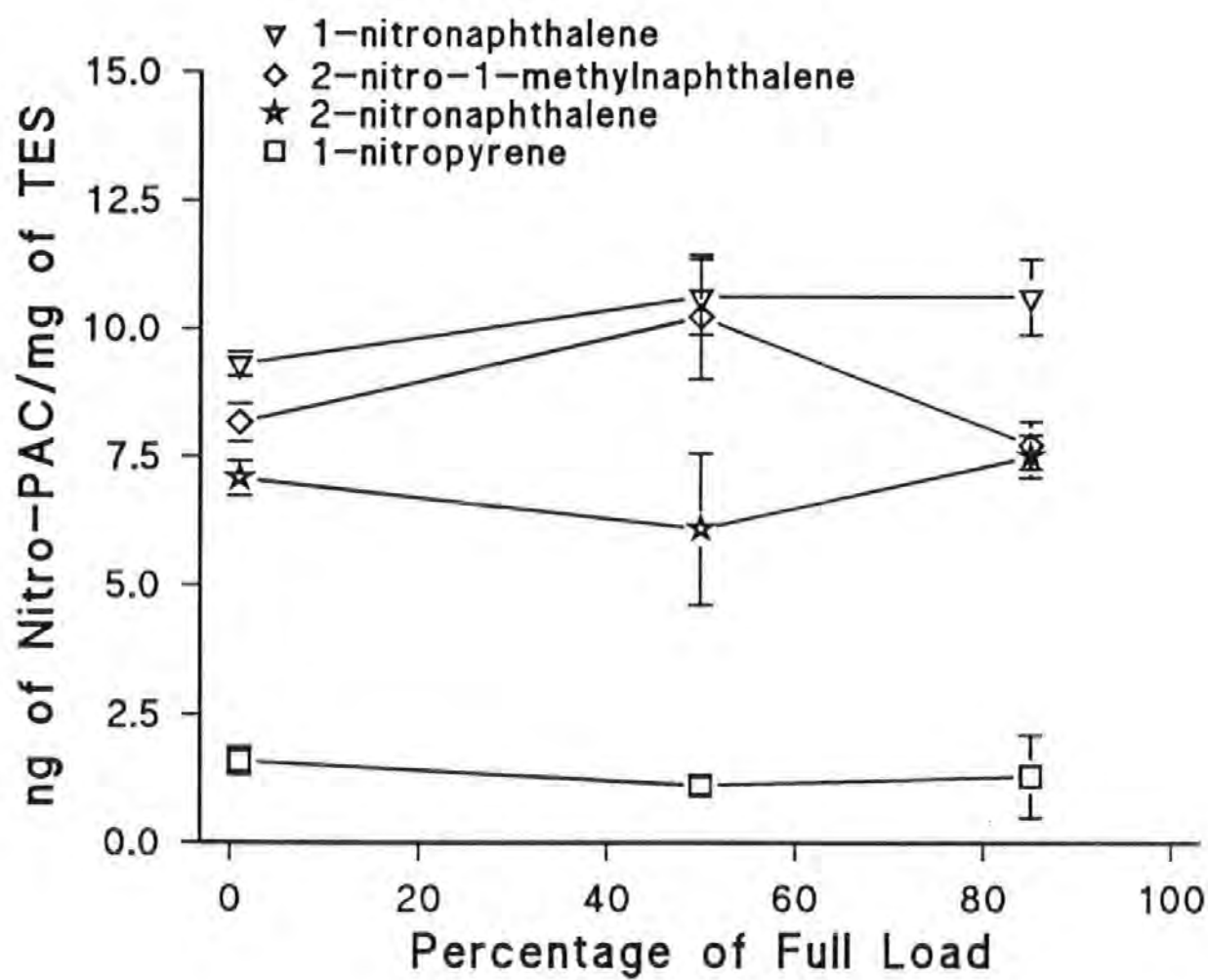


Figure 5.9 The effect of engine load on the nitro-PAC at 1500 rpm

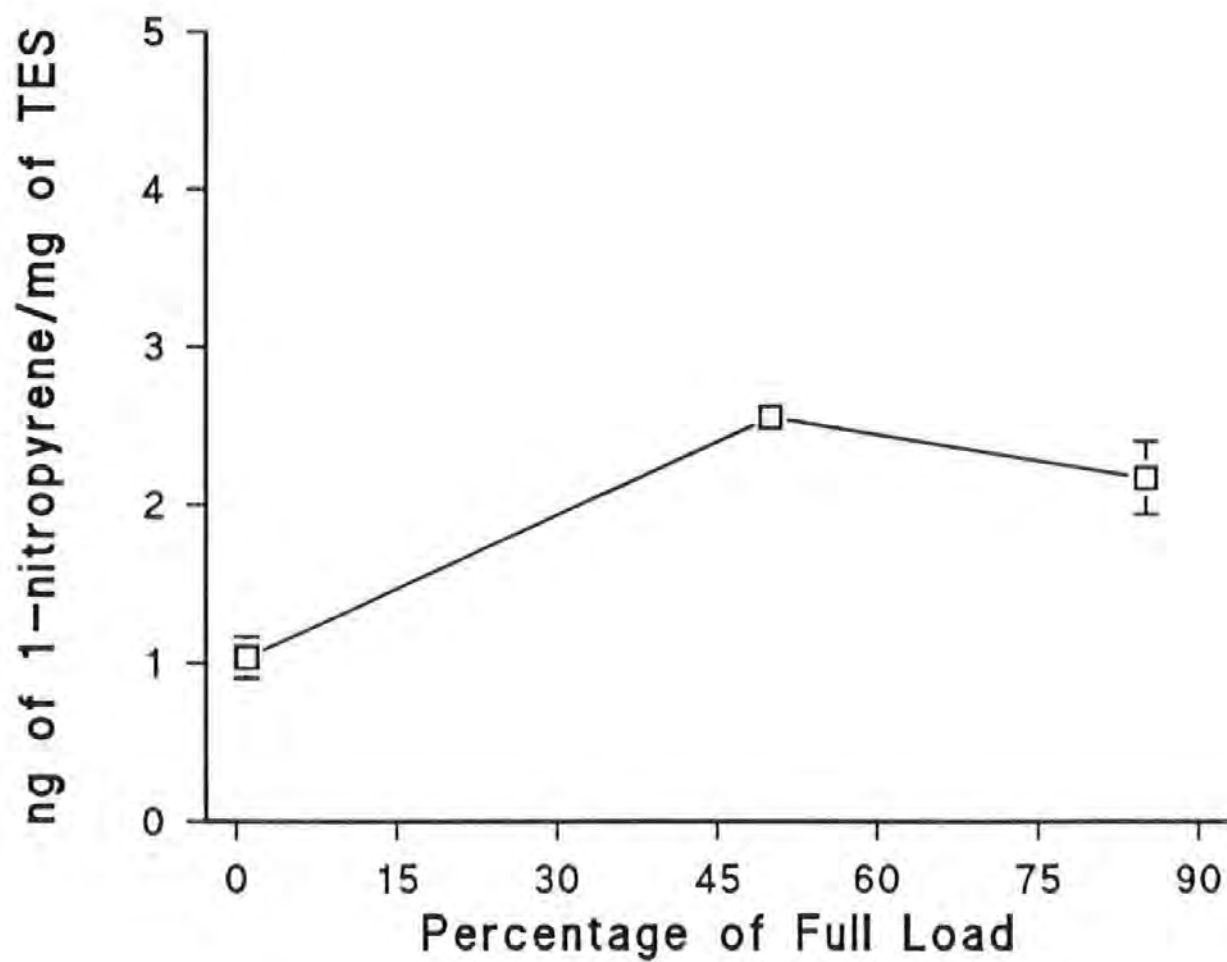


Figure 5.10 The effect of engine load on the nitro-PAC at 2500 rpm

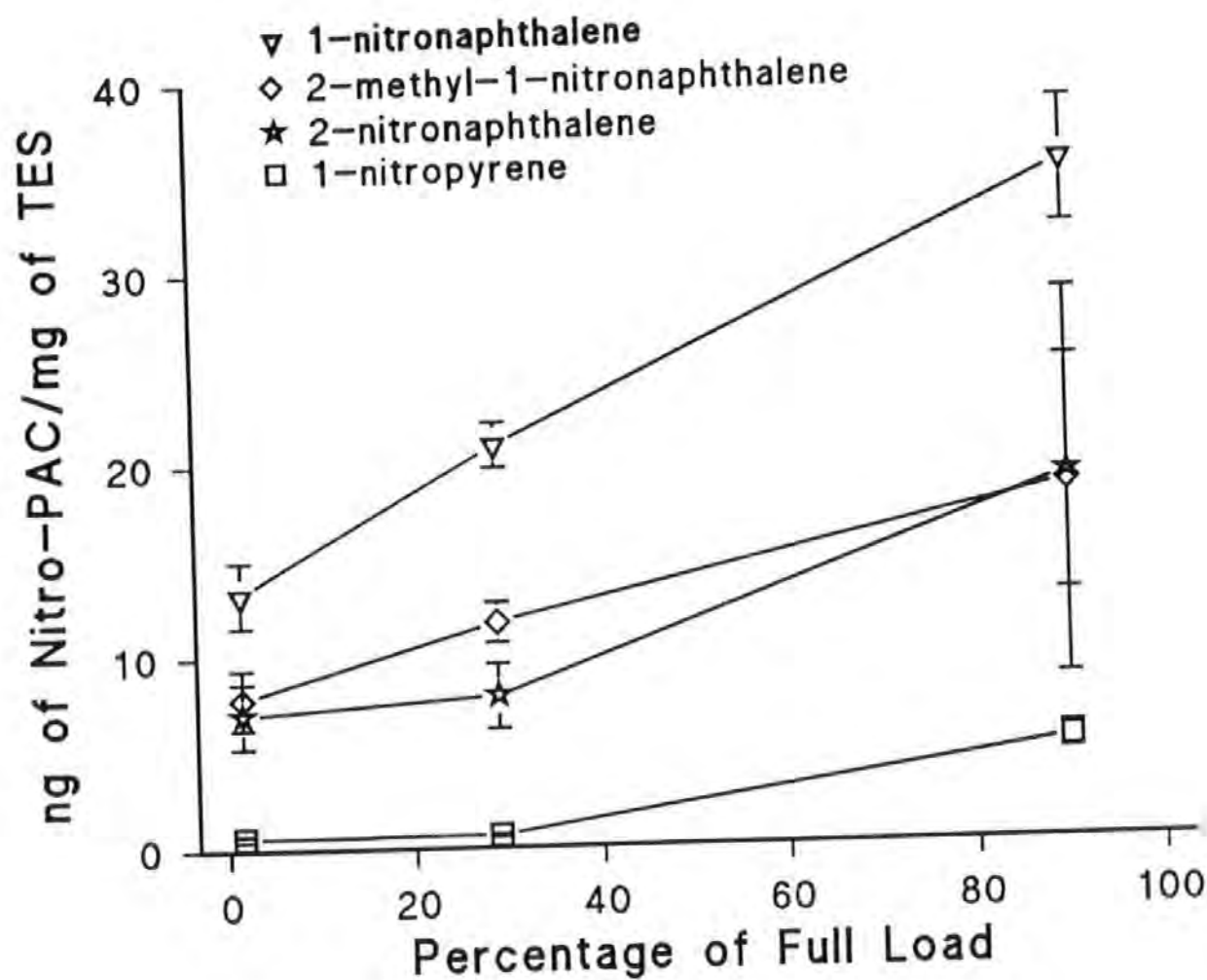


Figure 5.11 The effect of engine load on the nitro-PAC at 3500 rpm

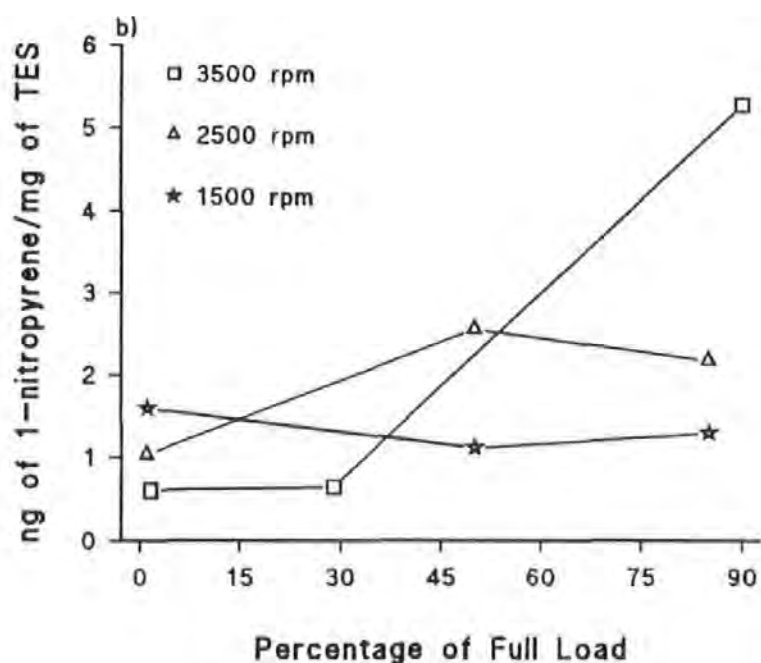
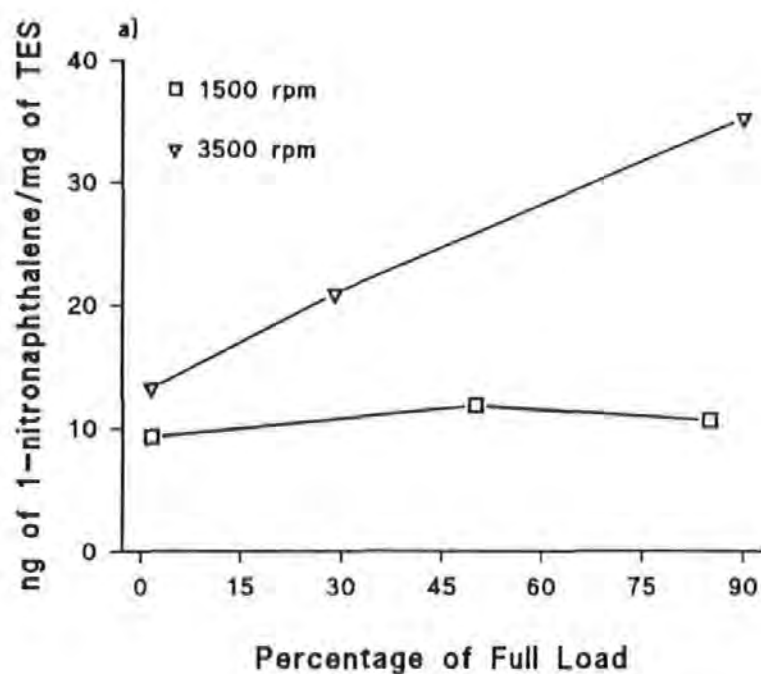


Figure 5.12 The combined effect of speed and load on a) 1-nitronaphthalene and b) 1-nitropyrene emissions.

The study by Schuetzle & Perez (1983) on heavy-duty diesels found the 1-nitropyrene extract concentrations initially increased with load and then severely decreased at high load for a speed of 2100 rpm. This agrees with the findings of this study at 2500 rpm, with a less severe decline in the 1-nitropyrene emissions at high load in this study. Schuetzle & Perez also found the emissions of 1-nitropyrene at mid- and high-loads for a lower speed of 1260 rpm were more stable in comparison with the emissions at the higher speed, as was the case in this study. The work also sampled at very low load and 700 rpm, whereupon the highest of 1-nitropyrene emissions out of all the sampling conditions was generated.

Bechtold *et al.* (1984) found that the emissions of 1-nitropyrene from a heavy-duty diesel increased with engine speed whilst under cruising conditions, as did NO<sub>x</sub> and temperature. This agrees with the 1-nitropyrene emissions found in this study at mid-load for increasing the speed from 1500 rpm to 2500 rpm, and also at high load where 1-nitropyrene increases as the speed was increased.

The study of heavy-duty diesel exhaust wall deposits on road tunnels by Handa *et al.* (1984) found that the emissions of 1-nitropyrene were higher at high load compared with low load for an estimated on-road speed of 1800 rpm. The lack of other engine conditions make it difficult to gauge the results to those found in this study. By contrast to the road tunnel study the 1-nitropyrene emissions at 1500 rpm were much more stable in this study, although at higher speeds the 1-nitropyrene emissions were highest at high load compared with low load.

Draper 1986 compared the nitro-PAC emissions from a heavy duty diesel engine at high load and moderate speed with the emissions at moderate load and high speed. The authors found that the nitro-PAC emissions were highest at moderate load and high speed. The fact that the study relied on only two sampling points combined with both speed and load changing at each point again makes comparisons difficult. Taking 1500 rpm as a moderate speed and 3500 rpm as the high speed reveals no correlations between the findings in this study to those by Draper and co-workers, except for 1-nitronaphthalene, which was higher at moderate load and high speed in both studies.

Veigl *et al.* (1994) found that the highest emissions of 1-nitropyrene emitted from a light-duty diesel were produced over the HWFET compared with a lower speed and fluctuating load FTP cycle. The increased nitro-PAC emissions at high speed, would tend to agree with the results from this study, however transient cycles are difficult to breakdown into whether it is speed or load which determines the emissions. The authors also profiled 1-nitropyrene emissions over a range of loads at constant speed of 1560 rpm for a medium-duty diesel. Within the error bars, some of which were large, the 1-nitropyrene emissions increased up to mid-load whereafter the emissions decreased slightly, a finding similar to that found at 2500 rpm in this study but not at 1500 rpm. The authors found the lowest emissions of 1-nitropyrene at low load and 600 rpm.

The comparison of the findings from this study with previous ones, has in some cases identified some correlations. However there are also major differences between not only this study and the other studies, but also amongst the other studies themselves. In most cases, many more sampling points would be needed to provide a better comparison. The majority of the studies compared to this study were based on heavy-duty engines. The similarity of heavy-duty and light-duty combustion in terms of nitro-PAC is unknown. In terms of the range of both engine conditions and nitro-PAC investigated the results from this study are the most comprehensive to date for light-duty diesel engines. Another major weakness of the majority of previous studies is the failing to attempt correlations between the emissions and nitration parameters, such as  $\text{NO}_x$  and temperature. The next section investigates the importance of such factors at specific engine conditions.

#### 5.2.1.5 Factors controlling the Nitration in the Combustion Chamber

The close proximity of TESSA to the Prima engine largely removes the post-combustion reactions simulated by dilution tunnel sampling systems. The short transfer line will allow some post-combustion reactions to proceed, but not to the same extent as the dilution tunnel. The greatly reduced post-combustion environment has resulted in much lower levels of nitro-PAC found in this study. This suggests that a significant proportion of nitro-PAC are derived following combustion processes. Indeed Kittelson *et al.* (1984) found that nitro-PAC were four times more likely to be found in the exhaust than in the combustion chamber.

The formation of nitro-PAC is primarily a function of the concentration of PAH and nitrating species, termed  $\text{NO}_x$ . The analysis of a nitro-PAC HPLC fraction by GC/MS NICI identified that a proportion of PAH present in the fuel had at some stage been converted into nitro-PAC (Section 5.2.1.2).

To examine the effect of  $\text{NO}_x$  on the nitro-PAC emissions, the  $\text{NO}_x$  concentrations were examined relative to the nitro-PAC emissions at varying engine conditions (Figure 5.13). Due to the greater information on nitro-PAC, the speeds corresponding to 1500 rpm and 3500 rpm are displayed. For all speeds tested, the gaseous  $\text{NO}_x$  concentrations increased with engine load up to around 80% of full load, and thereafter the  $\text{NO}_x$  levels declined slightly. There is little correlation between the nitro-PAC emissions with the  $\text{NO}_x$  concentrations at low and mid-engine speeds (R-sq for 1-nitronaphthalene and  $\text{NO}_x$  correlation = 0.327 and  $p = 0.612$ , at low speed.). At the higher engine speed, there is a strong correlation between  $\text{NO}_x$  and the nitro-PAC (R-sq for 1-nitronaphthalene and  $\text{NO}_x$  correlation = 0.989 and  $p = 0.067$ ).

The correlation of  $\text{NO}_x$  and nitro-PAC at high speed as opposed to lower speeds, may indicate that the nitro-PAC formation is temperature controlled to some extent. This suggests that the nitration reactions are favoured by the higher temperatures existing at high speed. Bechtold *et al.* (1984) also found a link between exhaust temperatures and the 1-nitropyrene emissions.

It is important to point out that the  $\text{NO}_x$  measurements were derived further down the exhaust system (Rhead *et al.* 1991). This work assumes that the overall  $\text{NO}_x$  trends with engine load are the same close to the combustion chamber as for further down the exhaust. The work of Pipho *et al.* (1991) showed the levels of  $\text{NO}_x$  within the combustion chamber were replicated further down the exhaust pipe.

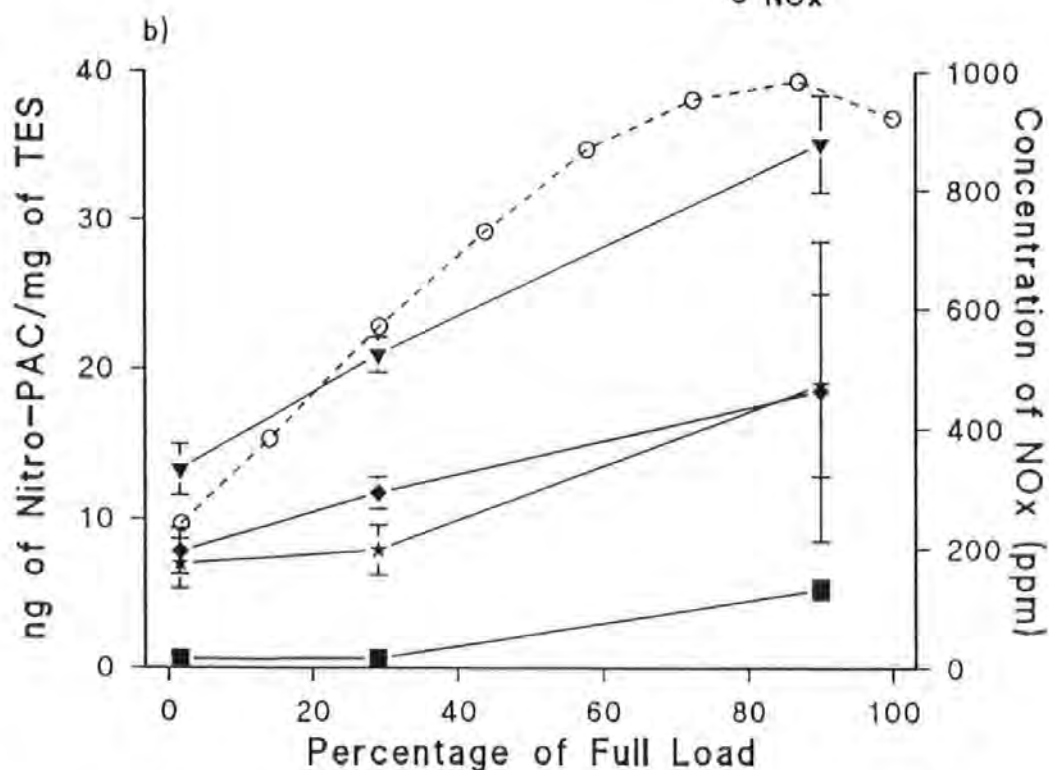
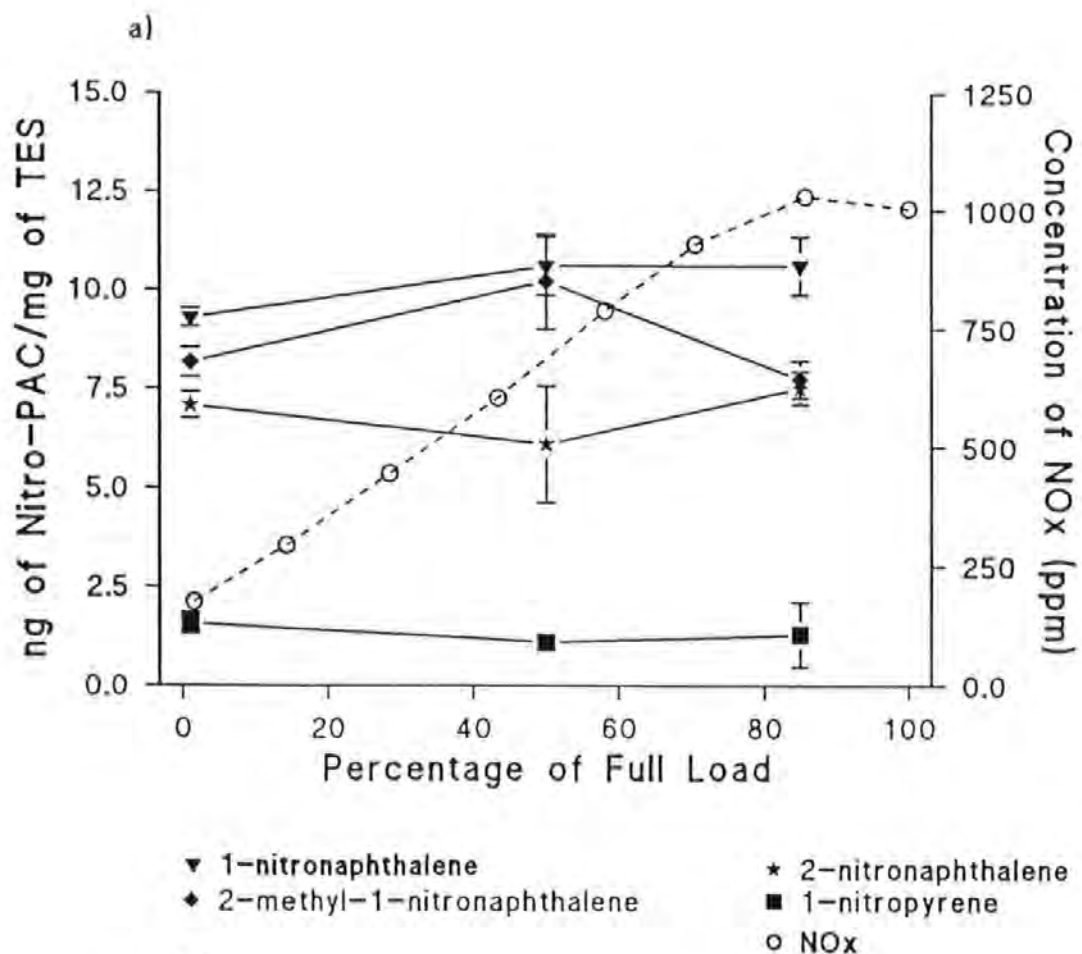


Figure 5.13 The investigation of correlations between the nitro-PAC and NO<sub>x</sub> emissions at a) 1500 rpm and b) 3500 rpm.



#### 5.2.1.6 Nitration mechanisms involved

Two nitration mechanisms have been proposed to account for the nitro-PAC emissions from diesel engines are:

1) Free radical reactions involving  $\text{NO}_x$  and PAH radicals.

2) Electrophilic substitution of PAH, involving  $\text{NO}_2$  in the presence of nitric acid.

(Scheepers & Bos 1992b)

It is important to note that it is only the  $\text{NO}_2$  fraction of  $\text{NO}_x$  involved in the electrophilic substitution nitration (Lindskog 1983 and Schuetzle 1983), whereas both NO and  $\text{NO}_2$  participate in the free radical nitrations (Scheepers & Bos 1992b). The primary  $\text{NO}_x$  species formed in the chamber is NO, with  $\text{NO}_2$  existing as a transient species at the flame front, before being converted to NO in the post-flame region (Arcoumanis 1992). Nitrogen dioxide can be emitted at low loads due to the conversion of  $\text{NO}_2$  to NO being quenched (Arcoumanis 1992). This translates to  $\text{NO}_2$  contributing *ca.* 50% to the total  $\text{NO}_x$  emitted at low loads compared with only 5% at high loads (Campbell *et al.* 1981, Lenner 1987, Pipho *et al.* 1991). The highest concentration of nitric acid, known to greatly enhance nitration, is also generated at low loads (Harris *et al.* 1987).

Free radical nitration reactions are favoured by conditions where both the  $\text{NO}_x$  and PAH radicals are abundant and sufficient potential exist for the reaction to proceed. The high temperature dependence of free radical reactions would suggest the variables for successful free radical nitration would exist following combustion and diminish with time thereafter. In contrast, nitration of PAH by electrophilic substitution with the nitronium ion,  $\text{NO}_2^+$ , is not governed by the same kinetics as free radical processes. Indeed, nitration involving the nitronium ion ( $\text{NO}^+$ ) in aqueous solutions will proceed at room temperature (Nielsen 1984 and Ross *et al.* 1988). It follows that the greatest potential for electrophilic substitution nitration occurs at conditions for which nitrogen dioxide and associated nitric acid can interact with PAH, ie. at the lower exhaust region temperatures.

In order to gain a further insight into the potential of the combustion and initial stages of exhaust to form nitro-PAC, the nitro-PAC, PAH, and  $\text{NO}_x$  were referred to the amount of fuel consumed. At low engine speed, 1-nitronaphthalene emissions, in terms of the fuel consumed, are highest at low load (Figure 5.14). The lowest combustion efficiency associated with low loads result in naphthalene also being highest at low loads (Chapter 4). By contrast, the gaseous  $\text{NO}_x$  emissions increase with engine load, but the actual contribution of  $\text{NO}_2$  to the  $\text{NO}_x$  decreases with increased load (assuming a 50% contribution of  $\text{NO}_2$  to  $\text{NO}_x$  at low loads compared with 5% at high loads). Similar trends are generated for 1-nitropyrene, pyrene, and  $\text{NO}_x$  emissions at 1500 rpm, with the exception that pyrene increases again at high load (Figure 5.15).

The high emission of nitro-PAC relative to the fuel consumed at low load and low speed, may indicate that under these engine conditions the greatest free radical interaction with  $\text{NO}_x$  and PAH occurs (mechanism 1). The other possibility is that low loads result in the nitration of the surviving PAH by substitution mechanisms involving  $\text{NO}_2$  and nitric acid, *via* the  $\text{NO}_2^+$  (mechanism 2). The higher  $\text{NO}_2$  and nitric acid combined with the higher survival levels of PAH (Chapter 4) at low loads, would represent the highest electrophilic substitution nitration potential during the expansion and exhaust stages (mechanism 2).

Hirakouchi *et al.* (1990) also found that the highest emissions of 1-nitropyrene and PAH, expressed relative to the fuel burned, were at low loads. The gaseous  $\text{NO}_x$  emissions relative to the fuel burned peaked at around mid-loads and then stabilised at higher loads, as in this study. The study using a mini-dilution tunnel found very good correlations with full flow dilution tunnels.

The dilution tunnel arrangement will favour exhaust electrophilic substitution reactions with  $\text{NO}_2$  and associated  $\text{HNO}_3$  (mechanism 2). Hence, the similar trends found by Hirakouchi and co-workers and by this study provides further evidence that the high level of nitro-PAC at low loads and low speeds are a consequence of PAH surviving combustion and undergoing nitration in the early stages of the exhaust/transfer line (mechanism 2). An extended transfer pipe between the engine and TESSA would enable verification of this theory (Section 6.3).

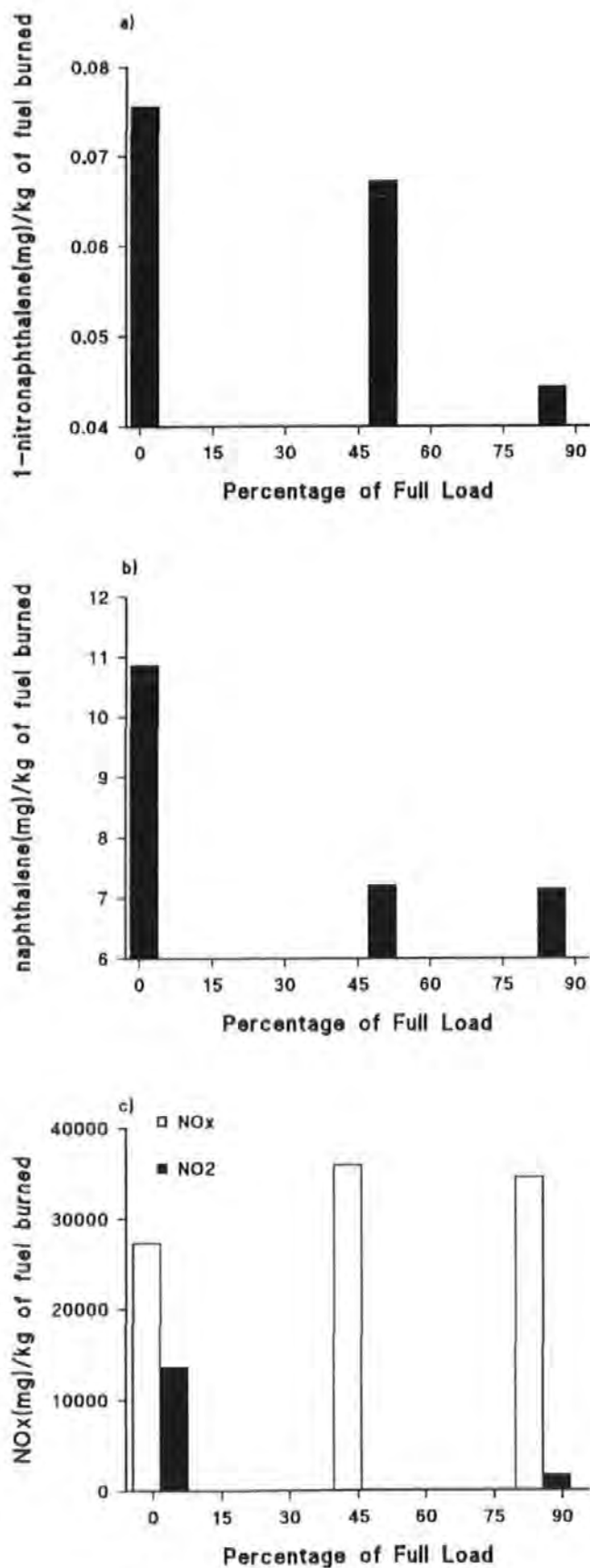


Figure 5.14 Emissions of 1-nitronaphthalene (a), naphthalene (b), and NO<sub>x</sub> (c) relative to the fuel burned at 1500 rpm.

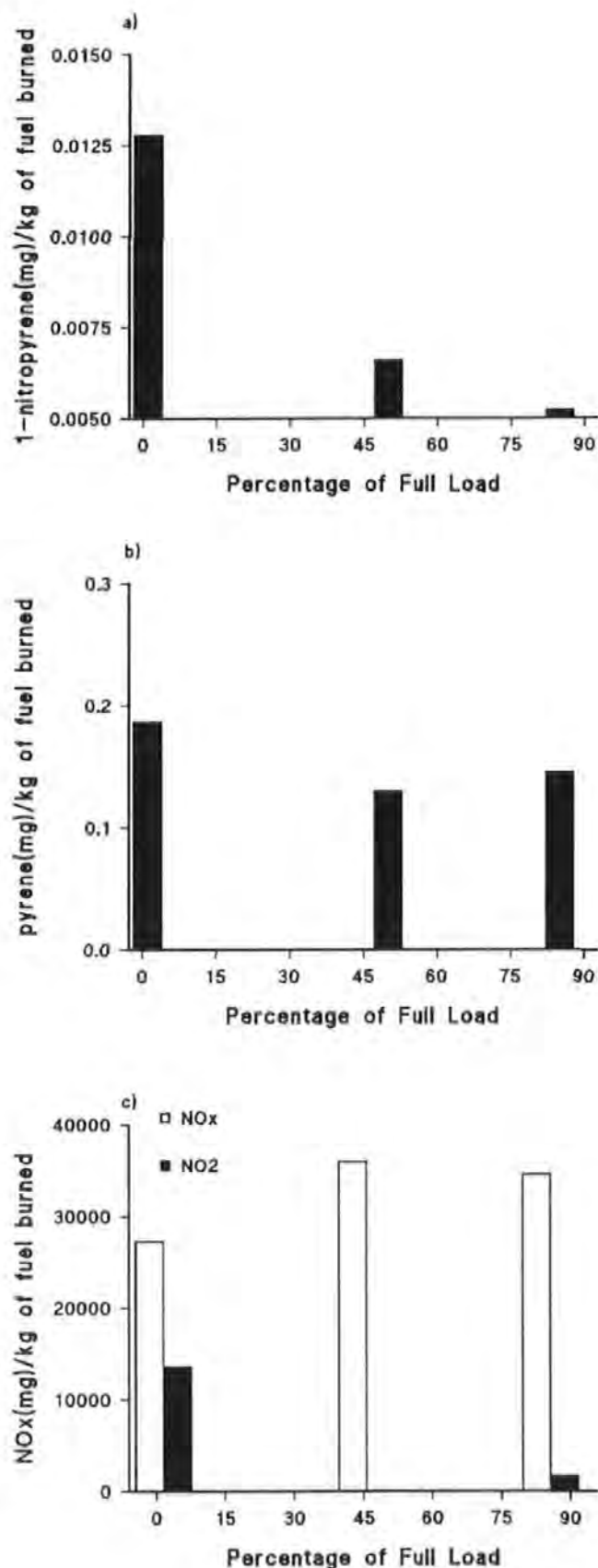


Figure 5.15 Emissions of 1-nitropyrene (a), pyrene (b), and NO<sub>x</sub> (c) relative to the fuel burned at 1500 rpm.

At the higher engine speed of 3500 rpm, the profile of 1-nitronaphthalene and  $\text{NO}_x$  relative to the total fuel consumed both peak at around 30% of full load (Figure 5.16). This may indicate that this engine condition represents the optimum conditions for free radical nitration of naphthalene. The possibility that 1-nitronaphthalene is derived from the electrophilic substitution of naphthalene by the  $\text{NO}_2^+$  is thought unlikely. This is due to the low  $\text{NO}_2$  and associated nitric acid concentrations that would exist at the temperatures involved with this load and speed. Secondly, the survival level of naphthalene that would be available is relatively lower than at the lowest loads.

The 1-nitropyrene emissions at 3500 rpm replicates the profile of pyrene across the load range (Figure 5.17). The close resemblance of the pyrene and 1-nitropyrene emissions relative to the total fuel consumed at high engine speed, suggests a direct link between pyrene and 1-nitropyrene at these engine conditions. In fact examination of the percentage recovery of pyrene relative to the other major PAH at high load and high speed revealed that the pyrene emissions were probably contributed to by a significant pyrosynthetic input (Section 4.3.2). The increased mass of pyrene causes a significant input to the formation of 1-nitropyrene, either by free radical or substitution processes. The possible pyrosynthetic contributions to pyrene combined with the high temperatures at extreme engine powers, suggest that the nitration takes place by free radical combustion chamber interactions between  $\text{NO}_x$  and pyrene.

To investigate the nitration potential as a function of engine speed, the profiles of 1-nitropyrene, pyrene, and  $\text{NO}_x$  relative to the total fuel consumed were plotted at low and high loads. The emissions of 1-nitropyrene, relative to the fuel consumed, at low load decrease with speed (Figure 5.18). By contrast, pyrene initially increases with speed and then decreases at higher speeds. Hence, the greatest interaction between  $\text{NO}_x$ /nitric acid and PAH (mechanism 2) exist at the low temperatures present in the expansion stages of low load. This may indicate that increased speed at low loads reduces the reaction time available for  $\text{NO}_2^+$  and PAH interactions. At high load, 1-nitropyrene emissions are the reverse to low load, and now increase with speed (Figure 5.19). As identified, pyrene has a significant input to the nitro-PAC emissions at high speed and high load. The trends at high load suggest that temperature is an important factor in the free radical formation of nitro-PAC emissions.

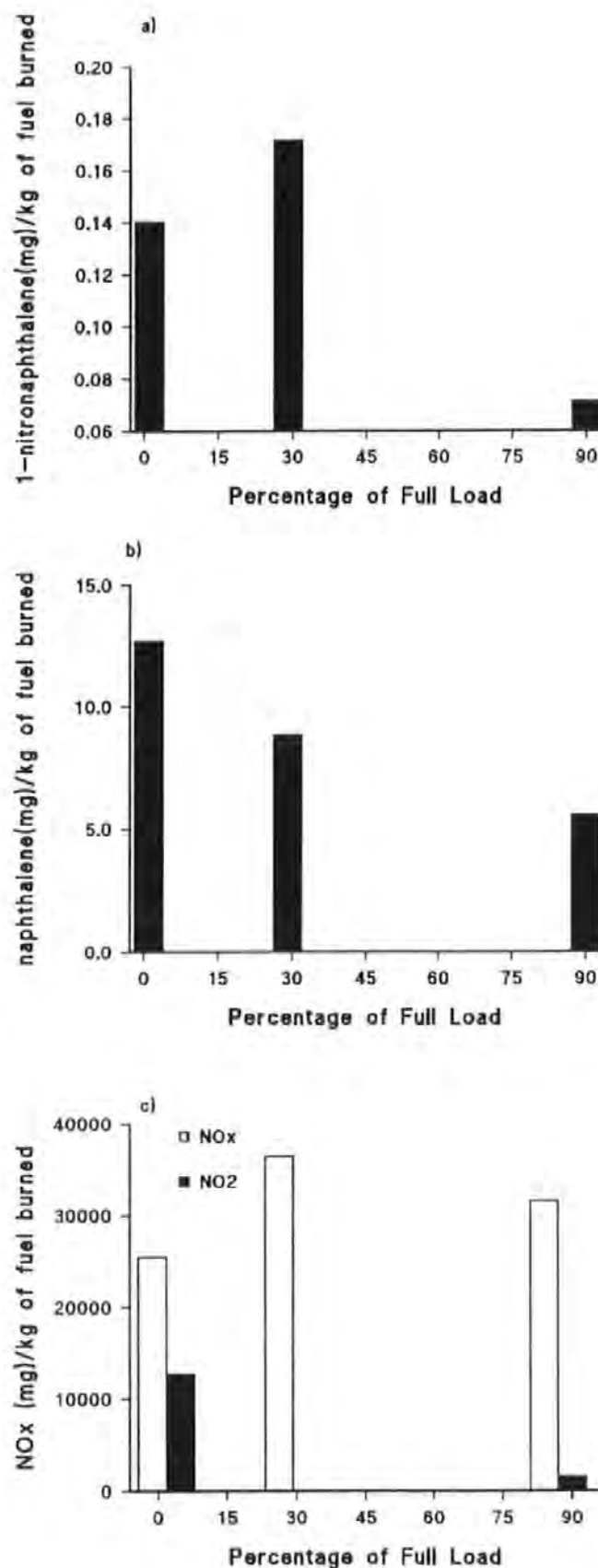


Figure 5.16 Emissions of 1-nitronaphthalene (a), naphthalene (b), and  $\text{NO}_x$  (c) relative to the fuel burned at 3500 rpm.

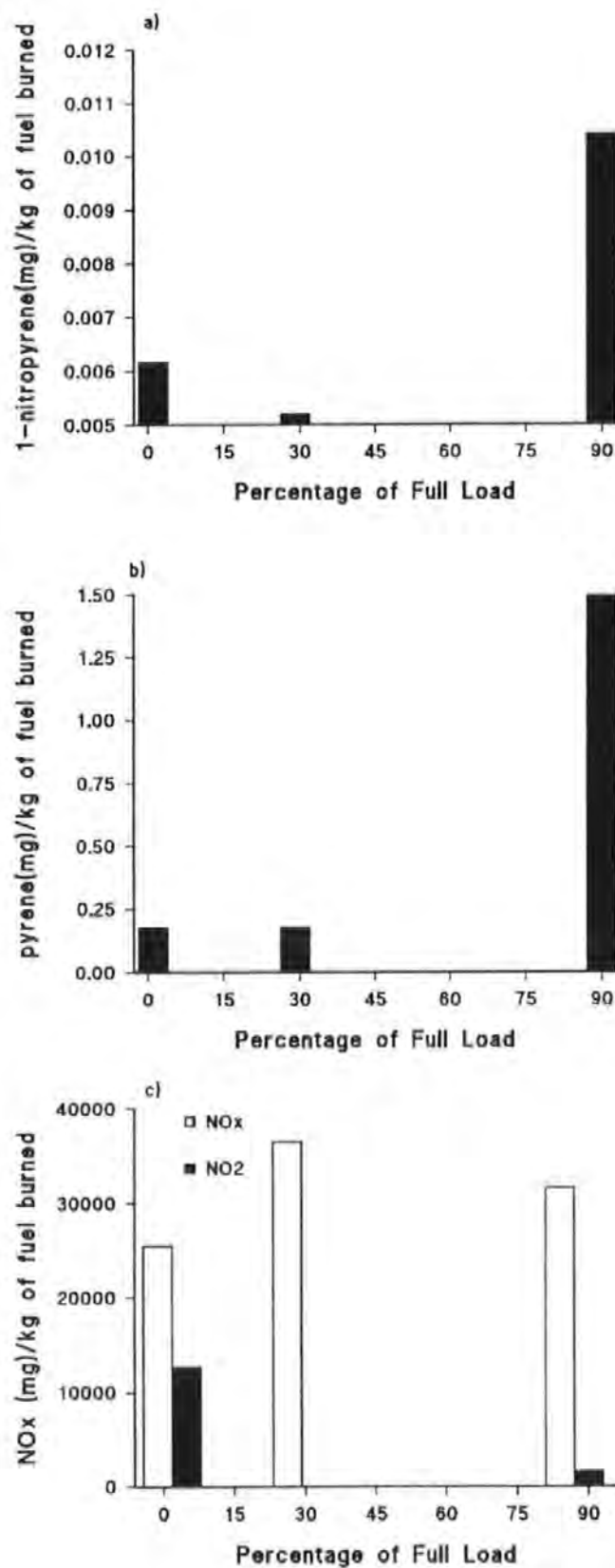


Figure 5.17 Emissions of 1-nitropyrene (a), pyrene (b), and NO<sub>x</sub> (c) relative to the fuel burned at 3500 rpm.

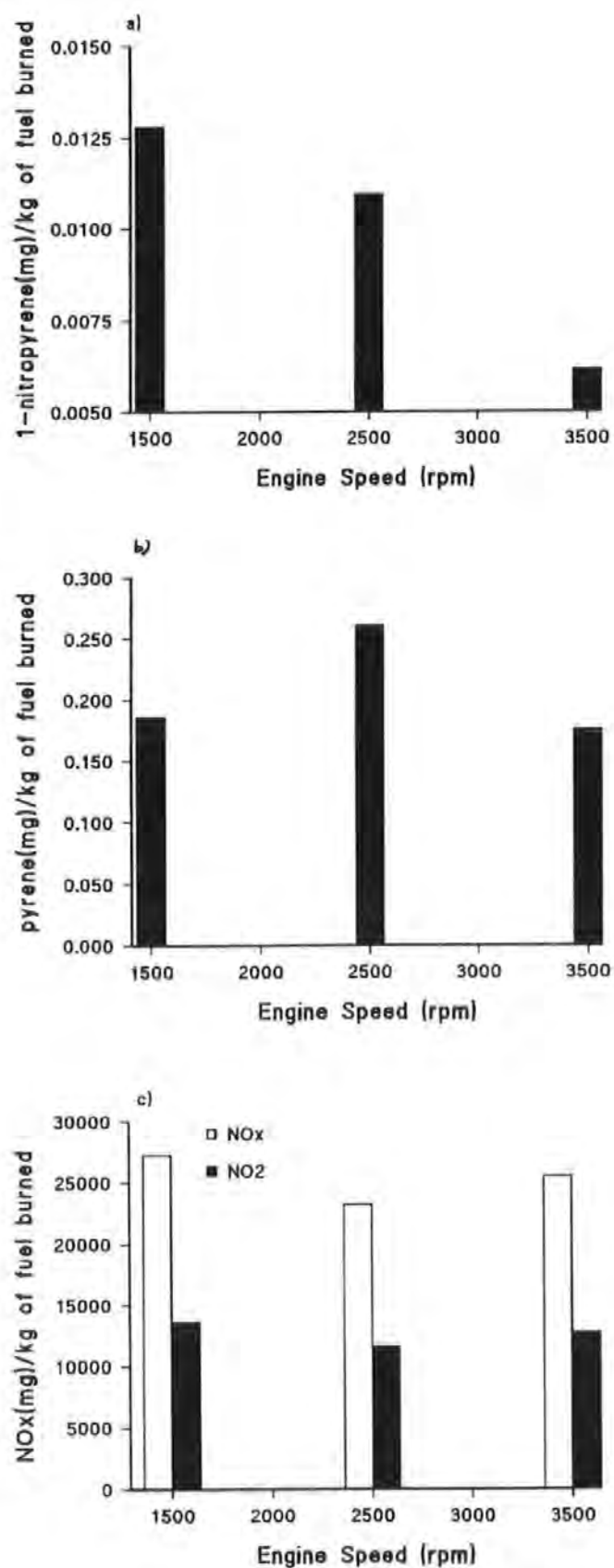


Figure 5.18 Emissions of 1-nitropyrene (a), pyrene (b), and NO<sub>x</sub> (c) relative to the fuel burned at low load.



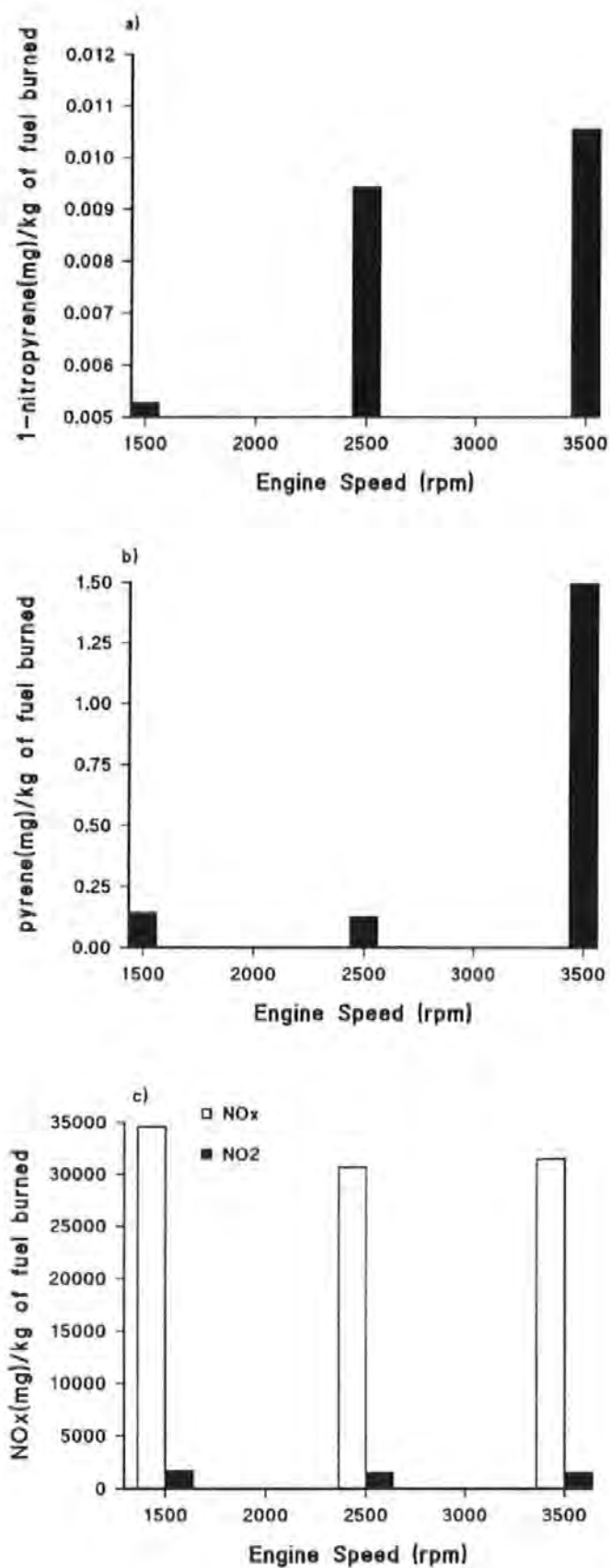


Figure 5.19 Emissions of 1-nitropyrene (a), pyrene (b), and NO<sub>x</sub> (c) relative to the fuel burned at high load.

### 5.2.2 Dinitro-PAC & Nitro-oxy-PAC Profiles for the Prima Diesel Engine

Following the large variations in mononitro-PAC at high speed, the HPLC fractions associated with the dinitro-PAC elution window were analyzed by GC-ECD for the three loads collected at high speed (Figure 5.20). There are a great deal of electrophilic compounds present in these HPLC fractions, and the distribution of the compounds for each load position are similar. This may indicate that there are common formation routes occurring to produce the compounds across the load range. At high load the greatest abundance of compounds are evident. This provides further evidence that high speed and high load favour combustion generation of secondary nitro-PAC. However, co-injection techniques could not find any dinitro-PAC. The dinitro-PAC levels from diesel exhaust are typically much lower than the mononitro-PAC (Nakagawa *et al.* 1983, Williams *et al.* 1986b, and Hayakawa *et al.* 1992). Given the low mononitro-PAC levels found in this study, it may not be surprising that the even with the sensitivity of GC-ECD no dinitro-PAC could be found in the Prima emissions.

The HPLC fractions corresponding to the nitro-oxy-PAC elution window collected at high speed and for the three loads were also analyzed by GC-ECD (Figure 5.21). The fractions also contain a vast amount of electrophilic compounds, again with a degree of similarity at each load, suggesting common origins. No identification of nitro-oxy-PAC were found by co-injection techniques. The ECD detector was very susceptible to becoming contaminated by the nitro-oxy-HPLC fractions.

### 5.3 Oxy-PAC Emissions

The excess air and high temperatures present in diesel combustion enables primary PAC emissions, such as fluorene, to be converted into oxy-PAC derivatives, in the case of fluorene, resulting in the formation of primarily fluoren-9-one. It has been proposed that some oxy-PAC may be responsible for significant mutagenic contributions to diesel extracts (Scheepers & Bos 1992a). In an attempt to gain further information on the potential of diesel combustion to generate oxy-PAC at different engine conditions, the oxy-PAC HPLC fractions and the polar fractions from the silica gel clean-up were analyzed by GC/MS in the EI mode (Section 3.4.3.2).

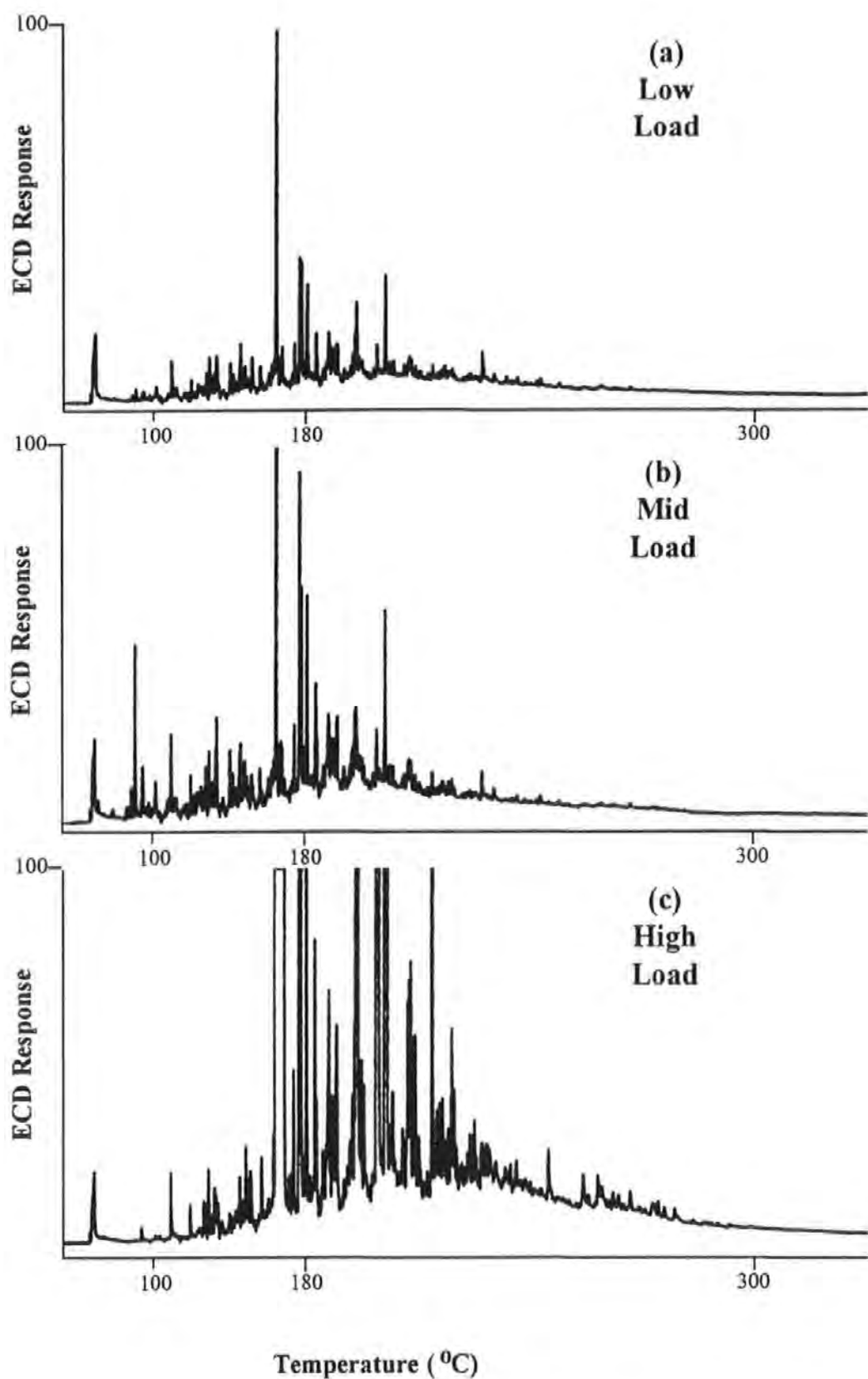


Figure 5.20 The gas chromatographic analysis of the dinitro-PAC HPLC fractions collected at 3500 rpm and a) low load, b) mid load, and c) high load by gas chromatography with electron capture detection (Chromatographic conditions given in Section 3.4.3.1.4.2).

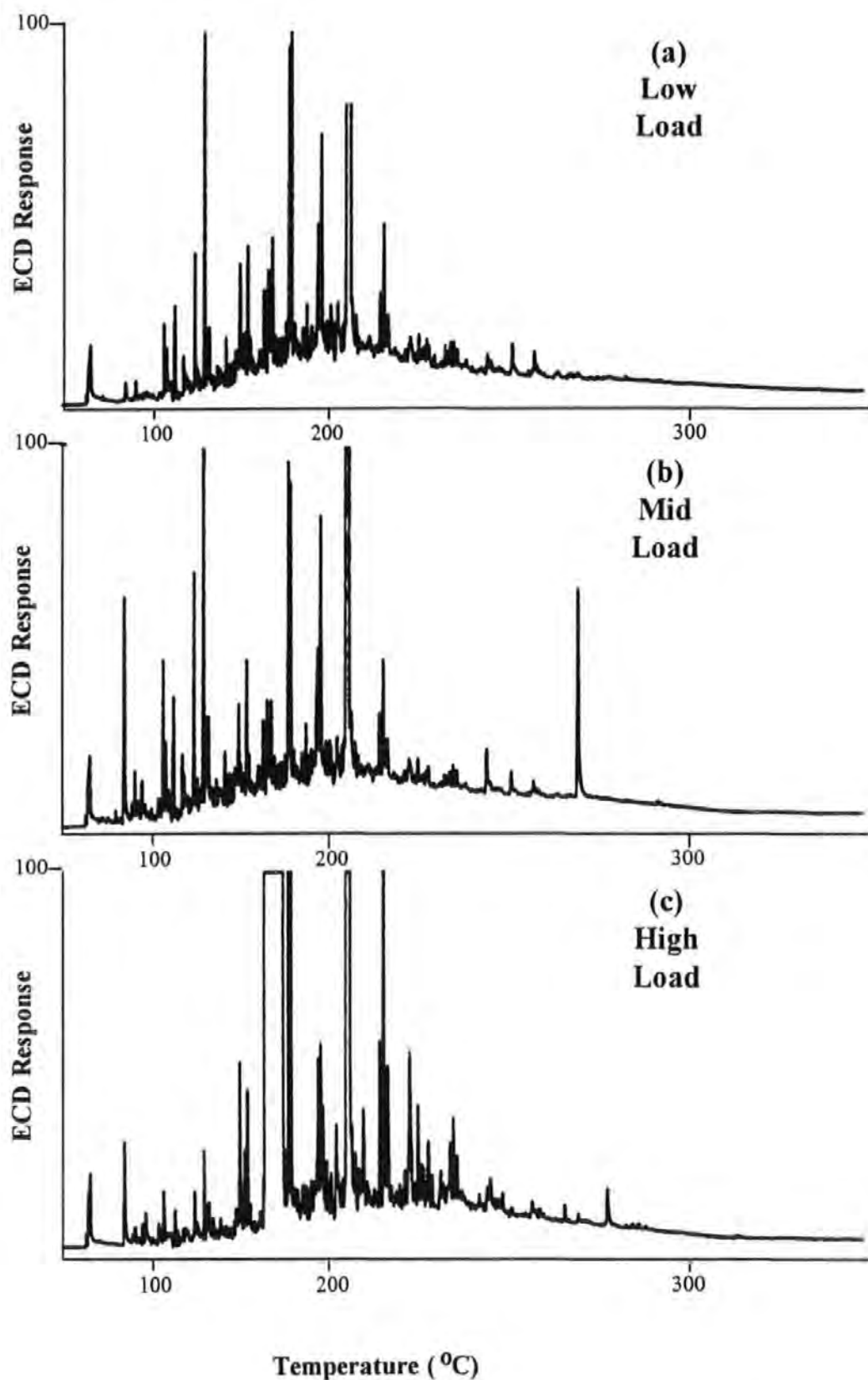


Figure 5.21 The analysis of the nitro-oxy-PAC HPLC fractions collected at 3500 rpm and a) low load, b) mid load, and c) high load by gas chromatography with electron capture detection (Chromatographic conditions given in Section 3.4.3.1.4.3).

In order to obtain a preliminary appraisal of the effect of engine conditions, the oxy-PAC HPLC fractions corresponding to 1500 rpm and low load were compared with the same fractions obtained at 3500 rpm and high load (Figure 5.22). The analysis shows few major peaks between the retention index markers. Presently, no identifications of the larger peaks have been ascertained. However, there is little difference between the two extremes of engine conditions. The preliminary profiles suggest that the pathways which lead to oxy-PAC and polar PAC formation are at least similar across many engine conditions. The exact structures and levels of compounds under different engine conditions requires further work, possibly using LC/MS (Galceran & Mayona 1994) or LC/GC (Kelly *et al.* 1992); techniques more suited to the more polar oxy-PAC.

The comparison of the polar methanol fractions from the silica gel clean-up at low and high engine power also shows a series of small peaks, with a few prominent ones interspaced between the retention index markers (Figure 5.23). There appears to be some matching of peaks between the two samples, suggesting that the compounds are derived from similar pathways. As for the oxy-PAC HPLC fractions, no firm identifications have yet to be made, and further analysis by LC/MS or LC/GC would be useful.

**Key**

Retention Index markers:

A = Naphthalene

C = Chrysene

B = Phenanthrene

D = Benzo(ghi)perylene

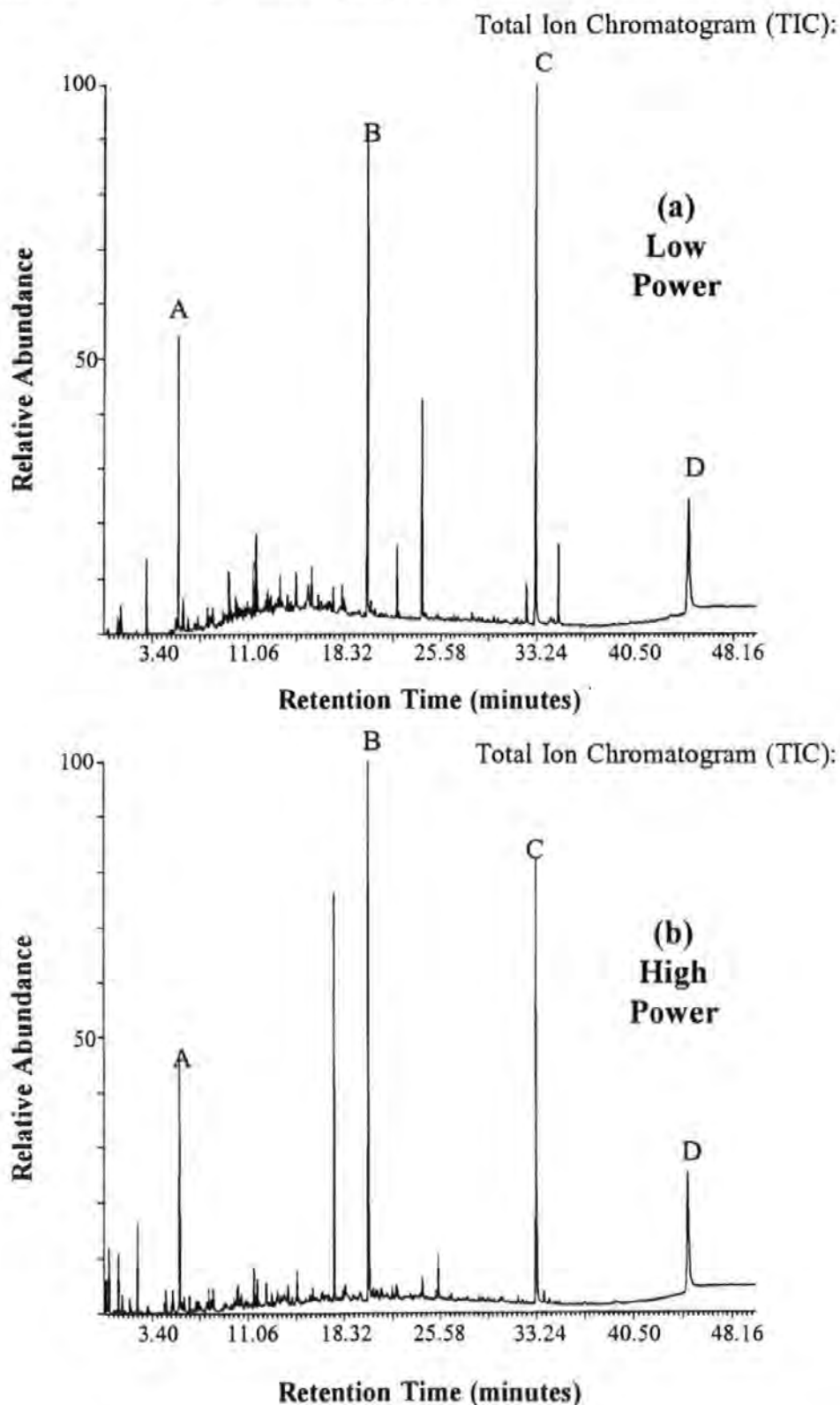


Figure 5.22 The analysis of the oxy-PAC HPLC fractions of TES collected at low engine power (a) and high engine power (b) by gas chromatography/mass spectrometry operated in the electron impact mode (Chromatographic conditions given in Section 3.4.3.2).

## Key

Retention Index markers:

A = Naphthalene

B = Phenanthrene

C = Chrysene

D = Benzo(ghi)perylene

Total Ion Chromatogram (TIC):

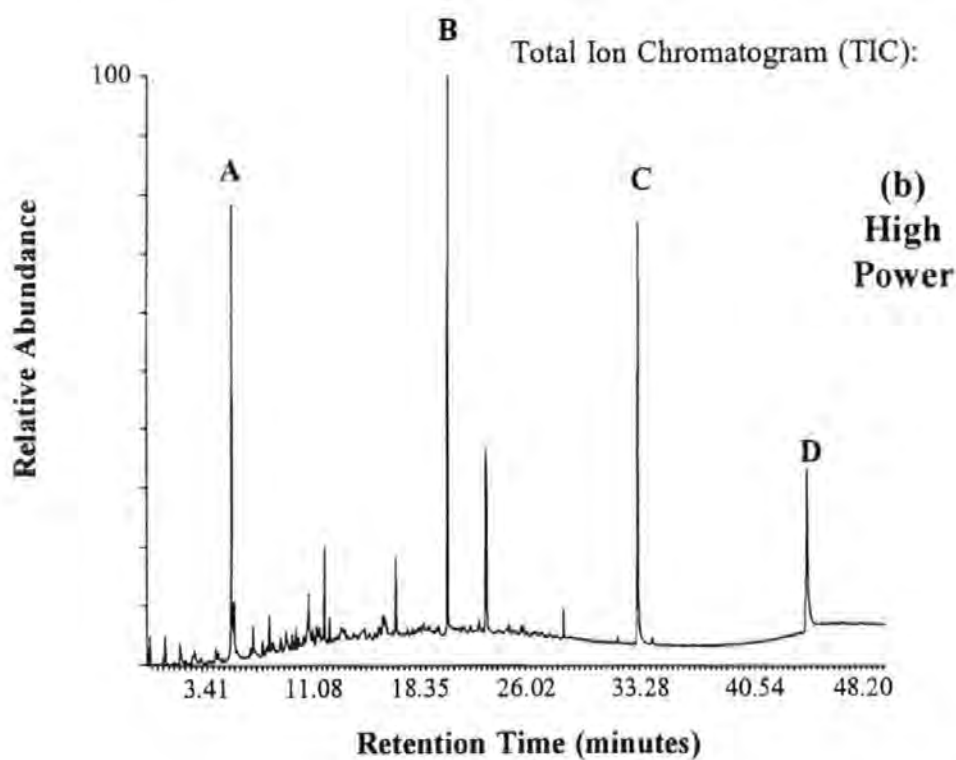
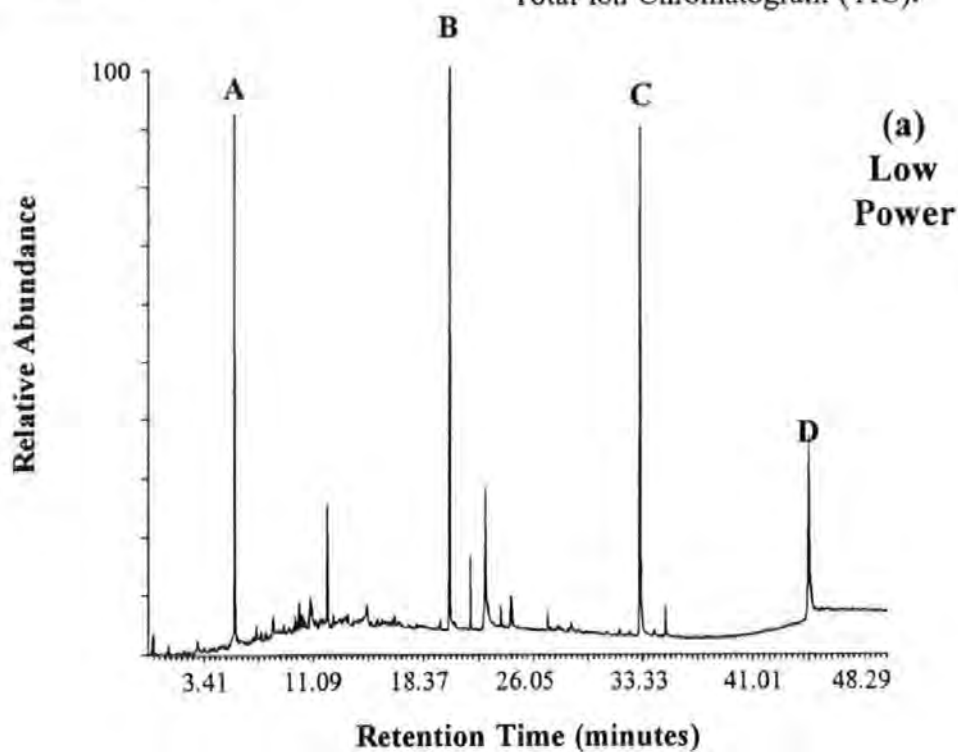


Figure 5.23 The analysis of the polar fractions from the silica gel clean-up of TES collected at low engine power (a) and high engine power (b) by gas chromatography/mass spectrometry operated in the electron impact mode (Chromatographic conditions given in Section 3.4.3.2).

#### 5.4 Summary of Findings for Secondary Nitro- and Oxy-PAC Emissions

- 1) Transformation of primary organic emissions to secondary emissions occurs in the combustion chamber. Mononitro-PAC were present in TES but not in the fuel nor oil.
- 2) Mononitro-PAC were found at low levels for all exhaust samples, analysed by GC-ECD and GC/MS NICI. The levels were much lower than those found with dilution tunnel sampling systems and as reported in the literature. This may mean that dilution tunnel/filter sampling results in enhanced nitration as a consequence of greater air dilution. Alternatively, the dilution tunnel sampling technique does not replicate the tailpipe and environment processes and instead leads to high nitro-PAC by artefact processes.
- 3) The GC/MS NICI results indicate that a proportion of the fuel after combustion undergoes nitration resulting in the exhaust distribution of the nitro-PAC derivatives similar to the PAH precursors in the fuel.
- 4) Different profiles of nitro-PAC with respect to engine load are found under varying speed regimes. Hence, it is not sufficient to rely on specific engine sampling positions to establish the processes controlling nitration reactions. In this study a full range of speeds and loads has for the first time been achieved for a light-duty diesel engine.
- 5) The concentration of mononitro-PAC at low- and mid-speeds did not correlate with gaseous  $\text{NO}_x$  concentrations. High speed resulted in an increase in the mononitro-PAC and  $\text{NO}_x$  concentrations with engine load, possibly indicating that the nitration is dependant on high temperature reactions, such as those involved with free radical reactions.
- 6) In terms per gram of fuel burned the highest nitro-PAC emissions were at low load under low engine speed, as were the PAH emissions. Hence, the conditions at low loads and low speed favour low temperature interactions of  $\text{NO}_2$ , in the presence of nitric acid, *via*  $\text{NO}_2^+$ , and PAH that have survived to the exhaust.



7) At high load and high speed, the formation of 1-nitropyrene is enhanced by the pyrene mass being increased, possibly through pyrosynthetic processes. The peak of 1-nitronaphthalene and  $\text{NO}_x$  at around 30% of full load suggest that free radical processes may be enhanced for 1-nitronaphthalene at these engine conditions. Hence, the high temperature environment at high speed and high load encourages free radical nitration reactions.

8) The analysis of the dinitro- and nitro-oxy-HPLC fractions by GC-ECD could not find any evidence for the presence of such compounds. The profiles at low-, mid-, and high-loads for the top speed of 3500 rpm were similar for both sets of dinitro- and nitro-oxy-PAC HPLC fractions. This shows that similar reactions may be occurring across the load range at high speed. Further analysis by GC/MS NICI may enable identifications of other such structures.

9) The preliminary search for oxy-PAC failed to make any positive identifications of structures. The profiles were similar at low and high engine power settings, suggesting that the pathways to polar PAC may be similar for both power settings. Further analysis is required, possibly using LC/MS.

## **Chapter 6-Final Discussions, Conclusions, & Future Work**

This chapter is divided into discussing the major findings from both the primary and secondary emission chapters (Section 6.1), listing the overall conclusions of the work (Section 6.2), and finally suggesting future work (Section 6.3).

### **6.1 Final Discussions**

The main purpose of this research was to produce emissions maps of specific classes of organic compounds for a range of speeds and loads. Emissions maps provide useful information for engineering and fuel companies alike. Such information will become increasingly important if legislation requires specific chemical criteria to be established over a range of speed and load test conditions before awarding engine certification.

The emission profiling was performed on a relatively modern naturally aspirated Perkins Prima DI light-duty diesel engine using the TESSA to sample the emissions close to the combustion chamber. The Prima was sampled for a total of 26 different speeds and loads and the samples characterised for the primary organic emissions and secondary emissions, using two versions of TESSA (Table 6.1).

Table 6.1 Overview of the Emission Profiling Research Programme

Speed (rpm)	Percentage of Full Load	TESSA version	Primary Emissions profiled	Secondary Emissions profiled
1000	1, 25, 50, 75, & 100	Initial	n-alkanes, PAH, PASH, & Alkyl-PAC	-
1000	1, 8, 17, & 25	Upgraded	Fluorene	-
1500	1, 50, & 85	Upgraded	n-alkanes, PAH, PASH, Alkyl-PAC	Nitro-PAC & Oxy-PAC
2000	1, 25, 50, 75, & 100	Initial	n-alkanes, PAH, PASH, & Alkyl-PAC	-
2500	1, 50, & 85	Upgraded	PAH, PASH, Alkyl-PAC	1-Nitropyrene
3000	1, 25, 50, 75, & 100	Initial	n-alkanes, PAH, PASH, & Alkyl-PAC	-
3500	1, 29, & 90	Upgraded	n-alkanes, PAH, PASH, Alkyl-PAC	Nitro-PAC, Oxy-PAC, & polars

Sampling with both the initial and the upgraded TESSA versions was found to be both rapid and reproducible (Sections 3.2.1, 3.3, and 3.4.1). The profiling of the primary organics was successfully achieved with a simple work-up and well established detection systems (Section 3.2). The secondary emissions were focused on the nitro-PAC, for which more complex work-up and specialised detection system were required (Section 3.4). The identification of nitro-PAC by GC-ECD and GC/MS NICI provided detailed quantitative measurements. The technique of reverse phase HPLC with fluorescence/chemiluminescence detection, with on-line pre-column reduction, was proved a valuable future detection technique.

The findings from both the primary PAH and *n*-alkane emissions and the secondary nitro- and oxy-PAC emissions were presented and discussed in Chapters 4 & 5 respectively. The following sections discuss further the major findings from those two chapters and investigate both the wider environmental implications and appropriate control strategies implied from the results. The discussions are divided into those relating to the primary organics (Section 6.1.1) and the secondary organic (Section 6.1.2) emissions.

#### 6.1.1 Primary Organic Emissions

One of the major findings from the primary organic emission profiling was the close resemblance of the aliphatic and aromatic fractions of emissions to those of the same fractions in the diesel fuel (Section 4.1). This provides strong evidence for fuel survival being a major contributory factor in the emissions composition (Andrews *et al.* 1983, Williams *et al.* 1986 & 1989, Barbella *et al.* 1988 & 1989, and Zeijewski *et al.* 1991). The highest levels of survival were associated with low loads, in agreement with previous light-duty DI studies (Andrews *et al.* 1983, Williams *et al.* 1986, Barbella *et al.* 1989, and Zeijewski *et al.* 1991) (Section 4.2.2.). In this study, the highest survivals of all were obtained at low load and low speed. This highlights the engine conditions at which light-duty DI engines are susceptible to poor combustion. Similar conclusions have been reached by a number of other researchers (Mills *et al.* 1984, Yoshida *et al.* 1986, and Assaumi 1992). The reasons for the inefficient combustion at low loads for the DI engine, comes from the low temperatures and insufficient air:fuel interactions. Further evidence that temperature on its own, has a strong effect on the combustion efficiency was illustrated by sampling the Prima with and without engine

conditioning (conditioning normally consists of 1 hour at 3000 rpm and 90 Nm followed by a further fifteen minute conditioning at the sampling position) (Section 4.3.1). The unconditioned sampling resulted in a higher survival of fluorene (1.31%) compared with conditioned sample (0.96%). It follows, that the higher emissions associated with the cold start were a result of the lower combustion chamber temperatures and greater combustion instability (Asou *et al.* 1992). The Earth Resources Research estimated that cold start conditions contributed approximately one third of the total volatile organic compound emissions from passenger cars in 1990 (Holman *et al.* 1993 cited by QUARG 1993).

The predicted rise in passenger diesels in the urban environment (QUARG 1993 and Parliamentary Office of Science & Technology 1994) and the increasing reliance on the DI, rather than IDI fuel injection configurations (Bulmer 1990, Dürnholtz *et al.* 1992, and Belardini *et al.* 1993) may be of significance to the urban environments. The inefficient DI diesel combustion occurs at the low speed and low load stop-start driving associated with congested city centres. The average car journey times in the UK are low with about 40% less than three miles (QUARG 1993). The short journey time would produce relatively higher emissions due to the low temperature existing during such driving periods (Martin and Shock 1989 cited by QUARG 1993). The cold-starting problem is more severe for petrol engines (QUARG 1993), but it follows that for very short trips, emissions from diesel engines would be aggravated by reduced ambient temperatures (Tritthart *et al.* 1993).

The similar recoveries experienced for different PAC and *n*-alkanes at each load position sampled at 1000 rpm, suggested that, for this low speed, the fuel survives combustion largely unchanged (Section 4.2.2). The *n*-alkanes had lower survivals, compared with those PAC with corresponding boiling points, suggesting that the straight chain-*n*-alkane structure is relatively easier to break down than that of the more stable ring PAC structures. The PAC may be supplemented by a greater combustion generation input (Section 4.2.5). Combustion studies using simple aliphatic fuels have been found to result in PAC emissions (Crittenden & Long 1973 and Cole *et al.* 1984). The higher PAC emissions found in this study may be a result of the higher combustibility of the aliphatics, especially in low temperature and oxygen zones needed for complete combustion of aromatics, and also by combustion generation of PAC

involving aliphatic radicals. The extent to which preferential survival and/or combustion chamber reactions contribute to the emissions at different engine conditions might be revealed in further  $^{14}\text{C}$  labelling experiments on the Prima at the University of Plymouth.

The similarity of the emission and fuel profiles means that the fuel composition will have an important role in determining the emissions entering the environment. The primary organic emissions, sampled close to the combustion chamber, found in this study replicate the trends with respect to speed and load as have been found by previous studies. However, there may be changes in the chemical composition of the exhaust further down the exhaust pipe not included in this study. Hayona *et al.* (1985) found that the transfer of combustion formed PAH into the exhaust caused a large decrease in the PAH emitted. By fitting an extended 3 m length of transfer pipe between an IDI Ricardo Hydra and TESSA, Trier (1988) found that the aliphatics were preferentially burned-out compared with the aromatic and polar constituents of fuel surviving combustion. Hence, of the fuel surviving combustion it is the more hazardous PAC which enter the environment compared with the much less harmful *n*-alkanes.

There are many thousands of PAC present in diesel fuel and only a selection of these have been evaluated for their mutagenic and carcinogenic effects (IARC 1989). Of those tested, the methyl-derivatives of fluorene, phenanthrene, anthracene, pyrene, chrysene, and methylbenzo( $\alpha$ )pyrene have been found to be carcinogenic (Melikian *et al.* 1983, IARC 1989, and Scheepers & Bos 1992b). The concentrations of the methyl derivatives of two to four ring PAH are higher in diesel fuels than such carcinogenic PAH as benzo( $\alpha$ )pyrene, and it may be that alkyl-PAH play an important part in the hazard associated with diesel emissions (Scheepers & Bos 1992b). Within each group of methyl derivatives, the precise position of the methyl group on the PAC ring structure is key to the potency of the compound. For example, the bay-regions associated with 5-methylchrysene result in a higher carcinogenic potency than 6-methylchrysene (Melikian *et al.* 1983 and IARC 1989).

By contrast to the poor combustion at low loads, the combustion efficiency was found to be greatest under high loads (Section 4.2.4 & 4.3.2). Similar conclusion have been reached by Andrews *et al.* (1983), Williams *et al.* (1986), Barbella *et al.* (1988), and Zeijewski *et al.*

(1991). Thus the DI system works effectively under high fuelling conditions, such as those encountered with steep gradients. However, in terms of the environment, high loads will result in a higher output of possible mutagens present in the fuel, such as benz( $\alpha$ )pyrene and the mutagenic alkyl-PAH, purely as a consequence of the greater fuel consumption.

The highest combustion efficiencies for organic emissions were associated with mid-speeds, between 2000 rpm and 2500 rpm, for low loads (Section 4.3.3). At higher loads, the effect of speed was minimal. Zeijewski *et al.* (1991) also correlated mid-speeds with the optimum swirl, reaction time, and temperatures for efficient combustion/power to develop. As with high loads, the greater fuel consumption at high speeds would result in the highest output of organics. Thus for high load sections of high-speed motoring, the greatest emissions of all will be produced, but the scope for improvement, in terms of combustion efficiency, is not as great as at low loads.

The large proportion of organic emissions derived from fuel surviving the combustion process and the extent to which different engine conditions affect the extent of the survival is of great significance to control strategies. Firstly, the lowest combustion efficiencies associated with low loads highlight the shortcomings of the Prima fuel injection system. In order to enhance combustion at low loads, a greater air:fuel interaction is required combined with higher temperatures (Dent 1980, Kamimoto *et al.* 1980, Karimi 1989, Walsh & Bradow 1991, & Konno *et al.* 1992b & 1993). Higher fuel injection pressures, increased fuel injector outlets, valve covered orifice injectors, reduced crevice volumes and improved combustion chamber geometry (including more radical designs to encourage turbulence) have all been shown to lower UHC emissions (Ning *et al.* 1991, Walsh & Bradow 1991, Akaska & Tamanouchi 1992, Kobayashi *et al.* 1992, Konno *et al.* 1992b & 1993, and Poulton 1994). It is vital that an integrated approach is adopted, to prevent specific improvements in some emissions at the expense of others. Increasingly, computer technology is being used to control the different systems and control the combustion process, allowing the optimum conditions for the lowest emissions to be achieved at varying engine conditions (Carroll 1991, Walsh & Bradow 1991, Amstutz & Del Re 1992, Bazari & French 1993, Ladommatos *et al.* 1993).

The close resemblance of the UHC emissions and primary organic emissions (Sections 4.2.2 & 4.2.3), may enable a significant reduction of the organic emissions to be achieved through improvements to the Prima engine. With respect to the Prima engine design, recent improvements have included two-stage injectors and turbocharging.

The two-stage injectors were introduced primarily to reduce noise, but may also reduce UHCs as a consequence of less fuel impingement on the chamber walls and improved spray characteristics (Shakal & Martin 1990, Arcoumanis *et al.* 1993, and Konno *et al.* 1993). Abbass *et al.* (1991b) studied the effect of turbocharged and natural aspiration on the organic emissions from a 4 l DI diesel. The authors found similar profiles for both engines, but with higher recoveries of exhaust PAH for the turbo version. This may reflect the higher temperatures and pressures associated with turbocharging, leading to relatively more pyrolysis compared with the naturally aspirated version. The authors point out that, sump oil and exhaust/engine deposits may have been responsible. Following the findings from Abbass *et al.* (1991b) the turbo version of Prima, may reduce overall UHCs whilst promoting specific combustion reactions under certain engine conditions. The effect of the improvements on the combustion of organics could be achieved by comparing the profiles of the up-to-date Prima using TESSA, with those presented in this study (Section 6.3).

The other control strategy that might reduce emissions, derived predominately from fuel survival, is manipulation of the fuel composition. By altering the fuel composition, for example, removing identified mutagenic components, it follows that the emissions would be improved. A great deal of research has attempted to identify the properties of fuels which determine the pollutants (Weaver *et al.* 1986, Yoshida *et al.* 1986, Miyamoto *et al.* 1992, Røj 1992, Naber *et al.* 1993, Ryan & Erwin, 1993, and Stradling *et al.* 1993). One of the major findings from these studies, was the link between particulate emissions and the aromatic content of fuels. Some studies however, dispute this, and propose that the link is a consequence of fuel density (Weidmann *et al.* 1988, Cowley *et al.* 1993, Fløysand *et al.* 1993, and Tritthart *et al.* 1993). The possible link between particulates and fuel aromatics led to the US state of California imposing a 10% upper limit on the aromatic content of diesel fuel, whilst in Sweden there are three specifications: a limit of 5% in class I, 20% in class II, and

25 % in class III (Cooper *et al.* 1993 and Nikanjam 1993). Such limits require substantial changes within the petrochemical industry to enable the hydrotreatment processes, capable of reducing the sulphur and aromatics, to be employed (Weaver *et al.* 1986 and Martin & Bigeard 1992). However, the introduction of new fuel blends enables the benefits to be realised immediately. Improvements in engineering designs take time before the new designs filter down into the car market. Severe changes in fuel composition can cause problems in terms of fuel pumps and associated hardware (Røj 1992 and Noble 1994).

The increased range of percentage recoveries for the different primary organics, such as fluorene compared with pyrene, at specific engine conditions, suggest that fuel survival unchanged is not solely responsible for the emissions. Thus at high speed and low load, it may be that at a greater range of temperatures as well as air:fuel ratios are generated in the chamber (Section 4.2.3). This may lead to some organics surviving relative to others, or alternatively the great range of temperatures may promote combustion chamber reaction pathways. Whether it is preferential survival and/or combustion generation which are favoured at specific engine conditions; improved air:fuel mixing and higher temperatures at low loads may reduce the emissions. A higher overall combustion chamber temperature confined within a narrow temperature gradient would increase the chance that different structures would be combusted to the same extent. Advanced injection would also provide higher temperatures and a greater reaction time, thus reducing UHCs and particulates, but possibly at the expense of higher NO<sub>x</sub> emissions (Zelenka *et al.* 1990 and Zhang *et al.* 1993). For this reason, a computer controlled injection system, which could control not only the precise quantity of fuel injected but also the time at which the injection started, is essential. Such fuel injectors are constantly under development and recently Cummins Ltd. have developed a fuel injector with infinitely variable fuel metering and injection timing for heavy-duty diesel engines (Bunting 1992).

The influence of methyl-derivatives on the environment may be reduced at high speeds and low loads, since under such conditions emissions of the methyl-PAC are lowered relative to the unsubstituted PAC (Section 4.2.6). The overall hazard of the emissions may be reduced at specific engine conditions as a consequence of the reduction in the methyl derivatives, some of which are more hazardous than the non-substituted PAC. The possibility that pyrosynthetic



reactions may be active under such engine conditions may result in the formation of more hazardous compounds. Fuel rich zones combined with the range of temperatures that may exist at low load and high speed may present the optimum conditions for pyrolysis reactions (Burrows & Lindsey 1961, Badger *et al.* 1964, and Tancell *et al.* 1995b). The work of both Burrows & Lindsey (1961) and Badger *et al.* (1964) showed that the greatest pyrolysis products from simple fuels were obtained at a optimum mid-range temperatures.

For instance, Burrows & Lindsey (1961) found that the greatest quantities of naphthalene, acenaphthylene, phenanthrene, pyrene, fluoranthene, anthracene, and coronene were formed at *ca.* 850°C (with temperatures tested ranging from 700°C to 1000°C) for ethylene and *ca.* 1070°C (with temperatures tested ranging from 900°C to 1100°C) for methane flames. The increase in the relatively lower molecular *n*-alkanes relative to the higher weight *n*-alkanes may be evidence for cracking reactions being promoted under such conditions (Nelson 1989). Thus the conditions of high speed and low loads may represent a wide range of temperatures, which allow specific combustion generations to occur to a greater extent than may be possible with the narrow range of temperatures associated with other engine conditions.

The extremes of 3500 rpm and close to full load resulted in a much higher recovery of pyrene relative to the other organics; this provided strong evidence that the high temperature conditions associated with these engine conditions resulted in significant combustion generation of pyrene. At other engine conditions, the yield of pyrene appeared atypical compared with other PAC. The <sup>14</sup>C-pyrene research by Tancell (1995a) has shown that the structure of pyrene is more easily pyrosynthesised than smaller ring PAC. Pyrene may be of significance to the formation of secondary organics emissions, specifically 1-nitropyrene, in the combustion chamber (Section 6.1.2).

The measurement of primary emissions shows that there is a common trend of fuel survival occurring to different extents depending on the temperature, reaction time, and air:fuel interactions associated with different engine conditions. Combustion generation reactions at specific engine conditions may also influence the emissions.

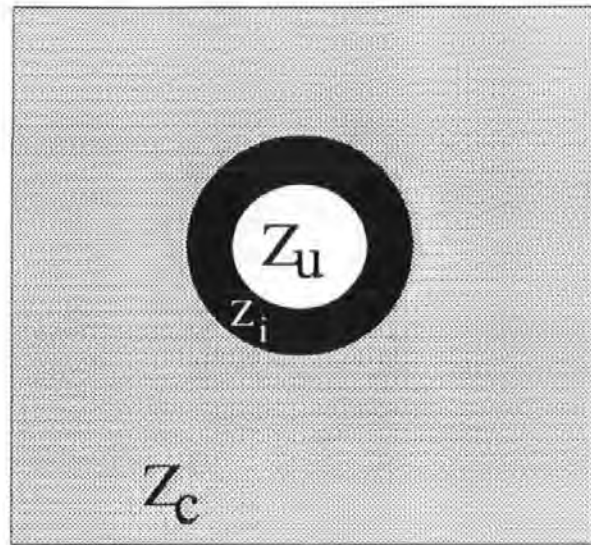
The situation can be shown as in Figure 6.1. By dividing the combustion chamber into different zones of temperature and time the effect of different speeds and loads can be envisaged. Thus at high loads the range of temperatures is narrow and hence compounds either survive in the low temperature zone ( $Z_L$ ) or are completely combusted in the high temperature zone ( $Z_H$ ) (Figure 6.1a). At low loads, a greater range of temperatures may exist in different temperature zones of the chamber, enabling differing combustion efficiencies and combustion reactions to proceed at specific temperatures (Figure 6.1b). The time available for combustion reactions will also effect the emissions, such that higher speeds will reduce the time available for total combustion to occur, thus allowing some compounds to undergo pyrosynthetic reactions rather than complete combustion.

### 6.1.2 Secondary Organic Emissions

The profiling of some of the highly mutagenic and possibly carcinogenic nitro-PAC was the ultimate aim of this study. The results relating to the mononitro-PAC, presented in Chapter 5 are unique in two ways. Firstly, the study covers a greater range of speeds and loads than published to date. Secondly, and more importantly, the study utilises the unique TESSA developed at the University of Plymouth. The close proximity of TESSA to the Prima engine allows the contribution of combustion generation to nitro-PAC emissions to be examined over different engine running conditions.

One of most important findings from the nitro-PAC profiling on the Prima using TESSA, was that the levels of mononitro-PAC emitted (average extract concentration of 1-nitropyrene of 5.3 ppm) were much lower compared with previous studies which relied on dilution tunnel/filter sampling systems (average of 1-nitropyrene in extracts of 627.9 ppm) (Section 5.2.1.3). The lower mononitro-PAC levels shortly after combustion agree with the levels (4.5 ppm of 1-nitropyrene in extract) found by sampling diesel exhaust with a cyclone particulate separator (Li & Westerholm 1994). This implies that extended exposure of primary organics to dilution enhances the formation of nitro-PAC. The increased nitro-PAC emissions found from dilution tunnels may in some cases be a consequence of the artefact potential associated with the filter collection used in such systems. In contrast, the TESSA design minimises the opportunity for artefact formation.

## High Load



Key

$Z_c$  = Complete combustion zone

$Z_i$  = Intermediate combustion zone

$Z_u$  = Unburnt fuel zone

## Low Load & High Speed

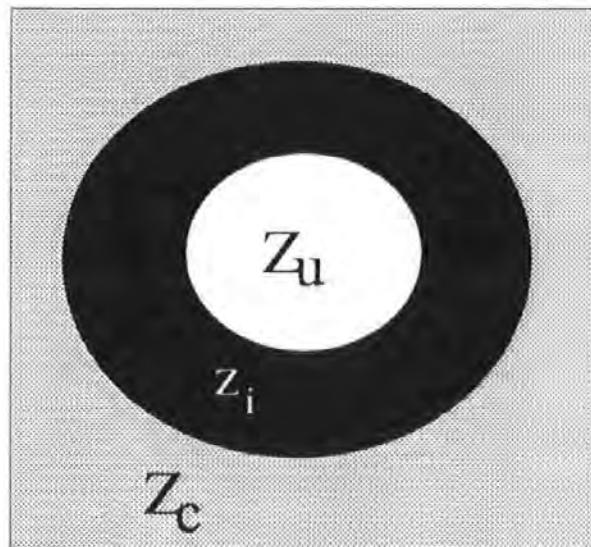


Figure 6.1 Concept of different temperature and time zones necessary for complete combustion. High loads result in the highest temperatures, resulting in a large complete combustion zone ( $Z_c$ ), and a much smaller zone in which fuel survives intact ( $Z_u$ ). The gradient in terms of the temperature and time existing in the intermediate combustion zone ( $Z_i$ ) is narrow. At low load and high speed the unburnt fuel zone is greater and the range of temperatures and time available for combustion is large, enabling preferential survival and/or combustion chamber generation of PAC.

The work-up procedure was also found not to produce artefacts. The nitro-PAC found in this study confirm that such compounds can be formed during combustion. Kittleson and co-researchers (1984) found that 1-nitropyrene was formed in the combustion chamber, but not to the same extent as in the exhaust.

Studies using dilution tunnel sampling have estimated that nitro-PAC can make significant contributions to the direct-acting mutagenicity associated with diesel extracts. For example, Schuetzle (1983) quoted that 66% of the total direct-acting mutagenicity was attributable to seven nitro-PAC. Other studies have put the contribution of 1-nitropyrene on its own, at between 10 to 40% of the total mutagenicity of diesel extracts (Schuetzle *et al.* 1981, Nakagawa *et al.* 1983, Schuetzle & Frazier 1986, & Veigl *et al.* 1994). The levels of 1-nitropyrene found in this study would put the mutagenic contributions significantly lower and more in line with on-road measurements of 1-nitropyrene (Gorse *et al.* 1983). Thus a key question in both terms of the nitro-PAC emissions and the associated mutagenicity centres on whether post-combustion reactions are responsible for nitro-PAC emissions.

The regular profile of nitro-PAC emissions at different speeds and loads suggesting that the conversion of fuel components occurs across a range of engine conditions (Sections 5.1 & 5.1.1) may be significant to controlling nitro-PAC emissions. The similar distributions of the nitronaphthalenes in the emissions compared with the distribution of the naphthalenes in the fuel provides further evidence for the fuel influencing the nitro-PAC emissions (Section 5.2.1.2).

The trends of nitro-PAC with respect to speeds and loads found in this study (Section 5.2.1.4) are comparable with previous findings. For example, at a mid-speed of 2500 rpm the increase in 1-nitropyrene emissions with engine load, followed by a decline at higher loads was also found by Schuetzle & Perez (1983) at 2100 rpm, and by Veigl *et al.* (1994) at 1560 rpm. The two studies also found 1-nitropyrene emissions to be more stable across the load range at lower speeds. Bechtold *et al.* (1984) found 1-nitropyrene to increase with speed, as did the 1-nitropyrene emissions at mid-loads and high loads in this study. Handa *et al.* (1984) found that the 1-nitropyrene emissions in road tunnels were highest at high loads compared with low

loads for a speed of 1800 rpm. A much higher speed of 3500 rpm, produced the highest nitro-PAC at high loads, in this study. There was a correlation between the higher levels of 1-nitronaphthalene at moderate load and high speed compared with high low and moderate speed in this study and that undertaken by Draper (1986).

The correlations are complicated by the studies being based on medium- and heavy-duty engines, whereas this study is based on a light-duty diesel. This may explain why Veigl and co-researchers (1994) found the same 1-nitropyrene emission trends to this study at a lower speed of 1560 rpm, and similarly the road tunnel study by Handa *et al.* (1984) found the same effects as found in this study at high speed, but at a much lower speed of 1800 rpm. However, there remain large discrepancies between some studies. Schuetzle & Perez (1983) found the highest levels of 1-nitropyrene at low load and 700 rpm, whereas Veigl *et al.* (1994) found the lowest emissions at low load and 600 rpm. This may reflect greater artefact contributions at the low temperatures associated with low engine power in the early study, which may not have occurred in the later study (even though no direct evaluation of artefact formation is reported by Veigl *et al.* 1994).

The range of steady state conditions sampled in this study for the light-duty Prima engine are the most comprehensive to date, and allow a greater insight into the nitration process under different driving conditions. The results show that high speed and high load motoring would result in the highest contribution of nitro-PAC to diesel extracts, whereas lower speeds more representative of urban areas, would be relatively enriched by PAH surviving combustion. In terms, of the nitro-PAC emissions emitted per gram of fuel burned, the greatest nitro-PAC would be emitted at low loads for low speeds. At high speed the greatest nitro-PAC emissions would be at higher loads (Section 5.2.1.6).

The correlation between the nitro-PAC, especially 1-nitronaphthalene, and the gaseous NO<sub>x</sub> emissions at 3500 rpm shows that specific engine conditions favoured the nitration reactions (Section 5.2.1.5). At the high speed of 3500 rpm, the associated temperatures may provide sufficient temperatures for the free radical combustion formation of nitro-PAC to proceed. In the case of 1-nitropyrene, a much greater supply of pyrene to the nitration process was

generated at high speed and high load, possibly also as a result of increased pyrosynthetic contributions (Section 4.3.2). The highest emission of 1-nitropyrene at high speed and high load, correlated with the greater pyrene available for nitration. At high engine powers the formation of 1-nitropyrene is controlled by the mass of available pyrene.

Thus the parameters controlling the nitration are the  $\text{NO}_x$ , PAH, and temperatures available at specific engine conditions. The correlation with  $\text{NO}_x$  and also temperature was also made for 1-nitropyrene emissions from a heavy-duty diesel (Bechtold *et al.* 1984). The formation of nitro-PAC by post-combustion reaction of  $\text{NO}_2$  in the presence of nitric acid, involving the nitronium ion, would be favoured at the lower exhaust temperatures associated with low loads and speeds. This arises from both the higher levels of  $\text{NO}_2$  and nitric acid in the exhaust, under low loads and speeds, and the greater primary PAH emissions which also survive combustion (Section 5.2.1.6).

The results from this study suggest two control strategies; firstly by the reduction of the PAH content of the fuel, such as the naphthalenes and pyrene by hydrotreatment, would remove the fuel survival source for nitration at low loads and speeds. There has been relatively little research into establishing whether different fuel blends can reduce nitro-PAC emissions. Saito *et al.* (1982) found higher levels of 1-nitropyrene per mile travelled with high cetane index, low specific gravity, and high top end distillations point fuels. The work of Saito *et al.* also showed that improved fuel injection systems resulted in both reduced overall UHC's and also 1-nitropyrene. Henderson *et al.* (1982, 1983, & 1984) found that a proportion of the fuel underwent nitration, whereas Shore (1986) could find no link between different fuel blends and the emission of 1-nitropyrene. Shore did show that DI engines emit significantly more 1-nitropyrene than the IDI version of the same engine, for most of the fuels tested. For example, testing of the standard US diesel produced  $11.1 \mu\text{g}/\text{hour}$  of 1-nitropyrene for the DI compared with only  $0.78 \mu\text{g}/\text{hour}$  for the IDI. As the author notes this was not attributable to  $\text{NO}_x$ , since the DI typically produced three to four times more  $\text{NO}_x$  than did the IDI.

The increased pyrosynthetic activity associated with the formation of both pyrene and 1-nitropyrene at high speeds may result in fuel measures being ineffective, and under these conditions a second control strategy, employing post-combustion control measures may be

necessary. Post-combustion measures, such as using oxidative catalysts, significantly reduce PAH precursors to nitro-PAH (Andrews *et al.* 1987, Henk *et al.* 1992, Davies *et al.* 1993, Fløysand *et al.* 1993, Zelenka *et al.* 1990, and Zelenka & Herzog 1993).

Research by Veigl *et al.* (1994) showed that oxidative catalysts lowered the emissions of 1-nitropyrene from a light-duty engine over the HWFET and FTP transient test cycles. The authors also found that the addition of fuel additives reduced the 1-nitropyrene emissions. In contrast, the study by Draper *et al.* (1988) found that the addition of a barium fuel additive aimed at suppressing smoke formation, resulted in significant increases of PAC emissions. Scheepers *et al.* (1994) found low levels of 1-nitropyrene emissions from light-duty diesels with oxidation catalysts, however how much of this was a result of the catalyst not possible to determine, since no comparative studies on the same engine without catalysts were performed.

The hardest nitration parameter to reduce is that of  $\text{NO}_x$  emissions. This is due to  $\text{NO}_x$  emissions being related to the peak temperature outputs, and hence the combustion efficiency itself (Fenn 1982). However, retardation of fuel injection using computer controlled systems can lower  $\text{NO}_x$  levels without causing other pollutants, typically particulates to rise. Schuetzle & Perez (1986) showed that retarding fuel injection reduced not only  $\text{NO}_x$  but also the level of 1-nitropyrene emitted. Pilot injection has also been found to lower  $\text{NO}_x$  emissions (Shakal & Martin 1990). Another method used to reduce  $\text{NO}_x$  is to re-circulate and mix the exhaust gases with the fresh inlet air going into the combustion chamber, a technique known as exhaust gas recirculation (EGR). The  $\text{NO}_x$  is reduced as a consequence of lower temperatures and reduced oxygen levels (Amstutz & Del 1992 and Dürnholtz *et al.* 1992). As with fuel injection retardation, an integrated approach would be needed so as not to increase particulates and UHC's. Veigl *et al.* (1994) found that EGR reduced the levels of 1-nitropyrene over the high temperature HWFET cycle but reduced much less the 1-nitropyrene emissions (and in one case the EGR actually resulted in higher 1-nitropyrene emissions) over the more varied and generally lower speed FTP cycle. This supports the idea that there are two modes of nitration, one favoured at high temperatures and the other at lower temperatures. Hence, EGR reduced the overall combustion temperatures, and in so doing increased the lower temperature  $\text{NO}_2$  & associated  $\text{HNO}_3$  nitration mechanism, whilst limiting combustion chamber nitrations.

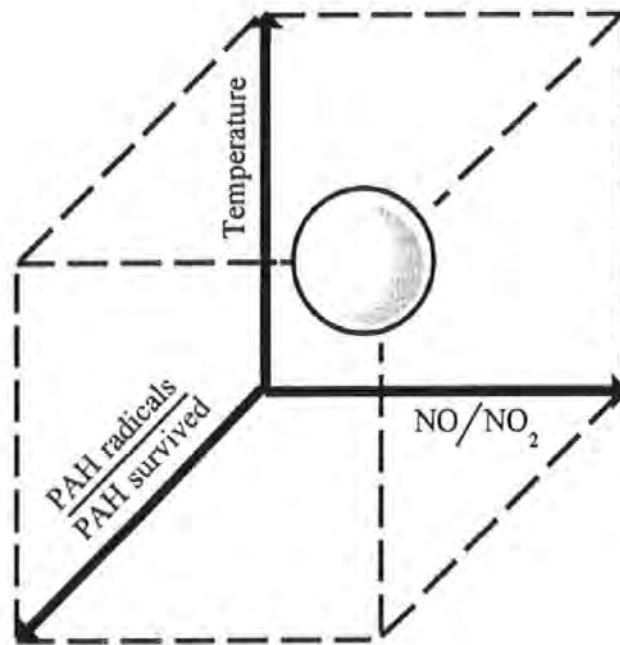
Specially designed combustion chambers such as the combustion chamber for disturbance (CCD) described by Konno *et al.* (1993) can be used to simultaneously reduce NO<sub>x</sub> and particulates by two stage combustion; in a much more controlled way than is feasible with fuel injection retardation. The NO<sub>x</sub> levels may also be reduced by reductive catalysts, commonly using copper ion-exchanged zeolites, which can reduce NO<sub>x</sub> even in the presence of oxygen (Konno *et al.* 1992a).

The realisation that reduction catalysts in diesel engines require enhancing the hydrocarbon input to the exhaust (thus requiring an additional oxidative catalyst) for the reaction to proceed, and the narrow reduction operating temperatures, has led to investigating selective non catalytic reduction (SNCR) or thermal deNO<sub>x</sub> techniques (Andrews & Gibbs 1993). The process uses chemical injections of gaseous HNCO or ammonia to react with NO (the major constituent of NO<sub>x</sub>) to form nitrogen, water, and in some cases carbon dioxide (Andrews & Gibbs 1993). The extent to which NO<sub>x</sub> reductions achieved by employing novel combustion chamber designs, reductive catalysts, and SNCR effect the levels of nitro-PAC remains uncharted work.

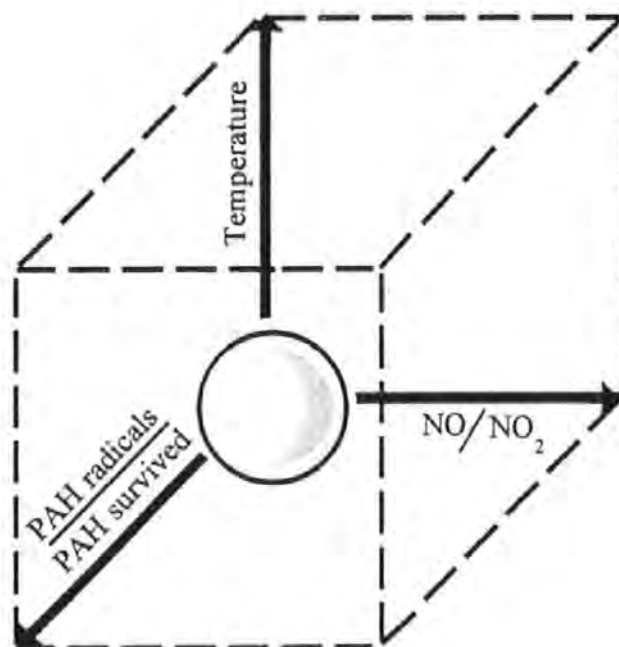
It is important to point out that diesel engines are not the only source of nitro-PAC emissions in the atmosphere. Nitro-PAC can also be formed by atmospheric reactions with primary organics, such as pyrene (Pitts 1985, Arey 1986 & 1987, Atkinson 1987a,b, & c, 1990a&b, Zeilinska *et al.* 1989a&b, Helmig *et al.* 1992, Ciccioli *et al.* 1993). These reactions form isomers of nitro-PAC not produced by diesels, for example 2-nitropyrene. However, since diesel engines in the urban environment will be in close proximity to human biological systems the direct emissions of nitro-PAC will be important over the limited time that such compounds can exist in the environment (Benson *et al.* 1981 and Stärk *et al.* 1985). Furthermore, the fact that diesel engines are responsible for a large proportion of the primary organic emissions in the atmosphere, necessitates measures which help to alleviate not only the nitration associated with diesels, but also later atmospheric reactions.

In a similar approach to the combustion of primary emissions, the formation of nitro-PAC can be described in terms of nitration zones, in which nitration is favoured under specific temperatures and where specific organic species are available for reaction (Figure 6.2).





(a)



(b)

Figure 6.2 Two zone nitration concept, such that the free radical combustion generation of nitro-PAC is favoured at high loads and high speeds (a), whereas electrophilic substitution of surviving PAC is favoured at low loads and low speeds (b).

It may be the case, that there are two types of zones which favour the proposed two modes of nitration. The first zone relates to high temperature combustion generation of nitro-PAC, in which the greatest PAH radicals and  $\text{NO}_x$  radicals exist (Figure 6.2a). The second zone corresponds to lower temperature  $\text{NO}_2$  and  $\text{HNO}_3$  interactions with unburnt fuel, which would be favoured by higher  $\text{NO}_2$  and PAH survivals (Figure 6.2b). These two types of nitration zones will be encountered at the extremes of engine power, ie. combustion generation favoured at high powers compared with  $\text{NO}_2$  &  $\text{HNO}_3$  at low powers.

## 6.2 Conclusions from research

1) The design of TESSA minimises the opportunity for artefact formations, and by employing rapid reproducible sampling a large range of engine conditions may be used on the same day. The profiling of organic emissions from the combustion chamber over a wide range speeds and loads is suited to TESSA, especially for trace nitro-PAC emissions.

2) The profiling of the primary PAH and  $n$ -alkane emissions showed that low loads result in the greatest carry over of fuel components to the exhaust stream, whereas the greatest combustion efficiencies were at high loads. The engine conditions associated with urban congested driving are those which require the greatest increase in combustion improvements. The optimum conditions for combustion at low loads would be assigned to a mid-speed of around 2000 rpm to 2500 rpm. The highest emission concentrations are at high loads and high speeds, but these are a consequence of the greater fuel consumption not poor combustion.

3) Significant improvements in primary emissions may be achieved by increasing the air utilization and combustion chamber temperatures in an integrated approach. A strong correlation with the fuel PAC input and PAC output may enable fuel modifications to be employed to reduce organics emissions. Greater combustion may give rise to increased pyrosynthetic/pyrolysis reactions. The conditions for complete combustion are favoured by a narrow band of high temperatures. A large range of temperatures, termed as a gradient, as may exist at low load and high speed, enables a range of combustion efficiencies to arise, as well as specific combustion reactions.

4) The wide variations in the recovery of different organic structures at low load and high speed, indicate pyrolysis reactions involving alkyl-PAC and pyrolytic cracking of larger  $n$ -alkanes into smaller units may be favoured. The much higher recovery of pyrene compared with naphthalene, fluorene, dibenzothiophene, and phenanthrene at high speed and high load is strong evidence for combustion generation of pyrene. The possible pyrolysis and cracking reactions are associated with the lower range of temperatures at low load, whereas the formation of pyrene is favoured by the extreme temperatures associated with high engine power.

5) Highly mutagenic nitro-PAC are produced during the combustion of standard diesel fuel, and the formation occurs over a range of speeds and loads. The much lower levels of nitro-PAC found from the combustion chamber sampled using TESSA compared with dilution tunnel/filter engine sampling, indicates that post-combustion reactions increase nitro-PAH, some of which may be artefacts formed on the filter.

6) Different speed regimes result in different relationships of the nitro-PAC emissions with engine load. High speed and high load motoring results in the highest contribution of nitro-PAC to the emissions and also highest output of nitro-PAC per gram of fuel burned. By contrast, at low speeds, associated with urban areas, the highest nitro-PAC per gram of fuel consumed is produced at low loads, where the diesel extracts are enriched by PAH surviving combustion.

7) Nitration can be formed in the engine by two pathways. Each pathway is favoured at a particular engine regime. Firstly, combustion generation of nitro-PAH is enhanced at high loads and high speeds where high chamber temperatures favour free radical combustion reactions forming both nitro-PAC precursors, such as pyrene, and the nitro-PAC. Secondly, low loads enable nitrogen dioxide and associated nitric acid to nitrate PAC, surviving combustion late, in the expansion and initial exhaust stages.

8) The close association between the fuel and the nitro-PAC emissions, presents a control strategy for nitro-PAC emissions based on improving combustion of the primary emissions or alternatively by lowering the aromatic precursors to nitro-PAC in the fuel. Combustion generation of nitro-PAC may necessitate post-combustion measures, including innovative techniques to reduce the important role of the oxides of nitrogen in the nitration reactions.

### **6.3 Future Research Proposals**

- 1) The engine test facilities now allow comparison between different engine specifications, for example the influence of different fuel injectors on the PAC emissions could be assessed. The facilities could be used to compare the organic profiles from the up-to-date Prima with that of the profiles presented in this study. In this way, the degree to which engineering developments, such as turbocharging and two-stage injectors, reduce organic emissions could be verified.
  
- 2) The nitro-PAC HPLC fractions contains many compounds of that class. Further analysis of nitro-PAC using gas chromatography with electron capture detection and gas chromatography/mass spectrometry operated in the negative ion chemical ionisation mode would enable a greater range of nitro-PAC to be studied. High-performance liquid chromatography with fluorescence/chemiluminescence detection should be developed to allow rapid screening of the HPLC fractions. The technique was hindered by the unreliable zinc reductive columns. Future research would be greatly improved by employing on-line catalytic reduction of nitro-PAC. Using these techniques and engine sampling with TESSA, further assessment of the nitration of PAC under high and low engine powers could proceed. The role of nitrogen containing PAC in the fuel to the formation of nitro-PAC would be of great interest.
  
- 3) Varying of the transfer line between the engine and TESSA would enable the role of post-combustion reactions to be determined. The ultimate design would incorporate a mini-dilution tunnel with TESSA in series, ie. TESSA as the collector instead of the filter. Such a system would enable a direct comparison of both forms of engine sampling, and associated artefact contributions.
  
- 4) Running the engine on fuel blends of varied PAH content would enable the effect of the fuel matrix on nitro-PAH to be determined. Such a study conducted with TESSA would enable the combustion chamber contribution to the nitro-PAC for different fuels to be established for the first time.

5) Enrichment of PAH components, such as pyrene, of low aromatic fuels, with specific PAH precursors to nitro-PAC, such as pyrene, would enable the range of nitration products to be established. Similarly, combustion of radiolabelled precursors to nitro-PAH followed by isolation of the specific radioactive compounds would provide information on the degree of nitration induced from one precursor. Such experimentation would require large amounts of radiolabelled precursor or alternatively combining of consecutive runs.

6) The high mutagenicity that may be attributable to the more polar constituents of the emissions, requires further research with the aim of detailed characterization and profiling the effects of combustion over a range of speeds and loads on polar PAC production. The volatility problems associated with the more polar fractions and the complexity therein, requires LC detection systems, such as LC/MS. Parallel to the chemical characterisation, a biological assessment of the identified PAC is essential, if the role of the more hazardous PAC is to be understood.

## Literature Cited

- Abbass, M.K., Williams, P.T., Andrews, G.E., & Bartle, K.D. (1987) The aging of lubricating oil, the influence of unburnt fuel and particulate SOF contamination. *Society of Automotive Engineers*. 872085.
- Abbass, M.K., Andrews, G.E., Williams, P.T., Bartle, K.D., Davies, I.L., & Tanui, L.K. (1988) Diesel particulate emissions: pyrosynthesis of PAH from hexadecane. *Society of Automotive Engineers*. 880345.
- Abbass, M.K., Andrews, G.E., Kennion, S.J., Williams, P.T., & Bartle, K.D. (1991a) The survivability of diesel fuel components in the organic fraction of particulate emissions from an IDI diesel. *Society of Automotive Engineers*. 910487.
- Abbass, M.K., Andrews, G.E., Ishaq, R.B., Williams, P.T., & Bartle, K.D. (1991b) A comparison of the particulate composition between turbocharged and naturally aspirated DI diesel engines. *Society of Automotive Engineers*. 910733.
- Aceves, M. & Grimalt, J.O. (1993) Seasonally dependent size distributions of aliphatic and polycyclic aromatic hydrocarbons in urban aerosols from densely populated areas. *Environmental Science & Technology*. 27, 2896-2908.
- Akasaka, Y. & Tamanouchi, M. (1992) Effect of fuel properties on the performance of DI diesel engine with fuel jet impingement. *Society of Automotive Engineers*. 922213.
- Alatas, B., Pinson, J.A., Litzinger, T.A., & Santavicca, D.A. A study of NO and soot evolution in a DI diesel engine via planar imaging. *Society of Automotive Engineers*. 930973.
- Alkidas, A.C. (1984) Relationships between smoke measurements and particulate measurements. *Society of Automotive Engineers*. 840412.
- Amann, C.A., Stivender, D.L., Plee, S.L., & MacDonald, J.S. (1980) Some rudiments of diesel particulate emissions. *Society of Automotive Engineers*. 800251.
- Amann, C.A. & Siegl, D.C. (1982) Diesel particulates - what they are and why. *Aerosol Science and Technology*. 1, 73-101.
- Amann, C.A. (1993) Technical options for energy conservation and controlling environmental impact in highway vehicles. *International Journal of Vehicle Design*. 14 (1), 59-77.
- Amstutz, A. & Del Re, L. (1992) EGR feedback control on a turbocharged DI diesel engine. *Institute of Mech Engineers*. C448/003, 83-88.
- Andoh, H. & Shiraishi, K. (1986) Influence on injection and combustion phenomena by elimination of hole nozzle sac volume. *Society of Automotive Engineers*. 860416.

Andrews, G.E., Iheozor-Ejiofor, I.E., Pang, S.W., & Oeapipatanakul, S. (1983) Unburnt hydrocarbon and polynuclear hydrocarbon emissions and their relationship to diesel fuel composition. *Institute of Mechanical Engineers*. C73/83, 63-74.

Andrews, P.A., Bryant, D., Vitakunas, S., Gouin, M., Anderson, G., McCarry, B.E., Quilliam, M.A., & McCalla, D.R. (1983) Metabolism of nitrated polycyclic aromatic hydrocarbons and formation of DNA-adducts in *Salmonella typhimurium*. Cooke, M. & Dennis, A.J. (Editors) *Polynuclear aromatic hydrocarbons: formation, metabolism and measurement*. 89-98.

Andrews, G.E. (1986) Diesel particulates: an introduction to factors that influence their production and occurrence. *A Short Course on Diesel Particulates*. University of Leeds, 22-24 April, Chapter 1.

Andrews, G.E., Iheozor-Ejiofor, I.E., & Pang, S.W. (1987) Diesel particulate SOF emissions reduction using an exhaust catalyst. *Society of Automotive Engineers*. 870251.

Andrews, G.E. & Gibbs, B.M. (1993) Chemical non-catalytic deNO<sub>x</sub>. *Institute of Mechanical Engineers Seminar: Worldwide engine emissions and how to meet them*. 137-153.

Aoyagi, Y., Kamimoto, T., Matsui, Y., & Matsuoka, S. (1980) A gas sampling study on the formation processes of soot and NO in a DI diesel engine. *Society of Automotive Engineers*. 800254.

Arcoumanis, C. (1992) Measurement and prediction of transient NO<sub>x</sub> emissions in DI engines. *Institute of Mechanical Engineers*. C448/039, 97-105.

Arcoumanis, C., Chang, J.-C., & Morris, T. (1993) Spray characteristics of single- and two-spring diesel fuel injectors. *Society of Automotive Engineers*. 930922.

Arey, J., Zielinska, B., Atkinson, R., Winer, A.M., Ramdahl, T., & Pitts, J.N., Jr. (1986) The formation of nitro-PAH from the gas-phase reactions of fluoranthene and pyrene with the OH radical in the presence of NO<sub>x</sub>. *Atmospheric Environment*. 20 (12), 2239-2345.

Arey, J., Zielinska, B., Atkinson, R., & Winer, A.M. (1987) Polycyclic aromatic hydrocarbon and nitroarene concentrations in ambient air during a wintertime high-NO<sub>x</sub> episode in the Los Angeles basin. *Atmospheric Environment*. 21 (6), 1437-1444.

Assaumi, Y., Shintani, M., & Watanabe, Y. (1992) Effects of fuel properties on diesel engine exhaust emission characteristics. *Society of Automotive Engineers*. 922214

Asou, Y., Fujimoto, H., Senda, J., Tsurutani, K., & Nagae, M. (1992) Combustion in a small DI diesel engine at starting. *Society of Automotive Engineers*. 920697.



Atkinson, R., Arey, J., Zielinska, B., Pitts, J.N., Jr., & Winer, A.M. (1987a) Evidence for the transformation of polycyclic organic matter in the atmosphere. *Atmospheric Environment*. 21 (10), 2261-2264.

Atkinson, R. & Aschmann, S.M. (1987b) Kinetics of the gas-phase reactions of alkyl naphthalenes with  $O_3$ ,  $N_2O_5$  and OH radicals at  $298 \pm 2$  K. *Atmospheric Environment*. 21 (11), 2323-2326.

Atkinson, R., Arey, J., Zielinska, B., & Aschmann, S.M. (1987c) Kinetics and products of the gas-phase reactions of OH radicals and  $N_2O_5$  with naphthalene and biphenyl. *Environmental Science Technology*. 21, 1014-1022.

Atkinson, R., Arey, J., Zielinska, B., & Aschmann, S.M. (1990a) Kinetics and nitro-products of the gas-phase OH and  $NO_3$  radical-initiated reactions of naphthalene- $d_8$ , fluoranthene- $d_{10}$ , and pyrene. *International Journal of Chemical Kinetics*. 22, 999-1014.

Atkinson, R., Tuazon, E.C., & Arey, J. (1990b) Reactions of naphthalene in  $N_2O_5$ - $NO_3$ - $NO_2$ -air mixtures. *International Journal of Chemical Kinetics*. 22, 1071-1082.

Badger, G.M., Kimber, R.W.L., & Novotny, J. (1964) The formation of aromatic hydrocarbons at high temperatures. XXI: The pyrolysis of n-butylbenzene over a range of temperatures from 300°C to 900°C at 50°C intervals. *Aust. J. Chem.* 17, 778-786.

Ball, D.J. (1982) Smoke from diesel vehicles - is it time for mass-based emission standard? *National Society for Clean Air*. 12 (2), 1-4.

Ball, D. (1987) Black lungs and black wall. *New Scientist*. Feb 12, 28-29.

Barbella, R., Bertoli, C., & Ciajolo, A., & D'Anna, A. (1988) Soot and unburnt liquid hydrocarbon emissions from diesel engines. *Combustion Science and Technology*. 59, 183-198.

Barbella, R., Ciajolo, A., & D'Anna, A. (1989) Effect of fuel aromaticity on diesel emissions. *Combustion and Flame*. 77, 267-277.

Bayona, J.M., Markides, K.E., & Lee, M.L. (1988) Characterization of polar polycyclic aromatic compounds in a heavy-duty diesel exhaust particulate by capillary column gas chromatography and high-resolution mass spectrometry. *Environmental Science & Technology*. 22, 1400-1447.

Bazari, Z. & French, B.A. (1993) Performance and emissions trade-offs for a HSDI diesel engine - an optimization study. *Society of Automotive Engineers*. 930592

Bechtold, W.E., Dutcher, J.S., Mokler, B.V., Lopez, J.A., Wolf, I., Li, A.P., Henderson, T.R., & McClellan, R.O (1984) Chemical and biological properties of diesel exhaust particles collected during selected segments of a simulated driving cycle. *Fundamental Applied Toxicology* 4, 370-377.

Beck, J.N, Uyehara, O.A., Prof. Emeritus, & Johnson, W.P. (1988) Effects of fuel injection on diesel combustion. *Society of Automotive Engineers*. 880299.

Beland, F.A., Heflich, R.H., Howard, P.C., & Fu, P.P. (1985) The in vitro metabolic activation of nitro polycyclic aromatic hydrocarbons. Harvey, R.G. (Editor). *Polycyclic hydrocarbons and carcinogenesis*. 371-396.

Belardini, P., Bertoli, C., Del Giacomo, N., & Iorio, B. (1993) Combustion and pollutant emissions from light duty diesel engines: the influence of mixing process and transient operating conditions. *The Science of the Total Environment*. 134, 285-293.

Benson, J.M., Brooks, A.L., Cheng, Y.S., Henderson, T.R., & White, J.E. (1981) Environmental transformation of 1-nitropyrene on glass surfaces. Bjorseth, A. & Dennis, A.G. (Editors) *Polynuclear Aromatic Hydrocarbons*. 77-85.

Benson, J.M., Brooks, A.L., Cheng, Y.S., Henderson T.R., & White, J.E. (1984) Cooke, M. & Dennis, A. (Editors) *Polynuclear Aromatic Hydrocarbons: Chemistry, characterization and carcinogenesis*. 77-85.

Bjorseth, A.C. (1983) *Handbook of Polycyclic Aromatic Hydrocarbons*. Marcel Dekker.

Boone, P.M. & Macias, E.S. (1987) Methyl alkanes in atmospheric aerosols. *Environmental Science & Technology*. 21 (9), 903-909.

Bradow, R.L., Zweidinger, R.B., Black, F.M., & Dietzmann, H.M. (1982) Sampling diesel engine particle and artifacts from nitrogen oxide interaction. *Society of Automotive Engineers*. 820182.

Braithwaite, A. & Smith, F.J. (1985) *Chromatographic Methods*. Chapman and Hall.

Brown, K.K. & Poole, C.F. (1984) Determination of 1-nitropyrene by thin-layer chromatography in a diesel exhaust particulate extract. *Journal of High Resolution Chromatography & Chromatography Communications*. 7, 520-524.

Bulmer, C. (1990) Towards 2000:- how future engines might be developed for the environment. *Automotive Engineer*. 15 (4), 42-44.

Bundt, J., Herbel, W., Steinhart, H., Franke, S., & Francke, W. (1991) Structure-type separation of diesel fuels by solid phase extraction and identification of the two- and three-ring aromatics by capillary GC-mass spectrometry. *Journal of High Resolution Chromatography*. 14, 91-97.

Bunting, A. (1992) Electronic diesel fuel injection: the developing science. *Automotive Engineer*. 17 (6), 38.

Burrows, I.E. & Lindsey, A.J. (1961) Formation of polycyclic aromatic hydrocarbons by pyrolysis of simple aliphatic hydrocarbons. *Chemistry and Industry*. Sept. 2, 1395.

Burtscher, H. (1992) Measurement and characteristics of combustion aerosols with special consideration of photoelectric charging and charging by flame ions. *Journal of Aerosol Science*. 23 (6), 549-595.

Calcote, H.F. (1981) Mechanisms of soot nucleation in flames - a critical review. *Combustion and Flame*. 42, 215-242.

Campbell, J., Scholl, J., Hibbler, F., Bagley, S., Leddy, D., Abata, D., & Johnson, J. (1981) The effect of fuel injection rate and timing on the physical, chemical, and biological character of particulate emissions from a direct injection diesel. *Society of Automotive Engineers*. 810996.

Campbell, R.M. & Lee, M.L. (1984) Capillary column gas chromatography determination of nitro polycyclic aromatic compounds in particulate extracts. *Analytical Chemistry*. 56, 1026-1030.

Carroll, J.E. (1991) Autoelectrics - development in engine management systems. *Electrotechnology*. Oct/Nov, 191-195.

Cartellieri, W. & Tritthart, P. (1984) Particulate analysis of light duty diesel engines (IDI & DI) with particular reference to the lube oil particulate fraction. *Society of Automotive Engineers*. 840418.

Castello, G. & Gerbino, T.C. (1993) Analysis of polycyclic aromatic hydrocarbons with an ion-trap mass detector and comparison with other gas chromatographic and high-performance liquid chromatographic techniques. *Journal of Chromatography*. 642, 351-357.

Chan, T.L. & Gibson, T.L. (1985) Sampling and atmospheric chemistry of particles containing nitrated polycyclic aromatic hydrocarbons. White, C.M. (Editor). *Nitrated Polycyclic Aromatic Hydrocarbons*. 237-266.

Chang, H.S., Wayte, R., & Spikes, H.A. (1993) Measurement of piston ring and land temperatures in a fired engine using infrared. *Tribology Transactions*. 36 (1), 104-112.

Chou, M.W. (1984) High performance liquid chromatographic separation of nitro-polycyclic aromatic hydrocarbons and their oxidized derivatives. Cooke, M. & Dennis, A.J. (Editors). *Polynuclear Aromatic Hydrocarbons: Chemistry, characterization and carcinogenesis*. 145-153.

Choudbury, D.R. (1982) Characterization of polycyclic ketones and quinones in diesel emission particulates by gas chromatography/mass spectrometry. *Environmental Science & Technology*. 16, 102-106.

- Ciccioli, P., Brancaleoni, E., Cecinato, A., Di Palo, C., Buttini, P., & Liberti, A. (1986) Fractionation of polar polynuclear aromatic hydrocarbons present in industrial emissions and atmospheric samples and their determination by gas chromatography-mass spectrometry. *Journal of Chromatography*. 351, 451-464.
- Ciccioli, P., Cecinato, A., Cabella, R., & Brancaleoni, E. (1993) The contribution of gas-phase reactions to the nitroarene fraction of molecular weight 247 present in carbon particles of northern Italy. *Atmospheric Environment*. 27A (8) 1261-1270.
- Cole, J.A., Bittner, J.D., Longwell, J.P., & Howard, J.B. (1984) Formation mechanisms of aromatic compounds in aliphatic flames. *Combustion and Flame*. 56, 51-70.
- Cooper, B.H., Stanislaus, A., & Hannerup, P.N. (1993) Hydrotreating catalysts for diesel aromatic saturation. *Hydrocarbon Processing*. June, 83-87.
- Cossali, G.E., Coghe, A., & Brunello, G. (1993) Effect of spray-wall interaction on air entrainment in a transient diesel spray. *Society of Automotive Engineers*. 930920.
- Cowley, L.T., Le Jeune, A., & Lange, W.W. (1993) Effect of fuel composition including aromatics content on emissions from a range of heavy-duty diesel engines. *Institute of Mechanical Engineers Seminar: Worldwide engine emission standards and how to meet them*. 225-244.
- Crittenden, B.D. & Long, R. (1973) Formation of polycyclic aromatics in rich premixed acetylene and ethylene flames. *Combustion and Flame*. 20, 359-368.
- Cuddihy, R.G., Griffith, W.C., & McClellan, R.O. (1984) Health risks from light-duty diesel vehicles *Environmental Science & Technology*. 18 (1), 14A-21A.
- Cuthbertson, R.D., Shore, P.R., Sundström, L., & Heden, P.-O. (1987) Direct analysis of diesel particulate-bound hydrocarbons by gas chromatography with solid sample injection. *Society of Automotive Engineers*. 870626.
- D'Agostino, P.A., Narine, D.R., McCarry, B.E., & Quilliam, M.A. (1983) Clean-up and analysis of nitrated aromatic hydrocarbons in environmental samples. Cooke, M. & Dennis, A.J. (Editors) *Polynuclear aromatic hydrocarbons: formation, metabolism and measurement*. 365-377.
- Davies, M.J., Blaikley, D.C.W., Jorgensen, N., Webster, D.E., & Wilkins, A.J.J. (1993) Catalytic control of diesel particulate emissions. *Institute of Mechanical Engineers Seminar: Worldwide engine emission standards and how to meet them*. 111-121.
- Dent, J.C. (1980) Turbulent mixing rate - its effect on smoke and hydrocarbon emissions from diesel engines. *Society of Automotive Engineers*. 800092.

- Draper, W.M. (1986) Quantitation of nitro- and dinitro-PAH in diesel exhaust particulate matter. *Chemosphere*. 15 (4), 437-447.
- Draper, W.M., Phillips, J., & Zeller, H.W. (1988) Impact of a barium fuel additive on the mutagenicity and polycyclic aromatic hydrocarbon content of diesel exhaust particulate emissions. *Society of Automotive Engineers*. 881651.
- Duleep, K.G. (1980) Analysis of automotive particulate sampling techniques. *Society of Automotive Engineers*. 800184.
- Dürnholtz, M., Eifler, G, & Endres, H. (1992) Exhaust-gas re-circulation - a measure to reduce exhaust emissions of DI diesel engines. *Society of Automotive Engineers*. 920725
- El-Shobokoshy, M.S. (1984) The effect of diesel engine load on particulate carbon emission. *Atmospheric Environment*. 18 (11), 2305-2311.
- Escrivá, C., Viana, E., Moltó, J.C., Picó, Y., & Mañes, J. (1994) Comparison of four methods for the determination of polycyclic aromatic hydrocarbons in airborne particulates. *Journal of Chromatography*. 676, 375-388.
- Farrar-Khan, J.R., Andrews, G.E., Ishaq, R., Williams, P.T., & Bartle, K.D. (1993) Quantitative diesel particulate analysis using gas-chromatography mass-spectrometry. *Institute of Mechanical Engineers*. 207 (2), 95-106.
- Fenn, J.B. (1982) *Engines, energy, and entropy*. W.H. Freeman & Company.
- Ferguson, C.R. (1986) *Internal Combustion Engines, Applied Thermosciences*. John Wiley & Sons.
- Fetzer, J.C. (1989) Gas and liquid-chromatographic techniques. Vo-Dinh, T. (Editor) *Chemical analysis of polycyclic aromatic compounds*. Chapter 3.
- Fløysand, S.Å, Kvinge, F., & Betts, W.E. (1993) The influence of diesel fuel properties on particulate emissions in a catalyst equipped European car. *Society of Automotive Engineers*. 932683.
- French, C.C.J. (1987) Power plants for nineties and beyond. *Society of Automotive Engineers*. 871214.
- Fu, F.P., Zhang, Y., Mao, Y.-L., Von Tungeln, L.S., Kim, Y., Jung, H., & Jun, M.-J. (1993) Relationships of structures of nitro-polycyclic aromatic hydrocarbons with high-performance liquid chromatography retention order. *Journal of Chromatography*. 642, 107-116.

Fukuda, M., Tree, D.R., Foster, D.E., & Suhre, B.R. (1992) The effect of fuel aromatic structure and content on direct injection diesel engine particulates. *Society of Automotive Engineers*. 920110.

Gaddo, P., Settis, M., & Giacomelli, L. (1984) Artifact formation during diesel particulate collection. Cooke, M. & Dennis, A.J. (Editors). *Polynuclear Aromatic Hydrocarbons*. 437-449.

Galceran, M.T. & Moyano, E. (1993) Determination of oxygenated and nitro-substituted polycyclic aromatic hydrocarbons by HPLC and electrochemical detection. *Talanta* 40 (5), 615-621.

Galceran, M.T. & Moyano, E. (1994) High-performance liquid chromatography-mass spectrometry (pneumatically assisted electrospray) of hydroxy polycyclic aromatic hydrocarbons. *Journal of Chromatography*. 683, 9-19.

Gachanja, A.N. (1993) Analysis of polycyclic aromatic hydrocarbons by liquid chromatography. *Chromatography and Analysis*. Feb/March, 5-7.

Gachanja, A.N. (1994) University of Plymouth, Personal Communication.

Gibson, T.L., Ricci, A.I., & Williams, R.L. (1981) Measurement of polynuclear aromatic hydrocarbons, their derivatives & their reactivity in diesel automobile exhaust. Bjorseth, A. & Dennis, A.G. (Editors) *Polynuclear Aromatic Hydrocarbons*. Battelle Press, 707-717.

Gibson, T.L. (1982) Nitro derivatives of polynuclear aromatic hydrocarbons in airborne and source particulate matter. *Atmospheric Environment*. 16 (8) 2037-2041.

Gomes, P.C.F & Yates, D.A. (1992) The influence of some engine operating parameters on particulate emissions. *Society of Automotive Engineers*. 922222.

González, M.A., Rodriguez, G.B., Galiasso, R., & Rodriguez, E. (1993) A low emission diesel fuel: hydrocracking production, characterization and engine evaluations. *Society of Automotive Engineers*. 932731.

Gorse, R.A., Jr., Riley, T.L., Ferris, F.C., Pero, A.M. & Skewes, L.M. (1983) 1-Nitropyrene concentration and bacterial mutagenicity in on-road particulate emissions. *Environmental Science & Technology*. 17, 198-202.

Grasso, P., Mann, A., & Irvine, D. (1988) Review of literature on the possible carcinogenicity of automotive emissions. Final Report. Robens Institute, University of Surrey.

Greeves, G. (1979) Response of diesel combustion systems to increase of fuel injection rate. *Society of Automotive Engineers*. 790037.

- Grosjean, D., Fung, K., & Harrison, J. (1983) Interactions of polycyclic aromatic hydrocarbons with atmospheric pollutants *Environmental Science & Technology*. 17, 673-679.
- Hamilton, R.S. & Mansfield, T.A. (1993) The soiling of materials in the ambient atmosphere. *Atmospheric Environment*. 274 (8), 1369-1374.
- Haddad, S.D. (1984) Combustion and heat release in diesel engines. Haddad, S.D. & Watson, N. (Editors) *Principles and performance in diesel engineering*. Ellis Horwood, Chapter 1.
- Hammerle, R.H., Shiller, J.W., & Schwarz, M.J. (1991) Global Climate Change. *Transactions of Engineering for gas turbines & power*. 113, 448-455.
- Handa, T., Yamauchi, T., Sawai, K., Yamamura, T., Koseki, Y., & Ishii, T. (1984) In situ emission levels of carcinogenic and mutagenic compounds from diesel and gasoline engine vehicles on an expressway. *Environmental Science & Technology*. 18 (2), 895-202.
- Hansen, A.M., Olsen, I.L.B., Holst, E., & Poulsen, O.M. (1991) Validation of a high-performance liquid chromatography/fluorescence detection method for the simultaneous quantification of fifteen polycyclic aromatic hydrocarbons. *Ann. Occup. Hyg.* 35 (6), 603-611.
- Hanson, R.L., Henderson, T.R., Hobbs, C.H., Clark, C.R., Carpenter, R.L., & Dutcher, J.S. (1983) Detection of nitroaromatics compounds on coal combustion particles. *Journal of Toxicology and Environmental Health*. 11 971-980.
- Harris, G.W., Mackay, G.I., Iguchi, T., Schiff, H.I., & Schuetzle, D. (1987) Measurement of NO<sub>2</sub> and HNO<sub>3</sub> in diesel exhaust by tunable diode laser absorption spectrometry. *Environmental Science & Technology*. 21, 299-304.
- Hartung, A., Kraft, J., Schulze, J., Kieß, H., & Lies, K.-H. (1984) The identification of nitrated polycyclic aromatic hydrocarbons in diesel particulate extracts and their potential formation as artifacts during particulate collection. *Chromatographia*. 19, 269-273.
- Haupais, A. (1982) A phenomenological approach of combustion modelling in DI diesel engines. *Institute of Mechanical Engineers*. C128/82, 229-236.
- Hayakawa, K., Butoh, M., & Miyazaki, M (1992) Determination of dinitro- and nitropyrenes in emission particulates from diesel and gasoline engine vehicles by liquid chromatography with chemiluminescence detection after precolumn reduction. *Analytica Chimica Acta*. 266, 251-256.
- Hayona, S., Jang-Ho, L., Furuya, K., Kikuchi, T., Someya, T., Oikawa, C., Iida, Y., Matsushita, H., Kinouchi, T., Manabe, Y., & Ohnishi, Y. (1985) Formation of hazardous substances and mutagenicity of PAH produced during the combustion process in a diesel engine. *Atmopsheric Environment*. 19 (6), 1009-1015.

Helmig, D., Arey, J., Atkinson, R., Hager, W.P., & McElroy, P.A. (1992) Products of the OH radical-initiated gas-phase reaction of fluorene in the presence of NO<sub>x</sub>. *Atmospheric Environment*. 26A (9), 1735-1745.

Henderson, T.R., Royer, R.E., Clark, C.R., Harvey, T.M., & Hunt, D.F. (1982) MS/MS analysis of diesel emissions and fuels treated with NO<sub>2</sub>. *Journal of Applied Toxicology* 2 (5), 231-237.

Henderson, T.R., Sun, J.D., Royer, R.E., Clark, C.R., Li, A.P, Harvey, T.M., Hunt, D.F., Fulford, J.E., Lovette, A.M., & Davidson, W.R. (1983) Triple-quadrupole mass spectrometry studies of nitroaromatic emissions from different diesel engines. *Environmental Science & Technology*. 17 (8), 443-449.

Henderson, T.R., Sun, J.D., Albert, L.P., Hanson, R.L., Bechtold, W.E., Harvey, T.M., Shabanowitz, J., & Hunt, D.F. (1984) GC/MS and MS/MS studies of diesel exhaust mutagenicity and emissions from chemically defined fuels. *Environmental Science & Technology*. 18 (6), 428-429.

Henein, N.A. (1973) Diesel engines combustion and emissions. Springer, G.S. & Patterson, D.J. (Editors) *Engine emissions. Pollutant formation and measurement*. Plenum Press. New York. 211- 266.

Henk, M.G., Williamson, W.B., & Silver, R.G. (1992) Diesel catalysts for low particulates and low sulfate emissions. *Society of Automotive Engineers*. 920368.

Herr, J.D., Dukovich, M., Letz, S.S., Yergey, J.A., Risby, T.H., & Tejada, S.B. (1982) The role of nitrogen in the observed direct microbial mutagenic activity for diesel engine combustion in a single-cylinder DI engine. *Society of Automotive Engineers*. 820467.

Hillier, V.A.W. (1991) *Fundamentals of Motor Vehicle Technology*. Stanley Thornes Ltd. England, Chapter 29.

Hirakouchi, N., Fukano, I., & Nagano, H. (1990) Measurement of unregulated exhaust emissions from heavy duty diesel engines with mini-dilution tunnel. *Society of Automotive Engineers*. 900643.

Hisamatsu, Y., Nishimura, T., Tanabe, K., & Matsushita, H. (1986) Mutagenicity of the photochemical reaction products of pyrene with nitrogen dioxide. *Mutation Research*. 172, 19-27.

Hites, R.A. (1989) Mass spectrometry of polycyclic aromatic compounds. Vo-Dinh, T. (Editor) *Chemical analysis of polycyclic aromatic compounds*. Chapter 8.



Hochhauser, A.M., Gorse, R.A., Jr., Reuter, R.M., Benson, J.D., Koehl, W.J., Rutherford, J.A., Burns, V.R., & Painter, L.J. (1992) Speciation and calculated reactivity of automotive exhaust emissions and their relation to fuel properties - Auto/oil air quality improvement research program. *Society of Automotive Engineers*. 920325.

Horrocks, R.W. (1993) Light duty diesels - an update on the emissions challenge. *Institute of Mechanical Engineers Seminar: Worldwide engine emissions and how to meet them*. 155-169.

Howard, J.B. & Longwell, J.P. (1983) Formation mechanisms of PAH and soot in flames. Cooke, M. & Dennis, A.J. (Editors) *Polynuclear aromatic hydrocarbons: formation, metabolism and measurement*. 27-62.

International Agency for Research on Cancer (IARC) (1989) *Monographs on the evaluation of carcinogenic risk to humans. Diesel and gasoline engine exhausts and some nitroarenes*. WHO, Lyon, France, 46.

Iida, N., Suzuki, Y., Sato, G.T., & Sawada, T. (1986) Effects of intake oxygen concentration on the characteristics of particulate emissions from a D.I. diesel engine. *Society of Automotive Engineers*. 861233.

Iida, N. & Sato, G.T. (1988) Temperature & mixing effects on NO<sub>x</sub> and particulate. *Society of Automotive Engineers*. 880424.

Imaizumi, N., Hayakawa, K., Miyazaki, M., Imai, K. (1989) Stability of bis(2,4,6-trichlorophenyl) oxalate in high-performance liquid chromatography for chemiluminescence detection. *Analyst*. 114, 161-164.

Imaizumi, N., Hayakawa, K., Suzuki, Y., & Miyazaki, M. (1990) Determination of nitrated pyrenes and their derivatives by high performance liquid chromatography with chemiluminescence detection after online electrochemical reduction. *Biomedical Chromatography*. 4 (3), 108-112.

Jäger, J. (1978) Detection and characterization of nitro derivatives of some polycyclic aromatic hydrocarbons by fluorescence quenching after thin-layer chromatography: application to air pollution analysis. *Journal of Chromatography*. 152, 575-578.

Jensen, T.E. & Hites, R.A. (1983) Aromatic diesel emissions as a function of engine conditions. *Analytical Chemistry*. 55 (4), 594-599.

Jensen, T.E., Richert, J.F.O., Cleary, A.C., LaCourse, D.L., & Gorse, R.A., Jr. (1986) 1-Nitropyrene in used engine oil. *Journal of the Air Pollution Control Association*. 36 (11), 1255-1257.

Jin, Z. & Rappaport, S.M. (1983) Microbore liquid chromatography with electrochemical detection for determination of nitro-substituted polynuclear aromatic hydrocarbons in diesel soot. *Analytical Chemistry*. 55, 1778-1781.

Kamimoto, T. & Yagita, M. (1989) Particulate formation and flame structure in diesel engines. *Society of Automotive Engineers*. 890436

Kamimoto, T. & Kobayashi, H. (1991) Combustion processes in diesel engines. *Prog. Energy Combust. Sci.* 17, 163-189.

Karcher, W., Fordham, R.J., Dubois, J.J., Glaude, P.G.J.M., & Ligthart, J.A.M. (1985) *Spectral atlas of polycyclic aromatic compounds*. Vol. I, D.Reidel.

Karimi, E.R. (1989) High-speed photography of fuel spray and combustion events in a production diesel engine and combustion bomb. *Institute of Mechanical Engineers*. 203, 269-281.

Kelly, G.W., Bartle, K.D., Clifford, A.A., & Robinson, R.E. (1992) Application of coupled LC-GC to the analysis of the polar fraction of diesel particulate matter. *Journal of High Resolution Chromatography*. 15, 526-530.

Kerswill, J. (1992) Diesel: pump it up. *The Guardian*. 19<sup>th</sup> October, 12.

Kingston, S.T. (1994) Genotoxicology of diesel engine exhaust emissions in cultered mammalian cells. Thesis, University of Plymouth, June.

Kittelson, D.B., Du, C.-J., & Zweidinger, R.B. (1984) Measurements of polycyclic aromatic compounds in the cylinder of an operating diesel engine. *Society of Automotive Engineers*. 840364.

Kobayashi, S. & Imai, K. (1980) Determination of fluorescent compounds by high performance liquid chromatography with chemiluminescence detection. *Analytical Chemistry*. 52, 424-427.

Kobayashi, S., Sakai, T., Nakahira, T., Komori, M., & Tsujimura, K. (1992) Measurement of flame temperature distribution in D.I. diesel engine with high pressure fuel injection. *Society of Automotive Engineers*. 920692.

König, J., Balfanz, E., Funcke, W., & Romanowski, T. (1983) Determination of oxygenated polycyclic aromatic hydrocarbons in airborne particulate matter by capillary gas chromatography and gas chromatography/mass spectrometry. *Analytical Chemistry*. 55, 599-603.

Konno, M., Chikahisa, T., Murayama, T., & Iwamoto, M. (1992a) Catalytic reduction of NO<sub>x</sub> in actual diesel engine exhaust. *Society of Automotive Engineers*. 920091.

Konno, M., Chikahisa, T., & Murayama, T. (1992b) Reduction of smoke and NO<sub>x</sub> by strong turbulence generated during the combustion process in D.I. diesel engines. *Society of Automotive Engineers*. 920467.

Konno, M., Chikahisa, T., & Murayama, T. (1993) An investigation on the simultaneous reduction of particulate and NO<sub>x</sub> by controlling both the turbulence and the mixture formation in DI diesel engines. *Society of Automotive Engineers*. 932797.

Kowalewicz, A. (1984) *Combustion systems of high-speed piston I.C. engines*. Elsevier

Kraft, J. & Lies, K.-H. (1981) Polycyclic aromatic hydrocarbons in the exhaust of gasoline and diesel vehicles. *Society of Automotive Engineers*. 810082.

Kruzel, E.L., Lafleur, A.L., Braun, A.G., Longwell, J.P., Thilly, W.G., & Peters, W.A. (1991) A high-yield sampler for toxicological characterization of complex mixtures in combustion effluents. *Environmental Health Perspectives*. 90, 305-314.

Kuhler, M., Kraft, J., Bess, H., Heeren, U., & Schürmann, D. (1994) Comparison between measured and calculated concentrations of nitrogen oxides and ozone in the vicinity of a motorway. *The Science of the Total Environment*. 146/147, 387-394.

Kwakman, P.J.M. & Brinkman, U.A.Th. (1992) Peroxyoxalate chemiluminescence detection in liquid chromatography. *Analytica Chimica Acta*. 266, 175-192.

Lach, G. & Winckler, J. (1988) Specific problems of sampling and measuring diesel exhaust emissions. *Society of Automotive Engineers*. 881763.

LaCourse, P.L. & Jensen, T.E. (1986) Determination of 1-nitropyrene in extracts of vehicle particulate emissions. *Analytical Chemistry*. 58 (8), 1894-1895.

Ladommatos, N., Horrocks, R., & Cooper, L. (1993) Control of the start of combustion in a direct injection diesel engine using an optical sensor. *Institute of Mechanical Engineers Seminar: Worldwide engine emission standards and how to meet them*. 183-196.

Laity, J.L., Malbin, M.D., Haskwell, W.W., & Doty, W.I. (1973) Mechanisms of polynuclear aromatic hydrocarbon emissions from automotive engines. *Society of Automotive Engineers*. 730835.

Langley, J. (1991) What's clean and lean and a godsend to a green? *The Daily Telegraph*. 30<sup>th</sup> January, Driving section, 1.

Later, D.W., Wilson, B.W., & Lee, M.L. (1985) Standardization of alumina and silica adsorbents used for chemical class separations of polycyclic aromatic compounds. *Analytical Chemistry*. 57, 2979-2984.

Lee, M.L., Novontny, M.V., & Bartle, K.D. (1981) *Analytical Chemistry of Polycyclic Aromatic Compounds*. Academic Press.

Lenner, M. (1987) Nitrogen dioxide in exhaust emissions from motor vehicles. *Atmospheric Environment*. 21 (1), 37-43.

Levin, J.-O., Nilsson, C.-A., & Norström, Å (1984) Sampling and analysis of polycyclic aromatic hydrocarbons (PAH) from two-stroke chain-saw engines. *Chemosphere*. 13 (3), 427-435.

Levine, S.P. & Skewes, L.M. (1982) High-performance semi-preparative liquid chromatography of diesel engine emission particulate extracts. *Journal of Chromatography*. 235, 532-535.

Li, C.-H. (1982) Piston thermal deformation and friction considerations. *Society of Automotive Engineers*. 820086.

Li, H. & Westerholm, R. (1994) Determination of mono- & di-nitro polycyclic aromatic hydrocarbons by on-line reduction and high performance liquid chromatography with chemiluminescence detection. *Journal of Chromatography*. 664, 177-182.

Liberti, A., Ciccioli, P., Cecinato, A., Brancaleoni, E. & Di Palo, C. (1984) Determination of nitrated-polyaromatic hydrocarbons (nitro-PAHs) in environmental samples by high resolution chromatographic techniques. *Journal of High Resolution Chromatography & Chromatography Communications*. 7, 389-397.

Lilly, L.C.R. (1984) *Diesel Engine Reference Book*. Butterworths.

Linder, W., Posch, W., Wolfbeis, O.S., & Tritthart, P. (1985) Analysis of nitro-PAHs in diesel exhaust particulate extracts with multi-column HPLC. *Chromatographia*. 20 (14), 213-218.

Lindskog, A. (1983) Transformations of polycyclic aromatic hydrocarbons during sampling. *Environmental Health Perspectives*, 47, 81-84.

Liu, T.-Y. & Robbat, A., Jr. (1991) High-performance liquid chromatography retention index and detection of nitrated polycyclic aromatic hydrocarbons. *Journal of Chromatography*. 539, 1-14.

MacCrehan, W.A., May, W.E., Yang, S.D., & Benner, B.A., Jr. (1988) Determination of nitro polynuclear aromatic hydrocarbons in air and diesel particulate using liquid chromatography with electrochemical and fluorescence detection. *Analytical Chemistry*. 60, 194-199.

Maher, W., Pellegrino, F., & Furlonger, J. (1989) Determination of polycyclic aromatic hydrocarbons in air particulate samples. *Microchemical Journal*. 39, 160-165.

Martin, B. & Bigeard, P.H. (1992) Hydrotreatment of diesel fuels - Its impact on light-duty diesel engine pollutants. *Society of Automotive Engineers*. 922268.

Matsui, Y. & Sugihara, K. (1986) Sources of hydrocarbon emissions from a small direct injection diesel engine. *Japanese Society of Automotive Engineering Review*. 7 (3), 4-11.

- Matsuoka, S. (1990) Combustion in the diesel engine. Weaving, J.H. (Editor) *Internal Combustion Engineering Science & Technology*. Elsevier Applied Science, 333-384.
- Mayer, W.J., Lechman, D.C., & Hilden, D.L. (1980) The contribution of engine oil to diesel exhaust particulate emissions. *Society of Automotive Engineers*. 800256.
- May, W.E. & Wise, S.A. (1984) Liquid chromatographic determination of polycyclic aromatic hydrocarbons in air particulate extracts. *Analytical Chemistry*. 56 (2), 225-232.
- Melikian, A.A., Lavoie, E.J., Hecht, S.S., & Hoffmann, D. (1983) On the enhancing effect of a bay-region methyl group in 5-methylchrysene carcinogenesis. Cooke, M. & Dennis, A.J. (Editors). *Polynuclear Aromatic Hydrocarbons: Formation, Metabolism, and Measurement*. Battelle Press. 861-875
- Mermelstein, R., Kiriazides, D., Butler, M., McCoy, E.C., & Rosenkranz, H.S. (1981) The extraordinary mutagenicity of nitropyrenes in bacteria. *Mutation Research*. 89, 187-198.
- Mills, G.A., Howarth, J.S., & Howard, A.G. (1984) The effect of diesel fuel aromaticity on polynuclear aromatic hydrocarbon exhaust emissions. *Journal of the Institute of Energy*. March, 273-286.
- Miyamoto, N., Ogawa, H., Shibuya, M., & Suda, T. (1992) Description of diesel emissions by individual fuel properties. *Society of Automotive Engineers*. 922221.
- Monaghan, M.L. (1981) High speed direct injection diesel for passenger cars. *Society of Automotive Engineers*. 810477.
- Montreuil, C.N., Ball, J.C., Gorse, R.A., Jr., & Young, W.C. (1992) Solvent extraction efficiencies of mutagenic components from diesel particles. *Mutation Research*. 282, 89-92.
- Muramatsu, G., Abe, A., Furuyama, M., & Yoshida, K. (1993) Catalytic reduction of NO<sub>x</sub> in diesel exhaust. *Society of Automotive Engineers*. 930135
- Murayama, T., Miyamoto, N., Chikahisa, T., & Yamane, K. (1986) Effects of combustion and injection systems on unburnt HC and particulate emissions from a DI diesel engine. *Society of Automotive Engineers*. 861232.
- Naber, D., Lange, W.W., Reglitzky, A.A., Schäfer, A., Gairing, M., & Le Jeune, A. (1993) The influence of fuel properties on exhaust emissions from advanced Mercedes Benz diesel engines. *Society of Automotive Engineers*. 932685.
- Nahum, A. (1989) Direct approach. *Autocar & Motor*. 10 May.

- Nakagawa, R., Kitamori, S., Horikawa, K., Nakashima, K., & Tokiwa, H. (1983) Identification of dinitropyrenes in diesel-exhaust particles. Their probable presence as major mutagens. *Mutation Research*. 124, 201-211.
- Nelson, P.F. (1989) Combustion-generated polycyclic aromatic hydrocarbons in diesel exhaust emissions. *Fuel*. 68, 283-286.
- Newton, D.L., Erickson, M.D., Tomer, K.B., Pellizzari, E.D., Gentry, P., & Zweidinger, R.B. (1982) Identification of nitroaromatics in diesel exhaust particulate using gas chromatography/negative ion chemical ionization mass spectrometry and other techniques. *Environmental Science & Technology*. 16, 206-213.
- Nielsen, T. (1983) Isolation of polycyclic aromatic hydrocarbons and nitro derivatives in complex mixtures. *Analytical Chemistry*. 55, 286-290.
- Nielsen, T., Ramdahl, T., & Bjørseth, A. (1983) The fate of airborne polycyclic organic matter. *Environmental Health Perspectives*. 47, 103-114.
- Nielsen, T. (1984) Reactivity of polycyclic aromatic hydrocarbons towards nitrating species. *Environmental Science & Technology*. 18, 157-163.
- Nikanjam, M. (1993) Development of the first CARB certified California alternative diesel fuel. *Society of Automotive Engineers*. 930728.
- Niles, R. & Tan, Y.L. (1989) Determination of polynuclear aromatic hydrocarbons and mononitrated derivatives in air and diesel particulates. *Analytica Chimica Acta*. 221, 53-63.
- Ning, M., Yuan-Xian, Z., Zhen-Huan, S., & Hu-Guo-dong (1991) Soot formation, oxidation and its mechanism in different combustion systems and smoke emission pattern in DI diesel engines. *Society of Automotive Engineers*. 910230.
- Noble, D. (1994) Perkins Technology, Peterborough, Personal communication.
- Obuchi, A., Aoyama, H., Ohi, A., & Ohuchi, H. (1984) Determination of polycyclic aromatic hydrocarbons in diesel exhaust particulate matter and diesel fuel oil. *Journal of Chromatography*. 312, 247-259.
- Oehme, M., Manø, S., & Stray, H. (1982) Determination of nitrated polycyclic hydrocarbons in aerosols using capillary gas chromatography combined with different electron capture detection methods. *Journal of High Resolution Chromatography & Chromatography Communications*. 5, 417-423.
- Oehme, M. (1985) Negative ion chemical ionization mass spectrometry - a useful technique for the selective detection of polar substituted polycyclic aromatic hydrocarbons with mutagenic properties. *Chemosphere*. 14 (9), 1285-1297.

Ohgaki, H., Negiski, C., Wakabayashi, K., Kusama, K., Sato, S., & Sugimura, T. (1984) Induction of sarcomas in rats by subcutaneous injection of dinitropyrenes. *Carcinogenesis*. 5 (5), 583-585.

Ohnishi, Y., Kachi, K., Sato, K., Tahara, I., Takeyoshi, H., & Tokiwa, H. (1980) Detection of mutagenic activity in automobile exhaust. *Mutation Research*. 77, 229-240.

Paputa-Peck, M.C, Marano, R.S., Schuetzle, D., Riley, T.L., Hampton, C.V., Prater, T.J., Skewes, L.M., Jensen, T.E., Ruehle, P.H., Bosch, L.C., & Duncan, W.P. (1983) Determination of nitrated polynuclear aromatic hydrocarbons in particulate extracts by capillary column gas chromatography with nitrogen selective detection. *Analytical Chemistry*. 55, 1946-1954.

Parliamentary Office of Science and Technology (1994) Breathing in our cities - urban air pollution and respiratory health. Report.

Pemberton (1995) University of Plymouth, Personal communication.

Petch, G.S., Trier, C.J., Rhead, M.M., Fussey, D.E. & Millward, G.E. (1987) The development of a novel exhaust sampling technique with particular relevance to polycyclic aromatic hydrocarbons. *Institute of Mechanical Engineers*. C340/87, 97-105.

Pederson, T.C. & Siak, J.-S. (1981) The role of nitroaromatic compounds in the direct-acting mutagenicity of diesel particle extracts. *Journal of Applied Toxicology*. 1 (2), 54-60.

Pfeffer, H.-U. (1994) Ambient air concentrations of pollutants at traffic-related sites in urban areas of North Rhine-Westphalia, Germany. *The Science of the Total Environment*. 146/147, 263-273.

Pipho, M.J., Kittelson, D.B., & Zarling, D.D. (1991) NO<sub>2</sub> formation in a diesel engine. *Society of Automotive Engineers*. 910231.

Pitts, J.N., Jr., Van Cauwenberghe, K.A., Grosjean, D., Schmid, J.P., Fitz, D.R., Belser, W.L., Jr., Knudson, G.B., & Hynds, P.M. (1978) Atmospheric reactions of polycyclic aromatic hydrocarbons: facile formation of mutagenic nitro derivatives. *Science*. 202, 515-519.

Pitts, J.N., Jr. (1983) Formation and fate of gaseous and particulate mutagens and carcinogens in real and simulated atmospheres. *Environmental Health Perspectives*. 47, 115-140.

Pitts, J.N., Jr., Arey, J., Zeilinska, B., Winer, A.M., & Atkinson, R. (1985) Determination of 2-nitrofluoranthene and 2-nitropyrene in ambient particulate organic matter: evidence for atmospheric reactions. *Atmospheric Environment*. 19 (10), 1601-1608.

Plee, S.L. & MacDonald, J.S. (1980) Some mechanisms affecting the mass of diesel exhaust particulate following a dilution process. *Society of Automotive Engineers*. 8001986.

Poole, C.F. (1982) The electron-capture detector in capillary gas chromatography. *Journal of HRC & CC*. 5, 454-471.

Poulton, M.L. (1994) *Alternative engines for road vehicles*. Computational Mechanics Publications.

Quality of Urban Air Review Group (QUARG) (1993). Diesel vehicle emissions and urban air quality. Second Report, December.

Ramdahl, T. & Urdal, K. (1982) Determination of nitrated polycyclic aromatic hydrocarbons by fused silica capillary gas chromatography/negative ion chemical ionization mass spectrometry. *Analytical Chemistry*. 54, 2256-2260.

Ramdahl, T. (1983) Polycyclic aromatic ketones in environmental samples. *Environmental Science & Technology*. 17, 666-670.

Ramdahl, T., Sweetman, J.A., Zielinska, B., Atkinson, R., Winer, A.M., & Pitts, J.N., Jr. (1985) Analysis of mononitro-isomers of fluoranthene and pyrene by high resolution capillary gas chromatography/mass spectrometry. *Journal of High Resolution Chromatography & Chromatography Communications*. 8, 849-853.

Rao, K.K., Winterbone, D.E., & Clough, E. (1993) Influence of swirl on high pressure injection in hydra diesel engine. *Society of Automotive Engineers*. 930978.

Rappaport, S.M., Jin, Z.L., & Xu, X.B. (1982) High-performance liquid chromatography with reductive electrochemical detection of mutagenic nitro-substituted polynuclear aromatic hydrocarbons in diesel exhausts. *Journal of Chromatography*. 240, 145-154.

Reece, C.E. & Scott, P.W. (1987) Quantitative analysis by gas chromatography. In: Katz, E. (Editor). *Quantitative analysis using chromatographic techniques*. 157-191.

Rhead, M.M., Fussey, D.E., Millward, G.E., & Trier, C.J. (1991) Pathways of PAH radio-tracers during transient testing of a modern HSDI diesel engine. Final report, SERC grant, GR/E/76780.

Rhead, M.M. & Trier, C.J. (1992) Fuel residues and organic combustion products in diesel exhaust emissions: sources, sampling and analysis. *Trends in Analytical Chemistry*. 11 (7), 255-259.

Richards, L.W., Bergstrom, R.W., Jr., & Ackerman, T.P. (1986) The optical effects of fine-particle carbon on urban atmosphere. *Atmospheric Environment*. 20 (2), 387-396.

Risby, T.H. & Lestz, S.S. (1983) Is the direct mutagenic activity of diesel particulate matter a sampling artefact ? *Environmental Science & Technology*. 17 (10), 621-624.



Rivers, K.J., Paassen, C.W.C., Booth, M., & Marriott, J.M. (1993) Future diesel fuel quality - balancing requirements. *Institute of Mechanical Engineers Seminar: Worldwide engine emission standards and how to meet them*. 209-223.

Robards, K. & Worsfold, P.J. (1992) Analytical applications of liquid-phase chemiluminescence. *Analytica Chimica Acta*. 266, 147-173.

Robbat, A., Jr., Corso, N.P., Doherty, P.J., & Wolf, M.H. (1986) Gas chromatographic chemiluminescent detection and evaluation of predictive models for identifying nitrated polycyclic aromatic hydrocarbons in a diesel fuel particulate extract. *Analytical Chemistry*. 58, 2078-2084.

Robbins, W.K. & McElroy, F.C. (1982) Rational selection of sample preparation techniques for the measurement of polynuclear aromatics. Cooke, M., Dennis, A.J., & Fisher, G.L. (Editors) *PAH's Physical and biological Chemistry*. 673-686.

Røj, A. (1992) Environmentally friendly diesel fuels - The Swedish experience. 11<sup>th</sup> European Automotive Symposium, Sorrento, November 19-20.

Rosenkranz, H.S. & Mermelstein, R. (1983). Mutagenicity and genotoxicity. All nitro-containing chemicals were not created. *Mutation Research*. 114, 217-267.

Ross, D.S., Hum, G.P., & Schmitt, R.J. (1988) Nitration of pyrene by NO<sub>2</sub> and N<sub>2</sub>O<sub>4</sub>. In Elbert, L.B. (Editor) *Polynuclear aromatic compounds*. American Chemical Society, Chapter 9.

Rubey, W.A., Hall, D.L., Torres, J.L., Dellinger, B., & Carnes, R.A. (1983) The thermal degradation behaviour of selected polynuclear aromatic hydrocarbons. Cooke, M. & Dennis, A.J. (Editors). *Polynuclear Aromatic Hydrocarbons: Formation, Metabolism, and Measurement*. Battelle Press. 861-875

Rudolf, W. (1994) Concentration of air pollutants inside cars driving on highways and in downtown areas. *The Science of the Total Environment*. 146/147, 433-444.

Ryan, T.W., III, Stroment, J.O., Wright, B.R., & Waytulonis, R. (1981) The effects of fuel properties and composition on diesel engine exhaust emissions-a review. *Society of Automotive Engineers*. 810953.

Ryan, T.W., III & Erwin, J. (1993) Diesel fuel composition effects on ignition and emissions. *Society of Automotive Engineers*. 932735.

Saito, T., Tokura, N., & Katoh, T. (1982) Analysis of factors affecting the formation of major mutagenic substances in diesel particulate extracts. *Society of Automotive Engineers*. 821244.

Saito, T., Daisho, Y., Uchida, N., & Ikeya, N. (1986) Effects of combustion chamber geometry on diesel combustion. *Society of Automotive Engineers*. 861186.

- Salmeen, I., Durisin, A.M., Prater, T.J., Riley, T., & Schuetzle, D. (1982) Contribution of 1-nitropyrene to direct-acting Ames assay mutagenicities of diesel particulate extracts. *Mutation Research*. 104, 17-23.
- Sasaki, Y., Endo, R. & Koido, Y. (1980) Direct mutagens in the gaseous component of automobile exhaust detected with *Bacillus subtilis* spores. *Mutation Research*. 79, 181-184.
- Scheepers, P.T.J. & Bos, R.P. (1992a) Combustion of diesel fuel from a toxicological perspective. II. Toxicity. *Int. Arch. Occup. Environ. Health*. 64, 163-77.
- Scheepers, P.T.J. & Bos, R.P. (1992b) Combustion of diesel fuel from a toxicological perspective. I. Origin of incomplete combustion products. *Int. Arch. Occup. Environ. Health*. 64, 149-161.
- Scheepers, P.T.J., Velders, D.D., Martens, M.H.J., Noordhoek, J., Bos, R.P. (1994) Gas chromatographic-mass spectrometric determination of nitro polycyclic aromatic hydrocarbons in airborne particulate matter from workplace atmospheres contaminated with diesel exhaust. *Journal of Chromatography*. 677, 107-121.
- Schenker, M.B. (1980) Diesel exhaust - an occupational carcinogen? *Journal of Occupational Medicine*. 22 (1), 41-46.
- Schindler, K.-P. (1992) Integrated diesel european action (IDEA): study of diesel combustion. *Society of Automotive Engineers*. 920591.
- Schmeltz, I. & Hoffman, D. (1976) Formation of polynuclear hydrocarbons from combustion of organic matter. Fredenthal, R.I. & Jones, P.W. (Editors) *Polynuclear aromatic hydrocarbons: Chemistry, metabolism, and carcinogenesis*. Vol. 1, Raven Press, 225-239.
- Schneider, E., Krenmayr, P., & Varmuza, K. (1990) A routine method for the analysis of the mononitro-PAH in immission and emission samples. *Monatshefte für Chemie Chemical Monthly*. 121, 393-401.
- Schuetzle, D., Lee, F.S-C., Prater, T.J., Tejada, S.B. (1981) The identification of polynuclear aromatic hydrocarbon (PAH) derivatives in mutagenic fractions of diesel particulate extracts. *Intern. J. Environ. Anal. Chem.* 9, 93-144.
- Schuetzle, T.L., Riley, T.L., Prater, T.J., Harvey, T.M., & Hunt, D.F. (1982) Analysis of nitrated polycyclic aromatic hydrocarbons in diesel particulates. *Analytical Chemistry*. 54, 265-271.
- Schuetzle, D. (1983) Sampling of vehicle emissions for chemical analysis and biological testing. *Environmental Health Perspectives*. 47, 65-80.

Schuetzle, D. & Perez, J.M. (1983) Factors influencing the emissions of nitrated-polynuclear aromatic hydrocarbons (nitro-PAH) from diesel engines. *Journal of Air Pollution Control Association*. 33 (8). 751-755.

Schuetzle, D. & Frazier, J.A. (1986) Factors influencing the emission of vapor and particulate phase components from diesel engines. Ishinishi, N., Koizumi, A., McClellan, R.O., & Stöber, W. (Editors) *Carcinogenic and mutagenic effects of diesel engine exhaust*. Elsevier, Amsterdam, 41-63.

Schulze, J., Hartung, A., Kieß, H., Kraft, J., & Lies, K.-H. (1984) Identification of oxygenated polycyclic aromatic hydrocarbons in diesel particulate matter by capillary gas chromatography and capillary gas chromatography/mass spectrometry. *Chromatographia*. 19, 391-397.

Seaton, A., MacNee, W., Donaldson, K., & Godden, D. (1995) Particulate air pollution & acute health effects. *The Lancet*. 345, 176-178.

Selleström, U., Jansson, B., Bergman, Å, & Alsberg, T. (1987) Selective and sensitive analysis of nitro-PAH. *Chemosphere*. 16 (5), 945-952.

Serageldin, M.A. (1981) Soot formation in small flames. *Society of Automotive Engineers*. 811197.

Shakal, J. & Martin, J.K. (1990) Effects of auxillary injection on diesel engine combustion. *Society of Automotive Engineers*. 900398.

Shay, E.G. (1993) Diesel fuel from vegetable oils: status and opportunities. *Biomass and Bioenergy*. 4 (4), 227-242.

Shioji, M., Kimoto, T., Okamoto, M., & Ikegami, M. (1989) An anlysis of diesel flame by picture processing. *JSME International Journal*. 32 (3), 434-442.

Shiozaki, T., Suzuki, T., & Shimoda., M. (1980) Observation of combustion process in D.I. diesel engine via high speed direct and schlieren photography. *Society of Automotive Engineers*. 800025.

Shore, P.R. (1984) The analysis of polycyclic aromatic hydrocarbon emissions. Report by Ricardo Consulting Engineers. Report

Shore, P.R. (1986) Alternative fuel effects on diesel engine PAH and nitro-PAH. Report by Ricardo Consulting Engineers. Report

Shundoh, S., Komori, M., Tsujimura, K., & Kobayashi, S. (1992) NO<sub>x</sub> reduction from diesel combustion using pilot injection with high pressure fuel injection. *Society of Automotive Engineers*. 920461.

- Signer, M. & Steinke, R.E. (1987) Future trends in diesel engine design and their impact on lubricants. *Society of Automotive Engineers*. 871271.
- Sigvardson, K.W. & Birks, J.W. (1984) Detection of nitro-polycyclic aromatic hydrocarbons in liquid chromatography by zinc reduction and peroxyalate chemiluminescence. *Journal of Chromatography*. 316, 507-518.
- Singal, S.K., Pundir, B.P., & Mehta, P.S. (1993) Fuel spray-air motion interaction in DI diesel engines: a review. *Society of Automotive Engineers*. 930604.
- Smith, O.I. (1981) Fundamentals of soot formation in flames with application to diesel engine particulate emissions. *Prog. Energy Combust. Sci.* 7, 275-291.
- Snook, M.E., Severson, R.F., Higman, H.C., Arrendale, R.F., & Chortyk, O.T. (1979) Methods for characterization of complex mixtures of polynuclear aromatic hydrocarbons. Jones, P.W. & Leber, P (Editors). *Polynuclear Aromatic Hydrocarbons*. Ann Arbor Science Publishers
- Sorrell, R.K. & Reding, R. (1985) Analysis of polynuclear aromatic hydrocarbons in environmental waters by high-pressure liquid chromatography. *Journal of Chromatography*. 348, 655-670.
- Springer, K.J. (1991) Global what? Control possibilities of CO<sub>2</sub> and other greenhouse gases. *Journal of Engineering for Gas Turbines and Power*. 113, 440-447.
- Stärk, G., Stauff, J., Miltenburger, H.G., & Stumm-Fischer, I. (1985) Photodecomposition of 1-nitropyrene and other direct-acting mutagens extracted from diesel-exhaust particulates. *Mutation Research*. 155, 27-33.
- Stenburg, U., Alsberg, T., & Westerholm, R. (1983) Emission of carcinogenic components with automobile exhausts. *Environmental Health Perspectives*. 47, 53-63.
- Stöber, W. (1992) Health aspects of combustion gases and diesel exhaust. *Journal of Aerosol Medicine*. 5 (2), 81-102.
- Stone, R. (1992) *Introduction to Internal Combustion Engines*. MacMillan.
- Stradling, R.J., Cowley, L.T., Lange, W.W., & Maillard, C. (1993) The influence of fuel properties and test cycle procedures on the exhaust particulate emissions from light-duty diesel vehicles. *Institute of Mechanical Engineers Seminar: Fuels for automotive and industrial engines*. 6<sup>th</sup>-7<sup>th</sup> April.
- Tanabe, H., Yamaguchi, H., Yamamoto, T., & Sato, T.G. (1992) Wall effects on SOF formation. *Society of Automotive Engineers*. 922211

Tancell, P.J., Rhead, M.M., Trier, C.J., Bell, M.A., & Fussey, D.E. (1995a) The sources of benzo( $\alpha$ )pyrene in diesel exhaust emissions. *The Science of the Total Environment*. 162, 179-186.

Tancell, P.J., Rhead, M.M., Trier, C., Pemberton, R., & Braven, J. (1995b) Diesel combustion of an alkylated polycyclic aromatic hydrocarbon. *Fuel*. awaiting publication.

Tancell (1995). The origin of polycyclic aromatic hydrocarbons in diesel exhaust emissions. Thesis, University of Plymouth, March.

Tejada, S.B., Zweidinger, R.B., & Sigsby, J.E., Jr. (1982) Analysis of nitroaromatics in diesel and gasoline car emissions. *Society of Automotive Engineers*. 820775.

Tejada, S.B., Zweidinger, R.B., & Sigsby, J.E., Jr. (1986) Fluorescence detection and identification of nitro derivatives of polynuclear aromatic hydrocarbons by on-column catalytic reduction to aromatic amines. *Analytical Chemistry*. 58, 1827-1834.

Theobald, N. (1988) Rapid preliminary separation of petroleum hydrocarbons by solid-phase extraction cartridges. *Analytica Chimica Acta*. 204, 135-144.

Tokiwa, H., Nakagawa, R., Kunimasa, M., & Ohnishi, Y. (1981) The mutagenicity of nitro derivatives induced by exposure of non-mutagenic compounds to nitrogen dioxide. *Mutation Research*. 85, 195-205.

Tokiwa, H. & Ohnishi, Y. (1986) Mutagenicity and carcinogenicity of nitroarenes and their sources in the environment. *CRC Critical Reviews in Toxicology*. 17 (1), 23-60.

Tomkins, B.A., Brazell, R.S., Roth, M.E., & Ostrum, V. (1984) Isolation of mononitrated polycyclic aromatic hydrocarbons in particulate matter by liquid chromatography and determination by gas chromatography with the thermal energy analyzer. *Analytical Chemistry*. 56, 781-786.

Tong, H.Y., Sweetman, J.A., & Karasek, F.W. (1983) Quantitation of 1-nitropyrene in diesel exhaust particulates by capillary gas chromatography-mass spectrometry and capillary gas chromatography. *Journal of Chromatography*. 264, 231-239.

Tong 1984, H.Y., Sweetman, J.A., Karasek, F.W., Jellum, E., & Thorsrud, A.K. (1984) Quantitative analysis of polycyclic aromatic compounds in diesel exhaust extracts by combined chromatographic techniques. *Journal of Chromatography*. 312, 183-202.

Trier, C.J. (1988) The origins of the organic fraction in diesel exhaust emissions. Thesis, University of Plymouth, June.

Trier, C.J., Fussey, D.E., Petch, G.S., & Rhead, M.M. (1988) A comparison of diesel exhaust emissions collected by an environmental protection agency recommended dilution tunnel/filter with the sample from a new solvent scrubbing system. *Institute of Mechanical Engineers*. C64, 135-144

Trier, C.J., Rhead, M.M., & Fussey, D.E. (1990) Evidence for the pyrosynthesis of parent polycyclic aromatic compounds in the combustion of a diesel engine. *Institute of Mechanical Engineers*. C394/003, 53-60.

Trier, C.J., Fussey, D.E., Ryder, D., & Graham, M.A. (1991) Development of radiotracer techniques for diesel fuel and exhaust emission research. *Institute of Mechanical Engineers*. C433/010, 159-164.

Trijonis, J. (1984) Effect of diesel vehicles on visibility in California. *The Science of the Total Environment*. 36, 131-140.

Trithart, P., Cichiocki, R., & Cartellieri, W. (1993) Fuel effects on emissions in various test cycles in advanced passenger car diesel vehicles. *Society of Automotive Engineers*. 932684.

Tsunemoto, H., Yamada, T., & Ishitani, H. (1986) Behaviour of adhering fuel on cold combustion chamber wall in direct injection diesel engines. *Society of Automotive Engineers*. 861235.

Uden, P.C. (1987) Detection in quantitative gas chromatography. Katz, E. (Editor) *Quantitative analysis using chromatographic techniques*. John & Wiley Sons, 99-155.

Viegl, E., Posch, W., Linder, W., & Trithart, P. (1994) Selective and sensitive analysis of 1-nitropyrene in diesel exhaust particulate extract by multidimensional HPLC. *Chromatographia*. 38 (3/4), 199-206.

Viras, L.G., Athanasiou, K., & Siskos, P. (1990) Determination of mutagenic activity of airborne particulates and of the benzo( $\alpha$ )pyrene concentrations in Athens atmosphere. *Atmospheric Environment*. 24B (2), 267-274.

Wade, J.F. & Newman, L.S. (1993) Diesel asthma. Reactive airways disease following overexposure to locomotive exhaust. *JOM*. 35 (2), 149-154.

Waldenmaier, D.A., Gratz, L.D., Bagley, S.T., Johnson, J.H., & Leddy, D.G. (1990) The influence of sampling conditions on the repeatability of diesel particulate vapor phase hydrocarbon and PAH measurements. *Society of Automotive Engineers*. 900642.

Walsh, M.P. & Bradow, R. (1991) Diesel particulate control around the world. *Society of Automotive Engineers*. 910130.

Weast, R.C. & Astle, M.J. (1985) *CRC Handbook of data on organic compounds*. Vol. I & II, CRC Press.

Weaver, C.S., Miller, C., Johnson, W.A., & Higgins, T.S. (1986) Reducing the sulfur and aromatic content of diesel fuel: costs, benefits, and effectiveness for emission control. *Society of Automotive Engineers*. 860622.

Wei, E.T. & Shu, H.P. (1983) Nitroaromatic carcinogens in diesel soot: a review of laboratory findings. *AJPH*. 73 (9), 1085-1088.

Weildmann, K., Menrad, H., Reders, K., & Hutcheson R.C. (1988) Diesel fuel quality effects on exhaust emissions. *Society of Automotive Engineers*. 881649.

Wheeler, R.H. (1984) Diesel exhaust emissions. Haddad, S.D. & Watson, N. (Editors) *Principles and performance in diesel engineering*. John Wiley & Sons. Chapter 6.

White, C.M., Robbat, A., Jr., & Hoes, R.M. (1984) Evaluation of a thermionic ionization detector for nitrated polycyclic aromatic hydrocarbons. *Analytical Chemistry*. 56, 232-236.

White, C.M. (1985). *Nitrated polycyclic aromatic hydrocarbons*. Huethig.

Williams, P.T., Bartle, K.D., & Andrews, G.E. (1986a) The relation between polycyclic aromatic compounds in diesel fuels and exhaust particulates. *Fuel*. 65, 1150-1158.

Williams, P.T., Andrews, G.E., & Bartle, K.D. (1987) The role of lubricating oil in diesel particulate and particulate PAH emissions. *Society of Automotive Engineers*. 872084.

Williams, P.T., Abbass, M.K., Andrews, G.E., & Bartle, K.D. (1989) Diesel particulate emissions: the role of unburned fuel. *Combustion and Flame*. 75, 1-24.

Williams, P.T. (1990) Sampling and analysis of polycyclic aromatic compounds from combustion systems: a review. *Journal of the Institute of Energy*. March, 22-30.

Williams, R.L. & Swarin, S.J. (1979) Benzo( $\alpha$ )pyrene emissions from gasoline and diesel automobiles. *Society of Automotive Engineers*. 790419.

Williams, R.L., Perez, J.M., & Griffing, M.E. (1985) A review of sampling condition effects on polynuclear aromatic hydrocarbons (PNA) from heavy-duty diesel engines. *Society of Automotive Engineers*. 852081.

Williams, R.L., Sparacino, C., Petersen, B., Bumgarne, J., Jungers, R.H., & Lewtas, J. (1986b) Comparative characterization of organic emissions from diesel particles, coke oven mains, roofing tar vapours and cigarette smoke condensate. *Intern. J. Environ. Anal. Chem.* 26, 27-49.

Williams, R.L., Meares, J., Brooks, L., Watts, R., & Lemieux, P. (1994) Priority pollutant PAH analysis of incinerator emission particles using HPLC and optimized fluorescence detection. *Inter. J. Anal. Chem.* 54, 299-314.

Wise, S.A., Chelser, S.N., Hilpert, L.R., May, W.E., Rebbert, R.E., Vogt, C.R., Nishioka, M.G., Austin, A., & Lewtas, J. (1985) Quantification of polycyclic aromatic hydrocarbons and nitro-substituted polycyclic aromatic hydrocarbons and mutagenicity testing for the character of ambient air particulate matter. *J. Environ. Int.* 11, 147-160.

Xu, X.B., Nachtman, J.P., Rappaport, S.M., Wei, E.T., Lewis, S., & Burlingame, A.L. (1981) Identification of 2-nitrofluorene in diesel exhaust particulates. *Journal of Applied Toxicology*. 1 (3), 196-198.

Xu, X.B., Nachtman, J.P., Jin, Z.L., Wei, E.T., & Rappaport, S.M. (1982) Isolation and identification of mutagenic nitro-PAH in diesel-exhaust particulates. *Analytica Chimica Acta*. 136, 163-174.

Yergey, J.A., Risby, T.H., & Letz, S.S. (1982) Chemical characterization of organic adsorbates on diesel particulate matter. *Analytical Chemistry*. 54, 354-357.

Yoshida, E., Nomura, H., & Sekimoto, M. (1986) Fuel and engine effects on diesel exhaust emissions. *Society of Automotive Engineers*. 860619.

Yu, M. & Hites, R.A. (1981) Identification of organic compounds on diesel engine soot. *Analytical Chemistry*. 53 (7), 951-954.

Yu, R.C., Wong, V.W., & Shaded, S.M. (1980) Sources of hydrocarbon emissions from direct injection diesel engines. *Society of Automotive Engineers*. 800048.

Yu, W.C., Fine, D.H., Chiu, K.S., & Biemann, K. (1984) Determination of nitrated polycyclic aromatic hydrocarbons in diesel particulates by gas chromatography with chemiluminescent detection. *Analytical Chemistry*. 56, 1158-1162.

Zelenka, P., Kriegler, W., Herzog, P.L., & Cartellieri, W.P. (1990) Ways toward the clean heavy-duty diesel. *Society of Automotive Engineers*. 900602.

Zelenka, P. & Herzog, P.L. (1993) Exhaust gas aftertreatment systems for diesel engines with respect to future emission legislation. *Institute of Mechanical Engineers Seminar: Worldwide engine emissions and how to meet them*. 123-135.

Zhang, L., Minami, T., Takatsuki, T., & Yokota, K. (1993) An analysis of the combustion of a DI diesel engine by photograph processing. *Society of Automotive Engineers*. 930594.

Zielinska, B., Arey, J., Atkinson, R., & Winer, A.M. (1989a) The nitroarenes of molecular weight 247 in ambient particulate samples collected in southern California. *Atmospheric Environment*. 23 (1), 223-229.

Zielinska, B., Arey, J., Atkinson, R., & McElroy, P.A. (1989b) Formation of methylnitronaphthalenes from the gas-phase reactions of 1- and 2-methylnaphthalene with OH radicals and N<sub>2</sub>O<sub>3</sub> and their occurrence in ambient air. *Environ. Sci. Technol.* 23, 723-729.



Ziejewski, M., Goettler, H.J., Cook, L.W., & Flicker, J. (1991) Polycyclic aromatic hydrocarbon emissions from plant oil based alternative fuels. *Society of Automotive Engineers*. 911765.

Ziejewski, M. & Goettler, H.J. (1992) Comparative analysis of the exhaust emissions for vegetable oil based alternative fuels. *Society of Automotive Engineers*. 920195.

Zierock, K.-H., Rothe, G., & Steppat, R. (1983) Polycyclic aromatic hydrocarbons in the particulate emissions of three diesel engines. *Society of Automotive Engineers*. 830458

Appendix A - GC-ECD analysis of Nitro-PAC collected using Upgraded TESSA																							
1-nitronaphthalene (1- <i>nn</i> )								calibration: $y = 60.6940x - 0.045$ where $y = \text{area}$ & $x = \text{wt injected (ng)}$															
								R-sq=0.998															
Speed	TES (mg)	Sub-fraction of TES cleaned-up (mg)	Aromatic Wt. from clean-up (mg)	Wt injected on HPLC (mg)	Multi-factor (if all TES used)	Dil. Vol. (ul)	Inj. Vol (ul)	Area #1	Area #2	Av. Area (b)	$j = 0.045$	$k/60.6940$	$\pm$ Dil. Vol.	ng of 1- <i>nn</i> emitted	1- <i>nn</i> /TES (ng/mg) (ppm)	Av. of duplicates	Time for 100ml of fuel to be consumed (secs)	Sampling time (secs)	Volume of Fuel Consumed over sampling period	Mass of fuel used (density = 0.863) (kg)	Mass of fuel from 1 cylinder (kg)	1- <i>nn</i> /total fuel consumed (mg/kg)	Av. of 1- <i>nn</i> /total fuel consumed (mg/kg)
$(a/b) \pm (a)(c) (1/d)$								$(h \pm g/2)$		$(i \pm f/g)$		$m \pm \text{Multi-factor (e)}$		$(n/a)$		$(r/q) \times 100$		$(s \pm 0.863)$		$(t/u)$		$(v/w)$	
	(a)	(b)	(c)	(d)	(e)	(f)	(g)	(h)	(i)	(j)	(k)	(l)	(m)	(n)	(o)	(p)	(q)	(r)	(s)	(t)	(u)	(v)	(w)
1500	21.6	21.6	5.5	4.4	1.25	100	0.5	49.2173	49.9806	49.5990	49.6440	0.8179	163.5877	204.5	9.5		365.41	30	13.68	0.0118	0.0030	0.0693	
1500	26.9	26.9	4.7	4.05	1.17	100	0.5	58.9804	68.5414	63.7359	63.7809	1.0509	210.1720	245.9	9.1		359.66	30	13.90	0.0120	0.0030	0.0820	0.0756
																9.3							
1500	33.5	33.5	5.9	5.62	1.05	100	0.5	151.7808	129.7916	130.7862	130.8332	2.1556	451.1174	452.7	13.5		152.73	30	32.74	0.0283	0.0071	0.0641	
1500	48.4	48.4	11.6	10.1	1.15	100	0.5	155.4531	124.3048	129.9290	129.9740	2.1415	428.2926	493.0	10.2		154.05	30	32.46	0.0280	0.0070	0.0704	0.0672
																11.8							
1500	44.1	44.1	10.1	9.2	1.10	100	0.5	123.0381	122.3781	122.6381	122.7031	2.0217	404.3335	444.8	10.1		96.7	30	51.71	0.0446	0.0112	0.0399	
1500	49.5	49.5	13.6	9.7	1.40	100	0.5	118.8491	119.8671	119.3581	119.4031	1.9673	393.4593	550.8	11.1		96.13	30	52.01	0.0449	0.0112	0.0491	0.0445
																10.6							
3500	83.2	52	8.5	8.1	1.68	500	0.5	35.4578	37.1219	36.2799	36.3249	0.5985	598.4916	1005.5	12.1		120	30	41.67	0.0360	0.0090	0.1118	
3500	107.2	50.5	8.7	4	4.62	100	0.5	98.6196	104.1683	101.5940	101.4390	1.6713	334.2635	1551.0	14.5		117.5	30	42.55	0.0367	0.0092	0.1689	0.1404
																13.3							
3500	121.7	54.5	10.7	9.7	2.46	500	0.5	63.9077	66.6238	65.2658	65.3108	1.0761	1076.0660	2647.1	21.8		70	30	71.43	0.0616	0.0154	0.1718	
3500	153.7	59.5	12.3	10.3	2.68	500	0.5	61.0165	59.6622	60.3393	60.3843	0.9949	994.8945	2686.2	20.1		69	30	72.46	0.0625	0.0156	0.1718	0.1718
																20.9							
1500	57	46.9	15.3	10.2	1.82	500	0.5	37.2058	66.8191	62.0125	62.0575	1.0225	1022.4643	1871.1	32.8		34.75	30	143.88	0.1242	0.0310	0.0603	
3500	68.6	50.6	17.6	9.8	2.43	500	0.5	62.1711	65.5612	63.8662	63.9112	1.0580	1053.0061	2569.3	37.5		34.615	30	144.45	0.1247	0.0312	0.0824	0.0714
																35.1							

Appendix A - GC-ECD analysis of Nitro-PAC collected using Upgraded TESSA																						
2-methyl-1-nitronaphthalene (2-Me-1-nna)								calibration: $y=69.4837x+0.269$ where $y=area$ & $x=wt$ injected (ng) $R^2=0.997$														
Speed	TES (mg)	Sub-fraction of TES cleaned up (mg)	Aromatic Wt. from clean-up (mg)	Wt injected on HPLC (mg)	Mult. factor (if all TES used)	Dil. Vol. (ul)	Inj. Vol. (ul)	Arm #1	Arm #2	Av. Area (b)	$1/69.4837$	$\pm$ Dil. Vol.	ng of 2-Me-1-nna injected	2-Me-1-nna/TES (ng/mg) (ppm)	Av. of duplicates	Time for 100ml of fuel to be consumed (secs)	Sampling time (secs)	Volume of Fuel Consumed over sampling period	Mass of fuel used (density = 0.863) (kg)	Mass of fuel from 1 cylinder (kg)	2-Me-1-nna/total fuel consumed (mg/kg)	Av. of 2-Me-1-nna/ total fuel consumed (mg/kg)
													$m \pm$ Mult. factor (a)	(n/a)	(g)	(q)	(r)	(r/q) $\times$ 100	(s $\times$ 0.863) (t)	(u/d)	(n/u)	(w)
	(a)	(b)	(c)	(d)	(e)	(f)	(g)	(h)	(i)	(j)	(k)	(l)	(m)	(n)	(o)	(p)	(q)	(r)	(s)	(t)	(u)	(w)
1500	21.6	21.6	5.5	4.4	1.25	100	0.5	46.2778	49.1113	47.6946	47.4256	0.6825	136.5084	170.6	7.9	365.41	50	13.68	0.0118	0.0030	0.0578	
1500	26.9	26.9	4.7	4.03	1.17	100	0.5	63.4345	71.7188	67.5767	67.3077	0.9687	193.7365	226.7	8.4	359.66	50	13.90	0.0120	0.0030	0.0756	
1500	33.5	33.5	5.9	5.62	1.05	100	0.5	108.5124	99.6105	104.0614	103.7924	1.4938	298.7531	313.7	9.4	152.73	50	32.74	0.0283	0.0071	0.0444	0.0667
1500	48.4	48.4	11.6	10.1	1.15	100	0.5	171.9577	152.0932	162.0255	161.7565	2.3280	465.5954	535.9	11.1	154.05	50	32.46	0.0280	0.0070	0.0765	0.0605
1500	44.1	44.1	10.1	9.2	1.10	100	0.5	103.6166	102.8642	103.2404	102.9714	1.4820	296.3901	326.0	7.4	96.7	50	51.71	0.0446	0.0112	0.0292	
1500	49.5	49.5	13.6	9.7	1.40	100	0.5	109.5045	88.8964	99.2005	98.9315	1.4238	284.7616	398.7	8.1	96.13	50	52.01	0.0449	0.0112	0.0355	0.0324
															7.7							
3500	81.2	52	8.5	8.1	1.68	300	0.5	24.1053	22.744	23.4247	23.1537	0.3333	333.2530	559.9	6.7	120	30	41.67	0.0360	0.0090	0.0623	
3500	107.2	50.5	8.7	4	4.62	100	0.5	89.4424	74.1742	71.8083	71.5393	1.0296	205.9168	955.5	8.9	117.5	50	42.35	0.0367	0.0092	0.1041	0.0832
3500	121.7	54.3	10.7	9.7	2.46	300	0.5	37.2923	38.7337	38.0130	37.7440	0.5432	543.2065	1336.3	11.0	70	30	71.43	0.0616	0.0154	0.0867	
3500	133.7	59.5	12.3	10.3	2.68	300	0.5	44.2032	42.1683	43.1858	42.9168	0.8177	617.6521	1667.7	12.5	69	50	72.46	0.0625	0.0156	0.1067	0.0967
3500	57	46.9	15.3	10.2	1.82	300	0.5	116.9714	131.2467	124.1091	123.8401	1.7823	356.4578	652.3	11.4	34.75	30	143.88	0.1242	0.0310	0.0210	
3500	68.6	50.6	17.6	9.8	2.43	300	0.5	246.0106	254.048	250.0293	249.7603	3.5945	718.9013	1754.1	25.6	34.615	30	144.45	0.1247	0.0312	0.0563	0.0386
															18.5							

Appendix A - GC-ECD analysis of Nitro-PAC collected using Upgraded TESSA

2-nitronaphthalene (2-*nn*)

calibration:

$$y = 51.4992x - 0.138 \text{ where } y = \text{area}$$

$$R^2 = 0.997$$

Appendix A - GC-ECD analysis of Nitro-PAC collected using Upgraded TESSA																									
2-nitronaphthalene (2- <i>nn</i> )										calibration: $y = 51.4992x - 0.138$ where $y = \text{area}$		R-sq=0.997													
Speed	TES (mg)	Sub-fraction of TES cleaned-up (mg)	Aromatic Wt. from clean-up (mg)	Wt injected on HPLC (mg)	Mult. factor (if all TES used)	Dil. Vol. (ul)	Inj. Vol (ul)	Area #1	Area #2	Av. Area (b)	$y \pm 0.138$	$\text{ci} \pm 1.4992$	x Dil. Vol.	ng of 2- <i>nn</i> emitted	2- <i>nn</i> /TES (ng/mg)	Av. of duplicates	Time for 100ml of fuel to be consumed (secs)	Sampling time (secs)	Volume of Fuel Consumed over sampling period	Mass of fuel used (density = 0.863) (kg)	Mass of fuel from 1 cylinder (kg)	2- <i>nn</i> /total fuel consumed (mg/kg)	Av. of 2- <i>nn</i> /total fuel consumed (mg/kg)		
$(c/b) \times 100$ (%)										$(d \pm \hat{d})/2$		$(f) \times (f/g)$		$m \times \text{Multi factor (e)}$		$(i/j)$		$(k/q) \times 100$		$(h \times 0.863)$		$(l/h)$		$(n/v)$	
(a)	(b)	(c)	(d)	(e)	(f)	(g)	(h)	(i)	(j)	(k)	(l)	(m)	(n)	(o)	(p)	(q)	(r)	(s)	(t)	(u)	(v)	(w)			
1500	21.6	21.6	5.5	4.4	1.25	100	0.5	29.0739	31.4471	30.2605	30.4185	0.5907	118.1319	147.7	6.8		365.41	50	13.68	0.0118	0.0030	0.0500			
1500	26.9	26.9	4.7	4.03	1.17	100	0.5	39.6899	46.3123	43.1012	43.2592	0.8400	167.9995	196.6	7.3		359.66	50	13.90	0.0120	0.0030	0.0635			
1500	33.5	33.5	5.9	5.62	1.05	100	0.5	59.2603	57.5169	58.3886	58.5466	1.1368	227.3690	238.7	7.1	7.1	152.73	50	32.74	0.0283	0.0071	0.0338	0.0578		
1500	48.4	48.4	11.6	10.1	1.15	100	0.5	57.5697	51.521	54.5454	54.7034	1.0622	212.4433	244.5	5.1		154.05	50	32.46	0.0280	0.0070	0.0349			
1500	44.1	44.1	10.1	9.2	1.10	100	0.5	80.7454	79.6844	80.2149	80.3729	1.5607	312.1326	345.3	7.8	6.1	96.7	50	51.71	0.0446	0.0112	0.0308	0.0344		
1500	49.5	49.5	13.6	9.7	1.40	100	0.5	71.8591	59.1861	65.5126	65.6706	1.2752	255.0154	357.0	7.2	7.5	96.13	50	52.01	0.0449	0.0112	0.0318	0.0315		
1500	83.2	52	8.5	8.1	1.68	500	0.5	14.3999	26.9458	20.6729	20.8309	0.4045	404.4888	679.5	8.2		120	50	41.67	0.0360	0.0090	0.0756			
1500	107.2	50.5	8.7	4	4.62	100	0.5	33.5602	35.1984	34.1793	34.5373	0.6706	134.1275	622.4	5.8	7.0	117.5	50	42.55	0.0367	0.0092	0.0678	0.0717		
1500	121.7	54.5	10.7	9.7	2.46	500	0.5	22.5251	23.4239	22.9745	23.1325	0.4492	449.1817	1105.0	9.1		70	50	71.43	0.0616	0.0154	0.0717			
1500	133.7	59.5	12.5	10.3	2.68	500	0.5	16.8949	16.9439	16.9439	17.1019	0.3321	332.0809	896.6	6.7	7.9	69	50	72.46	0.0625	0.0156	0.0574	0.0645		
1500	57	46.9	13.3	10.2	1.82	100	0.5	21.6798	24.9256	23.3027	23.4607	0.4556	455.5546	833.7	14.6		34.75	50	143.88	0.1242	0.0310	0.0269			
1500	68.6	50.6	17.6	9.8	2.43	500	0.5	32.8602	34.0333	33.4468	33.6048	0.6525	652.5296	1592.2	23.2	18.9	34.615	50	144.45	0.1247	0.0312	0.0511	0.0390		

Appendix A - GC-ECD analysis of Nitro-PAC collected using Upgraded TESSA

1-nitropyrene (1-np)

Calibration:  $y = 38.056x + 0.65$  where  $y$  = area &  $x$  = wt. injected (ng)

$R_{adj} = 0.997$

Speed	TES (mg)	Sub-fraction of TES cleaned-up (mg)	Aromatic Wt. from clean-up (mg)	Wt injected on HPLC (mg)	Multi factor (if all TES used)	Dil. Vol. (ul)	Inj. Vol (ul)	Area #1	Area #2	Av. Area (b)	j=0.65	k/38.0569	x Dil. Vol.	ng of 1-np emitted	1-np/TES (ng/mg) (ppm)	Av. of duplicates	Time for 100ml of fuel to be consumed (secs)	Sampling time (secs)	Volume of Fuel Consumed over sampling period	Mass of fuel used (density = 0.863) (kg)	Mass of fuel from 1 cylinder (kg)	1-np/total fuel consumed (mg/kg)	Av. of 1-np/ total fuel consumed (mg/kg)
	(a)	(b)	(c)	(d)	(e) = (b) x (1/d)	(f)	(g)	(h)	(i)	(j) = (f) x 2	(k)	(l)	(m) = (l) x (f/g)	(n) = Multi- factor (e)	(o) = (n/d)	(p)	(q)	(r)	(s) x 100	(t = 0.863) (l)	(u) = (t/d)	(v) = (n/u)	(w)
1500	21.6	21.6	5.5	4.4	1.25	100	0.5	6.1752	6.8401	6.5077	5.8777	0.1540	30.7998	38.5	1.8		365.41	50	13.68	0.0118	0.0090	0.0130	
1500	26.9	26.9	4.7	4.03	1.17	100	0.5	5.6271	7.9334	6.7803	6.1303	0.1612	32.2332	37.6	1.4		359.66	50	13.90	0.0120	0.0090	0.0125	
																1.6							0.0128
1500	33.5	33.5	5.9	5.62	1.05	100	0.5	6.4039	6.6882	6.4461	5.9961	0.1576	31.5275	33.1	1.0		152.73	50	32.74	0.0283	0.0071	0.0047	
1500	48.4	48.4	11.6	10.1	1.15	100	0.5	9.3914	11.6356	10.5135	9.8635	0.2593	51.8628	59.6	1.2		154.05	50	32.46	0.0280	0.0070	0.0085	
																1.1							0.0066
1500	44.1	44.1	10.1	9.2	1.10	100	0.5	14.5922	15.1182	14.8552	14.2052	0.3735	74.6917	82.0	1.9		96.7	50	51.71	0.0446	0.0112	0.0074	
1500	49.5	49.5	13.6	9.7	1.40	100	0.5	5.6615	5.3268	5.4942	4.8442	0.1274	25.4708	35.7	0.7		96.13	50	32.01	0.0449	0.0112	0.0032	
																1.3							0.0051
2300	59.2	39.5	23	10	3.45	140	0.5	3.3368	5.0606	3.2987	2.6487	0.0696	19.4978	67.2	1.1		195.24	50	25.61	0.0221	0.0055	0.0122	
2500	57.5	38.3	24.7	8	4.64	100	0.5	2.7822	2.9793	2.8808	2.2308	0.0566	11.7294	54.4	0.9		192.9	50	25.92	0.0224	0.0056	0.0097	
																1.0							0.0109
2500	71.7	35.9	21.9	10	4.57	100	0.5	8.2084	8.6878	8.4481	7.7981	0.2050	41.0028	179.3	2.5		81	50	61.73	0.0533	0.0133	0.0135	
2500	93.6	46.8	25.1	10	5.02	100	0.5	9.1091	10.6475	9.8785	9.2285	0.2426	48.5229	245.6	2.6		82	50	60.98	0.0526	0.0132	0.0185	
																2.6							0.0160
2500	82.1	28.2	18.1	10	5.27	100	0.5	7.5202	9.1302	8.3252	7.6752	0.2018	40.3566	212.7	2.3		53.8	50	92.94	0.0802	0.0201	0.0106	
2500	91.2	31.4	19.8	9.9	5.81	100	0.5	7.0619	5.1237	6.0928	5.4428	0.1431	28.6185	166.2	2.0		54.37	50	91.96	0.0794	0.0198	0.0084	
																2.2							0.0095
3500	83.2	52	8.5	8.1	1.68	100	0.5	7.7195	7.0043	7.3618	6.7118	0.1765	35.2910	59.5	0.7		130	50	41.67	0.0360	0.0090	0.0066	
3500	107.2	50.5	8.7	4	4.62	100	0.5	2.7135	2.912	2.8128	2.1628	0.0569	11.3719	52.5	0.5		117.5	50	42.55	0.0367	0.0092	0.0057	
																0.6							0.0062
3500	121.7	54.5	10.7	9.7	2.46	100	0.5	6.0727	6.3645	6.2186	5.5686	0.1464	29.2800	72.1	0.6		70	50	71.43	0.0616	0.0154	0.0047	
3500	133.7	59.5	12.3	10.3	2.68	500	0.5	2.5989	1.5201	1.9595	1.3095	0.0344	34.4271	92.4	0.7		69	50	72.46	0.0625	0.0156	0.0059	
																0.6							0.0051
3500	57	46.9	15.3	10.2	1.82	100	0.5	34.6693	34.7449	34.7071	34.0971	0.8954	179.0740	326.5	5.7		34.75	50	143.88	0.1242	0.0310	0.0105	
3500	68.6	50.6	17.6	9.8	2.43	100	0.5	26.0787	26.3486	26.2137	25.5637	0.0721	134.4150	327.5	4.8		34.815	50	144.45	0.1247	0.0312	0.0105	
																5.2							0.0105